

PB 196 972

REPORT

FLOOD PROTECTION AT CULVERT OUTLETS

By

D. B. Simons, M. A. Stevens and F. J. Watts

Prepared for

Wyoming State Highway Department

Planning and Research Division

in cooperation with the

U.S. Department of Transportation

Federal Highway Administration

Bureau of Public Roads

1970

CER69-70DBS-MAS-FJW4

103.017

PB 196 972

REPORT

FLOOD PROTECTION AT CULVERT OUTLETS

By

D. B. Simons, M. A. Stevens and F. J. Watts

Prepared for

Wyoming State Highway Department

Planning and Research Division

in cooperation with the

U.S. Department of Transportation

Federal Highway Administration

Bureau of Public Roads

1970

CER69-70DBS-MAS-FJW4

RESEARCH AND DEVELOPMENT REPORT
ABSTRACT AND EVALUATION

U.S. DEPARTMENT OF TRANSPORTATION
FEDERAL HIGHWAY ADMINISTRATION
BUREAU OF PUBLIC ROADS

DATE EVALUATED

Nov. 30, 1970

1. STATE Wyoming	2. STATE'S STUDY NO. 508	3. BPR ADMIN IDENT NO. 8	2421
4. STUDY TITLE Flood Protection of Bridges and Culverts			
5. REPORT TITLE Flood Protection at Bridge Crossings		6. AUTHOR(S) D. B. Simons and G. L. Lewis	
7. R&D DIVISION TO WHICH ASSIGNED Environmental Design and Control Division		8. PROGRAM AREA --	
9. STUDY CONDUCTED BY Colorado State University			
10. SPONSORING AGENCY: Wyoming State Highway Department and FHWA (BPR)			
11. TYPE OF R&D: <input checked="" type="checkbox"/> THEORETICAL <input type="checkbox"/> APPLIED <input type="checkbox"/> DEVELOPMENT <input type="checkbox"/> MT&E <input type="checkbox"/> OTHER R&D			
12. STUDY STATUS <input checked="" type="checkbox"/> ACTIVE <input type="checkbox"/> COMPLETE		3 YEAR OF A 3 YEAR STUDY	
13. ABSTRACT ORIGINAL BY: <u>Simons & Lewis</u>		(EDITED) (REVIEWED) BY: <u>H. E. Berger</u>	

Techniques for the design of stable rock-riprap protection in the vicinity of bridge crossings are computed from methods derived in other sources, and the properties are related to particle sizes for riprap protection of abutments and piers.

Design steps for prototype bridge crossings are enumerated so that the hydraulic engineer may use this report as a design manual. An example of the design protection for a prototype bridge crossing is included to clarify the suggested design procedures.

Riprap-protected spill-through abutments were constructed in the hydraulic facilities at Colorado State University in order to test the validity of the suggested design procedures.

PRICES SUBJECT TO CHANGE

14. STATE HOW THE RESULTS OF THIS RESEARCH CAN BE USED OR APPLIED. The results of this research will become the standard for establishing erosion protection required at bridges.	
15. COMMENTS: The report ties the protection of bridges to prior work on backwater, scour, rip-rap sizing and placement with suggested design procedures.	
TECHNICAL COORDINATOR Hugh E. Berger, Reg. Hydr. Engineer	DIVISION, REGION OR R&D DIVISION Region 9

REPORT

FLOOD PROTECTION AT CULVERT OUTLETS

By

D. B. Simons, M. A. Stevens and F. J. Watts

Prepared for

Wyoming State Highway Department

Planning and Research Division

in cooperation with the

U.S. Department of Transportation

Federal Highway Administration

Bureau of Public Roads

1970

CER69-70DBS-MAS-FJW4

id

AUTHORIZATION OF PROJECT

The problems to be investigated were formulated by the staff of the State Highway Commission of Wyoming in consultation with personnel of Colorado State University and the Bureau of Public Roads. The project was initiated by the signing of the agreement "Engineering Investigations Pertaining to Flood Protection of Bridges and Culverts," dated February 16, 1966.

DISCLAIMER

The opinions, findings and conclusions expressed in this publication are those of the authors and not necessarily those of the Wyoming State Highway Department or the Bureau of Public Roads.

ABSTRACT

FLOOD PROTECTION AT CULVERT OUTLETS

In this study several classes of information concerning flood protection at culvert outlets are presented. The information is related to the flow conditions at culvert outfalls and to the hydraulics of rigid basins and outlet basins stabilized with rock riprap. In addition, the characteristics of high tailwater and non-scouring, low tailwater basins are covered.

In this report it is intended that a hydraulic engineer can take the information contained in the text, examples, illustrations, and figures and apply it toward the design of an energy dissipator of maximum effectiveness.

The data on which the report is based were gathered mostly during an experimental program at Colorado State University. In some cases, adequate data were available from other sources. Where such information was needed, it was incorporated into the report.

TABLE OF CONTENTS

<u>Chapter</u>	<u>Page</u>
ABSTRACT	ii
NOTATION	v
LIST OF FIGURES	vii
SUMMARY ON RESEARCH IMPLICATION	xi
I INTRODUCTION	1
II FLOW CONDITIONS AT CULVERT OUTFALLS	5
2.1 Velocity Fields and Water Surface Contours	5
2.2 Energy and Momentum at the Outlet	11
2.3 Discharge-Brink Depth Relationship	17
2.4 Flow Conditions at the Culvert Outlet	19
III RIGID OUTLET BASINS	20
3.1 Hydraulic Design of a Smooth-floor Flared Basin	21
3.2 Hydraulic Design of a Smooth-floor Rectangular Basin	23
3.3 Rough-floor Rectangular Basin	23
3.4 The Combined Basin	30
IV ROCK RIPRAPPED BASINS	32
4.1 Introduction.	32
4.2 Parameters Used in the Design of Riprapped Basins	34
4.3 Standard Riprapped Basins	39
4.4 Metal End Section for Circular Pipes	47
4.5 Circular Outlets	51
4.6 Rectangular Outlets	53
4.7 Multiple Barrels	53
4.8 Optimum Culvert Design	55
V THE HIGH TAILWATER AND NON-SCOURING BASIN	56
5.1 Characteristics of Basins with High Tailwater	
BIBLIOGRAPHY	59
APPENDIX A - DESIGN EXAMPLES OF RIGID BOUNDARY AND ROCK RIPRAPPED BASINS	61
APPENDIX B - FIGURES	140
APPENDIX C - FLARE ANGLE AT THE CULVERT OUTLET	197

TABLE OF CONTENTS (Continued)

<u>Chapter</u>	<u>Page</u>
APPENDIX D - R-JUMP BASIN	205
APPENDIX E - TWO-DIMENSIONAL FLOW APPROXIMATION TO PREDICT SCOUR DEPTHS AT THE OUTFALL OF CIRCULAR AND RECTANGULAR CULVERTS	211

NOTATION

<u>SYMBOL</u>	<u>DEFINITION</u>	<u>UNITS</u>
A,B,C	Dimensions of rock basin	ft
A_o	Area of culvert outlet	ft
C_D	Drag coefficient	units
d_m	Effective diameter of rock mixture	ft
d_s	Depth of scour	ft
d_{to}	Tailwater depth at the outlet	ft
d_t	Tailwater depth	ft
D	Pipe diameter	ft
E_o	Specific energy	ft
F_o	Froude number at outlet	units
F_r	Drag force	lb
g	Acceleration of gravity	ft/sec ²
H_o	Height parameter	ft
K	Coefficient	units
L	Length parameter	ft
L_s	Length of scour hole	ft
M_o	Momentum flux	lb/ft
N	Counting function	units
q	Discharge per unit width	ft ³ /sec-ft
Q	Discharge	ft ³ /sec
T	Spacing between culverts	ft
t	Time	seconds
u	Flare slope of sidewall	ft/ft
V_o	Outlet mean velocity	ft/sec
W	Width parameter	ft

NOTATION (Continued)

<u>SYMBOL</u>	<u>DEFINITION</u>	<u>UNITS</u>
W_s	Width of scour hole	ft
x	Longitudinal coordinate	ft
Y	Vertical coordinate	ft
y_c	Critical depth	ft
y_o	Depth of culvert outlet	ft
z	Lateral coordinate	ft
α_1, α_2	Energy correction coefficients	1
β_1, β_2	Momentum correction coefficients	1
γ	Specific weight of water	lb/ft ³
ρ	Mass density of water	lb-sec ² /ft ⁴

LIST OF FIGURES

<u>Figure</u>		<u>Page</u>
1	Flow Type Definition (From Wyoming Highway Dept. "Hydraulic Design Practice")	141
2	Dimensionless Water Surface Contours Reproduced from Reference 14	142
3	Dimensionless Water Surface Contours and Relative Velocities, Rectangular Outfall	143
4	Dimensionless Water Surface Contours and Relative Velocities, Rectangular Outfall	144
5	Dimensionless Water Surface Contours and Relative Velocities, Rectangular Outfall	145
6	Dimensionless Water Surface Contours and Relative Velocities, Rectangular Outfall	146
7	Dimensionless Water Surface Contours and Relative Velocities, Rectangular Outfall	147
8	Dimensionless Water Surface Contours and Relative Velocities, Rectangular Outfall	148
9	Dimensionless Water Surface Contours and Relative Velocities, Circular Outfall	149
10	Dimensionless Water Surface Contours and Relative Velocities, Circular Outfall	150
11	Dimensionless Water Surface Contours and Relative Velocities, Circular Outfall	151
12	Dimensionless Water Surface Contours and Relative Velocities, Circular Outfall	152
13	Average Velocity in the Spreading Jet	153
14	Brink Depth, Energy and Momentum Coefficients for Rectangular Culverts	154
15	Brink Depth, Energy and Momentum Coefficients for Circular Pipes	155
16	Effect of Tailwater on Brink Depth: Horizontal and Mild Sloping Rectangular Culverts	156
17	Effect of Tailwater on Brink Depth: Horizontal and Mild Sloping Circular Culverts	157

LIST OF FIGURES (Continued)

<u>Figure</u>		<u>Page</u>
18	Smooth-floor Flared Basin	158
19	Dimensionless Water Surface Contours and Relative Velocities Smooth-floor Flared Basin	159
20	Smooth-floor Rectangular Basin	160
21	Dimensionless Water Surface Contours and Relative Velocities, Smooth-floor Rectangular Basin	161
22	Smooth Floor 45° Flare, $Q = 21.6$ cfs (from Watts, Reference 22)	162
23	Smooth Floor Plain End, $Q = 14.9$ cfs (from Watts, Reference 22)	162
24	General Relations Among F_1 , θ , β , y_2/y_1 and F_2 for Oblique Hydraulic Jumps (after A.T. Ippen, Reference 7) .	163
25	Definition Sketch for Backwater Computations, Smooth- floor Rectangular Basin	164
26	Definition Sketch for a Rough-floor Basin	165
27	Coefficients of Drag for Roughness Elements Rectangular Approach Pipe	166
28	Coefficients of Drag for Roughness Elements Rectangular Approach Pipe	166
29	Coefficients of Drag for Roughness Elements Rectangular Approach Pipe	167
30	Coefficients of Drag for Roughness Elements Rectangular Approach Pipe	167
31	Coefficient of Drag for Roughness Elements Circular Approach Pipe	168
32	Coefficient of Drag for Roughness Elements Circular Approach Pipe	168
33	Coefficients of Drag for Roughness Element Circular Approach Pipe	169
34	Coefficients of Drag for Roughness Element Circular Approach Pipe	169

LIST OF FIGURES (Continued)

<u>Figure</u>		<u>Page</u>
35	Coefficients of Drag for Roughness Element Circular Approach Pipe	169
36	Coefficient of Drag for Roughness Elements, Circular Approach Pipe	170
37	Coefficient of Drag for Roughness Elements, Circular Approach Pipe	170
38	Rough-floor Basin	171
39	Definition Sketch, Trajectory Equation	172
40	Definition Sketch of Riprapped Basin	173
41	Standard Non-Scouring Riprapped Basin	174
42	Standard Hybrid Riprapped Basin	175
43	Standard Scoured Basin	176
44	Metal End Section	177
45	Standing Waves	178
46	Non-Scouring Basin with a Metal End Section	179
47	Scouring Basin with a Metal End Section	180
48	Scour: Plain Rectangular Outlet	181
49	Scour: Plain Rectangular Outlet	182
50	Scour: Plain Circular Outlet	183
51	Scour: Plain Circular Outlet	184
52	Scour: Plain Circular Outlet	185
53	Length of Scour Hole	186
54	Length of Basin	187
55	Width of Scour Hole, Plain Outlets	188
56	Scour: Metal End Section	189
57	Gradation Curve, Example 1	190

LIST OF FIGURES (Continued)

<u>Figure</u>		<u>Page</u>
58	An Estimate of the Angle of Lateral Expansion for Horizontal and Mild Sloping Circular Culverts	191
59	An Estimate of the Angle of Lateral Expansion for Horizontal and Mild Sloping Rectangular Culverts	192
60	Distribution of Centerline Velocity for Flow from Submerged Outlets (after Reference 1)	193
61	Distribution of Longitudinal Velocity for $\frac{x}{D} < 6$ (after Reference 1)	194
62	Distribution of Longitudinal Velocity for $\frac{x}{D} > 6$	194
63	Comparison of Expansion Angles for Different Basin Geometries	195
64	Discharge Ratios for the Two-Dimensional Flow Approximation	196

SUMMARY ON RESEARCH IMPLICATION

The three concrete basins and the rock riprapped basin recommended in this report offer four options to the designer of culvert outlet energy dissipating structures. The final choice of a basin is an economical consideration; if the rock is readily available, the riprapped basin appears to be less expensive than the concrete alternatives.

The rock basin design procedure has been more or less standardized but the concrete basin design allows for some deviation from the presented procedures. These deviations depend on the physical limitations at the design site. Designers, after using the information as it is presented for several culvert installations, will be in a better position to formulate the best design. To assist the designer in interpreting the data or in extending the data to cover unusual design problems, examples of designs are given. Reference can be made to the text or to the Appendices for details on specific problems.

Potential benefits from implementing the research findings are savings in the initial investment of culvert outlet basins, savings in maintenance costs throughout the life of the structure and savings in the maintenance repair of existing structures. It is suggested that the concrete outlet basin be constructed at least partly under the embankment to reduce the cost of the barrel and to improve the aesthetics of the culvert structure.

All figures are presented in Appendix B. However, the various types of basins that were studied are illustrated in a single sketch for easy reference in Appendix A on page 63. This sketch is accompanied by example design problems.

Chapter I

INTRODUCTION

Scour at the outlet of a conduit is a familiar problem to hydraulic and highway engineers. Among the possible results of this scour are unstable scour holes, excessive deposition of scoured material downstream, and occasional structural collapse resulting from foundation removal.

Traditionally, energy dissipating basins such as the St. Anthony Falls basin (3), Bureau of Reclamation stilling basin (19), the New South Wales jump basin (10), or other experimentally developed basins have been placed at the outlet of large structures with high exit velocities. For small diameter conduits that flow infrequently and at moderate velocities (4 to 8 fps), various agencies have usually treated scour as a maintenance problem. If serious erosion occurs, the hole is usually filled with broken concrete or large rock; the extent of this maintenance usually depends on the judgment of the local foreman, rather than on specific design criteria.

Numerous publications by government agencies, such as "Shore Protection Planning and Design," Corps of Engineers (18), and "Bank and Shore Protection," California Division of Highways (4), do suggest design criteria. The suggestions usually consist of a chart of rock diameter or rock weight versus mean velocity or near bed velocity with empirical multiplying factors where flow is likely to impinge on the rock surface such as on the banks of bends.

Using formulas or design charts based on uniform mean flow conditions for the three-dimensional, highly turbulent, nonuniform, plunging flow found at culvert outlets is questionable. For this reason, the State

Highway Commission of Wyoming, in conjunction with the U.S. Bureau of Public Roads, inaugurated a basic research program to produce suitable design criteria for local scour with particular emphasis placed on culvert outlets.

The problems to be investigated were formulated by the State Highway Commission of Wyoming in consultation with D.B. Simons, other personnel of Colorado State University, and the Bureau of Public Roads. The project was initiated by signing the agreement "Engineering Investigations Pertaining to Flow Protection of Bridges and Culverts," February 16, 1966.

The project was divided into three phases:

Phase I - Channel stabilization in the vicinity of and downstream of culvert outlets;

Phase II - Channel stabilization in the vicinity of and downstream of bridges, and

Phase III - Investigation of the use of special materials and techniques to develop economical methods of stabilizing channels where there is no gravel or rock available and where special problems require the use of other materials and methods of stabilization. It is anticipated that this phase may be funded by commercial interests subsequent to phases I and II.

This report finalizes Phase I of the Colorado State University study. It is a summary of previous publications on rigid basins by Watts (22) and riprapped basins by Stevens (17).

The general purpose of this report is, as stated in the research agreement, "...to develop design criteria required to establish methods and the physical requirements of material necessary to control erosion downstream of highway culverts, contracted bridge sections, and other hydraulic structures."

The general problem of rapidly varied flow issuing from a culvert outlet is not amenable to analytical solution -- it is too complicated. All solutions must be based on empirical data. Therefore, data must be available for each design considered, or at least for the separate phenomena that comprise components of the design.

The design problem is presented in an applied sense -- that is, the report is meant to be a working tool for the design engineer. It must be realized, however, that if the data reported herein were generalized excessively, or if the design procedures were reduced to a level where no judgment was allowed, the benefits of the research would be lost. The cost of preserving the detail in the report is that very simple and direct design procedures are not developed. The benefits gained from this approach are that the designer is offered a chance to engineer true economy into his culvert and basin design.

In the event that design must be performed by personnel who are not trained in hydraulic principles, simpler procedures are available. These procedures do not indicate maximum economy of design however, nor do they always insure safe design.

The best use of this report would be its incorporation into a set of design aids or principles which would also include works by other researchers. Quite possibly the design procedure could be simplified by taking these studies and developing certain standard design from them. The standards could be used for the nominal cases of design, whereas the special procedures reported here could be used for the more difficult cases.

In this report three designs of rigid outlet basins are offered as possible economical outlet structures. Each structure has a slab floor

and relatively low sidewalls. Also, design principles for riprapped basins are provided. Since very large stones are generally required to resist scour completely, basins with limited scouring are suggested.

An additional feature of the report is a chapter on flow conditions at culvert outfalls (Chapter II). This subject is difficult to summarize because of the complicated nature of the flow. The methods advanced in this section are rather unique in that they provide a relatively simple, but reliable approach to this difficult problem. The engineer really has few resources at present from which to obtain information on this subject.

The final chapter of the report covers two special problems in detail: the case of the basin with high tailwater, and the non-scouring basin with low tailwater. These cases present special design problems in that the flow phenomena are complicated and little information is available.

Chapter II

FLOW CONDITIONS AT CULVERT OUTFALLS

A convenient place to start the design of a culvert outfall energy dissipator is at the vertical plane of the culvert outlet. However, before this can be accomplished, it is necessary to know the flow properties at this plane. Specifically, a knowledge of velocity and pressure fields, total energy and momentum, and flow depth is essential.

Culvert flow has been classified into seven general types as shown in Fig. 1 (23), Appendix B. A major objective of the study was to describe the outlet hydraulic conditions for Flow Types II and VI where there is considerable curvature of the flow at the plane of the outlet, see Fig. 1. Moreover, studies have been limited to the condition that the invert of the barrel and the bed of the downstream channel or structure be flush or tangent at the plane of the culvert outlet.

The bulk of the work presented in this chapter was previously reported by Watts (22). Reference can be made to Watts' work if details of the experimental program are needed. Only summaries are presented in this report.

2.1 Velocity Fields and Water Surface Contours

Introduction

For basin design it is necessary that the configuration of the water surface and the approximate magnitude and direction of velocity be predictable in the rapidly varied flow region adjacent to the culvert outlet. The information presented here is valid for any abrupt expansion continuing at the same slope where the floor is set at the elevation of

the approach pipe invert. It is assumed that the slopes of the basin and pipe are mild or horizontal and that the tailwater depth, d_t , is such that $d_t/y_o \leq 0.3$. Here, y_o is the depth of flow at the outlet and d_t is the tailwater depth adjacent to the jet at the outlet. Under these conditions, the flow in the region adjacent to the outlet will always be supercritical, and the outlet will be the control section.

Rectangular Sections

Rouse, Bhoota, and Hsu (14) have delineated the variables to be used in a study of abrupt expansions from rectangular sections with the flow conditions described in the Introduction. These variables are:

- 1) y_o and V_o , the depth and mean velocity at the outlet section;
- 2) W_o , the width of the rectangular channel;
- 3) x and z , the longitudinal and lateral coordinates measured from the outlet and channel centerline respectively;
- 4) y , the depth of flow at any point in the basin, and
- 5) g , the acceleration from gravity.

The variables were combined into the dimensionless relation,

$$\frac{y}{y_o} = f_1\left(\frac{x}{y_o}, \frac{z}{y_o}, \frac{W_o}{y_o}, \frac{V_o}{\sqrt{gy_o}}\right).$$

This means that the relative depth y/y_o at any point of the flow should depend on the relative coordinate location $(x/y_o, z/y_o)$, the relative width of the channel outlet W_o/y_o , and the Froude number of the approach flow $V_o/\sqrt{gy_o}$. Rouse, Bhoota, and Hsu then developed a graphical solution of the problem using the "method of characteristics." The "method of characteristics," in effect, reduces the above functional relation to the form

$$\frac{y}{y_0} = f_2 \left(\frac{x}{W_0}, \frac{z}{W_0}, \frac{V_0}{\sqrt{gy_0}} \right).$$

This is done by combining the relative coordinate terms x/y_0 and z/y_0 with the initial width-depth ratio W_0/y_0 . This entails the inherent assumption of hydrostatic pressure distribution at all points -- that is, the absence of appreciable vertical acceleration. The investigators then point out the discrepancy between the hydrostatic pressure assumption and the actual situation for various outlet width-to-depth ratios. Their experimental equipment made it possible to test three different width-to-depth ratios. They state that, "The deviations with W_0/y_0 are appreciable but nevertheless secondary to the variation with Froude number (14)".

Figure 2 is a reproduction of the authors' (14) generalization of experimental data for abrupt expansions. The experimental data for Froude numbers of 2, 4, and 8 group reasonably well; however, there is deviation in those data describing the dimensionless surface contour lines for a Froude number of 1 to 2. The range of Froude numbers from 1.0 to 2 is the region where many culverts operate.

Two other deviations or shortcomings of the information concerning energy basin design presented in the previously mentioned paper (14) are:

- 1) For a Froude number of one, dimensionless surface contours along the centerline are only presented for a distance of 1.7 pipe diameters.
- 2) No information is presented concerning the magnitude or direction of the velocities associated with the water surfaces.

To obtain sufficient information for energy basin design, extensive experimental data were collected in the study. A smooth rectangular approach pipe (1.25 ft by 1.25 ft) was used to convey water onto a flat

test basin (10 ft wide and 14 ft long) with vertical walls and a smooth horizontal aluminum floor. Water surface elevations and the direction and magnitude of velocity were measured at two and four pipe widths downstream from the outlet. Six discharges were examined with Froude numbers $V_o / \sqrt{gy_o}$ varying from 1.36 to 2.35.

The data were plotted and contour lines drawn through appropriate points as shown in Figs. 3 through 8. One additional dimensionless parameter, the ratio of the depth of flow at Station 0 over the width of the approach channel $\left(\frac{y_o}{W_o}\right)$, accompanies each of these diagrams. Because of the unpredictability of the pressure at the outlet section and its consequent effect on the flow field, this ratio must be approximately the same for model and prototype. This is important for Froude numbers up to 2, as shown by Fig. 2. For larger Froude numbers this ratio becomes progressively less significant, i.e., the pressure force, regardless of how it varies, no longer makes up a significant portion of the force-momentum quantity. Velocity dominates the quantity. Figure 2 is recommended for purposes of design where the exit Froude number is larger than 2.5.

Circular Sections

No information similar to that of Fig. 2 was found for circular approach pipes in the low Froude number range. Analysis indicates the same functional relation for the circular outlet as for the rectangular outlet, except for the circular pipe the diameter D is substituted for the width W_o . Hence the suggested expression for circular culverts discharging under conditions specified in the Introduction to this chapter is

$$\frac{y}{y_o} = f_3 \left(\frac{x}{D}, \frac{z}{D}, \frac{V_o}{\sqrt{gy_o}} \right) .$$

In the experimental program carried out by Watts (22), a smooth circular pipe (1.45 ft internal diameter) was used in conjunction with the same test basin used with the rectangular pipe. At stations 1D, 2D, and 3D downstream of the outlet, water surface profile data were collected every 0.3 ft transversely in the central portion of the basin and at 0.5 ft increments elsewhere. Velocity data were taken at stations 2D and 4D.

For the circular pipe, seven discharges were examined with the value of the parameter $Q/D^{2.5}$ varying from 3.87 to 9.28 cfs/ft^{5/2}. These discharges correspond to Froude numbers, $V_o/\sqrt{gy_o}$, varying from 1.25 to 2.07. It should be noted that the circular pipe flows full when $Q/D^{2.5} \geq 6.5$ cfs/ft^{5/2} and thereafter $y_o = D$ is a constant.

Part of the experimental data is shown in Figs. 9 through 12. Once again, the dimensional parameter y_o/D is added. Because of the difficulty of predicting the pressure distribution at the outlet section and its consequent effect on the flow field, this ratio must be approximately the same for model and prototype.

Summary

Figures 2 through 12 are essentially self explanatory. The relations are valid under three conditions:

- 1) the slope of the pipe is mild or horizontal
(steep pipes will be considered subsequently),
- 2) the floor of the basin is set at the elevation of the invert of the approach pipe and is at the same slope as the pipe, and
- 3) the tailwater depth is such that $d_t/y_o < 0.3$.

Given a pipe size and exit velocity (which can be estimated by conventional culvert hydraulics), the values of the parameters $F_o = \frac{V_o}{\sqrt{gy_o}}$,

$V_o = \frac{Q}{A_o}$, and $\frac{y_o}{D}$ are determined. The engineer then selects the dimensionless plot from Figs. 2-12 that most closely matches F_o and y_o/D and proceeds with plotting. Because of the rather close grouping of Froude numbers, it is probably not necessary to interpolate between plots, though it can be done. Further discussion of the use of these plots is deferred to Appendix A where procedures for applying the figures are described. The use of Fig. 2 is recommended for designing rectangular sections where the exit Froude number is larger than 2.5.

In cases where details of the surface geometry are not important and the engineer needs only mean depth for purposes of design, use can be made of the finding that $\frac{V}{V_o}$ does not vary much with x and z . Data in Figs. 3-12 can be summarized by two equations:

$$\left(\frac{V}{V_o}\right)_{ave} = 1.65 - 0.3 F_o \quad (\text{Rectangular}),$$

$$\left(\frac{V}{V_o}\right)_{ave} = 1.65 - 0.45 \frac{Q}{\sqrt{gD^5}} \quad (\text{Circular}).$$

These equations are valid for the design of basins provided the walls of the basin do not interfere with the spreading of the jet and $\frac{x}{D}$ or $\frac{x}{W_o}$ are not less than 2.

The direction of the velocity vector in Figs. 3-12 inclusive diverges from the centerline of the basin; the value of $\left(\frac{V}{V_o}\right)_{ave}$ plotted in Fig. 13 refers to the magnitude of the whole vector, not its component in the x direction. Nevertheless, the curves are recommended for calculations of the x component of mass and momentum flux; this recommendation is justified in the following paragraph.

The greatest deflection of the vector occurs near the edges of the jet at small values of x where the jet is shallow. At these values of x most of the mass is transported near the centerline, where the deflection is small. Further downstream, where the depth is more uniform, deflection of the vector is smaller. In both cases, the effect of deflection of the velocity vector on the longitudinal transport of mass and momentum is small.

2.2 Energy and Momentum at the Outlet

The design procedure for culvert outlet basins requires an accurate estimate of a momentum flux and pressure force term, computed for a specific discharge, at the outfall section of circular and rectangular culverts. Precise description of the energy line at the plane of the outlet is not required for the outlet basin design, but it can be useful in designing the barrel section.

The specific energy equation for flow at the outlet section can be written

$$E_o = \alpha_1 y_o + \alpha_2 \frac{(Q/A_o)^2}{2g}$$

in which α_1 and α_2 are correction coefficients that compensate for the nonhydrostatic pressure distribution and the variable distribution of velocity.

The most comprehensive treatment of the value of E_o for circular pipes is found in "Pressure and Resistance Characteristics of a Model Pipe Culvert," by J. L. French (6). In this publication the piezometric grade line is established for the interior uniform flow zone within the pipe and extended linearly through the plane of the outlet. The ratio

of the elevation of the piezometric line at this plane over the depth of flow is found. This ratio is designated as the correction factor. A relationship is established between the Froude number at the outlet section and the correction factor. Information is given for both rectangular and trapezoidal discharge channels downstream of a circular approach pipe for the condition where the jet is supported on the bottom by a floor and for the condition where the jet is allowed to fall freely without bottom support. Values of the correction factor range from 0.57 to 0.85.

The design methods developed during the study required similar correction factors for the pressure quantity in the momentum equation for both circular and rectangular approach pipes. These correction factors are defined in the equation for momentum at the outlet, M_o , or

$$M_o = \beta_1 \frac{\gamma y_o}{2} A_o + \beta_2 \rho Q V_o$$

in which W = width of the wetted section,

β_1 = correction factor which compensates for the nonhydrostatic pressure distribution,

β_2 = correction factor which compensates for the nonuniform distribution of velocity, and

ρ = mass density of the fluid.

A comprehensive experimental program was devised and carried out by Watts (22) whereby the energy level and momentum at the outlet and at successive stations throughout the basin were evaluated by integrating quantities obtained by direct measurement within the flow field. These quantities were then used to deduce appropriate correction factors.

The CSU test facility consisted of a rectangular basin with a horizontal aluminum floor 10 ft wide and 14 ft long with 12 in. vertical walls. Two approach pipe sections were examined: (1) a 1.45 ft diameter smooth circular pipe 20 ft long, and (2) a rectangular pipe 1.25 ft by 1.25 ft by 20 ft long. Both pipe inverts were horizontal and carefully matched to the basin floor so that there was no vertical discontinuity.

Rectangular Section

For the rectangular approach pipe (1.25 ft by 1.25 ft), six discharges varying from 6.75 cfs to 21.3 cfs were examined. The relative depth ratio, y_o/W_o , ranged from 0.61 to 0.94, and the Froude number, $V_o/\sqrt{gy_o}$, varied from 1.44 to 2.35, a normal range of culvert operation. Velocity, pressure, and water surface data were collected at stations 0.0, 2.5, 5.0, and 10.0 ft downstream of the culvert outlet.

The experiments reported by Watts (22) indicate that for small relative tailwater depths approximate values would be sufficient for culvert design:

$$\alpha_1 = 0.85$$

$$\beta_1 = 0.65$$

$$\alpha_2 = \beta_2 = 1.0 .$$

Stevens (17) later established the relationship between tailwater depth and α_1 and β_1 from a series of tests conducted on a 6 in. by 12 in. box culvert. He used Watts' findings that $\alpha_1 = \beta_1 = 1.0$ to show that

$$\alpha_1 = \left(\frac{y_o}{y_c}\right)^2 \left(3 - 2 \frac{y_o}{y_c}\right) ,$$

and

$$\beta_1 = \left(\frac{y_c}{y_0}\right)^2 \left(3 - 2 \frac{y_c}{y_0}\right)$$

when the water surface profile in the barrel is either a M2 or H2 profile.

The term y_c is the critical depth given by the equation

$$y_c = \frac{q^{2/3}}{g^{1/3}}$$

in which q is the flowrate per foot of width.

In the experimental model, the tailwater, d_t , was varied over the range

$$0.1 < \frac{d_t}{y_0} < 1.0 .$$

The results are plotted in Fig. 14. Using the curves in Fig. 13 must be limited to cases in which

$$y_c < H_0$$

and

$$d_t \leq y_0$$

and are applicable for only horizontal and mild sloping culverts.

For critical or steep sloping rectangular culverts, values of $\alpha_1 = \alpha_2 = \beta_2 = 1.0$ can be used for all tailwater depths.

If there is a vertical drop off at the culvert outlet ($d_t/y_0 < 0$), the ratio y_c/y_0 is 1.40 according to Rouse (13). Corresponding values for β_1 and α_1 are

$$\beta_1 = 0.392, \text{ and}$$

$$\alpha_1 = 0.803 .$$

Model studies on scouring rock basins indicate if the rocks were originally placed at the culvert outlet invert level, the ratio y_c/y_o would be the same as that given in Fig. 14.

Circular Section

The energy correction coefficients (α_1 for the pressure term and α_2 for the velocity term) and the momentum correction coefficients (β_1 for the pressure term and β_2 for the velocity term) at the outfall section were measured by both Watts (22) and French (6) for the case where the tailwater depth at the outlet is zero. Theoretically, expressions for α_1 and β_1 are

$$\alpha_1 = \frac{y_c}{y_o} \left\{ 1 - \frac{1}{2g} \left(\alpha_1 \left(\frac{A_c}{A_o} \right)^2 - 1 \right) \frac{(Q/D^{2.5})^2}{\left(\frac{A_c}{D^2} \right)^2 \left(\frac{y_c}{D} \right)} \right\}$$

and

$$\beta_1 = \frac{2 \frac{y_c}{y_o} \frac{A_c}{A_o}}{\frac{y_c}{D} \left(\frac{A_c}{D^2} \right)^2} \left\{ \frac{A_c}{D^2} \frac{P_c}{\gamma D^3} - \frac{1}{g} \left(\frac{Q}{D^{2.5}} \right)^2 \left(\beta_2 \frac{A_c}{A_o} - 1 \right) \right\}.$$

The subscripted variables refer to the critical flow section and P_c is the total pressure force in the direction of flow at the critical section.

It was found that for $Q/D^{2.5} \leq 3.50$ cfs/ft^{5/2}, y_c/y_o was nearly independent of $Q/D^{2.5}$. The relation is plotted in Fig. 15 and the data were taken from experiments by Stevens (17) on a 6-inch diameter pipe model.

Watts' data for α_2 is also shown in Fig. 15 so α_1 can be computed from the equation given previously and from the mean values of

y_c/y_0 taken from Fig. 15. To get good agreement between the calculated α_1 and that measured by Watts and French, it was necessary to let α_2 be at unity. The computed α_1 values are plotted in Fig. 15. Although the theoretical equation has been used beyond its apparent range of application ($Q/D^{2.5} \leq 3.5 \text{ cfs/ft}^{5.2}$), it still agrees fairly well with the measured α_1 . Therefore, assumption can be made that the family of curves are valid for circular pipes in which the water surface profile is either a M2 or H2 backwater profile.

The equation for β_1 does not correspond with the measured data obtained by Watts. The computed β_1 are about one-half the values that were measured. Therefore, it was assumed that the equation would predict the shape of the β_1 curves and the measured data would establish the position of the curves.

Once the pipe is flowing full with all streamlines straight and parallel at the outlet, β_1 can be calculated exactly for all tailwater depths. The β_1 curves have been dashed to these calculated β_1 values which are plotted at $Q/D^{2.5} = 8.0 \text{ cfs/ft}^{5/2}$; β_2 does not vary appreciably and can be assumed equal to 1.02, the mean of seven measurements taken by Watts.

For steep-sloping pipes with high velocity and converging flow (S2 backwater profile) in the barrel, the theory and Fig. 15 show it can be assumed that

$$\alpha_1 = 1.0$$

$$\alpha_2 = 1.03$$

$$\beta_2 = 1.02$$

and β_1 can be estimated depending on the conditions at the outlet.

2.3 Discharge-Brink Depth Relationship

It is convenient to have curves explicitly relating the brink depth, tailwater depth, and the discharge. These curves can be computed from the y_c/y_o versus d_t/y_o curves given in Figs. 14 and 15.

Rectangular Outlets

It can be shown that, for $g = 32.2 \text{ ft/sec}^2$,

$$\frac{y_c}{H_o} = 0.315 \left(\frac{Q}{W_o H_o^{3/2}} \right)^{2/3}$$

Also,

$$\frac{y_o}{H_o} = \frac{y_c}{H_o} / \frac{y_c}{y_o}$$

and

$$\frac{d_t}{H_o} = \frac{d_t}{y_o} \times \frac{y_o}{H_o}$$

Using these three equations and the y_c/y_o versus d_t/y_o relationship given in Fig. 13, the curves shown in Fig. 16 were developed. They are valid for box culvert flow if the water surface profile in the barrel is either a M2 or H2 profile.

The $Q/W_o H_o^{3/2}$ curves shown as dashed lines are estimates. It is assumed that the large box culverts will flow full at $Q/W_o H_o^{3/2} = 8.5 \text{ cfs/ft}^{5/2}$ when $d_t/y_o = 0$. There is a brink depth scale effect between different sizes of culverts which depends on the size and the roughness of the barrel. It is more convenient to discuss the scale effect for circular pipes where more information is known and the scale effect is more pronounced.

Circular Outlets

With circular pipes, the same procedure described previously was employed to derive the brink depth, tailwater depth, and discharge relationships shown in Fig. 17. Again, the curves are valid only if the water surface profile in the barrel is either a M2 or H2 profile.

Those curves for which $Q/D^{2.5} \geq 4.0$ cfs/ft^{5/2} are estimated. The assumption is that, in large pipes, the barrel will flow full at all tailwater depths if $Q/D^{2.5} \geq 6.50$ cfs/ft^{5/2}. For the 6-inch diameter CSU model, the pipe would flow full at the outlet if $Q/D^{2.5} \geq 5.3$ cfs/ft^{5/2}. Smith (16) has documented that a zone of fluid exists at the crown of the pipe in which the pressure is below atmospheric. If this zone is near the pipe outlet it will affect the brink depth. The brink depth is greater than that anticipated from theories. From the data presented by Smith (16) and Stevens (17) it can be estimated that, for $d_t/D = 0$, various sized smooth pipes will flow full according to the relationship:

<u>Pipe Diameter in inches</u>	<u>$Q/D^{2.5}$ cfs/ft^{5/2}</u>
4	4.7
6	5.3
8	5.9
12	6.1
36	6.5

The conclusion is that all pipes larger than 36 inches will flow full when $Q/D^{2.5} \geq 6.5$ cfs/ft^{5/2}.

2.4 Flow Conditions at the Culvert Outlet

For rock riprapped basins, it can be assumed that the tailwater level will be at the normal stream water surface elevation at the culvert outlet. In the CSU models, even though the flow in the outlet jet was rapidly varied supercritical flow, enough water moved upstream along and through the rock boundaries of the basin to maintain equal tailwater depths at the outlet and at the end of the basin. This is not the case for the concrete basins studied by Watts (22) or Rajaratnam and Subramanya (12).

For concrete basins, the tailwater depth at the pipe outlet depends on the geometry of the basin and on the flow properties at the outlet and throughout the basin. For $W_2/W_0 = 1.00$, there is no tailwater depth at the outlet per se. When W_2/W_0 approaches infinity, the tailwater at the outlet will be the normal channel tailwater.

Until the relationships among the discharge, the relative basin width W_2/W_0 or W_2/D , and the tailwater depth at the outlet and at the downstream end of the concrete basin are established, it will be necessary to assume the tailwater depth at the outlet is zero. More discussion related to this problem is given in Appendix C.

Chapter III

RIGID OUTLET BASINS

This chapter presents design criteria for energy dissipating basins at culvert outfalls. Design procedures based on continuity of flow and the balance of impulse and momentum between the inlet and outlet of the basin are presented for three types of basins. These basins were re-searched and developed at Colorado State University as potential standard, economical, rigid basin designs. The first basin has a smooth floor and flared vertical walls (smooth-floor flared basin); the second basin is a rectangular basin, with smooth floor and vertical walls (smooth-floor rectangular basin); the third basin is a rectangular basin with smooth, vertical walls and an artificially roughened floor (rough-floor basin).

Smooth concrete is an inefficient energy dissipator but it is very scour resistant and can be formed to provide passage of stock. The smooth-floor flared basin may be constructed with sloping walls resulting in a trapezoidal basin. In this case the height of the sloping walls should be increased to provide more freeboard since the flowing water and surface waves tend to ride up an inclined wall.

Another alternative is to build the smooth-floor flared basin of units of wire enclosed rock. This gives a stable basin using smaller rock than would otherwise be required. However, in gravel or rock bed streams the gravel and rock transported through the basin is very abrasive to the wire and will cause the structure to fail after a short time.

A brief discussion of the hydraulics of the basins and a step method of analysis for each of the basin types are presented.

The experimental development of the design criteria and design aids that are a necessary part of the analysis are discussed by Watts (22) in greater detail.

3.1 Hydraulic Design of a Smooth-floor Flared Basin

This basin, with flared vertical walls and a smooth floor, is illustrated in Fig. 18. The hydraulic jump induced in the basin dissipates energy and reduces the culvert exit velocity to a subcritical level. However, care must be taken to avoid degradation of the channel downstream of the basin which could cause loss of control and possible failure of the basin.

For given geometrical configurations of culvert barrel and basin, and a given design discharge Q , the momentum flux and resultant pressure forces at the inlet of the basin must balance the resultant pressure force and momentum flux at Station x , slightly downstream of the hydraulic jump. For the case of a rectangular approach section with a horizontal floor (Fig. 18b) this balance can be expressed:

$$\beta_1 \gamma \frac{y_o^2}{2} \frac{W_o}{2} + \beta_2 \rho V_o \frac{Q}{2} = \rho \frac{Q}{2} V_x + \frac{W_x}{2} \gamma \frac{y_x^2}{2}$$

in which

β_1 = the dimensionless correction factor for nonuniform pressure distribution at the outlet,

γ = the specific weight of the liquid,

y_o = the depth of flow at the outlet, or brink depth

W_o = width of the culvert barrel at the outfall,

β_2 = the dimensionless correction coefficient for nonuniform velocity distribution at the plane of the culvert outlet,

V_o = the exit velocity, $Q/y_o W_o$,

Q = design discharge,

ρ = mass density, γ/g

V_x = the average velocity at Station x , $Q/y_x W_x$,

W_x = width of the basin at Station x ,

y_x = mean depth of flow at Station x , or the tailwater depth.

The design discharge, Q , is known, y_o can be computed from conventional culvert hydraulics which are illustrated in the examples, W_o is known, $V_o = (Q/W_o y_o)$, and β_1 is readily obtained from Fig. 14 or Fig. 15; β_2 is approximately 1.00 for rectangular culverts and 1.02 for circular culverts. Therefore, all terms on the left side of the equation can be evaluated.

Examining the right hand side of the equation, y_x must be known (a function of Q and the downstream channel characteristics); W_x is a function of x ; V_x is a function of Q , W_x and y_x , and is known. There is only one value of x that will uniquely determine W_x and V_x in such a way that the equation will balance. This requires a trial and error solution. An example of a Smooth-floor Flared Basin (Fig. 18) with a rectangular culvert can be found in Appendix A, page 64.

Smooth-floor Flared Basin, Circular Culvert

Since Blaisdell's relation, $u = 3F_o$, is valid for circular pipes as well as rectangular sections the only changes that are required in the design procedure are the substitution of D for W_o , the use of Fig. 15 to evaluate β_1 and β_2 , the use of Figs. 9 to 12 to describe the dimensionless water surface contours, and the modification of the momentum at section 0 to

$$M_o = \beta_1 \gamma \frac{y_o}{2} A_o + \beta_2 \rho Q V_o ,$$

in which A_o is the wetted area and y_o is the centerline depth at the outfall.

3.2 Hydraulic Design of a Smooth-floor Rectangular Basin

This basin differs from the smooth-floor flared type in that it is rectangular in plan. Again, the design is based on vertical walls and the application of the momentum equation to locate the position of the hydraulic jump. If a trapezoidal cross section is considered rise up must be compensated for as with the smooth-floor flared basin.

The smooth-floor rectangular basin is the least tractable of the three types and should only be used with tailwater control. The simplest way to insure adequate tailwater is to slope the basin into the channel.

The R-Jump Basin

For high Froude number flows at the outlet, there is another possible alternate design, which is discussed in Appendix D; however, it cannot be used in this example.

3.3 Rough-floor Rectangular Basin

The rough-floor basin is a rectangular basin with vertical walls with roughness elements attached to the floor. The elements are of a selected size and are placed in an appropriate pattern so as to break up the high speed expanding jet downstream of the culvert outlet. They must be designed structurally and attached to the floor of the basin so that they adequately withstand the forces including the abrasion of sediment that they will be subjected to.

The method of analysis proposed for artificially roughened energy basins requires that the coefficient of drag, associated with a particular grouping and size of roughness elements in a basin of specific size, be known. Several circumstances complicate the problem. In the upper portion of the basin over the first few rows of elements, the flow is very irregular and turbulent. The flow, serrated and thrown into the air by the elements, is characterized by a high degree of air entrainment. In many cases, a large separation bubble or vacant gap, open to the atmosphere, forms in the lee of the element. The flow field is not continuous, therefore, no hope for a theoretical solution exists.

Watts (22) conducted an experimental study for the purpose of obtaining drag coefficients for various grouping of roughness elements of known dimensions installed in basins of given geometry.

Design Procedure

The design procedure is based on the impulse-momentum principle. With reference to Fig. 26, which shows the basin, the momentum equation written in the direction of flow between Station 0 and Station B is

$$\beta_1 \gamma \frac{y_0^2}{2} W_0 + \beta_2 \rho V_0 Q = F_T + F_R + \beta_3 \rho V_B Q + \beta_4 \gamma \frac{y_B^2}{2} W_B ,$$

in which F_T is the shear force exerted by the floor on the flow in the area upstream of the roughness elements and downstream of the outlet. Also, F_R is the drag force exerted on the flow by the combined group of roughness elements and is defined as:

$$F_R = C_D A N \rho \frac{V_a^2}{2}$$

in which

C_D = dimensionless drag coefficient,

A = frontal area of a roughness element,

N = number of elements, and

V_a = the approach velocity at the first row of roughness elements, defined as the value V , two pipe diameters downstream of the outlet. Knowing Q/A at the outlet, V_a is readily obtained from Figs. 3 through 12. The shear force F_T is a small quantity and henceforth it is included in the F_R term rather than being considered separately. Other variables in the equation have been previously defined.

Making use of the continuity equation $Q = V_B W_B Y_B$, where W_B and Y_B are the width and average depth of flow at section B, and V_B is the average velocity passing through the section,

$$Y_B = \frac{Q}{V_B W_B}$$

The expressions for the drag force and flow continuity are substituted into the momentum equation, to give:

$$\beta_1 \gamma \frac{y_o^2}{2} W_o + \beta_2 \rho V_o Q = C_D AN \rho \frac{V_a^2}{2} + \beta_3 \rho Q V_B + \beta_4 \frac{\gamma Q^2}{2 V_B^2 W_B}$$

This is the design equation for the rough-flow basin. For a given discharge, approach pipe, basin geometry, and a known C_D , an estimate of V_B , the exit velocity from the basin, can be readily obtained.

The drag coefficient, C_D , is closely related to the relative depth parameter, y/a . In the energy dissipating basin where the water is diverted upward by the element, it is obvious that, up to a limiting point at least, the deeper the flow over the element, the larger the quantity of water disturbed by the element and, consequently, the larger the apparent coefficient of drag.

Watts chose y as the scaling length, and the depth of flow two pipe diameters downstream of the outlet. Station 2D is the approximate location of the first row of elements. The depth should be measured in this vicinity to avoid the disturbance which they cause on the water surface. For design purposes, this depth is readily obtained in Figs. 3 through 12. Since the width of the expanding jet is not controlled by the walls at Station 2D, the depth of flow is significant for a basin of any width when considering only the first two rows of elements. This is not the case for the remaining rows of elements, i.e., the wider the basin, the shallower the flow for a given discharge. For this reason, an additional correlating factor W_2/W_0 , the basin width divided by the conduit width, is necessary.

The longitudinal spacing of the elements J has a significant effect but the lateral spacing of the element M is not considered critical. The important point is that the elements in each row should occupy half the width of the channel, and that the elements should be staggered in successive rows. This insures that there will be no smooth longitudinal corridors through the basin. So that the elements will serrate the flow and not act as a long sill, it is recommended that the ratio M/a should be in the range of 2 to 8.

Watts' experimental program included tests on 12 basin and element arrangements. Each basin was subjected to two discharges. The lower discharge was approximately the design discharge (based on the Wyoming Highway Department specifications) for the approach pipe. The higher discharge was approximately 50 percent larger.

In the model study, two heights of elements were used, $a = 1 \frac{1}{4}$ in. and $a = 2 \frac{1}{2}$ in., for each discharge. A variation of relative

depth (y/a) from 1.1 to 2.7 resulted from the combination of two discharges and two element heights.

One pattern of longitudinal and lateral spacing was used for all runs. With two element heights, a twofold variation of J/a , 6.0 and 12.0, was obtained.

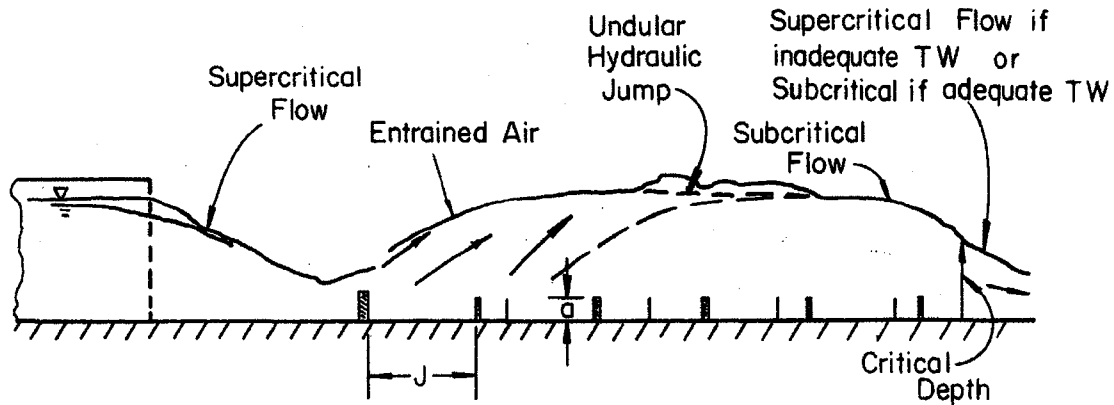
For the 1.25 ft square approach pipe, two basin widths, $W_2 = 5$ ft and $W_2 = 10$ ft, were tested. One width of basin, $W_2 = 10$ ft, was used with the 1.45 ft diameter circular approach pipe.

In addition to the runs described above, six special runs were made using the circular approach pipe and the 10-foot wide basin with two patterns of 4 in. by 1 in. elements. Significant differences between these basins and those used for the primary runs were the size and spacing of the elements. The 4-inch elements were spaced on 18-inch centers laterally; thus, large gaps existed between the elements. As expected, high speed cores of water were observed and measured downstream of the field of elements. The coefficient of drag deduced for the small, widely spaced elements was somewhat larger than comparable coefficients of drag for the elements 9 in. long. However, because of the probability of high speed cores of water occurring downstream of the basin, elements spaced laterally at more than twice their length are not recommended.

There is a uniform distribution of the flow downstream of the elements. If the tailwater is not sufficient, the flow returns to supercritical. This should be avoided in design.

The drag coefficients for the various basins and element arrangement are given in Figs 27 through 35.

Some features of the rough-floor basin are illustrated in the following sketch.



SKETCH. Centerline section, rough-floor basin

Basins with two rows of elements are not recommended. Distribution of the flow was not uniform downstream of the elements, particularly for the basins with relative width ratios of $W_2/W_0 = 7$ to 8.

Two rows of elements can be used for triggering a hydraulic jump. If tailwater conditions are known, the design equation is directly applicable. All terms would be known except the drag term, $C_D AN \frac{\rho V_0^2}{2}$. Selecting appropriate values of C_D from the design curves for two rows of elements, A , which are the required frontal area of the roughness element, is readily determined by trial and error.

The basins with a relative width ratio of four with four or six rows of elements performed in a more than satisfactory manner. The

rebouncing flow from the walls is directed back across the elements resulting in a uniform distribution of flow downstream of the elements.

For the wider basins, the flow was diverted to the sides where it tended to concentrate. There was little flow over the central elements, thus they were not effective.

The basins shown in Figs. 36 and 37, where the elements occupy less than one fourth of the basin width, are not recommended. Even with four rows of elements, high speed cores of water were noticeable downstream of the group of elements.

The coefficients of drag deduced from these studies were compared with values deduced from data published by the U.S. Bureau of Reclamation. In Engineering Monograph No. 25 (19), section 3, Table 4, data from 14 model tests of the Bureau of Reclamation type III basin are presented. In this type of basin, one row of elements is used to trigger the hydraulic jump. Using the data from these studies, it was possible, with a few assumptions, to obtain good estimates of C_D . The magnitude of C_D ranged from 0.68 to 0.92 for 13 of the 14 basins. The data from the other basin yielded a value of $C_D = 1.60$.

The CSU runs that were somewhat similar to these experiments had two rows of elements and a W_2/W_0 ratio of 4. Depending on the relative depth of flow, the values of C_D ranged from 0.45 to 0.72. The CSU values, as expected, were slightly lower because the front row elements shielded the second row.

The use of drag coefficients is not restricted to basins downstream of the outfall section. Box culverts could be designed with flared walls beginning under the fill slope and the elements installed within the flared portion, the last rows being on the apron between the wing-walls,

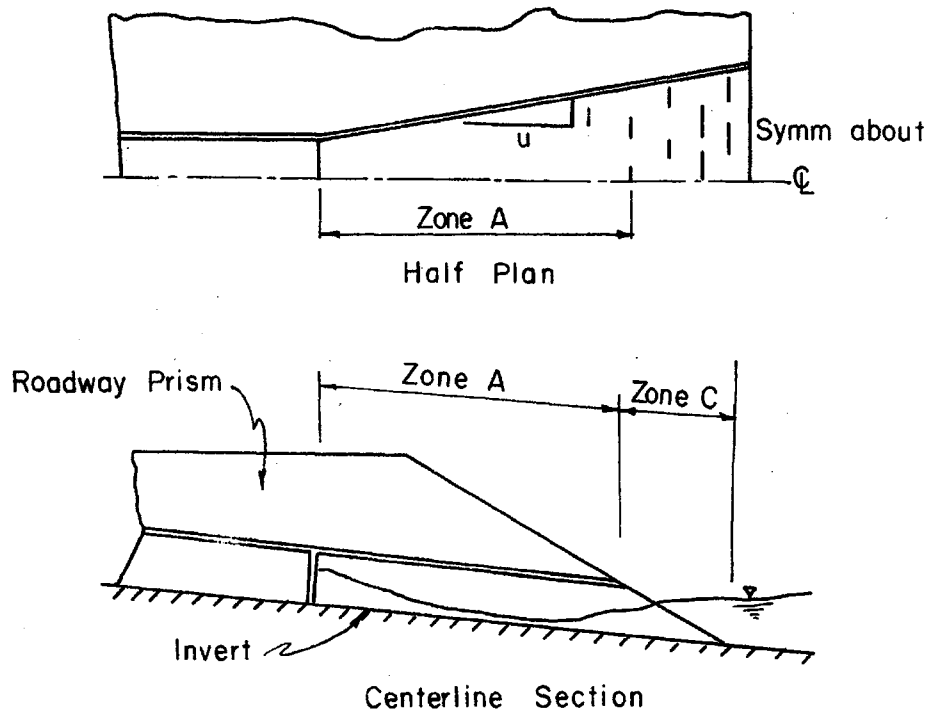
as shown below. This would appear to be more economical than the conventional culvert with a basin downstream. From an aesthetic point of view, the basin would be hidden from automobile drivers and would pose no problem to right-of-way maintenance personnel (mowing, etc.).

The use of the design graphs and suggested design procedures for the rough-floor basin are presented in an example found in Appendix A on page 79.

3.4 The Combined Basin

An alternate basin that would be equally effective and probably more economical than the rough-floor basin is shown below.

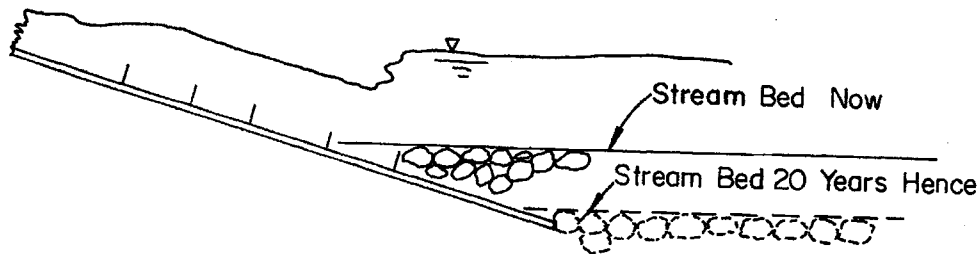
Zone A of the basin would be designed by the procedure described for smooth-floor flared basins. The depth and velocity of the flow at the



upstream row of elements can be estimated from the smooth-floor flared basin computations. Given the depth of flow and velocity at the first row of elements, the zone C portion of the basin is then designed as a rough-floor basin.

A particularly good feature of this arrangement is positive tailwater control. The invert elevation at the end of the basin can be set low enough to insure adequate tailwater.

If the channel downstream is degrading, the floor can be extended as far as necessary to accommodate future degradation.



SKETCH. Partial centerline section

The collection of silt around the elements could be a problem. However, deposition in the upper portion of the basin during periods of low flow should be rapidly eroded and washed downstream by the rigorous action of the water. High tailwater basins are discussed in Chapter V.

Chapter IV

ROCK RIPRAPPED BASINS

4.1 Introduction

As a part of the CSU study for the Wyoming Highway Commission circular and rectangular culvert outlet basins armored with or formed of rock riprap were studied. The aim was to supply further aids for the design of rock-riprapped basins.

An experimental program was implemented at the facilities of the CSU Engineering Research Center in 1967. Results for circular culverts were previously reported by Opie (11) and Stevens (17).

Initially, the project included tests conducted with four different culvert pipe sizes: 6-inch, 12-inch, 18-inch, and 36-inch with discharges ranging from 0.1 cfs in the 6-inch line to 100 cfs in the 36-inch. Rock mixtures consisting of a wide variation of angular and rounded materials were studied with values of d_m , the representative particle size, ranging from 0.049 ft to 0.613 ft. Combinations of rock and pipe sizes are detailed in Table 1. Only two pipe slopes were considered, one horizontal and one sloped at 3.75 percent. The majority of the study involved collecting data from the horizontal pipe. A methodology of design for basins with horizontal, intermediate and steep slopes was developed from these data, see paragraph 4.2.

In addition to the plain circular pipe culvert outlet, different types of metal end sections were tested to determine the advantages of allowing the flow from the pipe to diverge before it entered the rock basin. A standard metal end section, now available commercially from metal culvert manufacturers, and a special wide-angle expansion section were fabricated and tested.

TABLE 1. Combinations of Rock and Culvert Sizes Studied and Values of d_m/D or d_m/H_o

Circular Culverts

Rock Size d_m , ft	Pipe Size, D, ft			
	(6 in.)** 0.518 ft	(12 in.) 1.015 ft	(18 in.) 1.45 ft	(36 in.) 3.00 ft
.049	.0945*	----	----	----
.089	----	.0872	----	----
.106	.205	----	----	----
.137	.264	----	----	----
.207	.400	----	----	----
.225	----	----	----	.075
.287	----	.283	.198	----
.356	----	.351	----	----
.400	----	----	----	.133
.613	----	----	.422	.204

Note: *The numbers in the Table are d_m/D .

**Diameters in parentheses are nominal sizes.

Rectangular Culverts

Rock Size d_m , ft	Box Size, $H_o \times W_o$, ft x ft		
	0.488 x 1.0	0.488 x 1.5	0.488 x 2.0
.047	.096*	.096	.096
.024	.049	----	----
.0475	.0975	----	----

Note: *The numbers in the Table are d_m/H_o .

Besides the variations in culvert size, rock size, pipe slope, and pipe outlet section, various widths of rock basin were studied. The rock bed of the basin was constructed at the slope of the pipe, tangent to the pipe invert with a horizontal slope in the transverse direction. The sidewalls of the flume were vertical or had side slopes formed of the rock used in the bed.

A few tests were conducted to see if a systematic variation of discharge could cause more scour in the basin than a steady flow equal to the peak flow of the hydrograph.

Just three sizes of rectangular culverts were studied; only the width was varied while the height was held constant at 0.5 ft. Tests were limited to two rock sizes (Table 1) and the culvert slope to 0 percent and 3.75 percent. Metal end sections on rectangular sections were not considered.

4.2 Parameters Used in the Design of Riprapped Basins

Mild Sloping Culverts

Data for horizontal culverts should be applicable to all culverts with zero and mild slopes because the flow conditions at the outlet are not greatly changed by variations in slopes that do not appreciably accelerate the flow in the last 2 or 3 pipe diameters of the culvert.

Experimental evidence indicates that the scour phenomena can be scaled according to Froude criteria, at least over the range of rock sizes considered in this program (Table 1). For culverts discharging onto rock basins with a bed constructed to the culvert invert level, the most important parameters are:

1. $Q/D^{2.5}$ or $Q/W_o H_o^{3/2}$, a form of the Froude number for culvert flow;
2. y_o/D or y_o/H_o , the relative depth of flow at the culvert outlet;
3. d_t/D or d_t/H_o , the degree of submergence at the culvert outlet;
4. d_m/D or d_m/H_o , the size of the riprap material in terms of the culvert size, and
5. d_s/D or d_s/H_o , the depth of scour in terms of the culvert size.

The effective (grain-size) diameter of a rock mixture, d_m , was computed from

$$d_m = \left[\frac{\sum_{i=1}^{10} d_i^3}{10} \right]^{1/3}$$

in which

$$\begin{aligned} d_i(i=1) &= \frac{d_o + d_{10}}{2} \\ d_i(i=2) &= \frac{d_{10} + d_{20}}{2} \\ &\vdots \\ d_i(i=10) &= \frac{d_{90} + d_{100}}{2} \end{aligned}$$

The terms $d_o, d_{10} \dots d_{100}$ are the sieve diameters of the rock for which 0 percent, 10 percent, ... 100 percent, of the material (by weight) is finer.

This method of obtaining an effective grain size is based on knowledge that, of two rock mixtures having the same d_{50} , the one with the wider range of rock sizes will scour or degrade a lesser amount. In

computing the effective size in the manner given above, one weights the coarser material in the mix to a much greater extent than the finer material. Thus d_m is always greater than d_{50} . Moreover, comparing two materials having the same median size (d_{50}), the well graded material will always have larger d_m than the more uniform material.

The parameter d_m is used in reporting the data and in the dimensionless plots. The use of d_m did consolidate the data from a wide range of tests conducted using different rock mixtures into a reasonably compact and well correlated picture.

The evaluation of d_m implies the use of sieves to determine the size distribution of the riprap material. From this material d_i can be defined so that d_m can be computed. Because the sieving of riprap is time consuming and because it requires large samples and several sieves a simpler technique is desirable. This can be accomplished by using a light weight metal frame laced with twine to form a 0.1 ft grid. The grid can be placed over the material to be analyzed and a useful size distribution curve can be developed by sizing the representative sample of riprap through the grid. As a supplemental or alternate procedure the riprap sample can be photographed through the grid and a size distribution curve can be developed.

A special study should be conducted to develop improved simplified techniques for sizing riprap. Until this is done it is recommended that a small factor of safety of about 10 percent be added to the value of d_m estimated by the grid method.

The density of the rock material is an important factor but, in the CSU study, all materials had about the same specific gravity, 2.65 to 2.75.

When riprap with a larger or smaller specific gravity is used, compensate by multiplying the computed rock diameter by the ratio $(\gamma_1/\gamma_2)^{5/6}$ where γ_1 is about 2.70 and γ_2 is the specific weight of the available riprap. This relation is based on particle weight and fluid drag considerations.

The important dimensions of riprapped basins with scour are shown in Fig. 40. They are

W_s , the maximum width of the scour hole,

L_s , the length of the scour hole, and

L , the minimum required length of the basin.

Within the basin, there is an area of scour near the pipe outlet. The material moved from the scour hole is deposited in the region just downstream of the hole. This mound of material is an important feature of the local scour phenomena, for if it is removed the flow is capable of scouring into the bed to a still greater depth. Thus, it is felt that the required length of rock basin must include the deposition area. The quantity L is the dimension from the outlet to the most remote extent of the deposition of scoured material.

The width and length of the scour hole and the length of the basin are best described in terms of the effective grain size, d_m . The dimensionless parameters are then W_s/d_m , L_s/d_m , and L/d_m .

It would seem that if all other variables are constant, the effect of bed width, W_b , on scour can be accounted for in the tailwater parameter. A relative width, W_b/D , of 1 is the minimum that can be considered, and only if the rock will not scour. With scour, the bed must be wide enough so that the side slopes do not slip into the scour hole.

For basins that do not scour, the dimensions of the riprapped area are determined in a different manner. The function of the basin is to reduce the flow velocity at the culvert outlet to a level compatible with downstream channel conditions. This can be achieved by using knowledge of how the jet expands when it does not scour the bed. The only additional parameters required for a nonscouring basin (d_s/D or $d_s/H_o = 0$) are

- θ , the angle at which the jet expands in a lateral direction;
- W_b , the width of the basin where it can be terminated, and
- L , the length of the basin measured from the culvert outlet to the point where the basin is terminated.

In dimensionless form, these parameters become θ , W_b/D or W_b/H_o , and L/D or L/H_o . For situations not covered in the test program, interpolation is necessary. The interpolation procedure is illustrated in the subsequent section on design.

Steep Sloping Pipes

With regard to scour, steep sloping pipes have one characteristic greatly different from mildly sloping pipes; at the outlet the flow is parallel with the walls and floor of the conduit. With mild sloping pipes there is considerable curvature of the streamlines at the outlet and the velocity is more directed into the rock bed.

If the culvert flows full the streamlines are essentially straight and parallel at the outlet. Then the slope of the culvert has little or no affect on the depth of scour. Only the velocity, the tailwater depth, and the culvert size are important factors.

The method employed in this report is to convert the outfall flow conditions of the steep sloping culvert into equivalent conditions for a mildly sloping culvert flowing full. Examples are given in Appendix E.

The CSU scour data gathered on steep sloping and mildly sloping models flowing full agree well with tests conducted by Valentin (21) provided, in each case, that $d_s/d_m > 10$. Valentin's work will be used to cover situations not studied in the CSU project.

4.3 Standard Riprapped Basins

Three types of riprapped basins are presented as being most practical for field structures. After outlining the shape of each, data will be presented that will allow the designer to compute the dimensions of the basins. The most economic basin depends on the geometry and the hydraulics of the basin and the availability and characteristics of the available riprap. Larger rock will often require quarry operations. In general the non-scouring basin is most economical with regard to quantity, but if it requires a rock size that must be quarried it may not be the most economical with regard to cost.

Non-Scouring Basin

The non-scouring basin must be designed so that the high velocity jet at the culvert outlet can expand laterally until the flow velocity is reduced sufficiently to avoid instability in the natural channel. The basin shown in Fig. 41 is the recommended shape for the transition from the culvert to the natural channel. The length L depends on how rapidly the jet expands over the rock apron. The angle θ is chosen so that the side slopes match the boundary of the jet.

The basin has been divided into five sections: (1) the apron, (2) the end slope (3) the embankment slope, (4) the under slope, and (5) the side slopes. Rock of the same size is to be used for all components. Although difficult to justify, a more detailed theoretical analysis may show that smaller riprap could be used on the side and fill slopes.

1. Apron - If the rock size is chosen so that the apron will not scour at design flow, it should not scour for lesser flow. The apron should be placed level with the culvert invert at the outlet and should be sloped downstream at the same slope as the culvert barrel. The minimum recommended thickness of the apron, designated A, is either $2d_m$ or d_{100} whichever is greater. Let

$$f = d_{100}/d_m$$

and

$$h = A/d_m ,$$

then, the minimum h is the larger of f or 2.

The volume of rock in the apron is

$$\frac{1}{2} h d_m (W_o + W_b) L .$$

2. End Slope - The end slope terminates the apron and provides a hedge against any local scour at the end of the basin. If degradation is anticipated in the downstream channel, the end slope can be carried to a depth E to give some protection to the structure. The minimum recommended E is

$$E = A = h d_m ,$$

and the thickness of the end slope should be

$$B = f d_m = d_{100} .$$

The volume of rock in the end slope is

$$(f d_m) (E \sqrt{z_3^2 + 1}) (W_b)$$

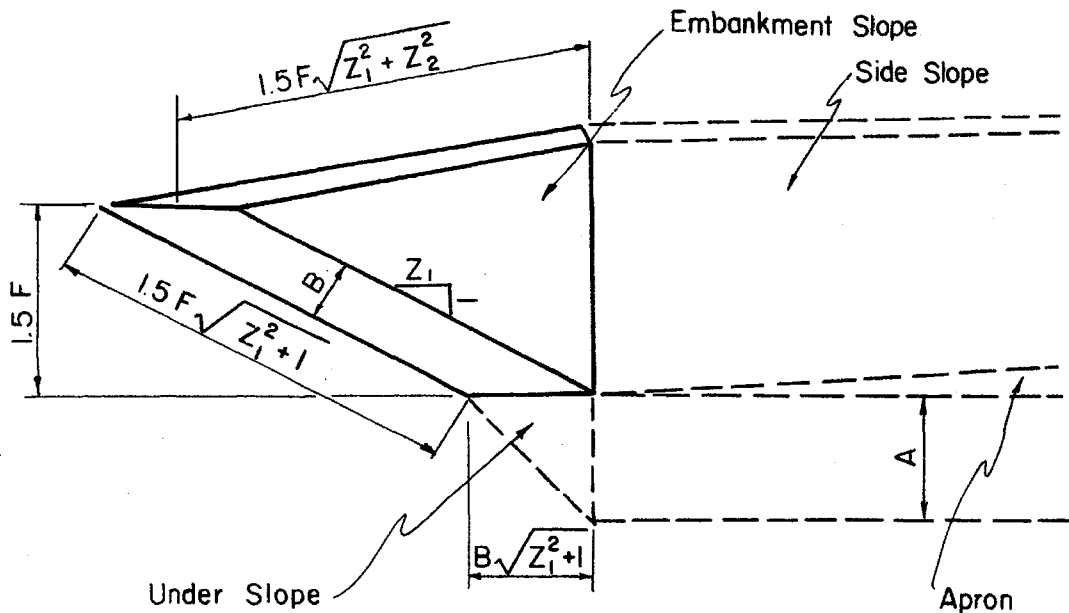
in which z_3 is the slope of the end slope. A value of 2:1 ($z_3 = 2$) or 1.5:1 ($z_3 = 1.5$) is suggested.

3. Embankment Slope - Riprap is required along the rock embankment in the immediate vicinity of the culvert outfall to protect against any splash or spray and to control the action of rollers that may form in the corners of the structure. It is recommended that F be made (in the sketch below) greater than y_0 or d_t , with z_1 the embankment slope and z_2 the side slope. Then the volume of riprap in the embankment slope is approximately

$$2[fd_m (1.5 F \sqrt{z_1^2 + 1}) (\frac{1.5}{2} F \sqrt{z_1^2 + z_2^2})]$$

or

$$1.5 fd_m F \sqrt{z_1^2 + 1} \sqrt{z_1^2 + z_2^2} .$$



4. Under Slope - The under slope joins together the embankment slope and the apron and is important because it prevents movement of materials out from under the culvert. The volume is

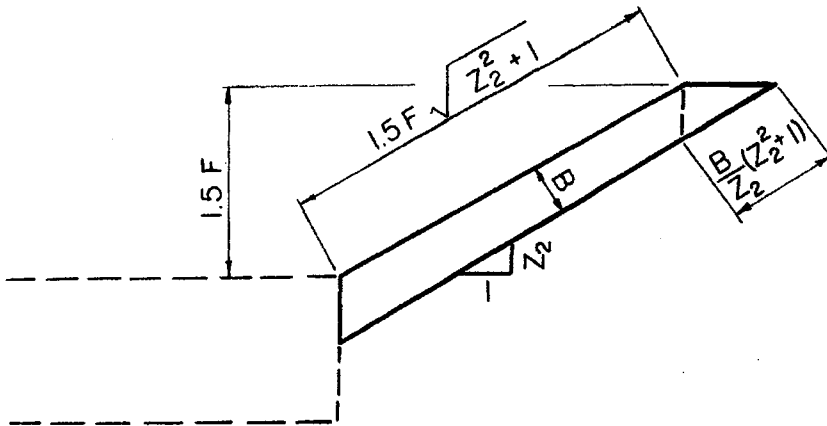
$$\frac{1}{2} (B \sqrt{z_1^2 + 1}) (A) (W_o)$$

or

$$\frac{1}{2} (fd_m \sqrt{z_1^2 + 1}) (hd_m) (W_o)$$

The culvert, as it joins the basin, may be either projecting or mitered. Also, a cutoff wall may be used in lieu of the under slope. It is suggested that the cutoff wall should extend downward a distance $2A$ below the apron.

5. Side Slopes - The side slopes extend from the culvert outlet to the termination point of the end slope. If the channel is not confined, this volume of riprap should be placed on the horizontal, in addition to the apron riprap. A typical cross section through the side slope is shown in the following sketch.



The volume required for side slopes at $z_2:1$ is approximately

$$2[(L \sec \theta + E \sqrt{z_3^2 + 1}) \frac{1}{2} (3F \sqrt{z_2^2 + 1} + \frac{B}{z_2} (z_2^2 + 1))(B)],$$

or

$$fd_m (L \sec \theta + E \sqrt{z_3^2 + 1}) (3F \sqrt{z_2^2 + 1} + fd_m \frac{(z_2^2 + 1)}{z_2}) .$$

The dimensions of a standard non-scouring basin for a circular pipe culvert are the same as the above except that W_o and H_o are replaced by D ; the pipe diameter and the volume would vary slightly due to the effect of change of culvert on embankment slope.

Hybrid Basin

The hybrid basin covers conditions where a basin scours slightly but not enough to give the efficient type of energy dissipation which results from basins with larger scour holes. Then, if

$$0 < \frac{d_s}{d_m} < 2.0 ,$$

an additional volume of rock is added to the apron and under the slope of the non-scouring basin (see Fig. 42) so that the jet will not penetrate the apron. The dimensions, W_b and L , of the hybrid basin are determined by computing $(W_s + 2H_o)$, L_s , and L for a scouring basin with $d_s/d_m = 2.0$ and by computing W_b and L for a non-scouring basin with $d_s/d_m = 0$. Then compute W_b and L for the hybrid basin and develop plots of W_b versus d_m and L versus d_m . This will be illustrated and applied in the examples in Appendix A.

The volume of rock in the apron is now

$$\frac{1}{2} L [(W_b + W_o) h d_m + \frac{1}{4} (W_b + 3 W_o) d_s]$$

and the volume in the under slope is increased to

$$\frac{1}{2} f d_m \sqrt{z_1^2 + 1} (d_s + h d_m) (W_o) .$$

Scoured Basin

It is permissible to allow a riprapped basin to scour if the basin is sized correctly. Flow energy in the jet plunging into the scour hole is rapidly dissipated in the boil and roller that forms in the hole. It is more convenient to place the riprap apron level with the culvert outlet and on the same slope as the barrel than it is to form the scour hole and mound (Fig. 43). The forming can be done by the water.

Generally, the volume of rock required for a scoured basin is more than for the hybrid and non-scouring basins. This basin may be used whenever the larger rock required for a non-scouring basin or hybrid basin is not available or whenever this basin is most economical considering the cost of obtaining large rock, hauling rock long distances, volume requirements, etc.

The design of the embankment slope, side slopes, end slope, and under slope is the same as for the previous two basins. The apron is now rectangular in plan and contains the major portion of the rock used in the structure. Volumes for the scoured basin are as follows.

1. Apron -

$$(B)(L)(W_s + 2C) + (d_s + A-B)(L_s)(W_s + 2C)$$

or

$$f d_m (L)(W_s + 2H_o) + [d_s + (h-f)d_m](L_s)(W_s + 2H_o) .$$

The recommended value for C is H_o .

2. End slope -

$$f d_m (E \sqrt{z_3^2 + 1}) (W_s + 2H_o);$$

3. Embankment slope -

$$(B)(W_s + 2C - W_o + 1.5 F \sqrt{z_1^2 + 1}) (1.5 F \sqrt{z_1^2 + 1})$$

or

$$f d_m (W_s + 2H_o - W_o + 1.5 F \sqrt{z_1^2 + 1}) (1.5 F \sqrt{z_1^2 + 1});$$

4. Under slope -

$$\frac{1}{2} B \sqrt{z_1^2 + 1} (W_s + 2C) (d_s + A)$$

or

$$\frac{1}{2} f d_m \sqrt{z_1^2 + 1} (W_s + 2H_o) (d_s + h d_m) ; \text{ and}$$

5. Side slopes -

$$2B \left(\frac{1.5}{2} F \sqrt{z_2^2 + 1} + L + E \sqrt{z_3^2 + 1} \right) \left(\frac{1}{2} \sqrt{z_2^2 + 1} \right) \left(3F + \frac{B}{z_2} \sqrt{z_2^2 + 1} \right)$$

or

$$f d_m \left[\sqrt{z_2^2 + 1} \left(3F + f d_m \frac{\sqrt{z_2^2 + 1}}{z_2} \right) \left(\frac{1.5}{2} F \sqrt{z_2^2 + 1} + L + E \sqrt{z_3^2 + 1} \right) \right]$$

For the scoured basin, the length of the basin is not governed by the allowable channel velocity downstream, but by the need to provide a landing area for that rock moved from the scour hole. The mound is an integral part of the structure and if it is somehow removed the scour hole would deepen and penetrate the apron resulting in partial failure or failure of the basin.

For circular barrels, the variables W_0 and H_0 in the above equations would be replaced by the pipe diameter D .

Filter Requirements

All side slopes about the outlet basin that are riprapped should be provided with suitable filters to prevent the movement of embankment materials through the riprap. That portion of the basin on the upstream side of the scour hole behind the embankment and under slope should always be provided with a filter. However, the rest of the bed may not require a filter. Fine material in the riprap tends to work down through the voids to form a filter. Therefore, a filter is not recommended for the bed when the riprap is well graded and the natural material is cohesive.

A comprehensive discussion of the subjects of riprap gradation and filter design is beyond the scope of this report. Serious consideration should be given to these subjects, however, in the design process. The U.S. Army Corps of Engineers (18) has been considering this aspect. The Corps has had considerable success using a filter cloth called filter x, which is manufactured by Corthage Mills, in place of the standard filter. This cloth is tough, easy to place, effective and reasonably inexpensive. The cloth may be placed between the natural material and the riprap whenever a filter is needed. The cloth does tend to clog with fine sediments, which reduce the percolation rate of water through the filter. But a cloth with a range of sizes of openings is presently being manufactured which will further improve the usefulness and versatility of the cloth filter. This material may be used in place of sand-gravel type filters whenever it can be economically justified.

Whether the function of the coarse material (riprap or filter) is to drain an embankment or to resist erosion, the same filter requirements

apply. The danger is that small particles may move upward through the large voids between coarse aggregates. In the case of riprap, such migration of small particles can result in the undermining of the riprap and subsequent failure.

The use of uniform graded riprap should be avoided where possible, especially when the natural bed is composed of material other than gravel. The best design of riprap gradation allows for a well graded transition from the largest stone to the particle size representative of the natural bed material.

Authoritative discussions of riprap gradation and filter design are given by Sherard, et al. (15) and by the Bureau of Reclamation (20).

4.4 Metal End Section for Circular Pipes

The metal end section, with dimensions shown in Fig. 44, can be effective in reducing the depth of scour only in certain restrictive cases:

1. $Q/D^{2.5} \leq 3.5 \text{ cfs/ft}^{5/2}$. For flow with $Q/D^{2.5}$ greater than $5.0 \text{ cfs/ft}^{5/2}$, the end section length (1.75D) is not sufficient and the flow plunges toward the bed at the end of the metal end section and the scour is nearly the same as if the end section were removed. Under some flow conditions, which have not been fully described, standing waves, as illustrated in Fig. 45, form and persist for long distances downstream. Therefore, it is recommended that, if a metal end section is used, angles as shown in Fig. 44 be employed. Then standing waves are eliminated. This procedure is recommended only if the effective rock size, d_m , is one-tenth the pipe diameter or larger. In smaller rock, the turbulence created by the roughness elements may cause unexpected scour depths such as those which occurred in the vicinity and downstream of the hydraulic

jump, possibly because of the change in the characteristics of turbulence of the flow.

If the angles are not used, then the discharge must be limited to $Q/D^{2.5} \leq 3.5$ cfs/ft^{5/2}. In model studies no standing waves formed in this range of flows.

2. The culvert barrel must be on a horizontal or mild slope. Standing waves did form at low $Q/D^{2.5}$ when model pipes were steeply sloped. Also, in models on a steep slope, it was possible to get a hydraulic jump in the metal end section. When this jump occurred the depth of scour in the basin was much greater than normal for that flow rate (17).

3. With $d_t/D \leq 0.33$. The tailwater may rise above the sides of the end section, then the jet is confined by the water that spills inward over the sides of the end section and the purpose of the end section is no longer completely effective. The end section is useful only when the jet can expand and be redirected parallel to the rock basin bed.

The recommended riprapped basins, which utilize metal end sections are shown in Figs. 46 and 47. The metal end section is supplied with a metal end wall that should extend into the rock basin a distance $d_s + A$ to protect the material under the transition from being pumped out from beneath the end section and pipe by the flow.

For the non scouring basins of Fig. 46 the volumes of rock required are:

1. Apron -

$$\left(\frac{2D + W_b}{2}\right)(L)(hd_m)$$

for $A = hd_m$;

2. End slope -

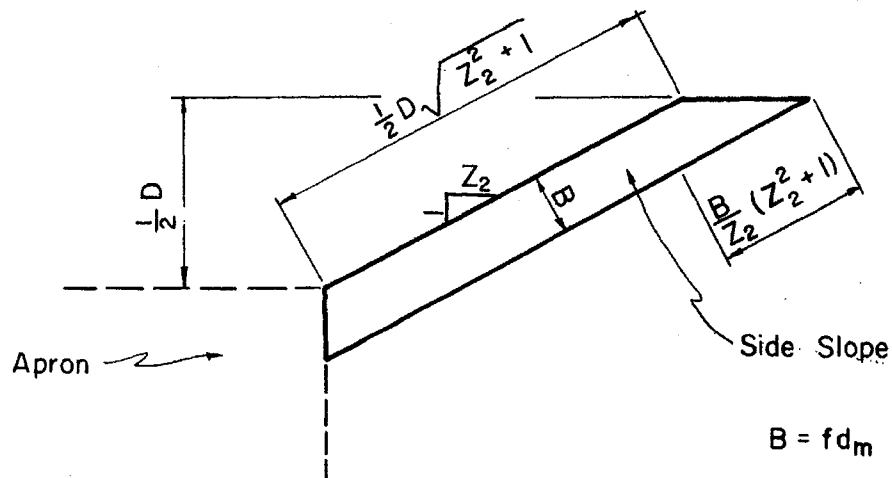
$$(fd_m) (E \sqrt{z_3^2 + 1}) (W_b)$$

for $B = fd_m$

and an end slope of $z_3:1$;

3. Side slopes -

A typical side slope is detailed in the sketch below.



It is necessary to extend the side slope to a distance $\frac{1}{2}D$ above the apron.

The length of one side slope is approximately

$$L \sec \theta + E \sqrt{z_3^2 + 1}$$

or $1.05 L + E \sqrt{z_3^2 + 1}$

because $\theta = 17^\circ$.

The approximate volume of rock is then

$$2f d_m (1.05 L + E \sqrt{z_3^2 + 1}) \left[\frac{D}{2} \sqrt{z_2^2 + 1} + \frac{f d_m}{2z_2} (z_2^2 + 1) \right].$$

Again, if

$$0 < \frac{d_s}{d_m} < 2,$$

the hybrid basin (Fig. 46) should be used.

All dimensions for the hybrid basin are the same as in the nonscouring basin except that an additional volume of rock

$$(6D + W_b) (d_s) \left(\frac{L}{8}\right)$$

is required in the apron. The total volume in the apron is now

$$\left(\frac{2D + W_b}{2}\right) (L) (hd_m) + (6D + W_b) (d_s) \left(\frac{L}{8}\right).$$

The scouring basin requires much more rock. The approximate volumes are:

1. Apron -

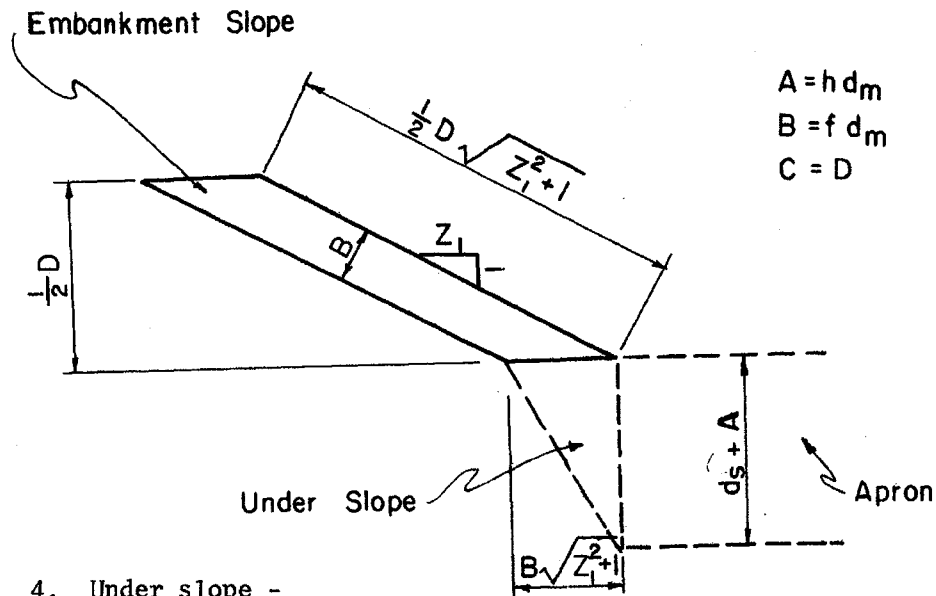
$$\begin{aligned} & (W_b) (L_s) (d_s + A) + (W_b) (L - L_s) (B) \\ & = (W_s + 2D) [(L_s) (d_s + hd_m) + f d_m (L - L_s)]; \end{aligned}$$

2. End slope -

$$\begin{aligned} & (B) (E \sqrt{z_3^2 + 1}) (W_s + 2C) \\ & = f d_m (E \sqrt{z_3^2 + 1}) (W_s + 2D); \end{aligned}$$

3. Embankment slope -

$$\begin{aligned} & \left(\frac{1}{2} D \sqrt{z_1^2 + 1}\right) (B) (W_s + 2C - 2D) \\ & = f d_m \left(\frac{1}{2} D \sqrt{z_1^2 + 1}\right) (W_s). \end{aligned}$$



4. Under slope -

$$\begin{aligned} & \left(\frac{B}{2} \sqrt{z_1^2 + 1}\right) (d_s + A) (W_s + 2C - 2D) \\ & = \frac{fd_m}{2} \sqrt{z_1^2 + 1} (d_s + hd_m) (W_s) ; \text{ and} \end{aligned}$$

5. Side slopes -

$$\begin{aligned} & 2B(L + E \sqrt{z_3^2 + 1}) \left[\frac{D}{2} \sqrt{z_2^2 + 1} + \frac{B}{2z_2} (z_2^2 + 1) \right] \\ & = fd_m (L + E \sqrt{z_3^2 + 1}) \left[D \sqrt{z_2^2 + 1} + \frac{fd_m}{z_2} (z_2^2 + 1) \right]. \end{aligned}$$

Filter requirements for metal end-section basins are the same as for the standard basins.

4.5 Circular Outlets

Data

Given the pipe discharge and tailwater depth at the end of the culvert, the depth of scour can be determined from the data plotted in Figs. 48, 49, 50, 51, and 52. A cross plot of depth of scour versus

rock size will yield a curve from which the depth of scour can be found for rock sizes not included in the above figures.

For basins that scour, the length of the scour hole is given in Fig. 53.

If no degradation is anticipated downstream of the structure, the length of the basin is given by

$$\frac{L}{d_m} = 1.9 \frac{L_s}{d_m}, \text{ see Fig. 54.}$$

When degradation is allowed, the basin can be protected for a longer time if it is assured that any scoured rock will be retained within the basin. To be certain of this the basin should be made longer; i.e., use

$$\frac{L}{d_m} = 2.4 \frac{L_s}{d_m}, \text{ see Fig. 54.}$$

The width of the scour hole is obtained from Fig. 55.

If a metal end section, with the geometry shown in Fig. 44, is employed, the depth of scour is found from the curves in Fig. 56. Figures 53, 54, and 55 are valid for metal end sections as well as plain outlets so they can be used to find the length of the scour hole and the length of the basin.

For plain outlets that do not scour, the angle of lateral expansion, θ , can be estimated from Figs. 58 and 59. Examples illustrating the design of hybrid, scoured, high tailwater and non-scouring rock riprap basins are given in Appendix A, page 86. Also, a field check of the design procedure is presented and discussed.

4.6 Rectangular Outlets

The procedure for designing rock basins at rectangular outlets is the same procedure for designing circular outlets. The required data are found in the following figures.

(a) Depth of Scour

Figs. 48 and 49 (use directly)

Figs. 50, 51, and 52 (must be modified by the procedure in Appendix E).

(b) Length of the Scour Hole

Fig. 53

(c) Length of the Basin

Fig. 54 (scouring basins)

Fig. 59 (non-scouring basins)

(d) Width of the Basin

Fig. 55 (scouring basins)

Fig. 59 (non-scouring basins)

4.7 Multiple Barrels

The design of rock basins for multiple-barrel culverts is essentially the same as for single barrels provided that all barrels are the same size. Assuming equal discharges in all barrels, the depth of scour and the length of scour hole and basin are computed by using the same procedure outlined in the examples given in Appendix A. That is, the scour depth and the length of scour hole and basin for a n -barrel culvert carrying Q_t , is the same as for a single barrel discharging Q_t/n . The width of the scour hole is given by the equation

$$W_{sn} = W_s + (n-1)(W_o + T)$$

or

$$W_{sn} = W_s + (n-1)(D + T)$$

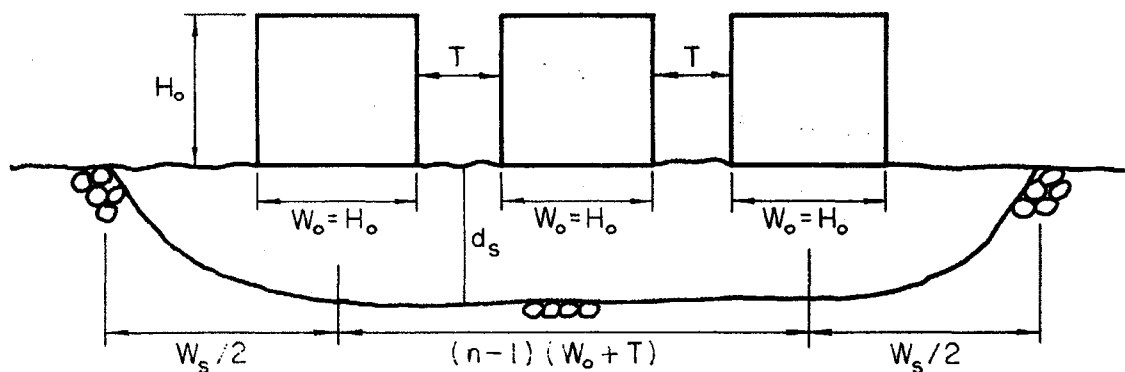
in which

W_{sn} = width of the scour hole for n barrels,

W_s = width of the scour hole for a single barrel (Fig. 55),

n = number of barrels, and

T = the spacing between the barrels, assumed to be the same between all the barrels.



SKETCH A: Width of Scour Hole for Multi-Barrel Culvert

There is a greater chance of failure in the riprapped basin for multi-barrel culverts than there is for single-barrel culverts. If one barrel of a multi-barrel culvert becomes blocked with debris, the remaining barrels carry more flow; this increase in flow may be great enough to fail the riprapped basin. The designer might consider

riprapping the flanking or outside barrels and side-slopes with larger rock than the design procedure would indicate. Failure below these two barrels would require more remedial work than a riprap failure below the interior barrels.

4.8 Optimum Culvert Design

In this report, it has been assumed that the barrel design has been completed and the outlet basin designed according to conditions at the outlet. It is possible that the cost of the basin can be reduced considerably if the barrel design is slightly changed. For example, when $d_t/y_o \geq 1.0$, non-scouring basins are very long. If the invert is raised, d_t/y_o can be decreased and the non-scouring basin becomes much shorter. However, the required rock size will be larger and if the flow is controlled by the outlet conditions, more headwater will be needed to obtain the design discharge.

It is suggested that small changes in the barrel design may considerably reduce the cost of the stilling basin.

Chapter V

THE HIGH TAILWATER AND NON-SCOURING BASIN

5.1 Characteristics of Basins with High TailwaterExperimental Data

High tailwater is defined as the condition where the water surrounding the high speed jet-like core of water downstream of the culvert outlet is as high as, or higher than, the elevation of the crown of the pipe. This situation occurs at culvert outlets where downstream channel constrictions create backwater or where the culvert discharges into a narrow, low gradient channel with high banks and a large normal depth.

Unknowns that confront the engineer faced with the problem of designing a stable energy dissipating basin where high tailwater conditions prevail are:

- (a) the rate of decay of the high speed velocity core,
- (b) the rate of lateral expansion of the core, and
- (c) the probability of the core being diverted off to one side, thus imperiling the banks.

The problem of two- and three-dimensional jets discharging into a large volume of quiescent ambient fluid has been studied in detail. Three significant papers on this subject are listed in the Bibliography, (1), (8), and (24).

It is necessary to determine how the diffusion characteristics of a jet of water bounded on the top by a free surface and on the bottom by a rough (rock lined), essentially rigid, boundary, compare to the characteristics of a jet diffusing in a basin of infinite size. During

the course of the CSU study limited data describing jet diffusion downstream of culverts were collected and reported by Watts (22).

Some data from the tests are shown in Fig. 60. Because the velocity distribution at the culvert outlet is nonuniform, in contrast to the uniform distribution for the orifice, it seemed more reasonable to compare the arithmetic mean of the velocities measured along a centerline vertical at Station x to an arithmetic mean of the velocities measured along a centerline vertical at the outlet. It should be noted that the maximum velocity for the orifice is equal to the mean velocity which is not the case for usual pipe flow. A plot of the data of $\frac{V_x \text{ ave}}{V_o \text{ ave}}$ versus the dimensionless longitudinal coordinate, $\frac{x}{D}$, is superimposed over the prediction curves (1) and (24) on Figure 60. In the range $x/D < 8.0$, the prediction curve is conservative except for the low tailwater runs. For the range $x/D > 8$, the culvert data follow the prediction curve.

The $V_o \text{ ave}$ to be used with Fig. 60 for basin design can be obtained from

$$V_o \text{ ave} = K Q/A ,$$

in which Q is the design discharge, A is the gross cross-sectional area of the culvert, and K is a constant relating Q/A to the arithmetic mean of the vertical velocity profile. For smooth approach pipes, K was evaluated using data from 34 runs. Values of K ranged from 0.96 to 1.16, with an arithmetic mean of 1.07. For purposes of design, the value $K = 1.10$ is suggested for smooth pipe.

Only two sets of data were available for corrugated pipe. The values of K were 1.14 and 1.21. The former value was associated with a typical maximum design discharge and the latter value with a Q well

over the usual design discharge. It is suggested that $K = 1.15$ be used for corrugated pipe.

Examining isovel plots from Watts (22) the following is apparent.

1. Lowering the tailwater only one-seventh of the approach pipe diameter allows the jet to plunge toward the floor. Where the jet discharges into the low tailwater basin, the location of the core of maximum velocity is at the surface, whereas the location is at mid-depth or lower for the high tailwater basins.

2. Theoretically predicted velocity profiles are in good agreement with measured values for both tailwater conditions (1).

3. Comparison of measured velocities with the theoretical velocities given by References (1), (8), and (24), at a distance $D/2$ above the floor are sufficiently good to warrant the use of the theoretical velocity prediction (Figs. 61 and 62) for design.

Whether or not the core of the jet is diverted to one side seems to depend on the ratio of the basin width to pipe diameter (W_b/D). With a large ratio, there is little danger of such an occurrence, but when $W_b/D \leq 4$, jet attachment to a bank or wall is a possibility.

There are two solutions to the scour problem for the high tailwater cases. One is to riprap the banks for a sufficient distance downstream and the other is to increase the cross-sectional area of the culvert so that the exit velocity is reduced. If a flare with the culvert box is sufficiently gradual, the entire section will be occupied by the flow; with large flare angles, the flow will separate from one wall and a large eddy in the basin will hold the flow against the other wall. An example of a non scour high tailwater basin design can be found in Appendix A, page 129.

BIBLIOGRAPHY

1. Albertson, M. L., Dai, Y. B., Jensen, R. A., and Rouse, H., "Diffusion of Submerged Jets," ASCE Trans. Vol. 115, pp. 639-697, 1950.
2. Blaisdell, Fred W., "Flow through Diverging Open Channel Transitions at Supercritical Velocities," Soil Conservation Service, U.S. Department of Agriculture, Washington, D.C., S.C.S. - TP-76, p. 15, April 1949.
3. Blaisdell, Fred W., "Development and Hydraulic Design, Saint Anthony Falls Stilling Basin," ASCE Trans. Vol. 113, pp. 483-520, 1948.
4. California Division of Highways, "Bank and Shore Protection in California Highway Practice," Sacramento, California, 1960.
5. Chow, Ven T., "Open Channel Hydraulics," McGraw Hill Book Co., New York, 1959.
6. French, John L., "Second Progress Report on Hydraulics of Culverts- Pressure and Resistance Characteristics of a Model Pipe Culvert," National Bureau of Standards, U.S. Department of Commerce, Washington, D.C., p. 4911, October 1956.
7. Ippen, Arthur T., "Mechanics of Supercritical Flow," ASCE Trans. Vol. 116, pp. 268-295, 1951.
8. Murota, A., and Muraoka, K., "Turbulent Diffusion of the Vertically Upward Jet," Proceedings of the Twelfth Congress of the IAHR, Vol. 4, Part I, Colorado State University, Fort Collins, Colorado, 1967.
9. Murphy, T. E., and Grace, J. L., "Riprap Requirements for Overflow Embankments," Highway Research Board Record, No. 30, Washington, D.C., 1963.
10. O'Loughlin, B. E., "Culvert Investigations by Hydraulic Models," Harbours and Rivers Branch, Hydraulic Laboratory, Manly Vale, N.S.W., Australia, 1960.
11. Opie, T. R., "Scour at Culvert Outlets," M.S. thesis, Colorado State University, Fort Collins, Colorado, December 1967
12. Rajaratnam, N., and Subramanya, K., "Hydraulic Jumps Below Abrupt Symmetrical Expansions," Journal of the Hydraulics Division, ASCE, Vol. 94, No. HY2, Proceedings Paper 5860, March, 1968.
13. Rouse, Hunter, "Fluid Mechanics for Hydraulic Engineers," Dover Publications, Inc., New York, 1961.

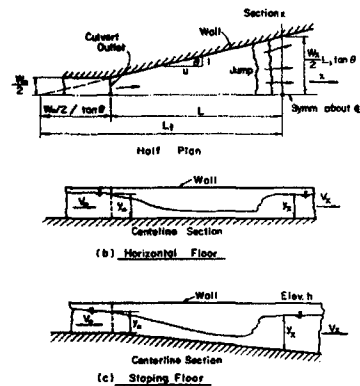
14. Rouse, Hunter, Bhoota, B. V., and Hsu, En-Yun, "Design of Channel Expansions," ASCE Trans. Vol. 116, pp. 347-363, 1951.
15. Sherard, J. L., Woodward, R. J., Gizienski, S. F. and Clevenger, W. A., "Earth and Earth-Rock Dams," John Wiley and Sons, Inc., New York, 1963.
16. Smith, C. D., "Brink Depth for a Circular Channel," Journal of the Hydraulics Division, ASCE, Vol. 88, No. HY 6, Proceedings Paper 3327, November 1962.
17. Stevens, M. A., "Scour in Riprap at Culvert Outlets," Ph.D. dissertation, Colorado State University, Fort Collins, Colorado, January 1969.
18. U.S. Army Corps of Engineers, "Shore Protection Planning and Design," Beach Erosion Board, Tech. Rep. No. 4, U.S. Government Printing Office, Washington, D.C., 1961.
19. U.S. Bureau of Reclamation, Engineering Monograph No. 25, "Hydraulic Design of Stilling Basins and Bucket Energy Dissipators," Technical Information Branch, Denver Federal Center, Denver, Colorado, 1958.
20. U.S. Bureau of Reclamation, "Design of Small Dams," Government Printing Office, 1965.
21. Valentin, F., "Considerations Concerning Scour in the Case of Flow Under Gates," Proceedings of the Twelfth Congress of the IAHR, Vol. 3, Colorado State University, Fort Collins, Colorado, 1967.
22. Watts, F. J., "Hydraulics of Rigid Boundary Basins," Ph.D. dissertation, Colorado State University, Fort Collins, Colorado, August 1968.
23. Wyoming Highway Department, "Hydraulic Design Practice," 1966.
24. Yevjevich, V., "Diffusion of Slot Jets with Finite Orifice Length-Width Ratios," Hydraulics Paper No. 2, Colorado State University, Fort Collins, Colorado, 1966.

APPENDIX A
DESIGN EXAMPLES OF RIGID BOUNDARY
AND ROCK RIPRAPPED BASINS

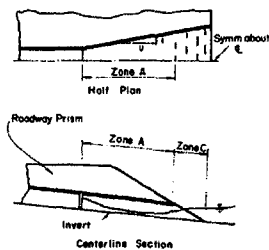
DESIGN EXAMPLES OF RIGID BOUNDARY AND ROCK RIPRAPPED BASINS

Design Examples

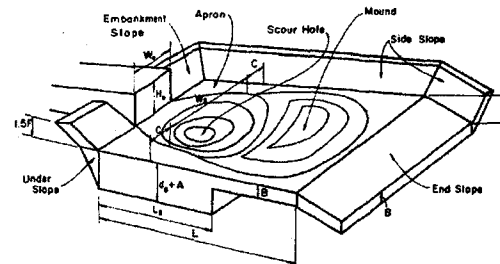
The design of the various types of rigid boundary and rock riprapped basins are presented. The common types of basins that will be considered are illustrated in the following figure.



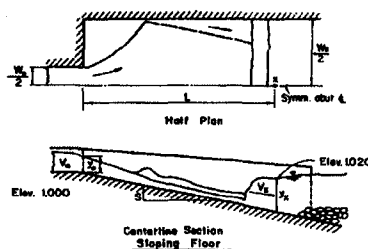
Smooth-Floor Flared Basin



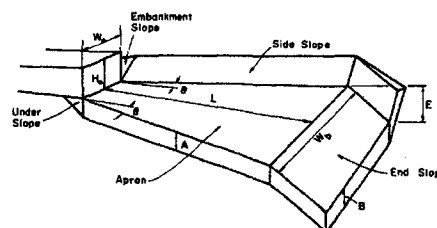
Combined Basin



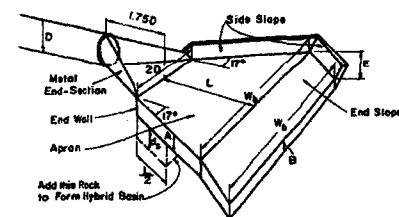
Standard Scoured Basin



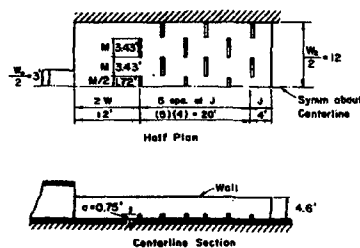
Smooth-Floor Rectangular Basin



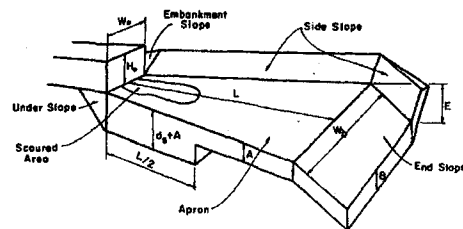
Standard-Non Scouring Riprapped Basin



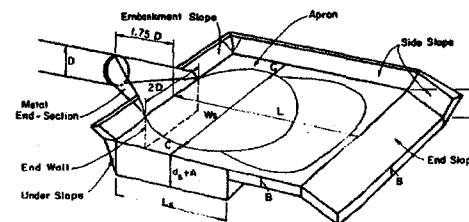
Non-Scouring Basin with a Metal End Section



Rough-Floor Rectangular Basin



Standard Hybrid Riprapped Basin



Scouring Basin with a Metal End Section

A - Smooth-floor Flared Basin (Fig. 18) Rectangular Culvert

1. Design a smooth-floor flared basin so that the hydraulic jump will occur within the diverging walls of the basin.

<u>Given</u>	6 ft x 6 ft box culvert	$W_o = 6$ ft
	Depth of flow at outfall of culvert	$y_o = 4$ ft
	Design discharge	$Q = 420$ cfs
	Downstream tailwater depth computed from channel hydraulics	$y_x = 4$ ft
	Horizontal apron	

Compute

$$V_o = \frac{Q/2}{A/2} = \frac{210}{(3)(4)} = 17.5 \text{ fps.}$$

Watts (22) has checked Blaisdell's criterion (2), for the flare angle, θ , and found it satisfactory for both rectangular and circular approach pipes. The equation suggested by Blaisdell is

$$u = 3F_o.$$

The quantity, u , is the longitudinal distance per transverse unit of divergence along a wall, and $F_o = V_o / \sqrt{gy_o}$ is the Froude number for the flow at the outlet of the culvert. Use of this flare angle assures that the entire width of cross section at section x will be occupied by flow in the downstream direction. See Appendix C for further discussion of the flare angle. In the example,

$$F_o = \frac{V_o}{\sqrt{gy_o}} = \frac{17.5}{\sqrt{(32.2)(4)}} = \underline{\underline{1.54}}$$

so $u = 3 F_o = 4.62.$

Use $\underline{u} = 4.5$

for which $\tan\theta = \frac{1}{u} = \frac{1}{4.5} = 0.222$.

With reference to Fig. 18, for a given Q and tailwater depth y_x , the momentum flux and pressure force at point x (slightly downstream of the hydraulic jump) is (assuming hydrostatic pressure variation and uniform distribution of velocity)

$$M_x = \rho(Q/2) V_x + \frac{W_x}{2} \frac{\gamma y_x^2}{2}$$

At point x ,

$$Q/2 = V_x \frac{W_x}{2} y_x$$

or

$$V_x = \frac{Q/2}{W_x/2 y_x}$$

and $W_x/2 = L_1 \tan\theta$.

Therefore,

$$M_x = \rho \left(\frac{Q}{2}\right) \left(\frac{Q/2}{L_1 \tan\theta y_x}\right) + \frac{L_1 (\tan\theta) (\gamma) (y_x)^2}{2}$$

Given Q , y_x , and θ , there is a value of M_x associated with each value of L_1 .

Compute values of M_x for several values of L_1 , i.e., let $L_1 = 25'$, $30'$, $35'$, etc., and determine M_x for each L_1 .

Substituting in the given values of Q , $\tan\theta$, y_x , ρ and γ , the momentum flux at section x becomes

$$M_x = \frac{(1.94)(2.1)^2}{L_1(0.222)(4)} + \frac{L_1(0.222)(62.4)(4)^2}{2}$$

$$M_x = \frac{96,500}{L_1} + L_1(110.7)$$

The solutions for selected values of L are tabulated.

Table 2

L_1 ft	L ft	96,500 L_1 lbs	L_1 (110.7) lbs	M_x lbs
35	21.5	2760	3880	6640
40	26.5	2410	4430	6840
45	31.5	2140	4990	7130
50	36.5	1930	5540	7470
55	41.5	1750	6100	7850
60	46.5	1610	6650	8260
65	51.5	1480	7200	8680
70	56.5	1380	7750	9130

The next step is to compute the momentum at the outfall section,

$$M_o = \frac{\beta_1 \gamma y_o^2}{2} \left(\frac{W}{2} \right) + \beta_2 \rho V_o Q/2 .$$

After recalling that $F_o = 1.54$, and that the culvert section is rectangular, Fig 14 is used to get

$$\beta_1 = 0.65 \quad (\text{assuming } d_t/y_o = 0 \text{ at the outlet});$$

also $\beta_2 = 1.00 .$

Then,

$$\begin{aligned} M_o &= (0.65)(62.4) \frac{(4)^2}{2} \frac{(6)}{2} + (1.00)(1.94)(17.5) \frac{(420)}{2} \\ &= 970 + 7130 = 8100 \text{ lb.} \end{aligned}$$

Comparing this value to the values of M_x versus L_1 in Table 2, it is apparent that $M_o \approx M_x$ at $55 \text{ ft} < L_1 < 60 \text{ ft}$. This is an estimate of the location of the hydraulic jump. Note that L_1 is not the length of the basin, L . With reference to the half plan (Fig. 18),

$$L = L_1 - \frac{W_o}{2} / \tan \theta .$$

Two mathematical solutions for L are possible. Select that solution on the upper branch of the M_x relation that gives the greatest length of basin. In this case the flow is decelerating (increasing in depth with distance) and the jump will be more stable and have its first opportunity to form in this position. For the alternate solution the jump would be very close to the outlet and would be much more likely to be drowned out and fail to adequately dissipate the energy of the expanding jet. This jet may cause failure of the basin as well as the channel downstream of the basin.

In the analysis, the shear force exerted by the floor on the flow and the pressure force exerted by the diverging walls on the flow have not been considered. The two forces tend to cancel each other but the floor shear is the larger of the two. By ignoring the wall and floor forces, a conservative estimate of L is obtained.

In using this method to compute the location of the jump, it is assumed that the tailwater depth, y_x , is constant. If a more precise estimate of L_1 is required, it is suggested that the surface profile of the supercritical flow through the diverging basin be computed. The flow is supercritical, therefore the control section (and starting point for flow profile computations) is upstream.

The rapidly varied flow region near the outfall section presents a problem. It is suggested that backwater computations be started at Station $\frac{x}{W_0} = 2$ where x is the distance from the culvert outlet to a point downstream on the centerline of the basin.

Using previously computed values of $F_0 = 1.54$ and $\frac{y_0}{W_0} = \frac{4'}{6'} = 0.67$, the dimensionless plot of water surface profiles and velocity vectors (Fig. 5) for flow with similar parameters ($F_0 = 1.57$ and $\frac{y_0}{W_0} = 0.83$)

is selected. This information is superposed over a half plan of the proposed basin as shown in Fig. 19.

At Station $\frac{x}{W_0} = 2.0$ it is apparent that the wall would have little effect on the flow field (the wall falls outside the $\frac{y}{y_0}$ contour of 0.2), therefore a good estimate of the average velocity can be obtained by averaging the $\frac{V}{V_0}$ values shown between the centerline of the basin and the wall:

$$\frac{V}{V_0} = \frac{1.18 + 1.18 + 1.15 + 1.10}{4} = 1.15 \quad .$$

The mean velocity passing the section is $V = 1.15 V_0 = (1.15)(17.5) = 20.1$ fps. The half-width of the basin at Station $\frac{x}{W_0} = 2$ is $3.0 + (2)(6)(\tan\theta) = (3.0) + (12)(0.222) = 5.67$ ft. The mean depth is

$$\frac{Q/2}{\frac{\text{width}}{2}(V)} = \frac{210}{(5.67)(20.1)} = 1.84' \quad .$$

With a known depth of flow and mean velocity at the starting section and given flare angle for the walls, a backwater computation using the standard step method (see Page 279, Ref. 5) is a well defined (though laborious unless computerized) procedure. In general the results are not sufficiently worth it to make this procedure routine.

To locate the jump, values of V_L (velocity at $x = L$) and y_L (depth at $x = L$) from the backwater computations are used to compute the quantity $M_L = \rho Q/2 V_L + \frac{\gamma y_L^2 W_L}{4}$. for various values of L . When M_L for a specific L equals the quantity shown in column 5 of Table 1 for an equal length, L , the jump will occur.

Regardless of the method used to locate the approximate position of the jump, the basin must be extended several feet beyond the theoretical

position. It is known that the length of the circular hydraulic jump (a situation similar to the flared basin) is about 3.5 to 4.5 times the depth of flow y_x at the heel of the jump. It is suggested that a minimum of $6 y_x$ be added to L (Fig. 18) to provide adequate safety against a downstream shift in the position of the jump due to changing resistance to flow degradation and other factors.

Additionally, exit velocities from the basin should be checked for the minimum tailwater condition. The standard step method carried out for the design length of a basin would yield this information. A means of shortening the basin is to increase the tailwater depth. One way of accomplishing this is to slope the basin steeply (1:6 maximum) into the ground.

In the analysis (see Figure 18c) it is assumed that tailwater height or elevation h , is a known quantity. To obtain quantities similar to those shown in Table 1, the variation of y_x must be considered, i.e.,

$$M_x = \frac{(1.94)(2.0)^2}{L_1(0.222)(y_x)} + \frac{L_1(0.222)(62.4)(y_x)^2}{2}$$

Knowing elevation h , the elevation of the invert at the culvert outfall, and the slope of the floor, the quantity y_x can be readily determined for any value of L_1 . Also, if the backwater curve is computed, the longitudinal slope of the floor must be considered.

In the design of this basin, the walls must be of sufficient height (greater than the depth of water) so that the tailwater cannot flow inward over the walls and submerge the high velocity flow upstream of the jump which would cause the high velocity jet to persist for a long distance downstream.

B - Smooth-floor Rectangular Basin (Fig. 20), Rectangular Culvert

Smooth-floor rectangular basin (Fig. 20) with sloping floor -

<u>Given</u>	6 ft x 6 ft box culvert	$W_o = 6$ ft
	Depth of flow at culvert outfall	$y_o = 4$ ft
	Design discharge	$Q = 420$ cfs
	Downstream tailwater elevation	102.0
	Invert elevation at culvert outlet	100.0
	Longitudinal slope of basin	10%
	Designer's choice $\frac{W_2}{W_o} = 4.0$	$W_2 = 24$ ft
	Work with 1/2 section.	
	Compute the momentum at outfall section.	
	See previous computations (smooth-floor flared basin)	
	$M_o = 8,100$ lbs.	

When the continuity equation,

$$V_x = \frac{Q/2}{(W_2/2)y_x}$$

is substituted into

$$M_x = \rho \frac{Q}{2} V_x + \frac{W}{2} \gamma \frac{y_x^2}{2}$$

the expression for the momentum in the x-direction at Station L (Fig. 20) is

$$M_x = \rho \left(\frac{Q}{2}\right) \frac{Q/2}{W_2/2 y_x} + \left(\frac{W_2}{2}\right) \frac{\gamma y_x^2}{2}$$

Next, equate M_x to M_o above and substitute known values of Q , ρ , γ , and W_2 , or

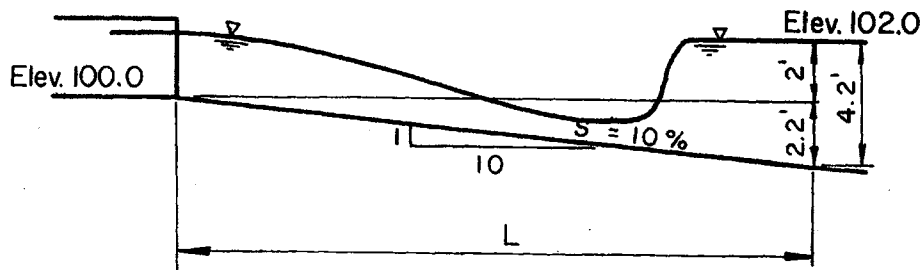
$$(1.94)(210) \left(\frac{210}{12}\right) \frac{1}{y_x} + \left(\frac{24}{2}\right) \left(\frac{62.4}{2}\right) y_x^2 = 8,100 .$$

Solving the above equation by trial and error for positive values of y_x gives:

$$y_x \text{ supercritical} = 0.9 \text{ ft, and}$$

$$y_x \text{ subcritical} = 4.1 \text{ ft,}$$

for an elevation of invert of 100.0 a tailwater elevation of 102.0, and basin slope of 10 percent as shown below,



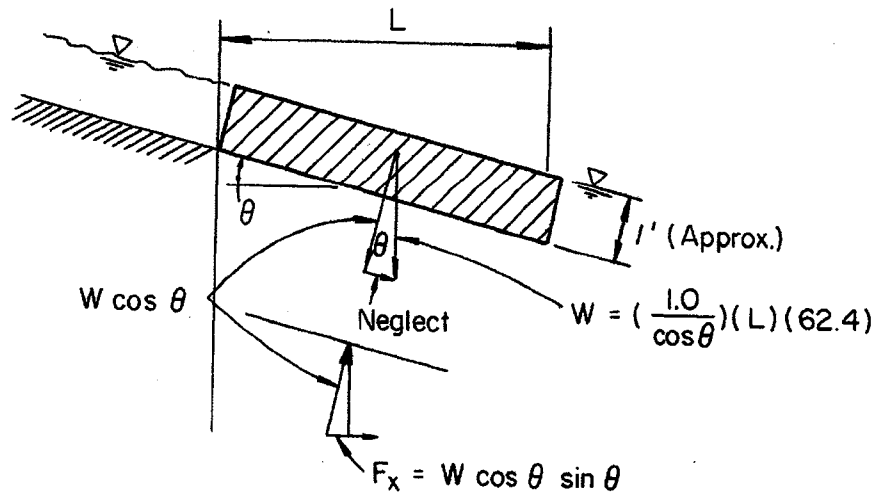
SKETCH. Hydraulic jump in a basin with sloping floor.

$$\frac{SL}{100} = 4.1 - 2.0,$$

or $L = \underline{21 \text{ ft}} .$

Note: The weight of the water has not been considered. There is a force component in the x-direction produced by the sloping floor on the body of water. There is also a shear force exerted by the floor on the water which partially cancels the weight force (the shear would, of course, exactly cancel the weight component if uniform flow existed).

By including the weight component the longer basin length required will be determined. Neglecting the shear force (which is difficult to estimate) will result in a conservative estimate.



SKETCH. Force diagram, sloping floor.

A first estimate of the weight force may be determined by adding an increment of length to the $L = 21$ ft originally determined. Let $L = 30$ ft. The weight component F_x will be

$$F_x = 1.0 (30) (12) (62.4) \frac{1}{10} = 2250 \text{ lb.}$$

With the additional weight force the balance of momentum is

$$(1.94) (210) \left[\frac{210}{12} \right] \frac{1}{y_x} + \left(\frac{24}{2} \right) \left(\frac{62.4}{2} \right) y_x = 8100 + 2250$$

or
$$\frac{7130}{y_x} + 375 y_x^2 = 10,350.$$

From the above equation:

$$\underline{y_x} \text{ subcritical} \approx 4.9 \text{ ft.}$$

The new value for L (Sketch D) is

$$\underline{L} = \frac{4.9 - 2.0}{.10} = \underline{29 \text{ ft}},$$

which is nearly the same as our initial estimate. The effect of considering the weight component is to lengthen the basin. If the floor of the basin is horizontal there will, of course, be no weight component. The effect of considering the shear force is to reduce the basin length.

Smooth-floor rectangular basin with horizontal floor - If a horizontal floor is required, the following procedure is suggested.

Given

6 ft x 6 ft box culvert	$W_o = 6 \text{ ft}$
Design discharge	$Q = 420 \text{ cfs}$
Depth of flow at culvert outlet	$y_o = 4 \text{ ft}$
Downstream tailwater	3 ft

The exit velocity is estimated from a smooth-floor rectangular basin with a horizontal floor.

The designer has a choice for W_2 . Pick

$$W_2 = 24 \text{ ft (i.e., } \frac{W_2}{W_o} = 4)$$

also

$$\frac{y_o}{W_o} = \frac{4}{6} = 0.67$$

and

$$F_o = \frac{17.5}{\sqrt{4g}} = 1.54 \text{ as before.}$$

The dimensionless water surface profile and velocity vectors, Fig. 5, are selected and superimposed on the rectangular basin with the wall at $z/W_0 = 2$ (Fig. 21).

Assumption 1: The $y/y_0 = 0.1$ contour extends to the wall. Its intersection with the wall is assumed to be the point of impingement and the impingement angle θ is scaled to be approximately 35° .

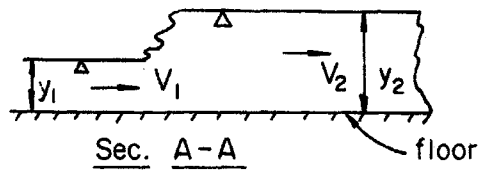
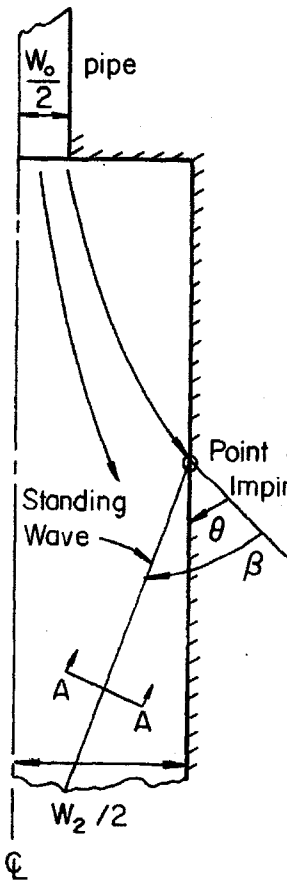
The supercritical flow striking the vertical side-wall results in an oblique hydraulic jump (Fig. 22) and it is this feature which is used to help reduce the high velocity at the culvert outlet to a lower value acceptable to the downstream channel.

Watts (22), in models of culvert outfalls, checked the relationships and curves established by Ippen (7) and concluded that Ippen's criteria (Fig. 24) were valid except for the conditions which subsequent sketches illustrate.

Watts found that for models with $4 \leq W_2/W_0 \leq 7$, good agreement between the predicted angle and the measured angle of the standing wave, β , verified Ippen's criteria. In the same group of tests, Watts found that the relative depth across the standing wave, y_2/y_1 , could be assumed constant and equal to 3.5. Then, for design of the smooth floor rectangular basin, the equation,

$$\frac{y_2}{y_1} = 3.5$$

is used.



$$\frac{y_2}{y_1} = \frac{1}{2} [\sqrt{1 + 8 F_1^2 \sin^2 \beta} - 1]$$

$$F_1 = \frac{V_1}{\sqrt{gy_1}} ; \frac{y_2}{y_1} = \frac{\tan \beta}{\tan(\beta - \theta)}$$

PLAN VIEW
$$\tan \theta = \frac{\tan \beta (\sqrt{1 + 8 F_1^2 \sin^2 \beta} - 3)}{2 \tan^2 \beta + \sqrt{1 + 8 F_1^2 \sin^2 \beta} - 1}$$

Equations and graphical solution to the above equations are shown on p. 287, Ref. 7.

SKETCH. Plan view of standing wave in a smooth-floor rectangular basin with horizontal floor.

In this example,

$$\frac{V_1}{V_0} = 1.07 \quad (\text{Fig. 21})$$

at the point of impingement (see Fig. 21) and

$$V_1 = 1.07 \times 17.5 = \underline{18.7 \text{ fps}} .$$

Assumption 2: Assume that

$$\frac{y_1}{y_0} = 0.1$$

at the point of impingement on the walls, or

$$y_1 = (0.1)(4) = 0.4 \text{ ft.}$$

The approach Froude number, F_1 , to be used in Ippen's chart (Fig. 24) is

$$F_1 = \frac{V_1}{\sqrt{gy_1}} = \frac{18.7}{\sqrt{(32.2)(0.4)}} = \underline{5.2}$$

If $\theta = 35^\circ$ and $F_1 = 5.2$ then Fig. 24 yields

$$\beta_1 = 47^\circ$$

and the sequent depth for the standing wave is

$$\underline{y_2} = 3.5 y_1 = (3.5)(0.4) = \underline{1.40 \text{ ft}}$$

(Watts' value of $y_2/y_1 = 3.5$ is used here). At Station x downstream of the intersection of the standing wave and the centerline,

$$V \approx \frac{Q/2}{(W_2/2) y_2} = \frac{210}{(12)(1.4)} = \underline{12.5 \text{ fps.}}$$

The momentum in the x -direction at Station x is

$$\begin{aligned} M_x &= \rho Q/2 V_x + \gamma \frac{y_x^2}{2} \frac{W_2}{2} = (1.94)(210)(12.5) + \frac{(62.4)(1.4)^2(12)}{(2)} \\ &= 5100 + 735 = \underline{5835 \text{ lb.}} \end{aligned}$$

Tailwater depth is given as 3 ft. Assuming the entire section is occupied by the flow the average velocity is

$$V \approx \frac{Q/2}{(W_2/2) y_x} = \frac{210}{(12)(3)} = 5.83 \text{ fps.}$$

The momentum of the flow 3 ft deep and 12 ft wide is

$$\rho \frac{QV}{2} + \frac{\gamma y_x^2 W_2^2 / 2}{2} = (1.94)(2.0)(5.83) + \frac{(62.4)(3)^2(12)}{2}$$

$$= 2370 + 3370 = \underline{\underline{5740 \text{ lbs}}}$$

This is slightly less than the momentum flux shown above (5835 lb); therefore, unless the tailwater depth was increased the jump would not occur within the basin. The outlet velocity would be approximately the velocity shown at Station x above, $V = 12.5 \text{ fps}$ -- still too high. However, without the basin, the velocity at the outfall of the culvert would have been $V = (1.18)(17.5) = \underline{\underline{21.6 \text{ fps}}}$. Other measures could be taken to insure information of a jump in the basin. For example, a sill could be constructed, or the basin floor could be lowered in accordance with the design principles of reference (19).

Smooth-floor rectangular basin, complex design procedure - If further refinement of the design procedure is warranted, the following method is suggested.

1. Superimpose the basin over the appropriate dimensionless water profile to determine the point of impingement and the bearing of the standing wave as described under Simple Design Procedure - Horizontal Floor.

2. Subdivide the basin into four (or more) stream tubes each carrying an equal discharge (see Fig. 25); that is,

$$Q/2 = 210 \text{ cfs,}$$

and

$$\frac{Q/2}{4} = 52 \text{ cfs.}$$

Begin computations at Station $x/W_0 = 2.0$. In the central portion of the basin where $V/V_0 = 1.18$ and $y/y_0 \approx 0.42$, then $V = (1.18)(V_0) = (1.18)(17.5) = 20.6$ fps and $y = (0.42)(4) = 1.68$ ft.

The width of the first stream tube is

$$W_1 = \frac{52}{yV} = \frac{52}{(1.68)(20.6)} = 1.50 \text{ ft.}$$

In the same manner W_2 and W_3 are computed and W_4 becomes the remaining width of the basin. With reference to Fig. 25, the surface profiles for stream tubes 1, 2, 3, and 4 are computed.

Considering stream tube W_2 :

1. Start at point A.

The depth, mean velocity and width of the stream tube (just computed) are known.

2. Assume the channel is subdivided downstream of the standing wave into four equal widths, W_D , and project the stream tube boundaries back to the standing wave.

3. Using the standard step procedure, compute the backwater curve for each of the four stream tubes from point A to point B. Determine the depth of flow at point B from back water computations.

4. Use the relationship $y_2/y_1 = 3.5$ to estimate depth of flow downstream of the wave.

5. Estimate the velocity of the flow downstream of the standing wave, $V = \frac{Q/8}{W_D y_2}$.

6. Continue the backwater computations in the downstream direction using y_2 , W_D , and V from Step 5.

7. Periodically check the depth of flow from tube to adjacent tube to insure the depths are approximately equal. If they are not, average the depths and use this new depth in the computations.

8. From point C on downstream, the backwater curve is assumed common for all tubes. The location of the jump for this point on downstream (or the estimate of exit velocity from the basin) is routine. An example is presented in Reference 5, page 403.

The basin must be designed in such a way that the jet will not be totally submerged (for basins with high tailwater see Chapter V). The flow must plunge and spread so that a high Froude number jump can occur. To insure this, the invert of the pipe at the outlet section must be set sufficiently high. In addition, the walls of the basin must be higher than the tailwater so that water cannot flow over the walls, flow back toward the outlet and spill into the basin and submerge the jet which allows the jet to continue through the basin.

From the previous calculations it can be seen that the problem is to apply a certain force to the water in order to induce a hydraulic jump. This may be done in a variety of ways. Smooth-floor flared and smooth-floor rectangular basins depend on bed shear to produce this force. In those situations where loss of control of tailwater elevation, or perhaps greater control of the position of the jump is necessary it may be desirable to use a sill or other obstruction to help the jump form (19). The hydraulic considerations necessary for such design are covered in detail in (5) and (20).

C - Rough-floor Rectangular Basin, (Fig. 38)

<u>Given</u>	Design discharge	$Q = 420$ cfs
	6 ft x 6 ft box	$W_o = 6$ ft
	Depth of flow at outfall of box	$y_o = 4$ ft

Designer's choice: $\frac{W_2}{W_0} = 4, \frac{y}{a} = 1.1, 6$ rows
of elements, working with $1/2$ of the basin,

$$\frac{W_2}{W_0} = 4, \quad W_2 = 4W_0 = (4)(6) = 24 \text{ ft,}$$

$$\frac{Q}{2} = 210 \text{ cfs, } y_0 = 4 \text{ ft, } \frac{W_0}{2} = 3 \text{ ft,}$$

$$V_0 = \frac{Q/2}{\text{Area}} = \frac{210}{W_0/2(y_0)} = \frac{210}{(3)(4)} = \underline{\underline{17.5 \text{ fps}}},$$

and

$$F_0 = \frac{V_0}{\sqrt{gy_0}} = \frac{17.5}{\sqrt{(32.2)(4)}} = \underline{\underline{1.54}}.$$

From Fig. 14 $\beta_1 = \underline{\underline{0.65}}$ (assuming $d_t/y_0 = 0$ at the outlet), and

$$\beta_2 = \underline{\underline{1.00}}.$$

From Fig. 5, an estimate of y/y_0 at $x = 2W_0$ is

$$\frac{y}{y_0} = 0.21$$

or

$$y = (0.21)(4) = \underline{\underline{0.84 \text{ ft}}}.$$

Also,

$$\frac{V_a}{V_0} = 1.18$$

and

$$V_a = 1.18 \times 17.5 = 20.6 \text{ fps.}$$

Height of Element a

Designer's choice, $y/a = 1.1$

$y = 0.84$, $y/a = 1.1$; therefore, $a = 0.76$ ft, but use $a = \underline{0.75}$ ft.

Length of Element M

From Fig. 27, $M = \frac{W_2/2}{3.5} = \frac{12}{3.5} = 3.43$ ft.

Area of element = $M(a) = (3.43)(0.75) = \underline{2.57}$ sq ft.

Longitudinal Spacing of Elements J

From Fig. 27 for $y/a = 1.1$, $J/a = 6.0$, and $J = (6.0)(0.75) = \underline{4}$ ft.

Number of Elements N

Count those shown in Fig. 27, $N = \underline{10.5}$

Determine C_D

In Figure 27, for six rows of elements, $y/a = 1.1$, so $C_D = \underline{0.23}$.

The velocity at the outfall of the basin, V_B , is estimated by employing the design equation,

$$\beta_1 \gamma \frac{y_o^2}{2} \frac{W_o}{2} + \beta_2 \rho V_o \frac{Q}{2} = C_D N A \rho \frac{V_a^2}{2} + \beta_3 \rho \frac{Q}{2} V_B + \beta_4 \frac{\gamma (Q/2)^2}{2 V_B^2 W_B/2}$$

In this example,

$$\gamma = 62.4 \text{ lb/ft}^3$$

$$\rho = \frac{1.94 \text{ slug}}{\text{ft}^3}$$

$$C_D = 0.23$$

$$\beta_1 = 0.65$$

$$\beta_2 = 1.00$$

$$\beta_3 = \beta_4 = 1 \text{ (assume uniform flow at the end of the basin)}$$

$$V_o = 17.5 \text{ fps}$$

$$y_o = 4 \text{ ft}$$

$$W_o = 6 \text{ ft}$$

$$W_B = W_2 = 24 \text{ ft}$$

$$Q = 420 \text{ cfs,}$$

so

$$(0.65)(62.4) \frac{(4)^2}{2} \left(\frac{6}{2}\right) + (1.00)(1.94)(17.5)(210) = (0.23)(10.5)(2.57) --$$

$$--(1.94) \frac{(20.6)^2}{2} + (1.94)(210) V_B + \frac{(62.4)}{2} \frac{(210)^2}{V_B \frac{2(24)}{2}},$$

or

$$407 V_B + \frac{114,600}{V_B^2} = 5540 .$$

There are three possible values of V_B , one value is negative and meaningless, the other two are significant. The lower value is associated with subcritical flow, the higher value is the conjugate velocity.

Solving for V_B :

$$V_B \text{ subcritical} = 6.1 \text{ fps and}$$

$$V_B \text{ supercritical} = 11.5 \text{ fps.}$$

The depths of flow at the outfall corresponding to these velocities are

$$d_B = \frac{Q/2}{(W_2/2) V_B},$$

then

$$d_B \text{ subcritical} = \frac{210}{(12)(6.1)} = 2.9 \text{ ft,}$$

and

$$d_B \text{ supercritical} = \frac{210}{(12)(11.5)} = 1.5 \text{ ft .}$$

for basins with $y/a < 1.5$, the jump always occurred within the angle field. If insufficient tailwater existed, the flow passed back through the critical depth resulting in supercritical flow in the channel downstream of the basin.

If tailwater is less than 1.5 ft, flow will be supercritical and the outfall velocity will be about 12.0 fps. If tailwater is 2.9 ft or higher (in most cases a natural channel will not carry 420 cfs at a depth less than this), the exit velocity will be about 5.9 fps or less.

If the exit velocity and depths are satisfactory, the basin dimensions are:

$$\text{Length} = 2W_o + 5 J + 1 J \text{ (Add } J \text{ downstream of last row of elements)}$$

$$= (2)(6) + (5)(4) + 4 = 36 \text{ ft}$$

$$\text{Width} = (4)(W_o) = (4)(6) = 24 \text{ ft}$$

$$\text{Height of basin walls} = d_B \text{ subcritical} + \text{freeboard}$$

$$= 2.9 + 1.5 = 4.4 \text{ ft.}$$

Size of element: 0.75 ft x 3.43 ft

Number of elements required: $2 \times 10.5 = 21$

Longitudinal spacing of elements = 4 ft

Lateral spacing of elements = $2 M = \underline{\underline{6.8 \text{ ft} .}}$

If V_B deduced from the design equation is close to critical velocity (this was not the case in the example solved above) and the tailwater depth downstream of the basin is, coincidentally, near critical depth, an unstable water surface with standing waves is probable. If tailwater depth is near critical, the basin should be redesigned in such a way as to insure adequate depth. Widening the basin or lowering the downstream portion of the basin are two effective means of attaining a suitable depth. The latter solution is generally more economical.

Even though V_B is near critical velocity, this does not imply that the exit velocity from the basin is near critical velocity. What it does imply is that the momentum of the flow has been reduced to the minimum level possible for the particular combination of discharge and basin width. If the tailwater depth is near critical depth, the exit velocity will be near critical velocity. If the tailwater depth is larger than critical depth the exit velocity will be subcritical. If the tailwater depth is less than critical velocity the exit velocity will be supercritical.

One other problem exists, the problem of rooster tails of water downstream of the first two rows of elements. Referring to Fig. 39, a method of estimating the trajectory of the rooster tails is shown. The method is based on the energy equation.

At the first row of elements, using the criteria of Fig. 5,

$$V = (1.07)(17.5) = 18.7 \text{ fps.}$$

Also, $y/y_0 \approx 0.1$, $y = (0.1)(4) = 0.40 \text{ ft}$, i.e., $d_1 = \underline{0.40 \text{ ft}}$.

The vertical height of the jet trajectory is approximately

$$y = V_{oy}(t) - 1/2 g(t)^2 .$$

Assume $\phi = 45^\circ$,

$$V_{ox} = V_o \cos 45^\circ = (18.7)(0.707) = 13.2 \text{ fps,}$$

$$V_{oy} = V_o \sin 45^\circ = 13.2 \text{ fps .}$$

Determine t @ $y = 0$

$$0 = 13.2(t) - \frac{32.2}{2} t^2$$

or

$$t = 0.82 \text{ sec .}$$

$$\text{Then, } y_{\max} \approx V_{oy} \left(\frac{t}{2}\right) - \frac{1}{2} g \left(\frac{t}{2}\right)^2$$

$$= (13.2)(0.41) - \frac{1}{2} (32.2)(0.41)^2$$

$$= 5.4 - 2.7 = 2.7 \text{ ft .}$$

The maximum height of the top of the water above the floor is:

$$a + y_{\max} + \text{depth of flow or } d_1 = 0.75 + 2.7 + 0.4 = \underline{\underline{3.85 \text{ ft.}}}$$

The distance to y_{\max} is

$$x = V_{ox} \left(\frac{t}{2}\right) = (13.2)(0.41) = \underline{\underline{5.4 \text{ ft.}}}$$

By superimposing these values on the plan of the basin (Fig. 39) it can be determined if the walls are high enough to contain the (rooster tails) jets.

D - Rock Riprapped Basins

This example considers culverts with (1) plain outlet, mild slope and an M2 water surface profile; (2) plain outlet, steep slope and S2 profile; and (3) metal end sections.

1. Plain outlet, mild slope (M2 profile) -

<u>Given</u>	Slope	S = 1.7%
	Discharge	Q = 680 cfs
	Pipe	1 - 108" SPP, D = 9.0 ft
	Tailwater	$d_t = 3.6$ ft
	Brink depth	$y_o = 5.3$ ft
	Natural channel properties	Sketch A

Note: W_a is defined by the expression $W_a = \frac{Q}{d_t V_{ch}}$, in which V_{ch} is the average velocity in the channel for any flow rate, Q.

The flow parameters at the outlet are:

$$\frac{Q}{D^{2.5}} = \frac{680}{9^{2.5}} = \frac{680}{243} = 2.80 \text{ cfs/ft}^{5/2}$$

$$\frac{d_t}{D} = \frac{3.6}{9} = 0.40$$

$$\frac{d_t}{y_o} = \frac{3.6}{5.3} = 0.68$$

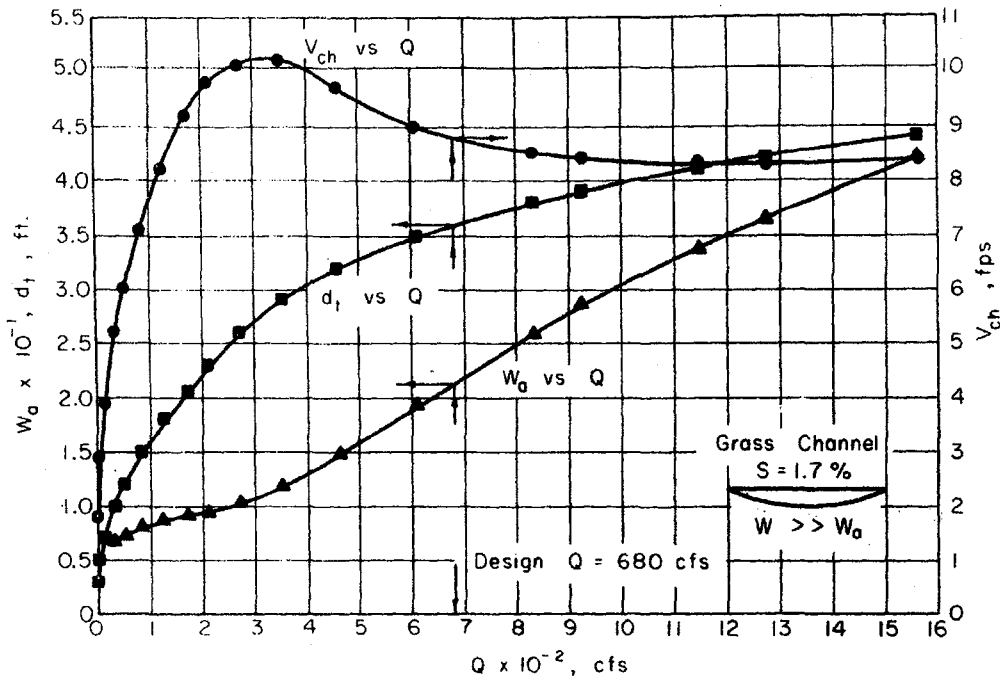
$$\frac{y_o}{D} = \frac{5.3}{9} = 0.59$$

The above value of y_o/D should be checked with that given in Fig. 17.

For

$$\frac{Q}{D^{2.5}} = 2.80 \text{ cfs/ft}^{5/2}$$

and



Sketch A

$$\frac{d_t}{D} = 0.40 .$$

Figure 17 indicates that for a mild sloping pipe (M2 backwater curve)

$$\frac{y_o}{D} = 0.59 .$$

Thus, Figs. 48 to 52 can be used without the modification that is required for steep-sloping pipe.

Computation of the depth of scour

From the data in Figs. 48, 50, and 51, the depth of scour d_s , is found for various mean rock diameters, d_m .

$\frac{d_m}{D}$	d_m ft	$\frac{d_s}{D}$	d_s ft	Reference
.049	0.44	1.80	16.2	Fig. 48, see below.
.0945	0.85	0.61	5.5	Fig. 50
.205	1.85	0.0	0	Fig. 51

The depth of scour for the $d_m/D = 0.049$ can be found in Fig. 48 by converting the flow parameter, $Q/D^{2.5}$, into an equivalent flow in a box culvert. (See Appendix E for a more complete explanation).

From Fig. 64, for

$$\frac{y_o}{D} = 0.59 ,$$

$$\frac{Q/W_o H_o^{3/2}}{Q/D^{2.5}} = 1.26 .$$

Therefore, the equivalent box culvert flow is

$$\frac{Q}{W_o H_o^{3/2}} = 1.26 \times 2.80 = 3.53 \text{ cfs/ft}^{5/2}$$

for the same relative brink depth; i.e.,

$$\frac{y_o}{H_o} = \frac{y_o}{D} = 0.59 .$$

Then, from Fig. 48,

$$\frac{d_s}{H_o} = \frac{d_s}{D} = 1.80$$

for

$$\frac{d_t}{H_o} = \frac{d_t}{D} = 0.40 .$$

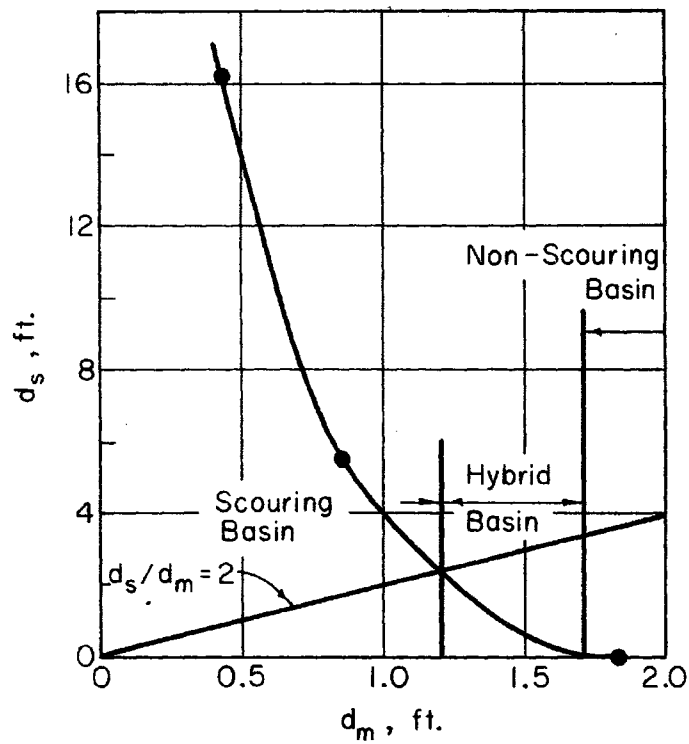
Hence,

$$\frac{d_s}{D} = 1.80$$

and

$$d_s = 1.8 \times 9 = 16.2 \text{ ft.}$$

Plot d_s versus d_m .



Sketch B

Computation of the length of the scour hole

In Fig. 53, the multiplication factor for a slope of 1.7% is

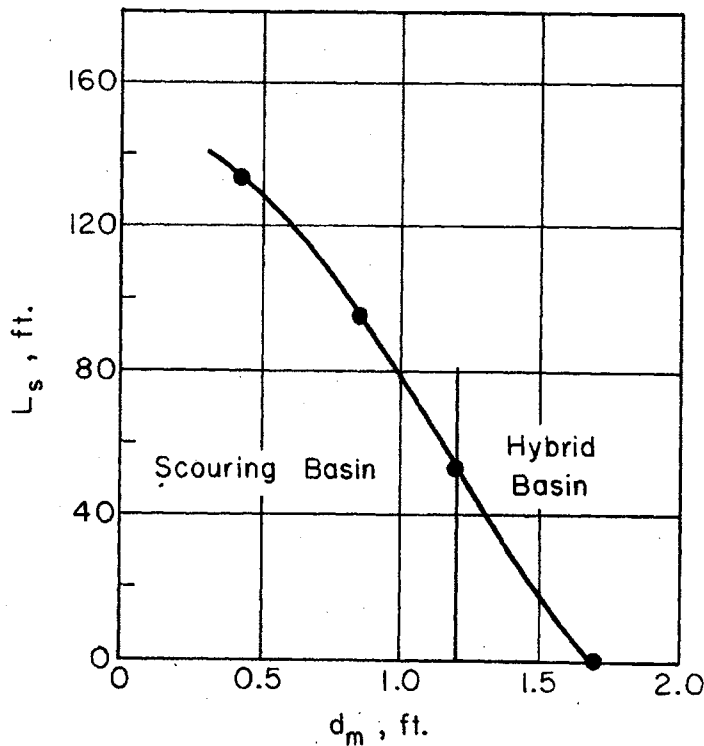
$$M = 1 + 0.05 \times 1.7 = 1.085.$$

Also, recall that

$$\frac{d_t}{y_o} = 0.68 .$$

d_s ft	d_m ft	$\frac{d_s}{d_m}$	$\frac{L_s/d_s}{d_t/y_o}$ from (Fig. 53)	M	$\frac{L_s/d_s}{d_t/y_o}$	$\frac{L_s}{d_s}$	L_s ft
16.2	0.44	37	11		12	8.2	133
5.5	0.85	6.5	23.5		25.5	17.3	95
2.4	1.20	2.0	30		32.6	22.1	53
0.0	1.70	0	0		0	0	0

Plot L_s versus d_m .



Sketch C

Computation of the required length of the basin

When no long-term degradation is anticipated, the length of the basin, L , is given by the expression

$$\frac{L}{d_m} = 1.9 \frac{L_s}{d_m}, \quad \text{see Fig. 54}$$

provided $d_s/d_m \geq 2.0$.

d_m ft	L_s ft	L ft	Reference
0.44	133	253	Fig. 54
0.85	95	181	Fig. 54
1.20	53	101	Fig. 54
1.70	-	62.5	* Fig. 58

For the rock size that does not scour ($d_m = 1.7$ ft), the length of the basin will depend on the maximum allowable average velocity in the downstream channel (V_{ch}). * Figure 58 is valid for pipes in which the flow profile at the outlet is an M2 backwater profile.

$$\text{For } d_t/y_o = 0.68,$$

$$\tan\theta = 0.10.$$

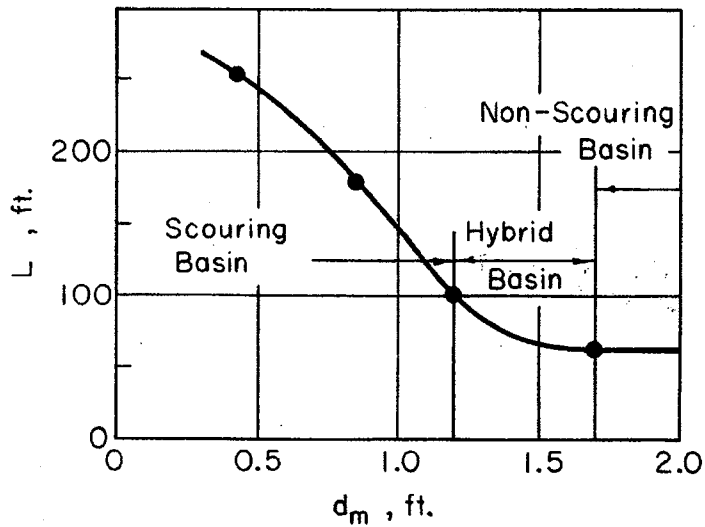
The depth, at the distance L , downstream of the culvert outlet is

$$y = d_t$$

if it is assumed that d_t is the normal depth for the design discharge. Then the average velocity at L will be V_{ch} if the basin is terminated at

$$\begin{aligned}
 L &= \frac{1}{2 \tan \theta} \left(\frac{Q}{d_t V_{ch}} - D \right) \\
 &= \frac{1}{0.2} \left(\frac{680}{8.8 \times 3.6} - 9 \right) \\
 &= 5 (21.5 - 9) \\
 &= 62.5 \text{ ft.}
 \end{aligned}$$

Plot L versus d_m .



Sketch D

Computation of the width of the scour hole and basin

The width of the scour hole, W_s , is obtained from Fig. 55 and the width of the basin apron, W_b , is given by the equation

$$W_b = W_s + 2D.$$

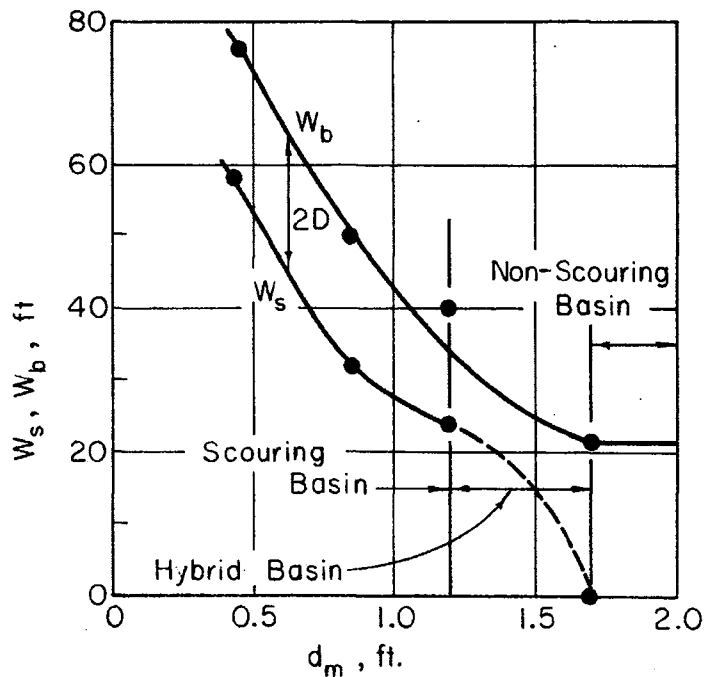
d_s ft	d_m ft	$\frac{d_s}{d_m}$	$\frac{W_s}{d_m}$	W_s ft	W_b ft	Reference
16.2	0.44	37	134	58	76	Fig. 55
5.5	0.85	6.5	38	32	50	Fig. 55
2.4	1.20	2.0	18	22	40	Fig. 55
0.0	1.70	0	-	-	22	*

For $d_m \geq 1.70$ ft

there is no scour and the width of the basin, W_b , at a distance L downstream of the pipe outlet is

$$\begin{aligned}
 *W_b &= 2L \tan\theta + D \\
 &= 2 \times 62.5 \times 0.10 + 9 \\
 &= 12.5 \times 9 \\
 &= 21.5 \text{ ft.}
 \end{aligned}$$

Plot W_s and W_b versus d_m .



Sketch E

Also, Sketch E gives the basin width at the termination point of the hybrid basin by locating a smooth curve through the plot of W_b versus d_m for scouring d_m and joining that curve to W_b at $d_m = 1.70$ ft.

From Sketches D and E, it is seen that the non-scouring basin is shorter and narrower than the scouring basin. Since it does not scour, less rock is needed in the apron.

Computation of the volume of rock required

The volume of rock required in each of the three standard basins (scouring, non-scouring, and hybrid) is found by employing the equations developed in Section 4.3.

Assume that:

- a. $z_1 = 4$, i.e., embankment slope is 4:1;
- b. $z_2 = 1.5$, i.e., side slope is 3:2; and
- c. $z_3 = 2.0$, i.e., end slope is 2:1.

Let

$$f = \frac{d_m}{d_{100}} = 2$$

$$E = A = hd_m, \text{ the minimum recommended}$$

$$h = 2.$$

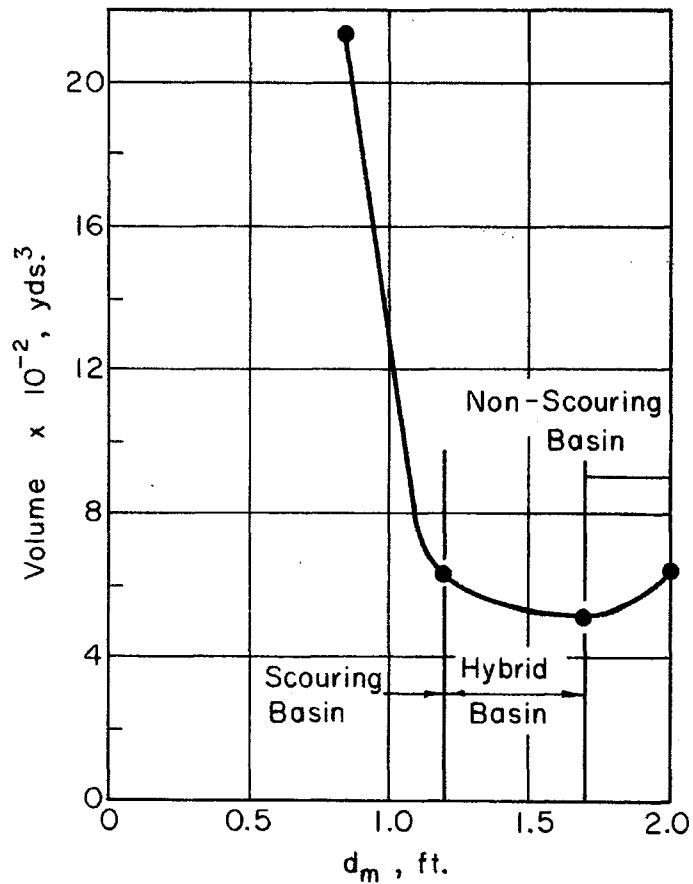
Also $F = y_o = 5.4$ ft.

d_m ft	Apron	End slope	Volume of riprap required, ft ³			Total	Reference Section
			Embankment slope	Under slope	Side slope		
2.00	3820	770	560	300	11750	17,200	4.3, Non-scouring
1.70	3240	560	470	210	9420	13,900	4.3, Non-scouring
1.20	6990	810	340	210	8620	16,970	4.3, Hybrid
0.70	41400	320	4100	1260	10520	57,600	4.3, Scouring

The volumes are converted to units of cubic yards.

$\frac{d_m}{ft}$	ft^3	<u>Volume</u> yds^3
2.00	17,200	637
1.70	13,900	515
1.20	16,970	628
0.70	57,600	2,130

Plot volume versus d_m .



Sketch F

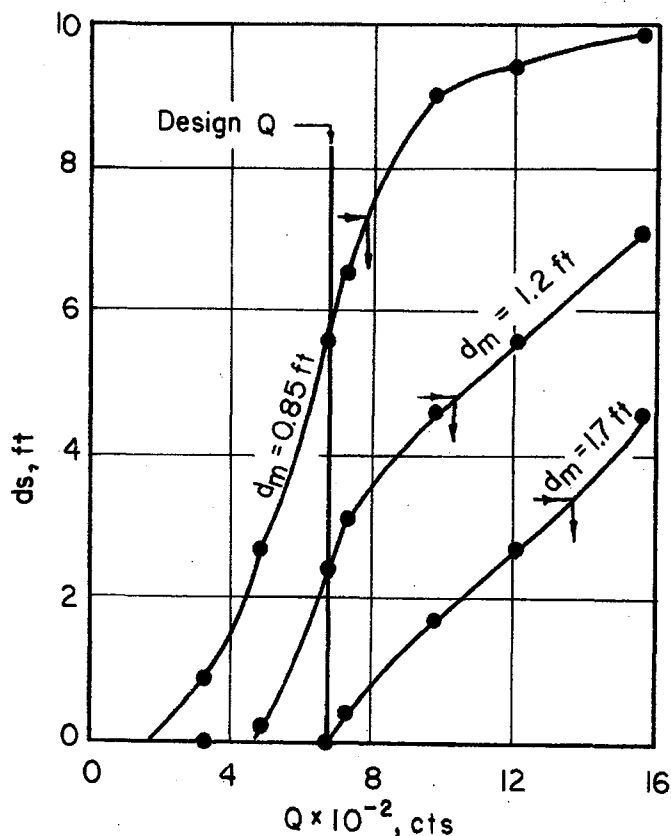
The minimum-volume basin is obtained if a rock size of $d_m = 1.70$ ft is chosen. The smallest rock that should be considered is $d_m = 1.20$ ft.

The effect of a change in design discharge

If a flood greater than the design flood should occur, each of the above standard basins would be damaged. The next step is to establish the effect of higher discharges on the basin.

For the three possible rock sizes, $d_m = 0.85, 1.20,$ and 1.70 ft, the scour depths for the various discharges are found in the same manner as for those in Sketch B. In Sketch G, the scour depth is plotted against discharge. For purposes of illustration it has been assumed that the flow in the barrel is subcritical for all discharges.

One measure of the safety of the rock basin is the inverse of the ratio of the design discharge, Q_d , to that discharge, Q_f , which would scour the apron down to the original channel material. The depth of material in each of the three basins is $d_s + A = d_s + 2d_m$ in this example.



Sketch G

d_m ft	d_s ft	$d_s + A$ ft	Q_d cfs	Q_f^* cfs	Q_f/Q_d
0.85	5.5	7.2	680	785	1.15
1.20	2.4	4.8	680	1035	1.52
1.70	0	3.4	680	1375	2.02

*From Sketch G

One achieves more security from failure due to larger than design discharges with the 1.70 ft rock ($Q_f/Q_d = 2.02$). The 1.20 ft rock is acceptable but only a 15 percent increase over the design discharge would scour through the apron of the 0.85 ft rock. Therefore, the basin should be designed with rock in the range

$$1.2 \text{ ft} \leq d_m \leq 1.7 \text{ ft}$$

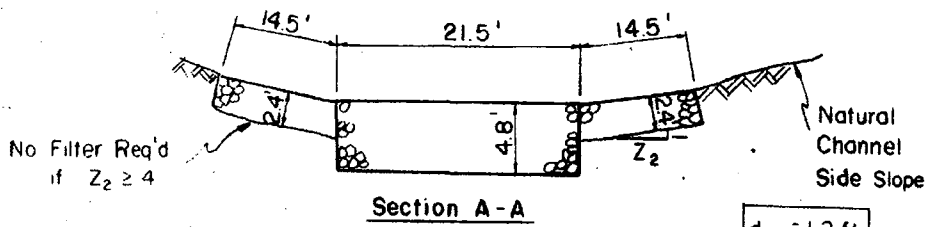
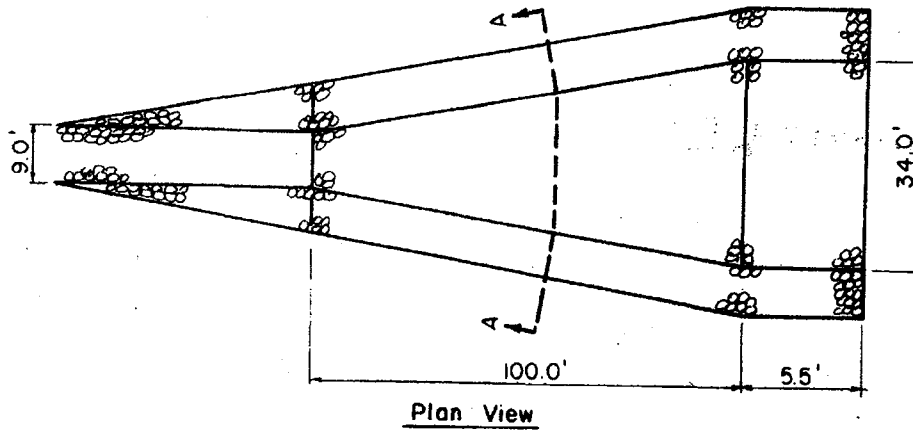
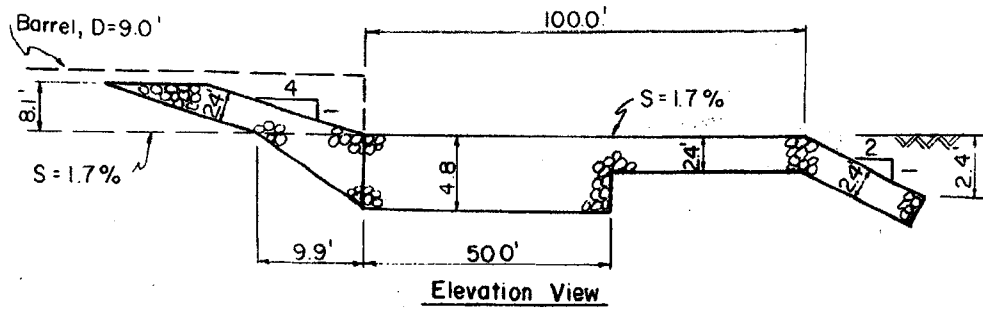
for minimum volume of riprap and maximum safety.

The recommended basins

In this design example, the volume of rock in the side slopes was calculated assuming a side slope of 1.5:1; the side slope was to extend up from the level of the apron to a vertical height $1.5 \times y_0$ above the apron. When natural-channel side slopes are less than 1.5:1, it is recommended that the same volume of rock be placed on the natural-channel side slope. Furthermore, when the side slope is 4:1 or less, no filter should be required under the side slope material.

An example of an acceptably graded rock is given in Fig. 57. The dimensions of the two recommended basins are given in Sketch H and I.

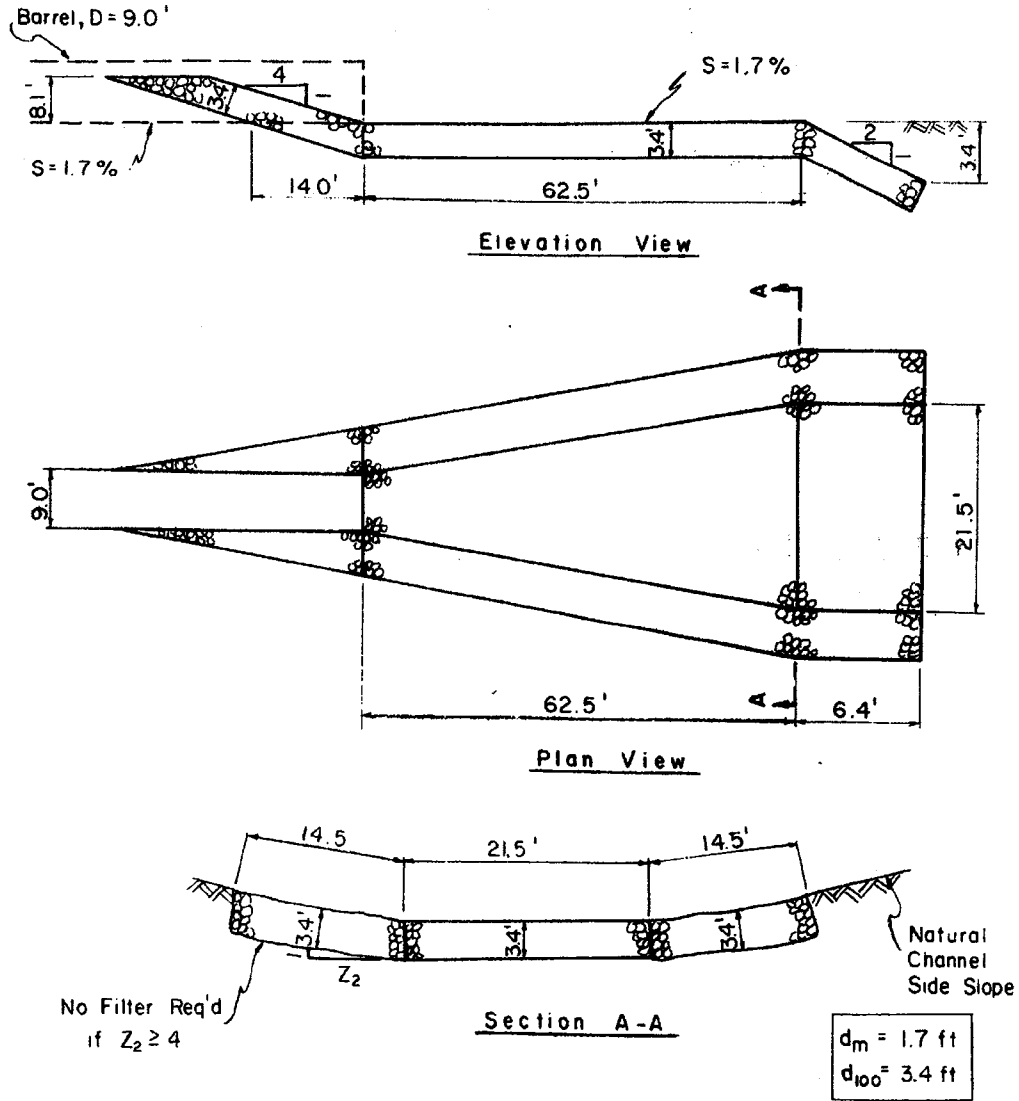
Dimensions of the basin when $d_m = 1.2$ ft



$d_m = 1.2$ ft
 $d_{100} = 2.4$ ft

Sketch H

Dimensions of a basin when $d_m = 1.7$ ft



Sketch I

2. Plain Outlet Steep Slope (S2 profile)

To illustrate the solution to the steep-sloping pipe problem, one example is presented.

<u>Given</u>	Slope	$S = 5\%$
	Discharge	$Q = 680 \text{ cfs}$
	Pipe	1 - 108" SPP, $D = 9.0 \text{ ft}$
	Tailwater	$d_t = 3.6 \text{ ft}$
	Brink depth	$y_o = 4.5 \text{ ft}$
	Natural channel properties,	Same as Sketch A for

the plain outlet within mild slope examples.

Computation of the flow parameters at the outlet

The flow parameters at the outlet are:

$$\frac{Q}{D^{2.5}} = \frac{680}{9^{2.5}} = 2.80 \text{ cfs/ft}^{5/2}$$

$$\frac{d_t}{D} = \frac{3.6}{9} = 0.40$$

$$\frac{d_t}{y_o} = \frac{3.6}{4.5} = 0.80$$

$$\frac{y_o}{D} = \frac{4.5}{9.0} = 0.50$$

$$A_o = \frac{1}{2} \times \frac{\pi D^2}{4} = \frac{\pi}{8} \times 81 = 31.8 \text{ ft}^2$$

$$V_o = \frac{Q}{A_o} = \frac{680}{31.8} = 21.4 \text{ fps}$$

$$\frac{V_o}{\sqrt{g y_o}} = \frac{21.4}{\sqrt{g \times 4.50}} = 1.78$$

Because the value of y_o/D is less than that given in Fig. 17, Figs. 48 to 52 cannot be used without modifications.

Computation of the depth of scour

First, it is necessary to convert the flow parameter $Q/D^{2.5}$ to an equivalent $Q/D^{2.5}$ for a pipe flowing full with

$$y_o = D = 4.5 \text{ ft,}$$

$$V_o = 21.4 \text{ fps}$$

and

$$d_t = 3.6 \text{ ft .}$$

The equivalent $Q/D^{2.5}$

$$= (21.4 \times \frac{\pi}{4} \times 4.5^2) / 4.5^{2.5}$$

$$= \frac{\pi}{4} \times \frac{21.4}{\sqrt{4.5}}$$

$$= 7.93 \text{ cfs/ft}^{5/2}$$

$$\frac{d_t}{D} = \frac{3.6}{4.5} = 0.80.$$

The equivalent box culvert would have an equivalent

$$\frac{Q}{W_o H_o^{3/2}} = 7.93 \times 1.275 = 10.1 \text{ cfs/ft}^{5/2}$$

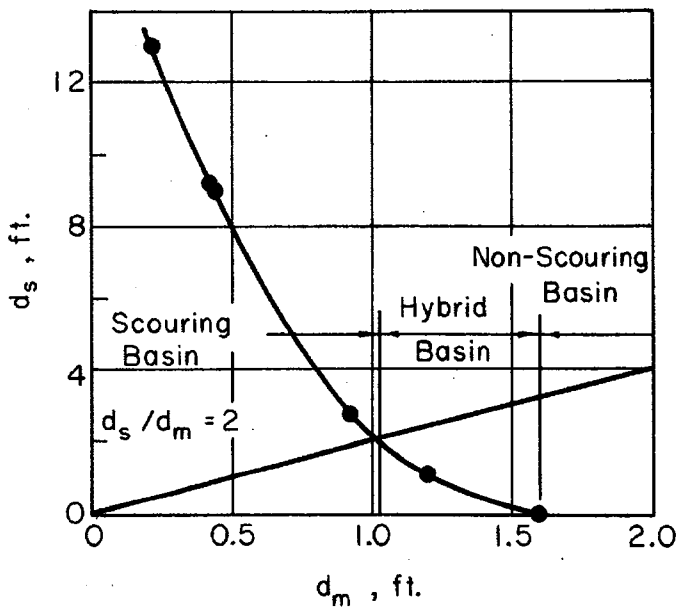
and

$$\frac{d_t}{H_o} = \frac{3.6}{4.5} = 0.80.$$

$\frac{d_m}{H_o}$	d_m ft	$\frac{Q}{W_o H_o^{3/2}}$ cfs/ft ^{5/2}	$\frac{d_s}{H_o}$	d_s ft	Reference
.049	.220	10.1	2.9	13.0	Fig. 48
.0975	.438	10.1	2.0	9.0	Fig. 49

$\frac{d_m}{D}$	d_m ft	$\frac{Q}{D^{2.5}}$ cfs/ft ^{5/2}	$\frac{d_s}{D}$	d_s ft	Reference
.0945	.425	7.93	2.04	9.2	Fig. 50
.205	.923	7.93	.60	2.7	Fig. 51
.264	1.19	7.93	.25	1.1	Fig. 52

Plot d_s versus d_m and extrapolate to find d_m for $d_s = 0.0$ ft;
Sketch A.



Sketch A

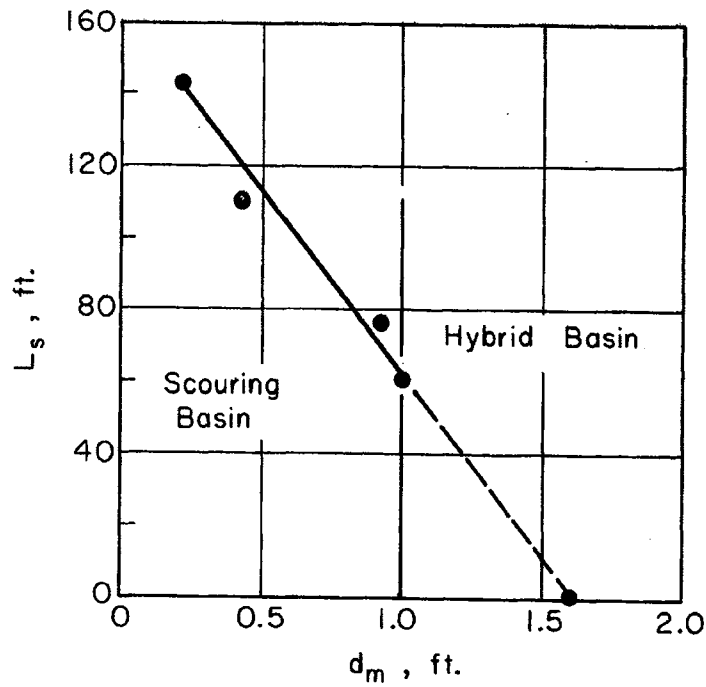
Computation of the length of the scour hole

In Fig. 53, the multiplication factor for a slope of 5.0% is

$$M = 1 + 0.05 \times 5 = 1.25 .$$

d_s ft	d_m ft	$\frac{d_s}{d_m}$	$\frac{L_s/d_s}{d_t/y_o}$ (Fig. 53)	$\frac{ML_s/d_s}{d_t/y_o}$	$\frac{L_s}{d_s}$	L_s ft
13.0	.22	59	11	13.7	11	143
9.2	.425	21.6	12	15.0	12	110
2.7	.923	2.9	28	35.1	28	76
2.0	1.00	2.0	30	37.5	30	60
0	1.60	0	-	-	0	0

Plot L_s versus d_m .



Sketch B

Computation of the required length of basin

Again, if no long-term degradation is anticipated,

$$\frac{L}{d_m} = 1.9 \frac{L_s}{d_m}, \text{ see Fig. 54 .}$$

d_m ft	L_s ft	L ft	Reference
.220	143	272	Fig. 54
.425	110	209	Fig. 54
.923	76	144	Fig. 54
1.00	60	114	Fig. 54
1.60	-	89.5	Fig. 64 See below

For the non-scouring rock basin ($d_m = 1.60$ ft), the basin length depends on the lateral expansion of the jet. Figure 59 is valid for horizontal and mild-sloping pipes only. Some modification must be made for flow from a steep-sloping pipe.

The value of Froude number, $F_o = V_o / \sqrt{gy_o}$, varies very little with discharge if the horizontal or mild-sloping pipe is partially full (17). The Froude number varies between 1.40 and 1.60. Hence, the curve plotted in Fig. 58 can be considered valid for

$$F_o = 1.50$$

in most cases.

For steep-sloping pipes, $\tan\theta$ is found by the relation

$$(\tan\theta)_r = \left(\frac{1}{F_o}\right)_r$$

which was originally proposed by Blaisdell (2) and later used by Watts (22). The subscript r means the ratio.

In this case,

$$F_o = 1.78$$

$$\frac{d_t}{y_o} = 0.80$$

and for the horizontal pipe

$$\tan\theta = 0.07 .$$

Then, for the steep-sloping pipe,

$$\tan\theta = 0.07 \times \frac{1.50}{1.78}$$

$$= 0.059 .$$

However, as shown in Fig. 59, the minimum $\tan\theta$ that can be obtained when $d_t/y_o = 0.8$ is

$$\tan\theta = 0.07 .$$

Hence, $\tan\theta = 0.07$ is used.

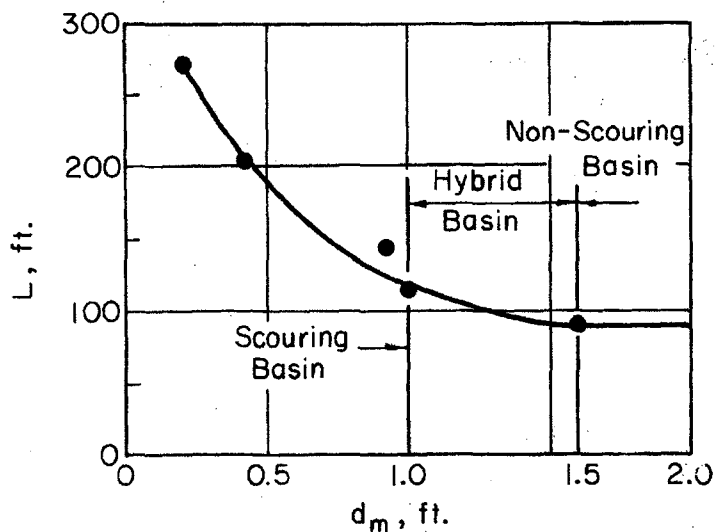
The depth, at the distance L , downstream of the culvert outlet is

$$y = d_t$$

if it is assumed that d_t is the normal depth for the design discharge.

The average velocity (V_{ch}) at L will be 8.8 fps and

$$\begin{aligned}
 L &= \frac{1}{2 \tan \theta} \left(\frac{Q}{d_t v_{ch}} - D \right) \\
 &= \frac{1}{2 \times .07} \left(\frac{680}{3.6 \times 8.8} - 9 \right) \\
 &= 7.15 (21.5 - 9) \\
 &= 89.5 \text{ ft.}
 \end{aligned}$$



Sketch C

Computation of the width of the scour hole and basin

The width of the scour hole, W_s , is obtained from Fig. 55 and the width of the basin apron, W_b , is given by the equation

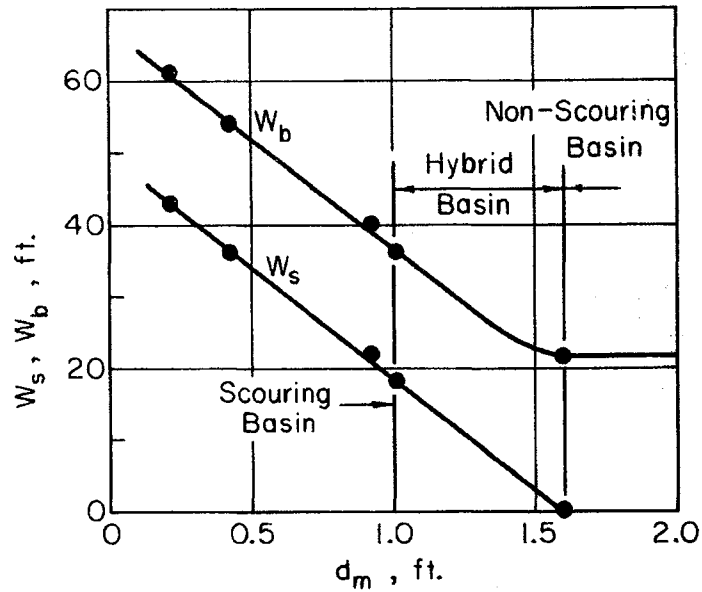
$$W_b = W_s + 2D.$$

d_s ft	d_m ft	$\frac{d_s}{d_m}$	$\frac{W_s}{d_m}$	W_s ft	W_b ft	Reference
13.0	.220	59	195	43	61	Fig. 55
9.2	.425	21.6	85	36	54	Fig. 55
2.7	.923	2.9	23.5	22	40	Fig. 55
2.0	1.00	2.0	18	18	36	Fig. 55
0.0	1.60	0	-	-	21.5	

When $d_m = 1.60$ ft, there is no scour and the basin width at the termination point L ft downstream from the outlet is

$$\begin{aligned} W_b &= 2L \tan\theta + D \\ &= 2 \times 89.5 \times .07 + 9 \\ &= 12.5 + 9 \\ &= 21.5 \text{ ft} \end{aligned}$$

Plot W_s and W_b versus d_m .



Sketch D

Computation of the volume of rock required

In computing the volume of rock required, assume

$$z_1 = 4$$

$$z_2 = 1.5$$

$$z_3 = 2.0$$

and let

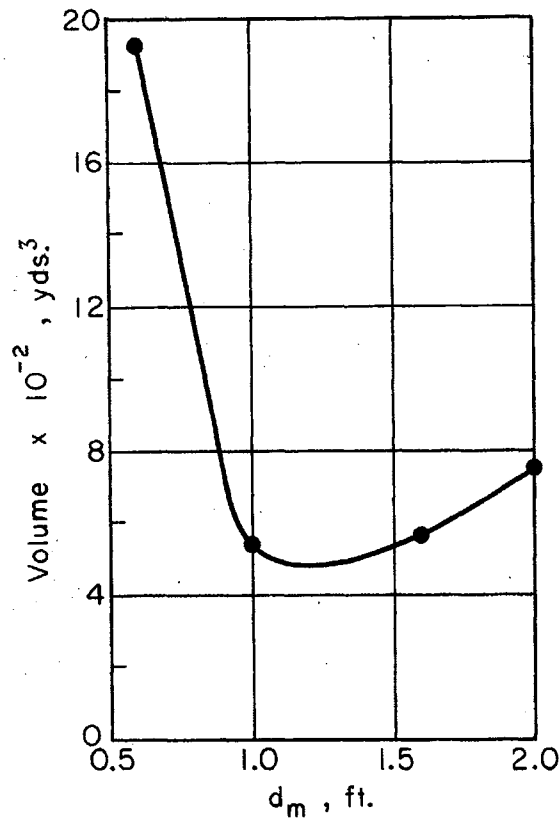
$$f = d_m / d_{100} = 2$$

$$E = A = h d_m = 2 d_m$$

Also let $F = y_o = 4.5$ ft.

d_m ft	Apron	End slope	Volume of riprap required, ft^3				Total Volume yds	Reference Section
			Embankment slope	Under slope	Side slope	Total		
2.00	5490	770	480	300	13100	20140	747	4.3, non-scouring
1.60	4400	490	430	190	9740	15250	565	4.3, non-scouring
1.00	6930	320	240	150	6850	14490	537	4.3, hybrid
.60	42800	160	2260	930	5820	51970	1925	4.3, scouring

Plot volume versus d_m , Sketch E.



Sketch E

Safety of the rock basin

As in the previous example, a measure of the safety of a riprapped basin is the inverse of the ratio of the design discharge, Q_d , to that discharge, Q_f , which would scour the apron down to the original soil material; that is, the Q that would scour a depth

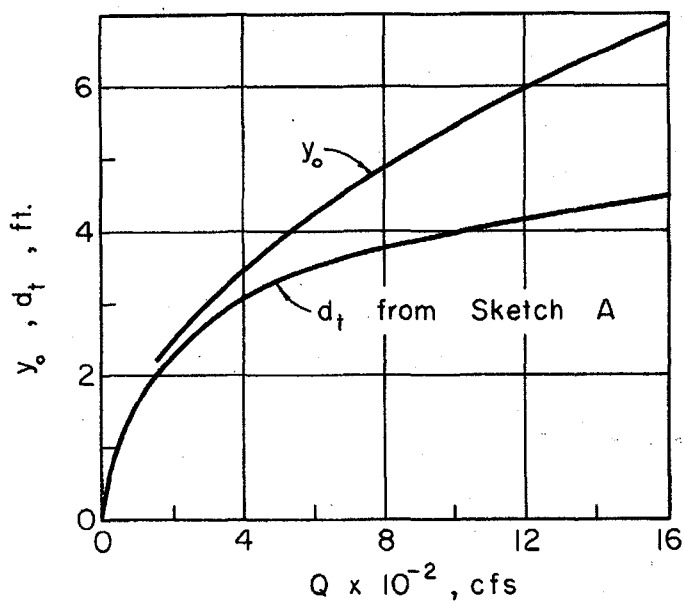
$$d_s + A = d_s + 2 d_m$$

in this example.

It is necessary to compute y_o for different values of discharge through the culvert. It is possible that for some of the selected discharges the flow would no longer be supercritical in the barrel. For this example, assume that y_o and Q are related by the curve drawn in Sketch F. This curve would be established by the designer when he is working with the hydraulics of the inlet and the barrel. Check the d_t/y_o ratio for all discharges up to 1600 cfs and compare with Fig. 17.

Q cfs	d_t ft	y_o ft	$\frac{Q}{D^{2.5}}$ cfs/ft ^{5/2}	$\frac{d_t}{D}$	$\frac{y_o}{D}$	$\frac{y_o}{D}$ (From Fig. 17)	Flow is
200	2.2	2.45	.823	.245	.273	.315	supercritical
400	3.05	3.45	1.64	.339	.384	.455	supercritical
600	3.5	4.2	2.47	.389	.467	.56	supercritical
800	3.75	4.9	3.29	.417	.545	.635	supercritical
1000	4.00	5.4	4.11	.445	.600	.71	supercritical
1200	4.15	5.95	4.94	.462	.662	.77	supercritical
1400	4.3	6.4	5.77	.478	.712	.99	supercritical
1600	4.45	6.9	6.59	.495	.767	>1.00	supercritical

This analysis shows that the flow, in this example, is always supercritical.



Sketch F

Computation of the velocities for various discharges

Q cfs	y_o ft	$\frac{y_o}{D}$	$\frac{A_o}{D^2}$	A_o ft ²	V_o fps
400	3.45	.384	.2778	22.5	17.8
600	4.20	.467	.3597	29.1	20.6
800	4.90	.545	.4377	35.4	22.6
1000	5.40	.600	.4920	39.8	25.1
1200	5.95	.662	.5518	44.7	26.9
1400	6.40	.712	.5982	48.4	29.0
1600	6.90	.767	.6469	52.4	30.5

Computing the equivalent $Q/D^{2.5}$ (see Appendix E), it can be found that $Q/D^{2.5}$ is

$$\frac{V_o \times \frac{\pi}{4} \times y_o^2}{y_o^{2.5}} = \frac{\frac{\pi}{4} V_o}{\sqrt{y_o}}$$

and the equivalent d_t/D is d_t/y_o . Also, the equivalent $Q/W_o H_o^{3/2}$ is the equivalent $Q/D^{2.5} / 1.275$ (Fig. 64), and the equivalent d_t/H_o is d_t/D .

Q cfs	y_o ft	d_t ft	V_o fps	$\frac{Q}{D^{2.5}}$ cfs/ft ^{5/2}	$\frac{d_t}{D}$	Equivalent	
						$\frac{Q}{W_o H_o^{3/2}}$ cfs/ft ^{5/2}	$\frac{d_t}{H_o}$
400	3.45	3.05	17.8	7.5	.88	9.6	.88
600	4.20	3.5	20.6	7.9	.83	10.1	.83
800	4.90	3.75	22.6	8.0	.77	10.2	.77
1000	5.40	4.0	25.1	8.5	.74	10.8	.74
1200	5.95	4.15	26.9	8.7	.70	11.1	.70
1400	6.40	4.3	29.0	9.0	.67	11.5	.67
1600	6.90	4.45	30.5	9.1	.64	11.6	.64

Compute the depth of scour when $d_m/H_o = 0.049$ (Fig. 48) and remember that $H_o = y_o$.

Q cfs	Equivalent		$\frac{d_s}{H_o}$	H_o ft	d_s ft	d_m ft
	$\frac{Q}{W_o H_o^{3/2}}$ cfs/ft ^{5/2}	$\frac{d_t}{H_o}$				
400	9.6	.88	2.6	3.45	9.0	.17
600	10.1	.83	2.9	4.20	12.2	.25
800	10.2	.77	3.1	4.90	15.2	.24
1000	10.8	.74	3.3	5.40	17.8	
1200	11.1	.70	3.45	5.95	20.5	.29
1400	11.5	.67	3.65	6.40	23.3	.35
1600	11.6	.64	3.7	6.90	25.5	.34

Compute the depth of scour for $d_m/D = 0.0945$ (Fig. 50).

Q cfs	Equivalent		$\frac{d_t}{D}$	$\frac{d_s}{D}$	D ft	d_s ft	d_m ft
	$\frac{Q}{D^{2.5}}$ cfs/ft ^{5/2}						
400	7.5		.88	1.75	3.45	6.0	.326
600	7.9		.83	2.0	4.20	8.4	.397
800	8.0		.77	2.1	4.90	10.3	.463
1000	8.5		.74	2.3	5.40	12.4	.510
1200	8.7		.70	2.45	5.95	14.6	.562
1400	9.0		.67	2.55	6.40	16.3	.605
1600	9.1		.64	2.65	6.90	18.3	.652

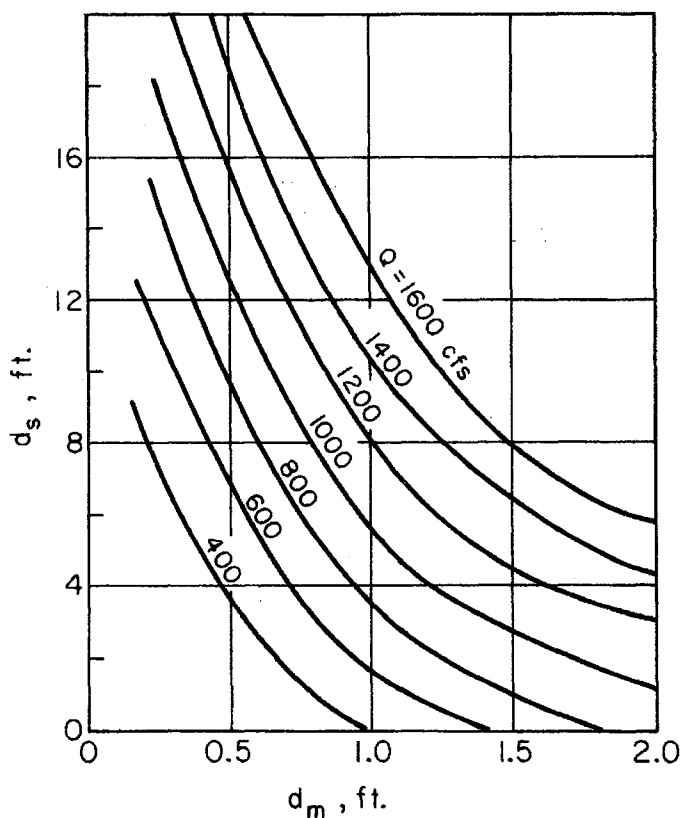
Compute the depth of scour for $d_m/D = .205$ (Fig. 51).

Q cfs	Equivalent		$\frac{d_s}{D}$	D ft	d_s ft	d_m ft
	$\frac{Q}{D^{2.5}}$ cfs/ft ^{5/2}	d_t/D				
400	7.5	.88	.42	3.45	1.5	.707
600	7.9	.83	.56	4.20	2.3	.861
800	8.0	.77	.60	4.90	2.9	1.00
1000	8.5	.74	.85	5.40	4.6	1.10
1200	8.7	.70	1.0	5.95	6.0	1.22
1400	9.0	.67	1.2	6.40	7.7	1.31
1600	9.1	.64	1.25	6.90	8.6	1.41

Compute the depth of scour for $d_m/D = .264$ (Fig. 52).

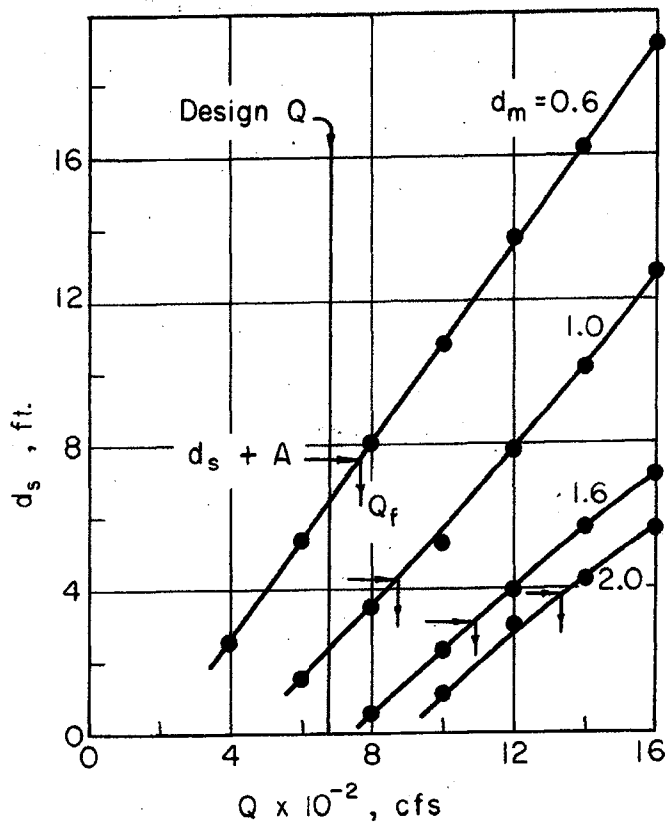
Q cfs	Equivalent $Q/D^{2.5}$ cfs/ft ^{5/2}	d_t/D	$\frac{d_s}{D}$	D ft	d_s ft	d_m ft
400	7.5	.88	.1	3.45	.3	.912
600	7.9	.83	.3	4.20	1.3	1.11
1800	8.0	.77	.45	4.90	2.2	1.29
1000	8.5	.74	.6	5.40	3.2	1.42
1200	8.7	.70	.7	5.95	4.2	1.57
1400	9.0	.67	.85	6.40	5.4	1.69
1600	9.1	.64	.90	6.90	6.2	1.82

Prepare a plot of d_s versus d_m for the various discharges as shown in Sketch G.



Sketch G

Then from Sketch A, a plot of scour depth versus discharge is made for the range of rock sizes that are of interest, i.e., $d_m = 0.6, 1.0, 1.6,$ and 2.0 ft.



Sketch H

From Sketch H, the following tabulation is made:

d_m ft	d_s ft	$d_s + A$ ft	Q_d cfs	Q_f^* cfs	Q_f/Q_d
.60	6.5	7.7	680	770	1.13
1.00	2.4	4.4	680	870	1.28
1.60	0.0	3.2	680	1090	1.60
2.00	0.0	4.0	680	1330	1.96

*From Sketch G.

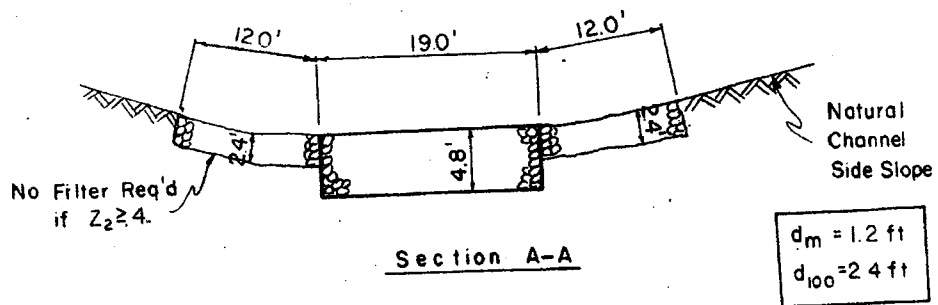
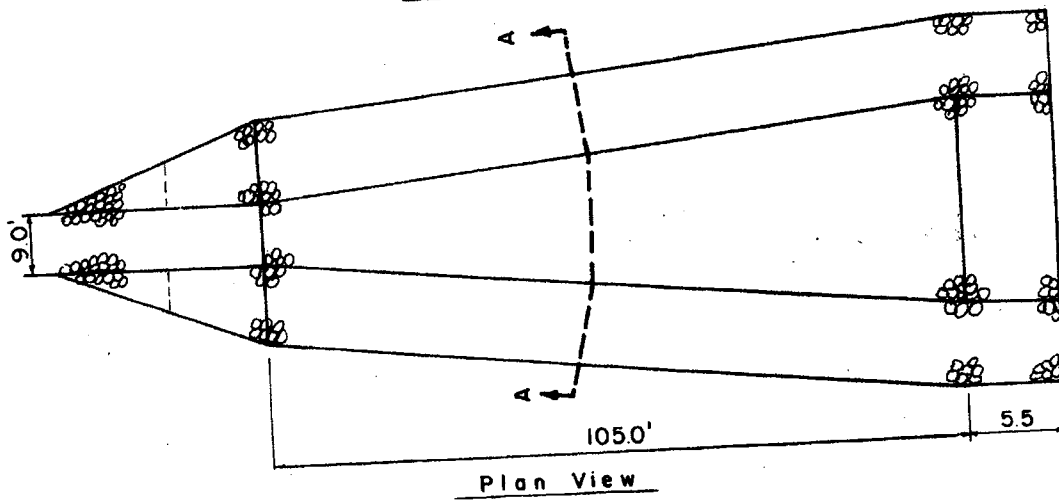
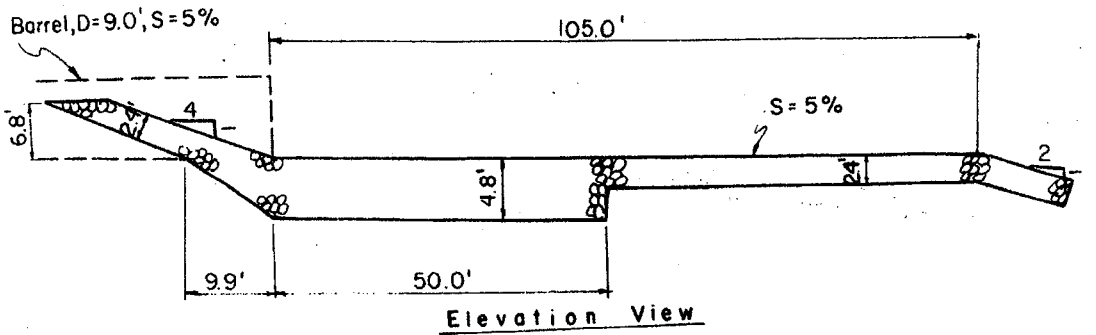
After considering the volume of rock required (Sketch F), the length of the basin (Sketch D), and the factor of safety Q_f/Q_d , it is recommended the rock size be limited to the range

$$1.20 \text{ ft} \leq d_m \leq 1.60 \text{ ft.}$$

Sketches of the recommended basins

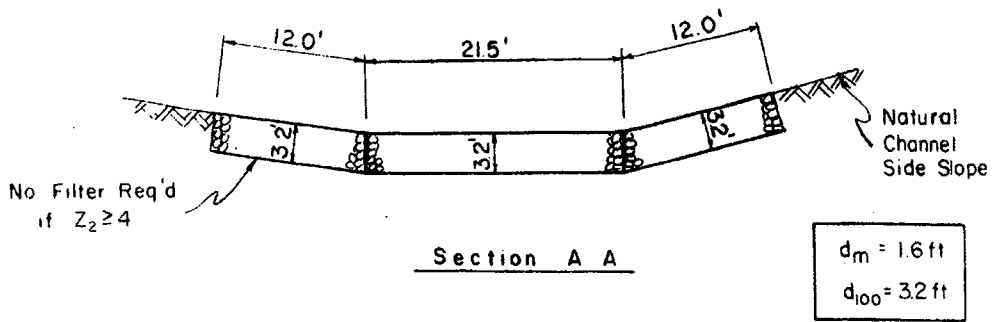
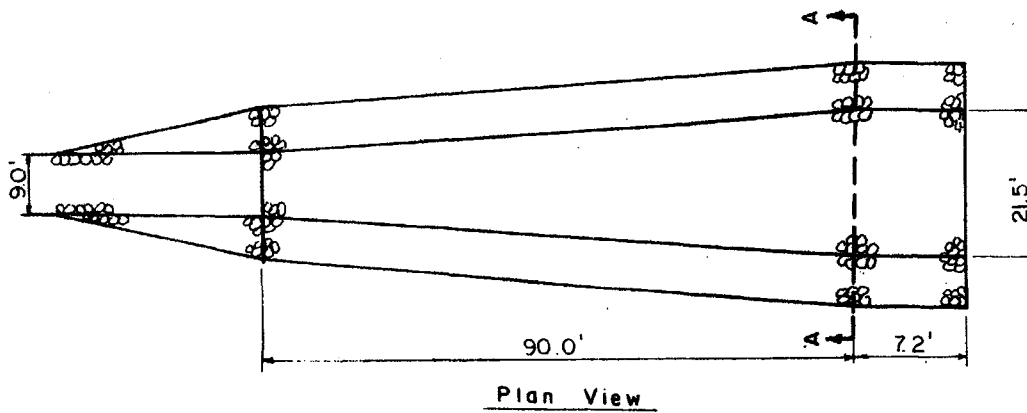
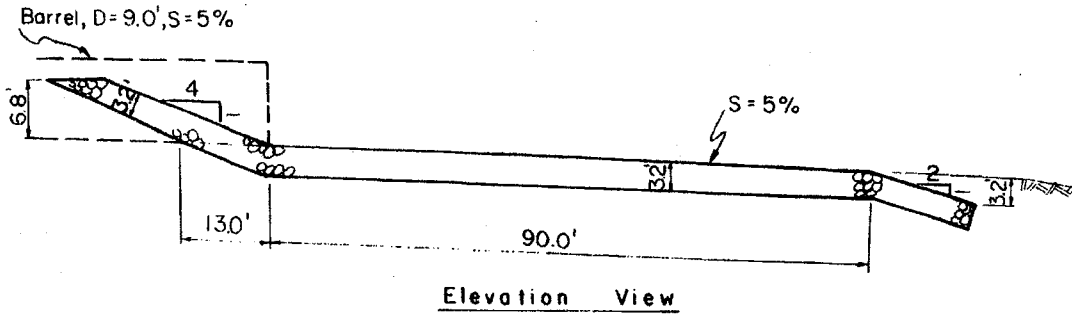
The dimensions of the recommended basins for $d_m = 1.20 \text{ ft}$ and $d_m = 1.60 \text{ ft}$ are drawn in Sketches J and K, respectively. Refer to the design example for the plain circular outlet on a mild slope for comments on the side-slope material.

Dimensions of the basin for $d_m = 1.2$ ft



Sketch J

Dimensions of the basin for $d_m = 1.6$ ft



Sketch K

3. Metal End Section

The metal end section can form an economical transition between the outlet of the barrel and the rock basin. If it is to be employed, an example that illustrates the method of sizing the riprap for the basin can be found in the following example.

Design example illustrating the use of the metal end section

<u>Given</u>	Discharge	$Q = 96$ cfs
	Slope	$S = 1.7\%$
	Pipe diameter	$D = 4$ ft
	Tailwater	$d_t = 1.2$ ft
	Brink depth	$y_o = 2.4$ ft
	Allowable channel velocity	$V_{ch} = 5$ fps

The flow parameters at the outlet can be computed:

$$\frac{Q}{D^{2.5}} = \frac{96}{32} = 3.00 \text{ cfs/ft}^{5/2}$$

$$\frac{d_t}{D} = \frac{1.2}{4} = 0.30$$

$$\frac{y_o}{D} = \frac{2.4}{4} = 0.60$$

From Fig. 17

$$.57 \leq \frac{y_o}{D} \leq .59$$

for $\frac{Q}{D^{2.5}} = 3.00 \text{ cfs/ft}^{5/2}$

and $0 \leq \frac{d_t}{D} \leq 0.3$

so the flow in the pipe has either a M2 or H2 water surface profile.

The limitations (Section 4.4) that

$$\frac{Q}{D^{2.5}} \leq 3.5 \text{ cfs/ft}^{5/2}$$

and

$$\frac{d_t}{D} \leq 0.33$$

have been satisfied so a metal end-section can be used.

Possibility of a hydraulic jump forming in the metal end section

The momentum at the outfall is

$$M_o = \beta_1 \gamma \frac{y_o}{2} A_o + \beta_2 Q \rho V_o$$

and

$$A_o = 7.88 \text{ ft}^2$$

$$y_o = 2.4 \text{ ft}$$

$$\gamma = 62.4 \text{ lb/ft}^3$$

$$\rho = 1.94 \text{ lb sec}^2/\text{ft}^4$$

$$Q = 96 \text{ cfs}$$

$$V_o = 12.2 \text{ fps}$$

$$\beta_1 = 0.54 \quad (\text{From Fig. 15 assuming } d_t/y_o = 0 \text{ at the pipe outlet})$$

$$\beta_2 = 1.02$$

Hence,

$$\begin{aligned} M_o &= 0.54 \times 62.4 \times \frac{2.4}{2} \times 7.88 + 1.02 \times 96 \times 1.94 \times 12.2 \\ &= 318 + 2320 \\ &= 2640 \text{ lb.} \end{aligned}$$

If a jump forms in the end-section the sequent depth would be

$d_t = 1.2 \text{ ft}$, the velocity

$$V_e = \frac{96}{1.2 \times 2 \times 4} = 10 \text{ fps,}$$

and the momentum at the end of the end-section would be approximately

$$\begin{aligned}
 M_e &= 1.0 \times 62.4 \times \frac{1.2}{2} \times 1.2 \times 2 \times 4 \\
 &+ 1.0 \times 96 \times 1.94 \times 10 \\
 &= 360 + 1860 \\
 &= 2220 \text{ lb.}
 \end{aligned}$$

Since $M_o > M_e$, no jump should form in the metal end-section.

Computation of the depth of scour

From Fig. 56, the depth of scour can be determined for two rock sizes:

$$\text{a) } \frac{d_m}{D} = 0.0945,$$

$$d_m = 0.0945 \times 4 = 0.38 \text{ ft,}$$

$$\frac{d_s}{D} = 0.3, \text{ and}$$

$$d_s = 0.3 \times 4 = 1.2 \text{ ft;}$$

$$\text{b) } \frac{d_m}{D} = 0.205,$$

$$d_m = 0.205 \times 4 = 0.82 \text{ ft,}$$

$$\frac{d_s}{D} = 0, \text{ and}$$

$$d_s = 0 \text{ ft.}$$

This is not much scour depth information so the two-dimensional flow approximation (Appendix E) will be employed to help establish the d_s versus d_m curve.

From Fig. 13 it can be seen that

$$\left(\frac{V}{V_o}\right)_{\text{ave}} = 1.65 - 0.45 \frac{Q}{\sqrt{gD^5}}$$

at $\frac{x}{D} = 2$. So, if the end-section is extended out to $2D = 8$ ft

$$\begin{aligned} \left(\frac{V}{V_o}\right)_{\text{ave}} &= 1.65 - 0.45 \times \frac{3.0}{\sqrt{g}} \\ &= 1.65 - 0.24 \\ &= 1.41, \end{aligned}$$

or the velocity leaving the end-section, V_e , would be on the average

$$\begin{aligned} V_e &= 1.41 \times 12.2 \\ &= 17.2 \text{ fps,} \end{aligned}$$

and the depth, y_e , would be

$$\begin{aligned} y_e &= \frac{Q}{2D \times V_e} \\ &= \frac{96}{8 \times 17.2} \\ &= 0.70 \text{ ft.} \end{aligned}$$

Now, the flow from the end of the metal end section can be treated as a box culvert flowing full with

$$\begin{aligned} H_o &= y_e = 0.70 \text{ ft,} \\ W_o &= 2D = 2 \times 4 = 8 \text{ ft,} \\ V_o &= 17.2 \text{ fps,} \\ d_t &= 1.2 \text{ ft, or} \end{aligned}$$

$$\frac{Q}{W_o H_o^{3/2}} = \frac{96}{8 \times 0.70^{3/2}} = 20.5 \text{ cfs/ft}^{5/2}$$

$$\frac{y_o}{H_o} = 1.0$$

$$\frac{d_t}{H_o} = \frac{1.2}{0.7} = 1.7$$

Since none of the curves in Figs. 48 and 49 extends to values of $Q/W_o H_o^{3/2} = 20.5$, Valentin's modified equation (Appendix E) will be employed. It is known that the depth of scour for $d_t/H_o = 1.7$ would be no more than the scour depth for $d_t/H_o = 1$. So, assume

$$\frac{d_t}{H_o} = 1.0, \text{ and}$$

$$F_o = \frac{17.2}{\sqrt{g \times .7}} = 3.62,$$

with

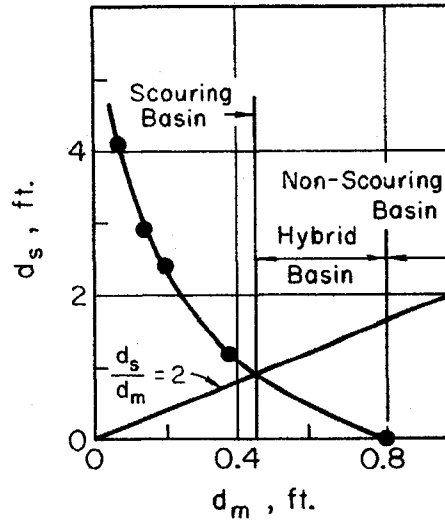
$$\left(\frac{d_s}{H_o}\right) \left(\frac{d_m}{H_o}\right)^{1/2} = e^{\frac{3.62-2}{2.03}} - .373 = 1.85,$$

provided

$$\frac{d_s}{d_m} \geq 10 \text{ to } 15.$$

d_m ft	$\frac{d_m}{H_o}$	$\frac{d_s}{H_o}$	d_s ft	$\frac{d_s}{d_m}$	Comments
.14	.2	4.14	2.9	20.7	OK
.28	.4	2.93	2.05	7.3	Not valid
.07	.1	5.85	4.1	58	OK
.20	.286	3.46	2.42	12.1	OK

The plot of d_s versus d_m .



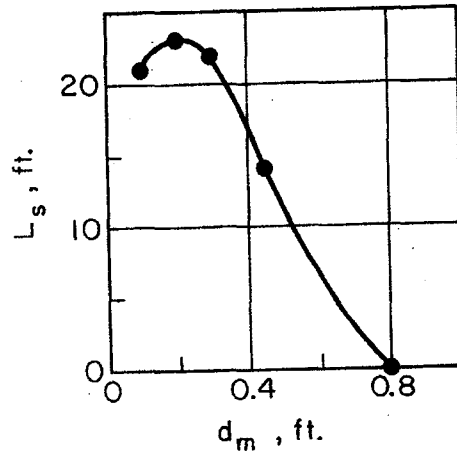
Sketch A

Computation of the length of the scour hole

The curve in Fig. 53 is applicable for metal-end sections. The multiplication factor M is $1.0 + 1.7 \times .05 = 1.085$.

d_m ft	d_s ft	d_s/d_m	L_s/d_s d_t/y_o	$M L_s/d_s$ d_t/y_o	d_t y_o	L_s d_s	L_s ft
0.1	3.5	35	11	12	0.5	6.0	21
0.2	2.4	12	18	19.5	0.5	9.8	23
0.3	1.6	5.3	25	27.1	0.5	13.6	22
0.45	.9	2	30	32.5	0.5	16.3	15

The plot of L_s versus d_m .



Sketch B

Computation of the required length of basin

The equation

$$\frac{L}{d_m} = 1.9 \frac{L_s}{d_m}$$

is valid. Hence,

d_m ft	L_s ft	L ft	Reference
.1	21	40	Equation
.2	23	44	Equation
.3	22	42	Equation
.45	15	28.5	Equation
.8	0	20	See below

Assuming, in the non-scouring basin, that the flow expands over the rock bed at the flare angle of the end-section, the continuity equation indicates that the basin could be terminated at

$$L = \left(\frac{Q}{v_{ch} d^2} - 2D \right) / 2 \tan \theta .$$

The flare angle θ is $17^\circ.4$ so

$$2 \tan \theta = .628 .$$

Hence,

$$\begin{aligned} L &= \left(\frac{96}{5 \times 1.2} - 8 \right) / .628 \\ &= \frac{13.7 - 8}{.628} = 9 \text{ ft.} \end{aligned}$$

However, the high velocity flow exiting from the metal end section must be decelerated by the bed roughness to such an extent that it will flow at a depth of 1.2 ft and at an average velocity of 5 fps; it is doubtful if 9 ft of bed roughness is sufficient to cause the required deceleration. Model studies on the 3-foot diameter pipe indicate that the minimum basin length should be about $8D$ if the basin is rectangular in plan and if the same width as the outlet of the metal end section. However, if the basin is flared at the same angle as the end-section, it does not need to be as long.

In the absence of quantitative data, a flared basin length of $5D$ is the recommended minimum length. One can expect an 80 percent reduction in specific energy between the outlet of the pipe and the end of the rock basin. This reduction was achieved in the models with rectangular rock basins of width $2D$ and for $Q/D^{2.5} \leq 4 \text{ cfs/ft}^{5/2}$.

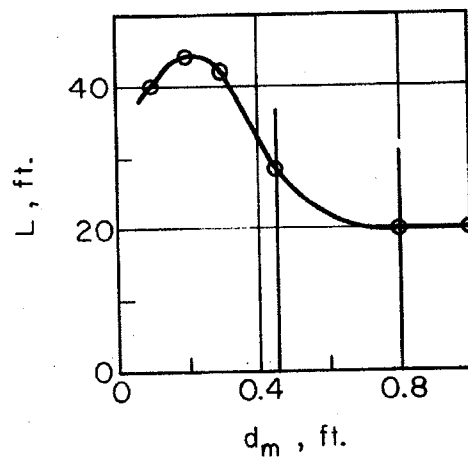
In the example, then, use

$$L = 5D = 5 \times 4 = 20 \text{ ft}$$

when

$$d_m = 0.8 \text{ ft.}$$

The plot of L versus d_m



Sketch C

Computation of the width of the scour hole and basin

The width of the scour hole can be obtained indirectly from Fig. 55 which gives the scour width for plain outlets. With the metal end section, the scour hole is wider by one pipe diameter (the end-section expands, to a width $2D$) than scour below a plain outlet.

Hence,

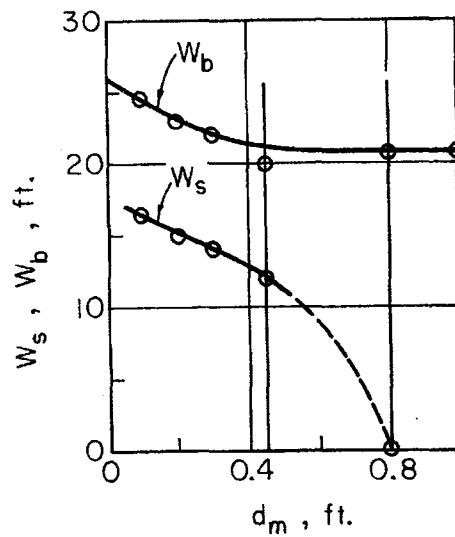
$$W_s \text{ (metal end-section)} = W_s \text{ (Fig. 55)} + D .$$

d_m ft	d_s ft	d_s/d_m	Plain Outlet		Metal end section
			W_s/d_m Fig. 51	W_s ft	W_s ft
.1	3.5	35	125	12.5	16.5
.2	2.4	12	55	11	15
.3	1.6	5.3	34	10	14
.45	.9	2	18	8	12

The recommended basin width, W_b , is the width of the scour hole plus $2D$ for basins that scour. For the rock that does not scour

$$\begin{aligned}
 W_b &= 2D + 2L \tan\theta \\
 &= 8 + 20 \times .628 \\
 &= 20.5 \text{ ft.}
 \end{aligned}$$

The plot of W_s and W_b versus d_m



Sketch D

Computation of the volume of riprap required

Assume that

$$z_1 = 4,$$

$$z_2 = 1.5$$

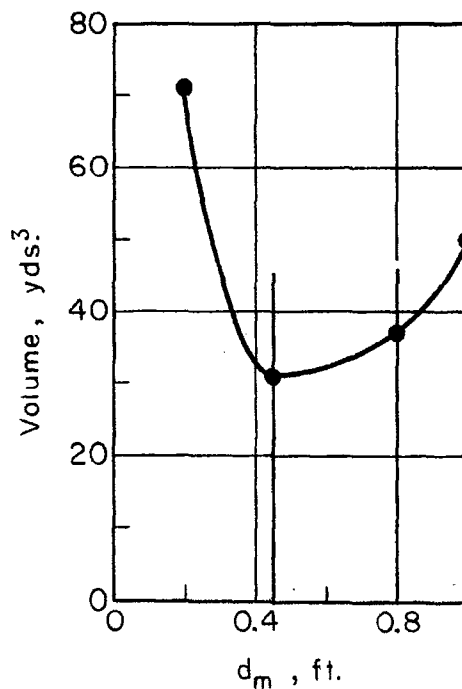
$$z_3 = 2.0,$$

$$f = d_m/d_{100} = 2, \text{ and}$$

$$E = A = hd_m = 2d_m, \text{ and}$$

compute the volume of riprap.

d_m ft	Volume of riprap required, ft ³						Total volume yds ³	Reference section
	Apron	End slope	Embankment slope	Side slope	Under slope	Total		
1.0	570	180	-	590	-	1340	50	4.4 non-scouring
.8	460	120	-	420	-	1000	37	4.4 non-scouring
.45	520	40	-	270	-	830	31	4.4 hybrid
.2	1670	10	50	145	35	1910	71	4.4 scouring

The plot of volume of riprap versus d_m 

Sketch E

The final step would be to compute the safety factor associated with each rock size. The procedure is the same as for the two previous examples and is not repeated here.

E - High Tailwater Non-scouring Basin Design

<u>Given</u>	Discharge	$Q = 330$ cfs
	Pipe diameter	$D = 6$ ft
	Tailwater	$d_t = 6$ ft

The rock size required to prevent scour can be computed:

$$\frac{Q}{D^{2.5}} = \frac{330}{6^{2.5}} = 3.74 \text{ cfs/ft}^{5/2},$$

$$\frac{d_t}{D} = \frac{6}{6} = 1.00,$$

and

$$\frac{y_o}{D} = \frac{6}{6} = 1.00.$$

From Fig. 50 it is apparent that for

$$d_m = 0.0945 \times 6 = 0.57 \text{ ft},$$

$$\frac{d_s}{D} = 0.$$

Computation of the centerline velocities

With a smooth pipe, $K = 1.1$ and

$$\begin{aligned} V_{o \text{ ave}} &= K \frac{Q}{A} \\ &= 1.10 \times \frac{Q}{D^{2.5}} \times \frac{D^{2.5}}{\frac{\pi}{4} D^2} \end{aligned}$$

or

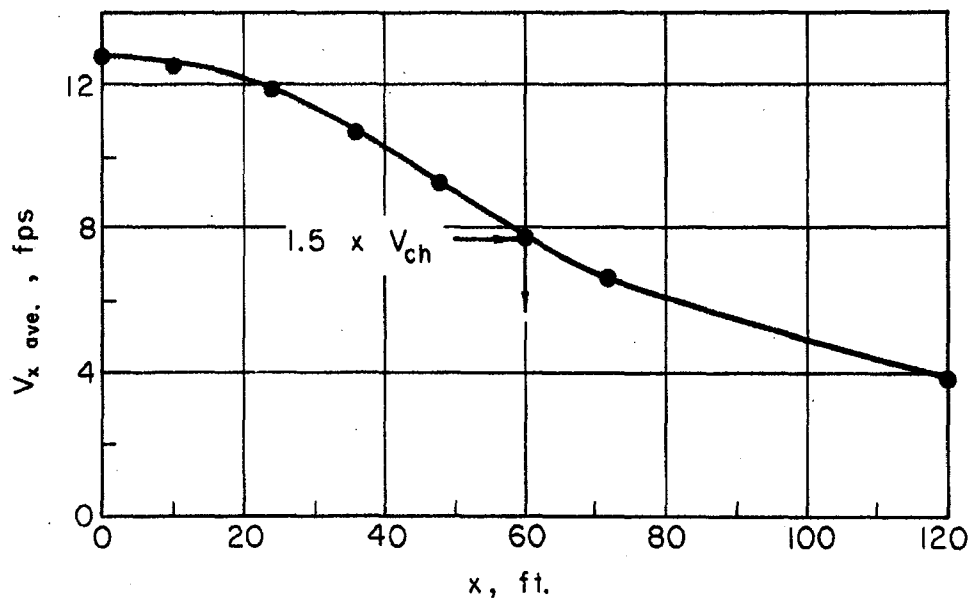
$$\underline{V_o \text{ ave}} = 1.4 \frac{Q}{D^{2.5}} \times \sqrt{D}$$

$$= 1.4 \times 3.74 \times 2.45 = \underline{12.8 \text{ fps.}}$$

x	$\frac{x}{D}$	$\frac{V_{x \text{ ave}}}{V_o \text{ ave}}$	$V_{x \text{ ave}}$
12	2	.98	12.5
24	4	.92	11.8
36	6	.83	10.6
48	8	.72	9.2
60	10	.60	7.7
72	12	.52	6.6
120	20	.30	3.8

Fig. 60

The plot of $V_{x \text{ ave}}$ versus x



Sketch A

Since $V_{x \text{ ave}}$ is the mean vertical velocity on the centerline, the basin can be safely terminated when the allowable average velocity in the natural channel, V_{ch} , is $\frac{2}{3} V_{x \text{ ave}}$.

In the example if

$$V_{ch} = 5.1 \text{ fps,}$$

then

$$V_{x \text{ ave}} = 1.5 \times 5.1 = 7.7 \text{ fps,}$$

and the basin could be terminated at

$$x = 60 \text{ ft.}$$

The lateral velocity distribution at a distance $D/2 = 3 \text{ ft}$ above the bed and 60 ft downstream of the outlet can be estimated using Fig. 62.

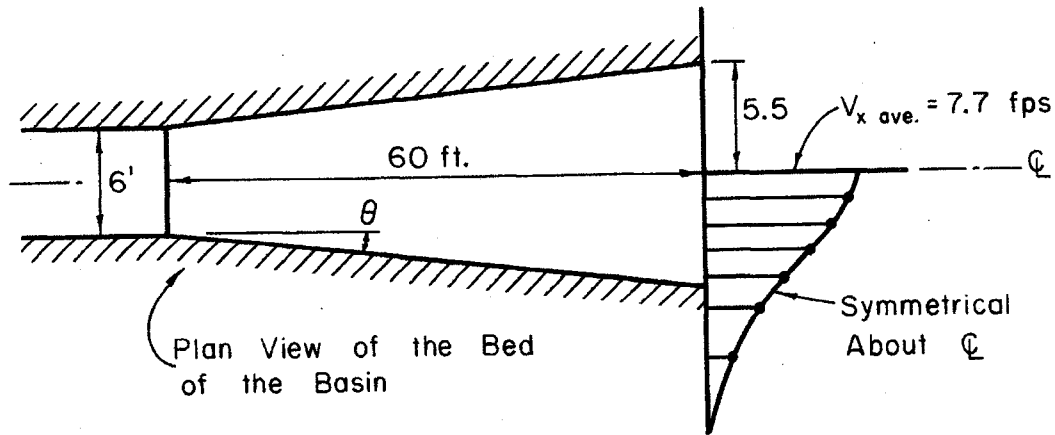
The procedure for this is: compute

$$\frac{V_{o \text{ ave}} D}{x} = \frac{12.8 \times 6}{60} = 1.28 .$$

Select values of $\frac{V_x}{V_{o \text{ ave}}} \frac{x}{D} = 6, 5, 4, \text{ etc.}$, and use these values of $\frac{V_x}{V_{o \text{ ave}}} \frac{x}{D}$ to obtain values of $\frac{r}{x}$ from Fig. 62, then compute r and V_x .

$\frac{V_x}{V_{o \text{ ave}}} \frac{x}{D}$	$\frac{r}{x}$	$r = x \left(\frac{r}{x}\right)$	$V_x = \left(\frac{V_x}{V_{o \text{ ave}}} \frac{x}{D}\right) \left(\frac{V_{o \text{ ave}} D}{x}\right)$
6	0.03	1.8 ft	7.7 fps
5	0.06	3.6	6.4
4	0.075	4.5	5.1
3	0.100	6.0	3.8
2	0.13	7.8	2.5
1	0.17	10.3	1.8
0	0.24	14.4	0

Plot the V_x velocity profile from the preceding table as in Sketch B. Sketch B shows the lateral velocity profile $D/2 = 3$ ft above the bed at $x = 60$ ft.



Sketch B

The required width of the basin is computed by applying the continuity equation

$$W_b = \frac{Q}{d_t V_{ch}} = \frac{330}{6 \times 5.1} = 11 \text{ ft.}$$

By superimposing the lateral velocity profile and the proposed geometry of the basin, it can be seen that the profile extends beyond the outline of the bed of the basin. There will be no problem for rock basins because the side slopes will provide more width at $D/2 = 3.0$ ft above the bed, and then roughness provided by the side slopes will offset any lateral restraint in basin width.

If the basin were constructed with concrete and vertical walls, one should consider making the basin slightly wider at the outlet.

The basin designed in the above manner is the same as that designed by using Fig. 58. In Fig. 58, for $d_t/y_o = 1.00$, $\tan\theta = 0.05$. Whereas,

with the procedure outlined in this chapter

$$\tan\theta = \frac{2.5}{60} = 0.042.$$

The design procedure presented in this chapter gives the designer a better insight into the fluid mechanics of the high tailwater case. For box culverts, the procedure is the same except that x/W_0 is used instead of x/D .

F - Field Check of Design Procedure

The Wyoming Highway Commission has started a program of gathering field data on scour holes that have occurred downstream of large culverts where the USGS has established hydraulic data. One such culvert, South of Worland, Wyoming, is immediately South of Little Gooseberry Creek and just above the railroad bridge that was damaged by the flood.

This concrete culvert is circular in cross-section but is slightly deformed in that the height is 16 ft and the width is 15 ft. The USGS has established that during the flood,

$$Q = 1980 \text{ cfs}$$

$$S = 1.14\%$$

$$d_t = 5.45 \text{ ft}$$

Flow type = II in Fig. 1.

The Highway Commission has surveyed the area in the vicinity of the culvert outfall. This data is shown in the sketch below. It was estimated that the riprap that was used to protect the outlet varied from 25# to 200# rock and that the mean weight was about 100#. A 100# rock is equivalent to a 1-foot diameter rock.

The centerline profile indicates that the maximum depth of scour was 12.3 ft at a distance 46 ft downstream from the barrel outlet. When the survey was taken, the soundings indicated that the scour hole bottom was covered with mud and it is not known if there is any riprap in the hole. The succeeding analysis is based on the assumption that there was a layer of riprap and mud in the scour hole.

Other dimensions of the scour hole were

$$L_s = 105 \text{ ft}$$

$$L = 170 \text{ ft}$$

$$W_s = 60 \text{ ft (approximately).}$$

The flow parameters at the outlet are:

$$\frac{Q}{D^{5/2}} = \frac{1980}{16^{5/2}} = 1.93 \text{ cfs/ft}^{5/2}.$$

$$\frac{d_t}{D} = \frac{5.45}{16} = 0.34 .$$

Since the flow is Type II, Fig. 17 shows that

$$\frac{y_o}{D} = 0.49$$

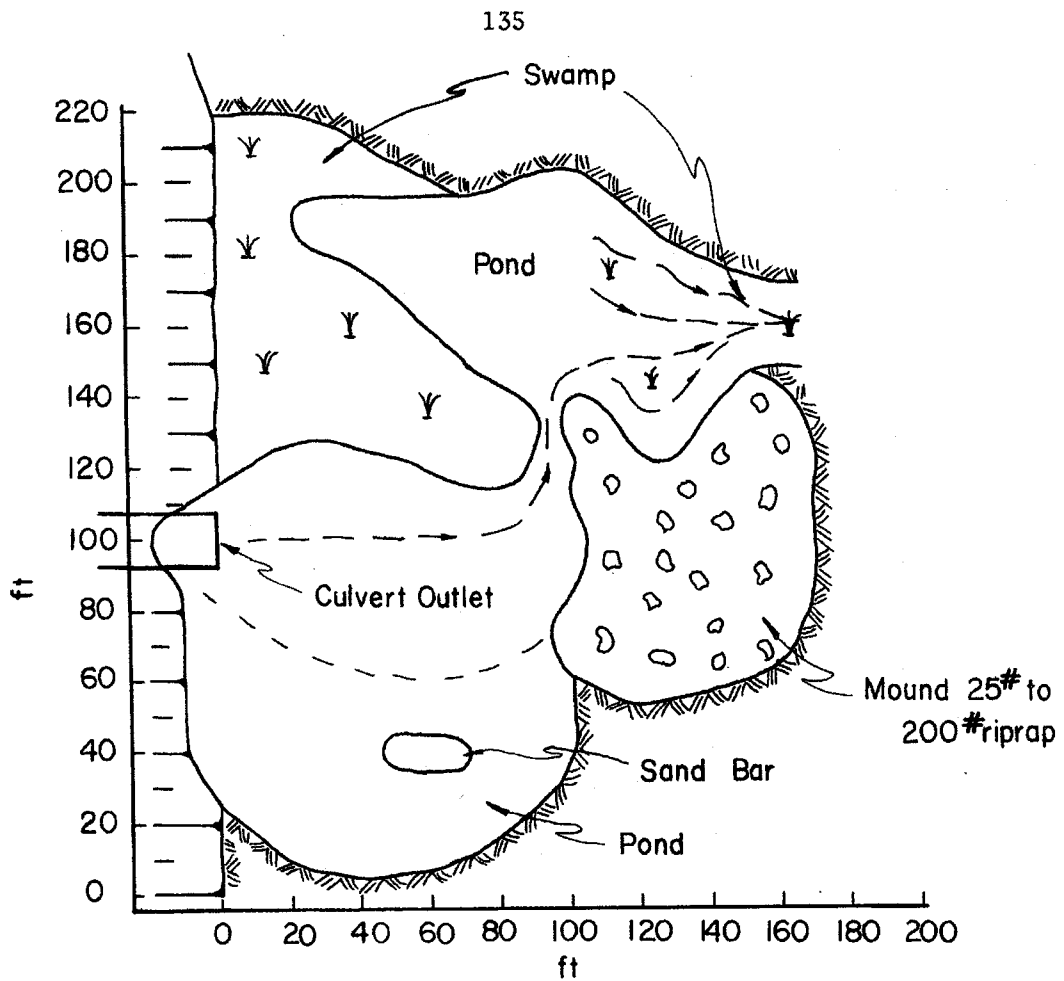
so that the brink depth, y_o , was

$$y_o = 0.49 \times 16 = 7.85 \text{ ft.}$$

For the above flow conditions Fig. 50 indicates that

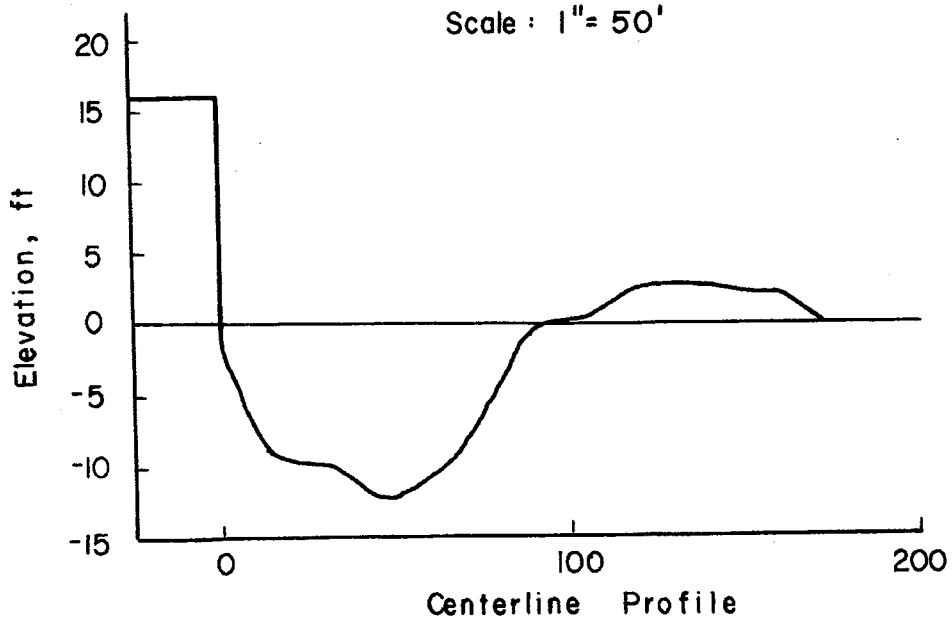
$$\frac{d_s}{D} = 0.27$$

for $\frac{d_m}{D} = 0.0945$



Plan

Scale : 1" = 50'



Plan and Profile of Little Gooseberry Creek Culvert Outlet.

and Fig. 51 that

$$\frac{d_s}{D} = 0.0$$

for

$$\frac{d_m}{D} = 0.205 .$$

The flow in an equivalent 16' x 16' box culvert is given by the two dimensional flow approximation. From Fig. 64,

$$\begin{aligned} \frac{Q}{W_o H_o^{3/2}} &= 1.37 \times \frac{Q}{D^{5/2}} \\ &= 1.37 \times 1.93 = 2.64 \text{ cfs/ft}^{5/2} . \end{aligned}$$

for $\frac{y_o}{H_o} = 0.49$

and $\frac{d_t}{H_o} = 0.34 .$

Now, from Fig. 48

$$\frac{d_s}{H_o} = 1.20$$

for $\frac{d_m}{H_o} = 0.049$

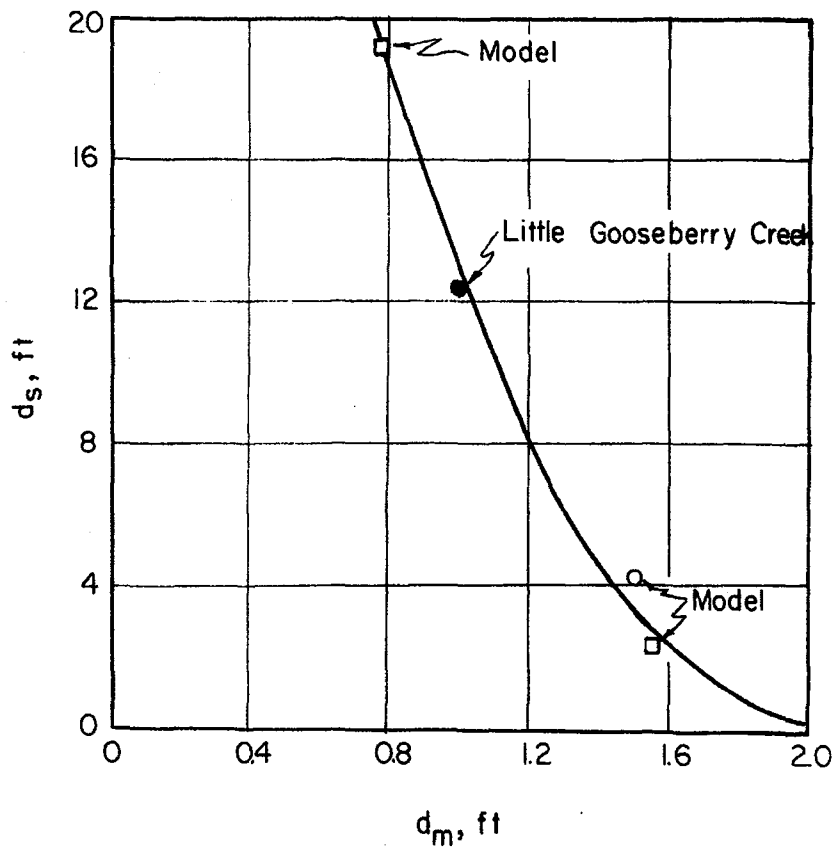
and from Fig. 49

$$\frac{d_s}{H_o} = .15$$

for $\frac{d_m}{H_o} = 0.0974 .$

For the flow conditions that existed at the Little Gooseberry Creek culvert model tests indicate scour depths for various rock sizes given in the table and sketch below:

$\frac{d_m}{D}$ or $\frac{d_m}{H_o}$	$\frac{d_s}{D}$ or $\frac{d_s}{H_o}$	d_m ft	d_s ft
0.0945	0.27	1.5	4.3
0.205	0.00	3.3	0.0
0.049	1.20	0.8	19.2
0.0974	0.15	1.6	2.4



Sketch

As shown in the sketch above, the scour depth at Little Gooseberry Creek agrees very well with the scour depth predicted from CSU Model tests. If the scour hole had been formed in a basin riprapped with 1-foot diameter rock to a depth greater than 12 feet, then it could be concluded that the model and field tests agree extremely well. The same conclusion can be reached if it is assumed that the bottom of the scour hole is still covered with riprap. However, if all the riprap had been removed and the flow was scouring in the original soil, then the agreement shown in the sketch above is only a very improbable coincidence.

Model tests predict a length of scour hole given by the curve in Fig. 53 or

$$\begin{aligned} \frac{L_s/d_s}{d_t/y_o} &= (1.0 + 0.05 \times 1.14) \times 17.5 \\ &= 18.5 \end{aligned}$$

for

$$\frac{d_s}{d_m} = \frac{12.3}{1} = 12.3$$

so

$$\frac{L_s}{d_s} = 18.5 \times \frac{5.45}{7.85} = 12.85$$

and

$$\begin{aligned} L_s &= 12.85 \times 12.3 \\ &= 158 \text{ ft.} \end{aligned}$$

The actual length of the scour hole was only 105 ft. The design curve presented in Fig. 53 overestimated the length of the scour hole by about 30 percent in this case.

In Fig. 54, the ratio of the length of the basin to the length of the scour hole is

$$\frac{L}{L_s} = 1.9$$

on the average. At little Gooseberry Creek

$$\frac{L}{L_s} = \frac{170}{105} = 1.62.$$

The agreement is very good.

The width of the field scour hole, $W_s = 60$ ft, was estimated taking into account the width of the mound downstream. The model test indicate a width of 57 ft, so again the agreement between model and field data is very good.

The study of the Little Gooseberry Creek scour hole does indicate that the design curves given in this report are valid for field culvert outlet basins. The agreement between model and field scour depth is not conclusive because it is not known if there is any riprap in the scour hole. The design curves overestimated the length of the scour hole by approximately 50 percent. The design curve given in Fig. 53 envelopes all model test data and is therefore the upper limit on the length of the scour hole. All field data should fall on or below this curve.

Both the length to the end of the mound and the width of the scour hole agrees very well with the design curves.

In order to have to prevent a scour hole from forming at the Little Gooseberry Creek culvert outlet, riprap with a 2-foot diameter mean size would have been required.

APPENDIX B
FIGURES

TYPE	EXAMPLE	TYPE	EXAMPLE
I Critical Depth at inlet $\frac{HW}{D} \approx 1.5$ $\frac{TW}{d_c} \approx 1.5$ $S_o > S_c$	(A) INLET CONTROL 	V Rapid Flow at Inlet $\frac{HW}{D} \approx 1.5$ $\frac{TW}{D} \approx 1.0$	(E) INLET CONTROL $d_n = \text{open channel flow depth in culvert}$
II Critical Depth at Outlet $\frac{HW}{D} \approx 1.5$ $\frac{TW}{d_c} \approx 1.0$ $S_o \approx S_c$	(B) OUTLET CONTROL $S_c = \left[\frac{V_c}{1486 R_c^{2/3}} \right]^2$ where $V_c = \frac{Q}{A_c}$ $R_c = \frac{A_c}{WP_c}$ 	VI Full Flow Free Outflow $\frac{HW}{D} \approx 1.5$ $\frac{TW}{D} \approx 1.0$	(F) OUTLET CONTROL $d_n = \text{open channel flow depth in culvert}$
III Tranquil Flow Throughout $\frac{HW}{D} \approx 1.5$ $\frac{TW}{D} \approx 1.0$ $\frac{TW}{d_c} \approx 1.0$	(C) OUTLET CONTROL 	VII Part Full Flow $\frac{HW}{D} \approx 1.5$ $HW \approx D + (1 + K_e) \frac{V^2}{2g}$ $D < d_n$ $D > d_c$	(G) OUTLET CONTROL $V = \text{mean velocity for full culvert}$ $d_n = \text{open channel flow depth culvert}$
IV Submerged Outlet $\frac{HW}{D} \approx 1.0$ $\frac{TW}{D} \approx 1.0$	(D) OUTLET CONTROL 		

Fig. 1 Flow Type Definition (From Wyoming Highway Dept. "Hydraulic Design Practice")

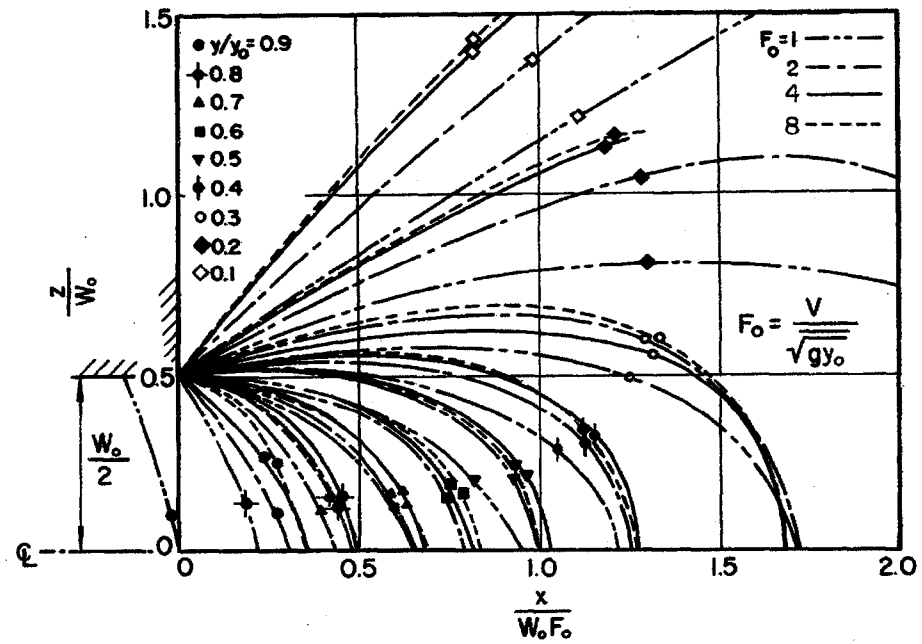


Fig. 2 Dimensionless Water Surface Contours Reproduced from Reference 14

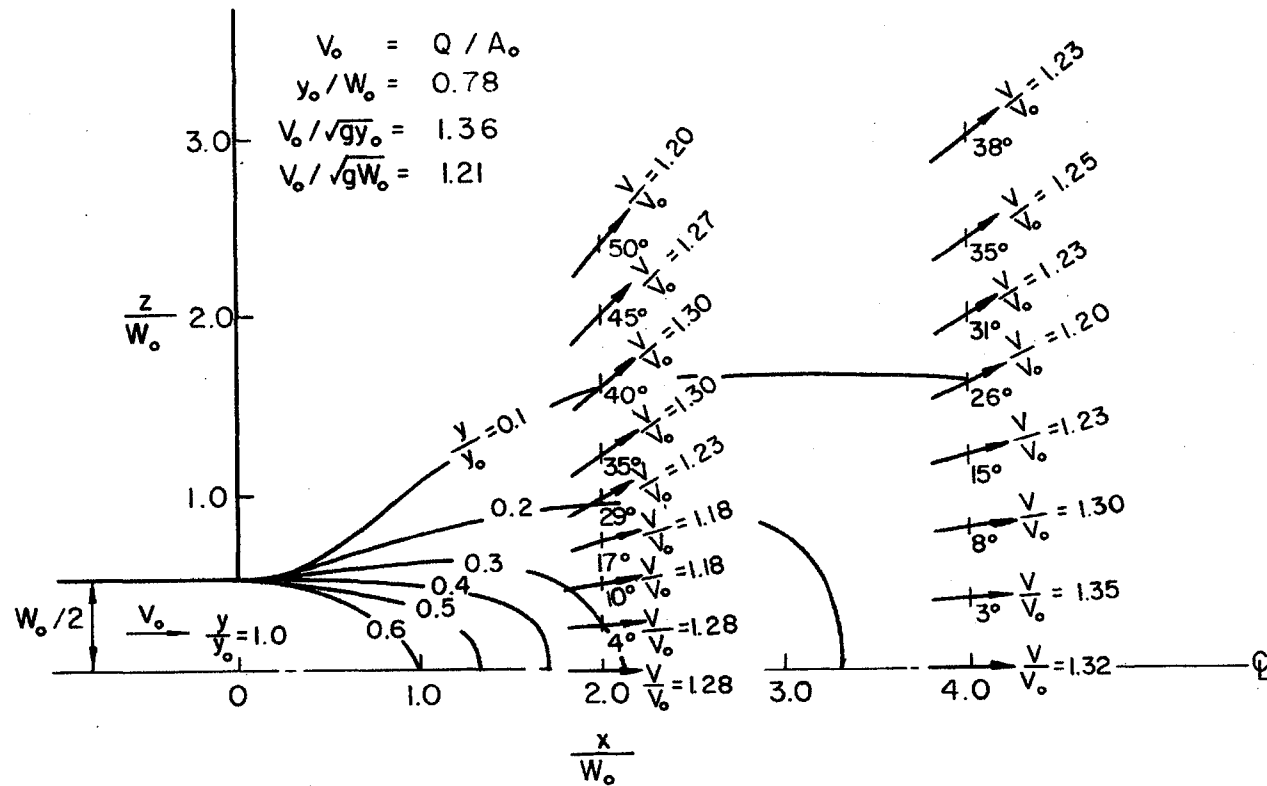


Fig. 4 Dimensionless Water Surface Contours and Relative Velocities, Rectangular Outfall

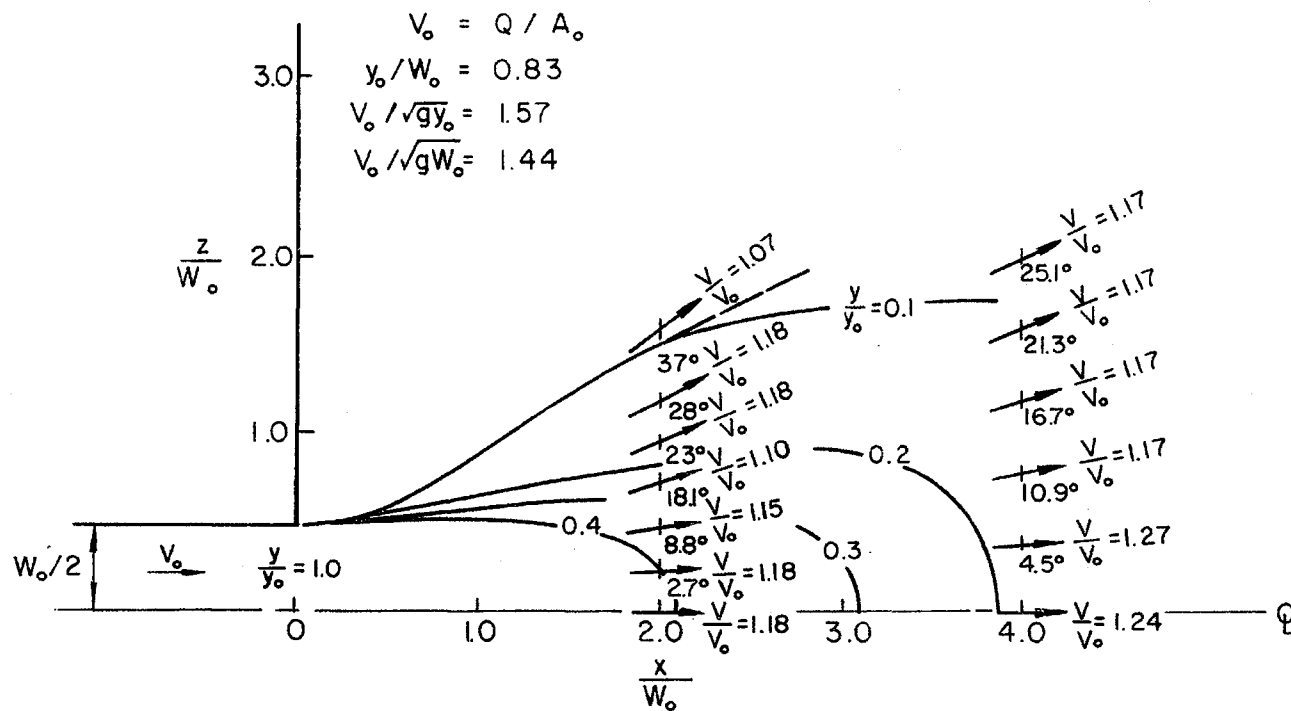


Fig. 5 Dimensionless Water Surface Contours and Relative Velocities, Rectangular Outfall

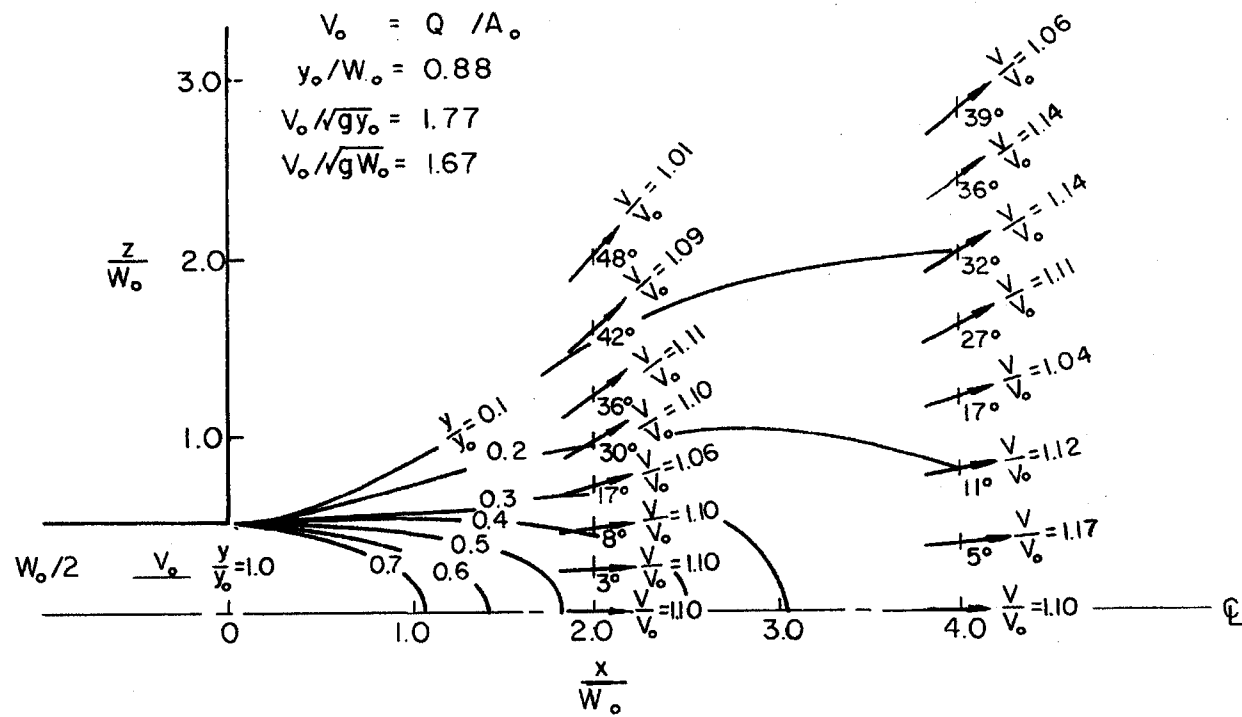


Fig. 6 Dimensionless Water Surface Contours and Relative Velocities, Rectangular Outfall

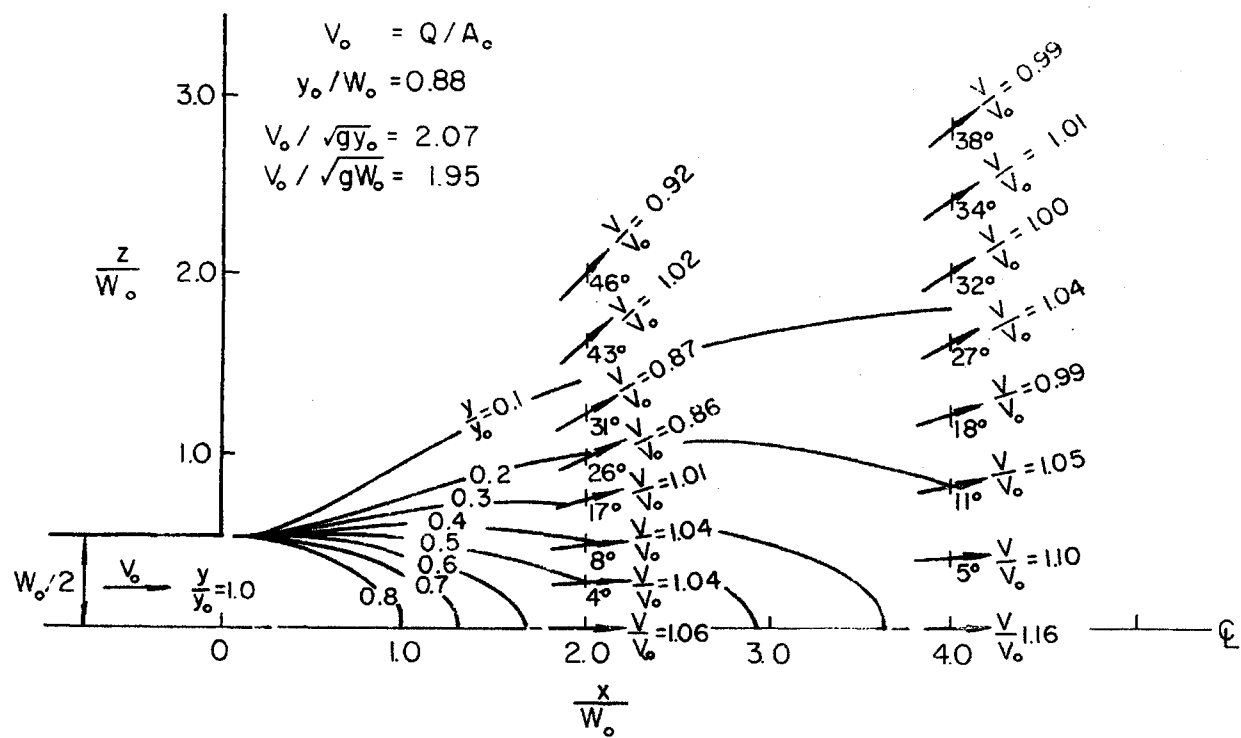


Fig. 7 Dimensionless Water Surface Contours and Relative Velocities, Rectangular Outfall

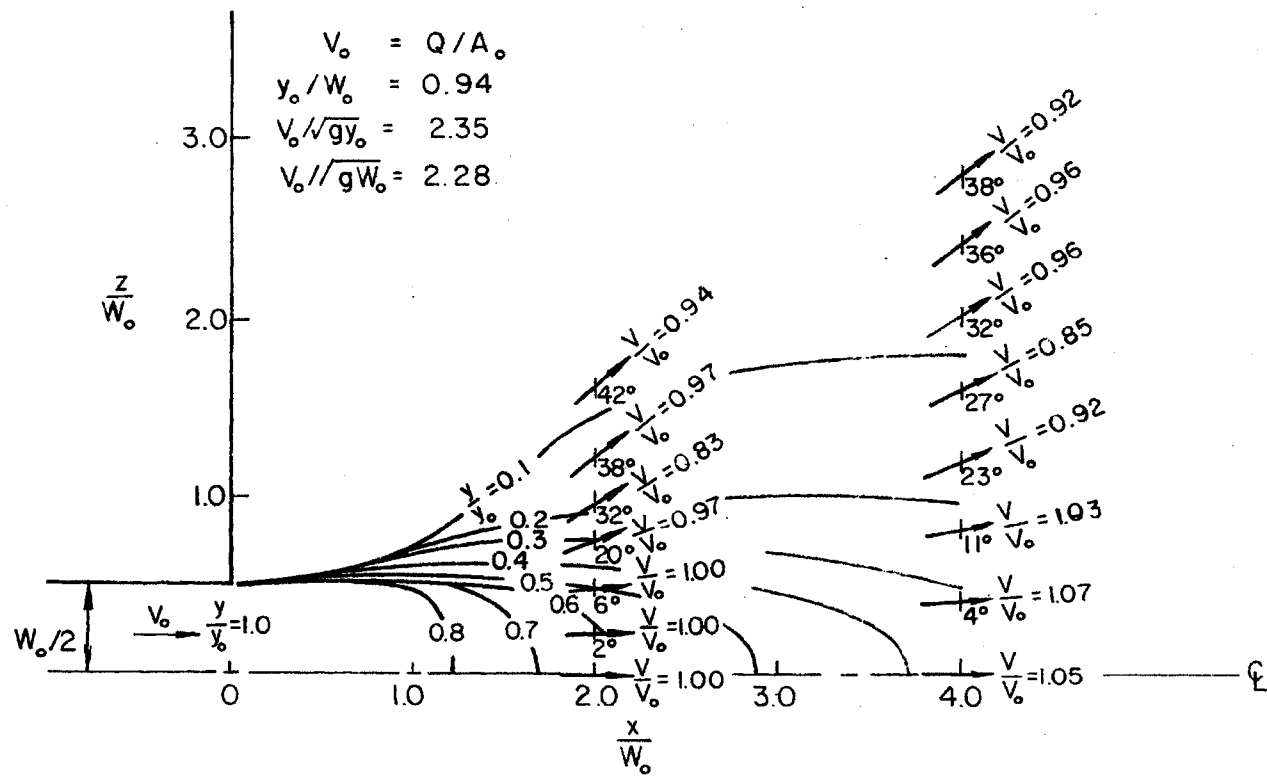


Fig. 8 Dimensionless Water Surface Contours and Relative Velocities, Rectangular Outfall

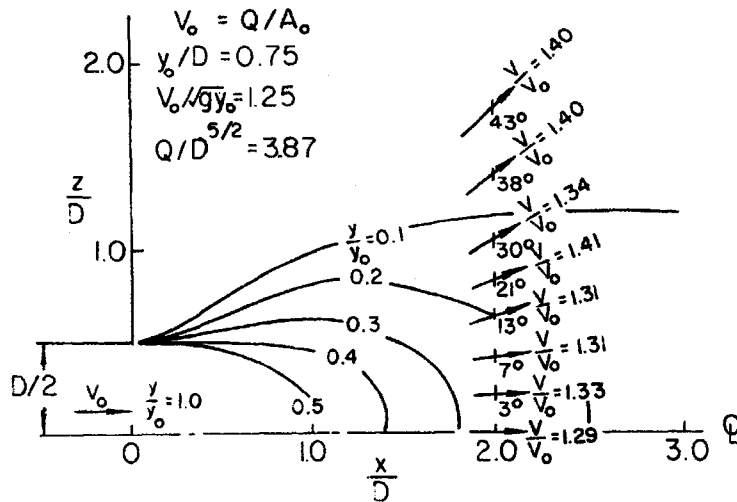
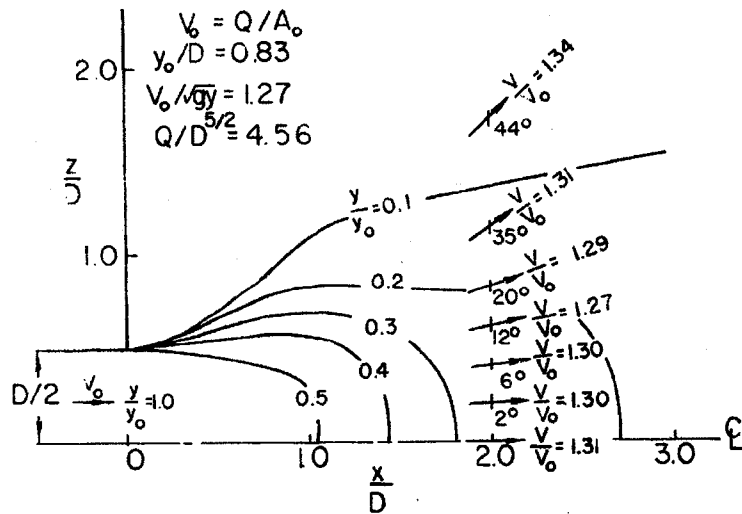


Fig. 9 Dimensionless Water Surface Contours and Relative Velocities, Circular Outfall

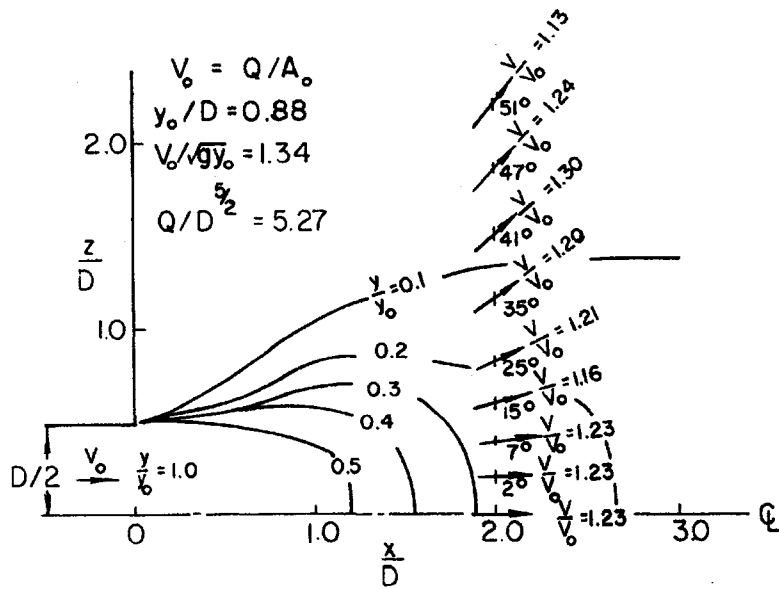
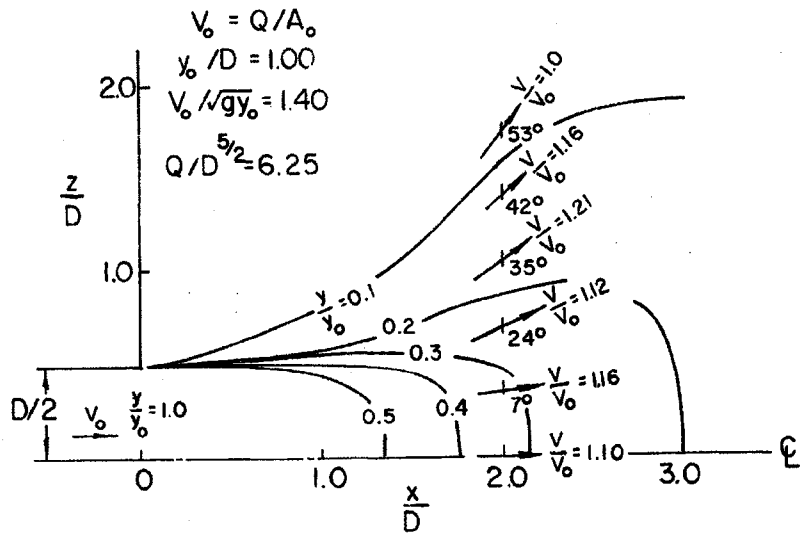


Fig. 10 Dimensionless Water Surface Contours and Relative Velocities, Circular Outfall

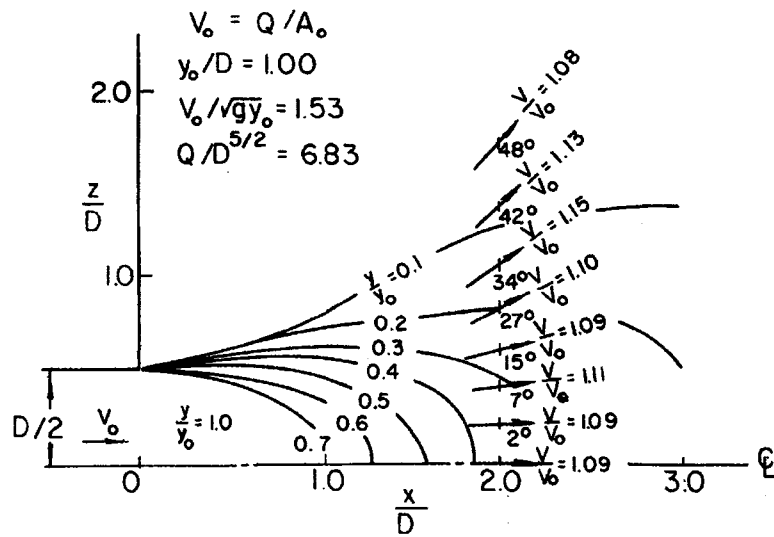
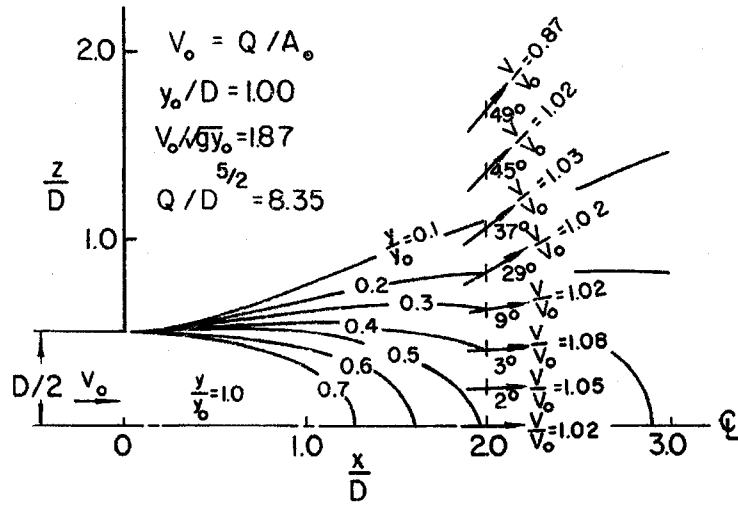


Fig. 11 Dimensionless Water Surface Contours and Relative Velocities, Circular Outfall

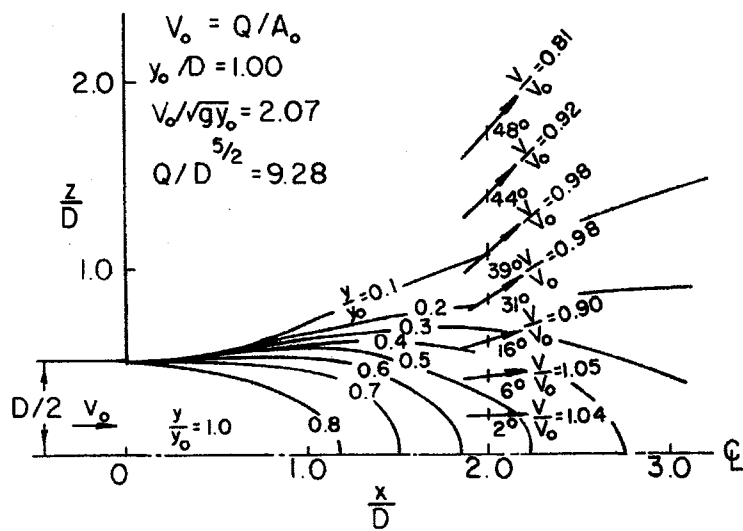


Fig. 12 Dimensionless Water Surface Contours and Relative Velocities, Circular Outfall

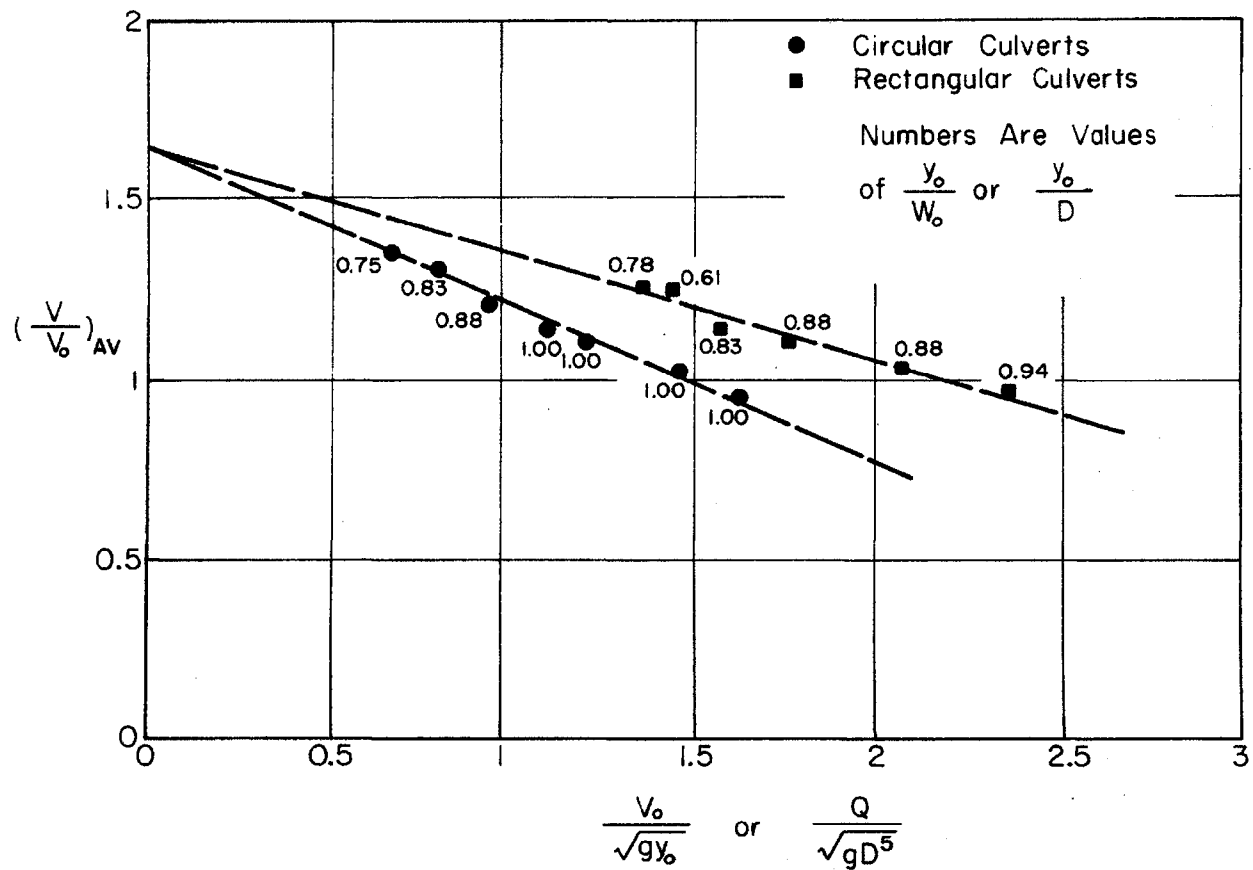


Fig. 13 Average Velocity in the Spreading Jet

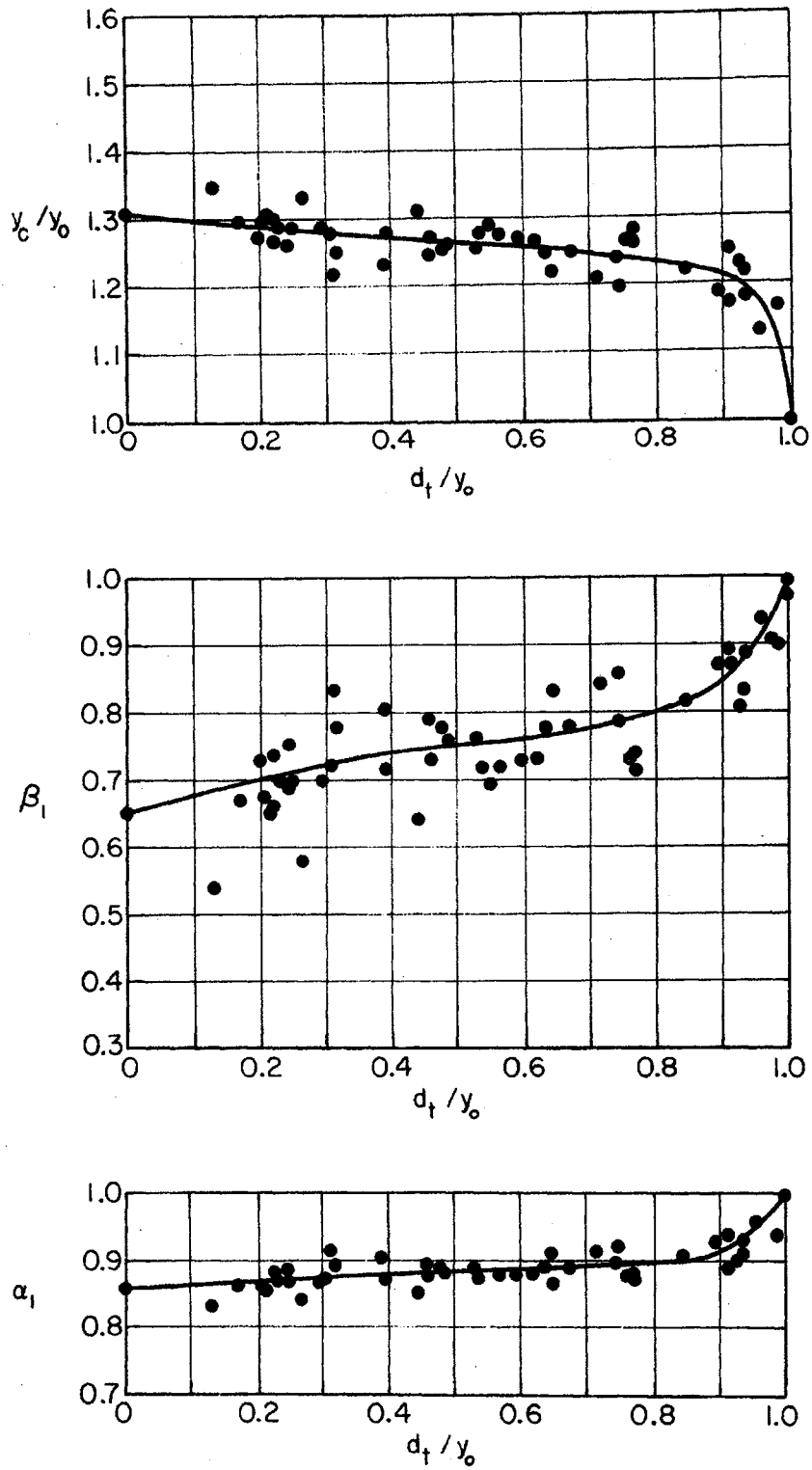


Fig. 14 Brink Depth, Energy and Momentum Coefficients for Rectangular Culverts

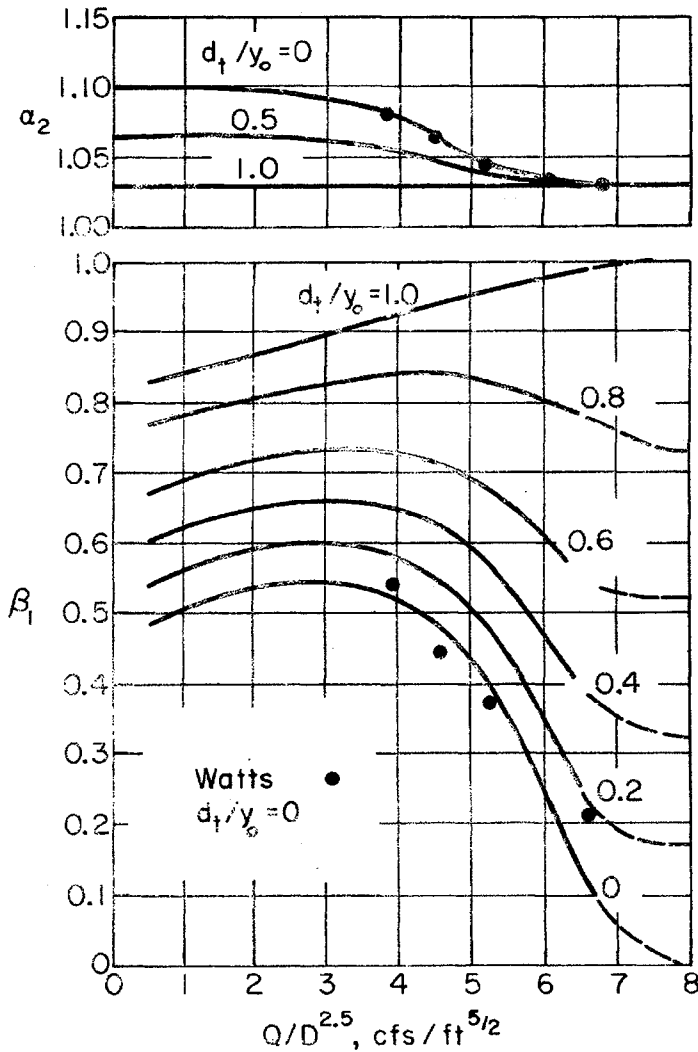
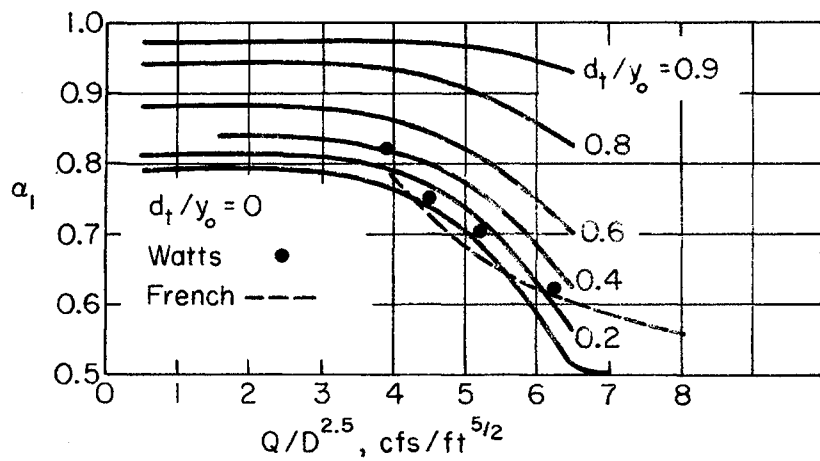
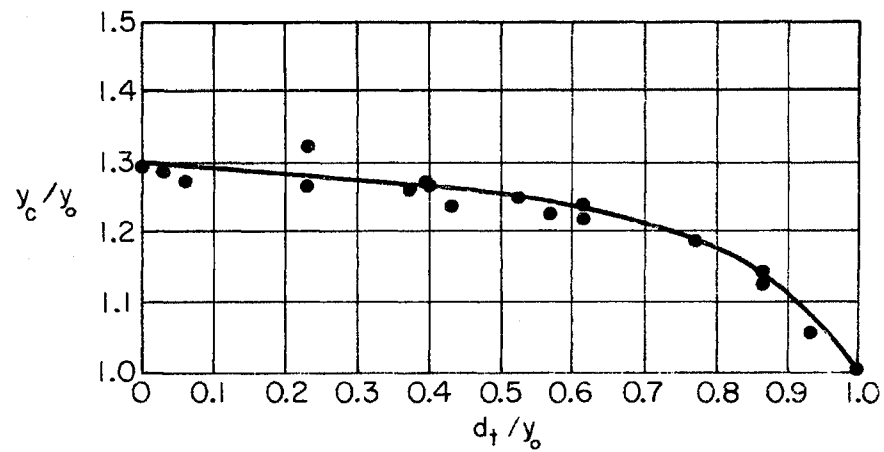


Fig. 15 Brink Depth, Energy and Momentum Coefficients for Circular Pipes

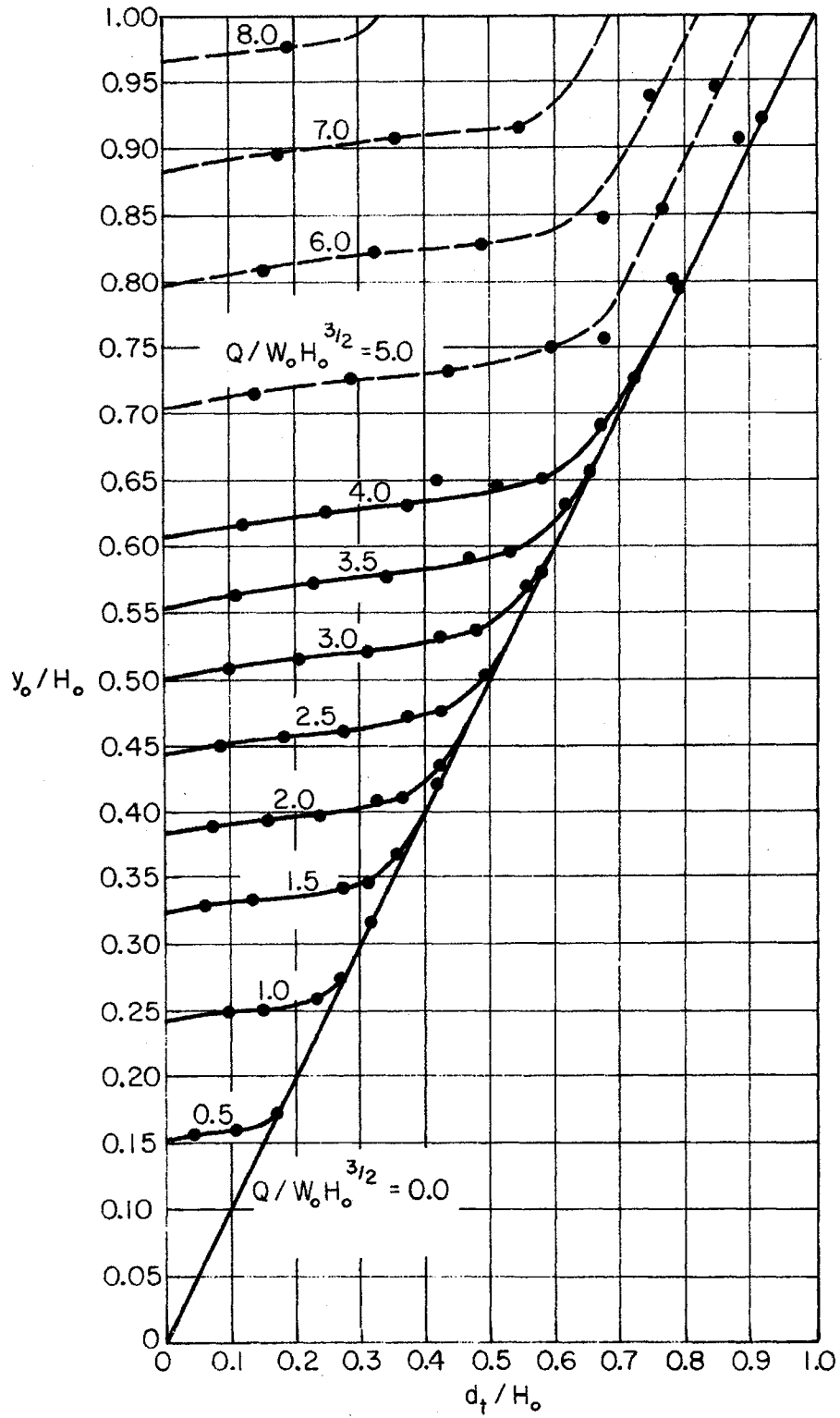


Fig. 16 Effect of Tailwater on Brink Depth: Horizontal and Mild Sloping Rectangular Culverts

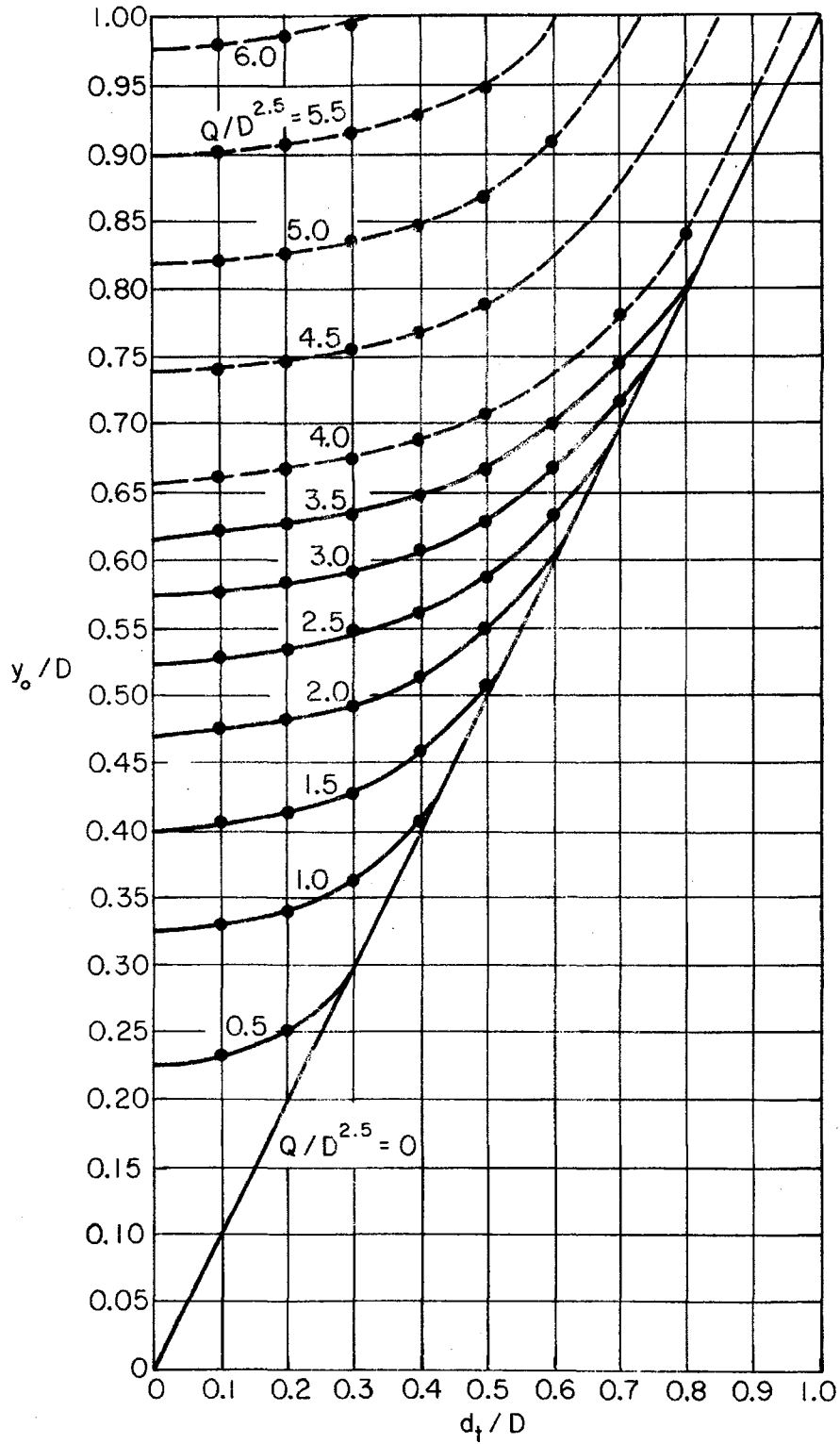
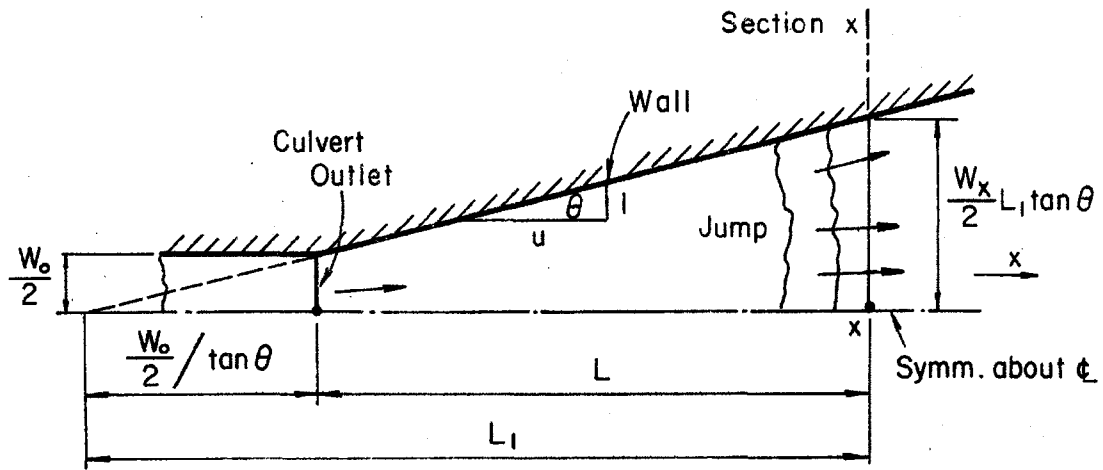
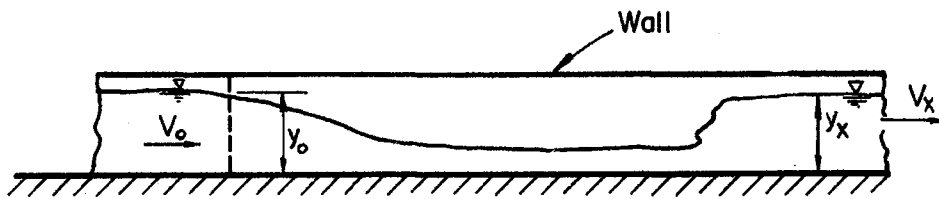


Fig. 17 Effect of Tailwater on Brink Depth: Horizontal and Mild Sloping Circular Culverts

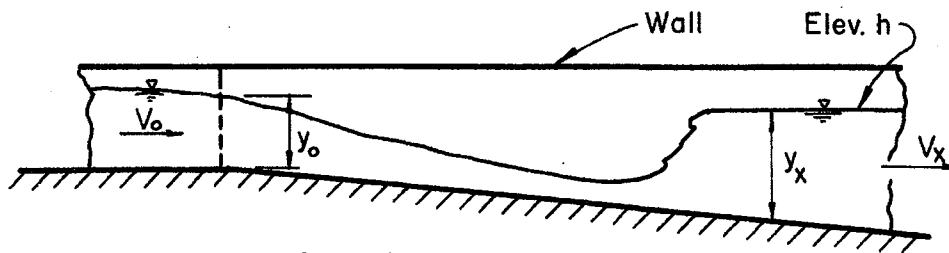


(a) Half Plan



Centerline Section

(b) Horizontal Floor



Centerline Section

(c) Sloping Floor

Fig. 18 Smooth-floor Flared Basin

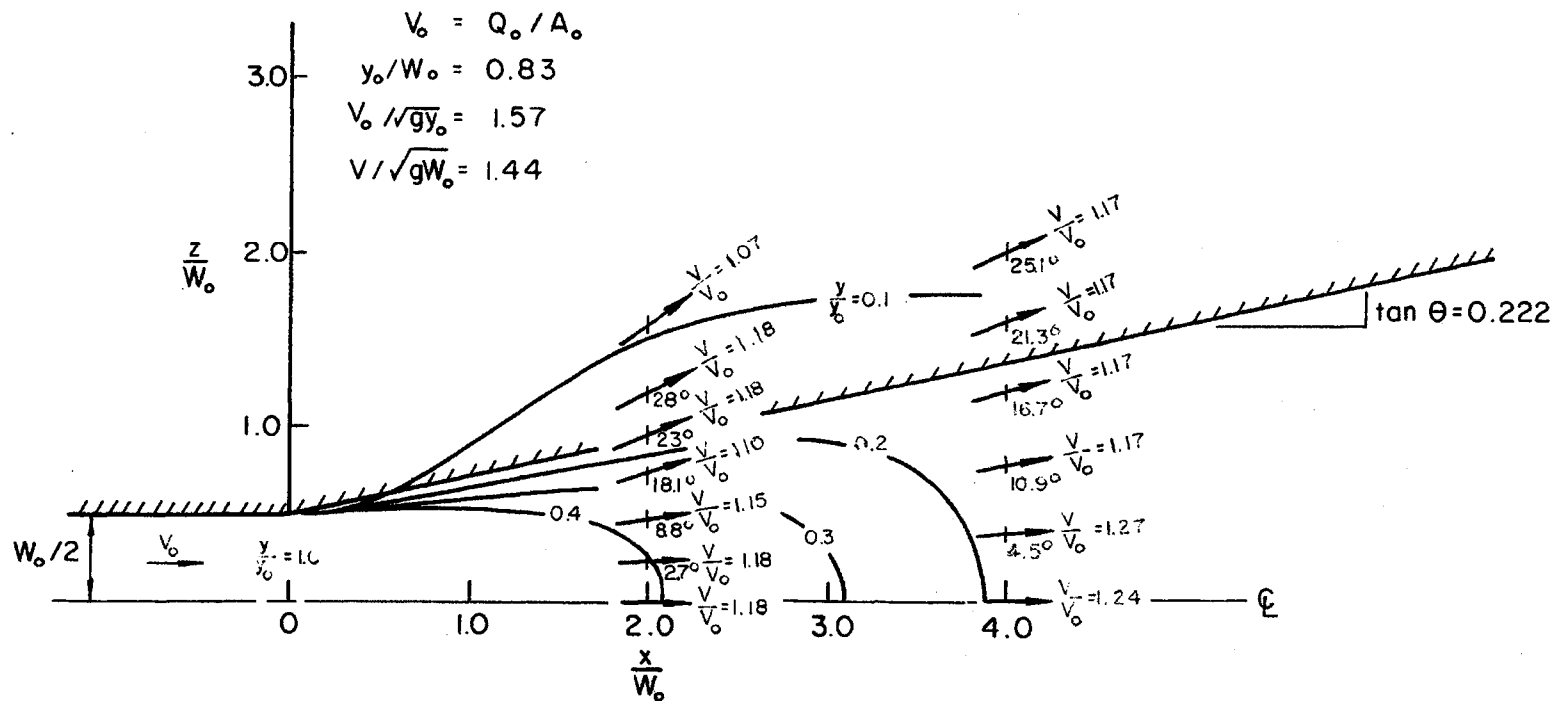


Fig. 19 Dimensionless Water Surface Contours and Relative Velocities
Smooth-floor Flared Basin

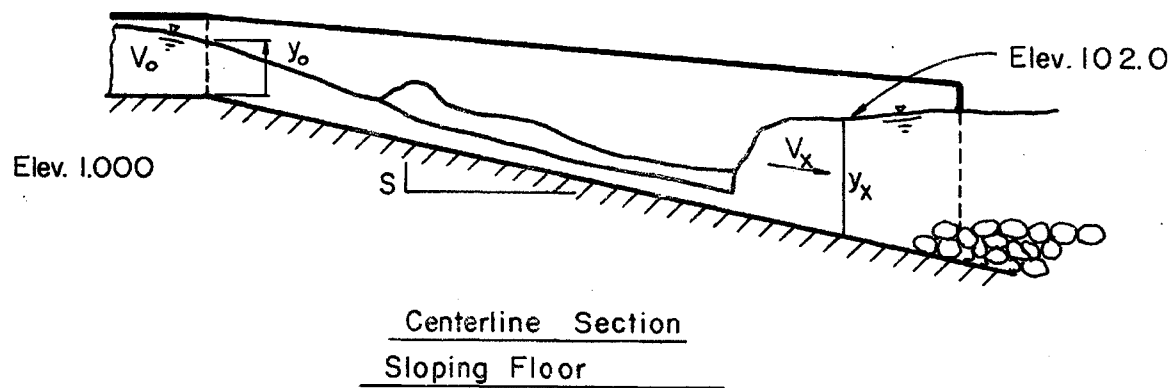
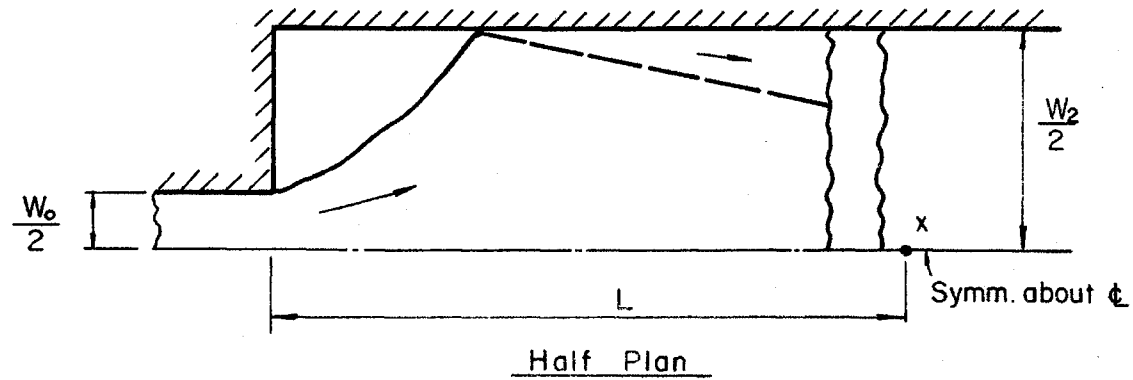


Fig. 20 Smooth-floor Rectangular Basin

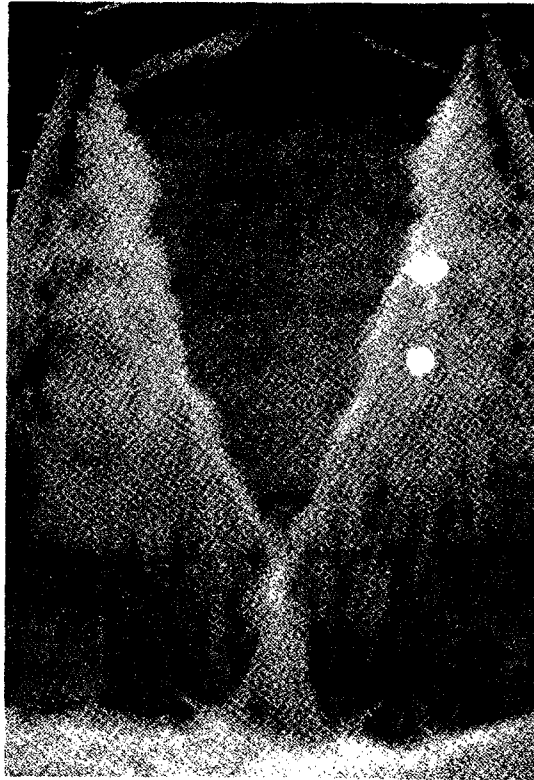


Fig. 22 Smooth Floor 45° Flare, $Q = 21.6$ cfs (from Watts, Reference 22)

This page is reproduced at the back of the report by a different reproduction method to provide better detail.

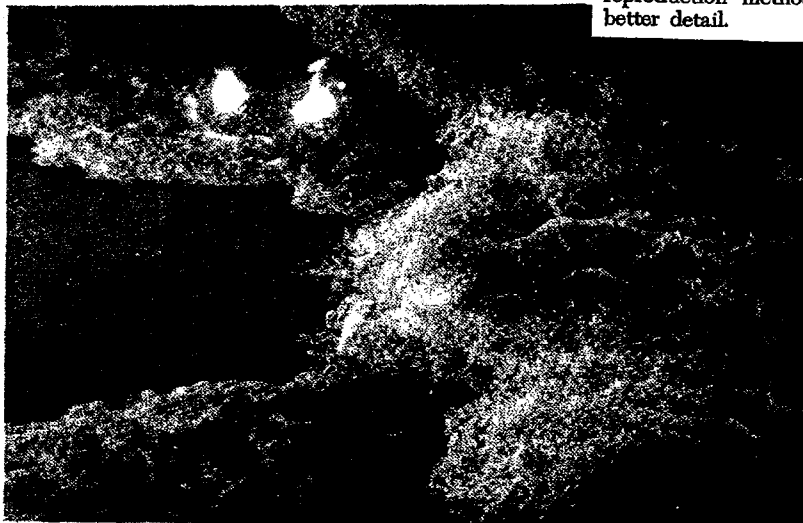


Fig. 23 Smooth Floor Plain End, $Q = 14.9$ cfs (from Watts, Reference 22)

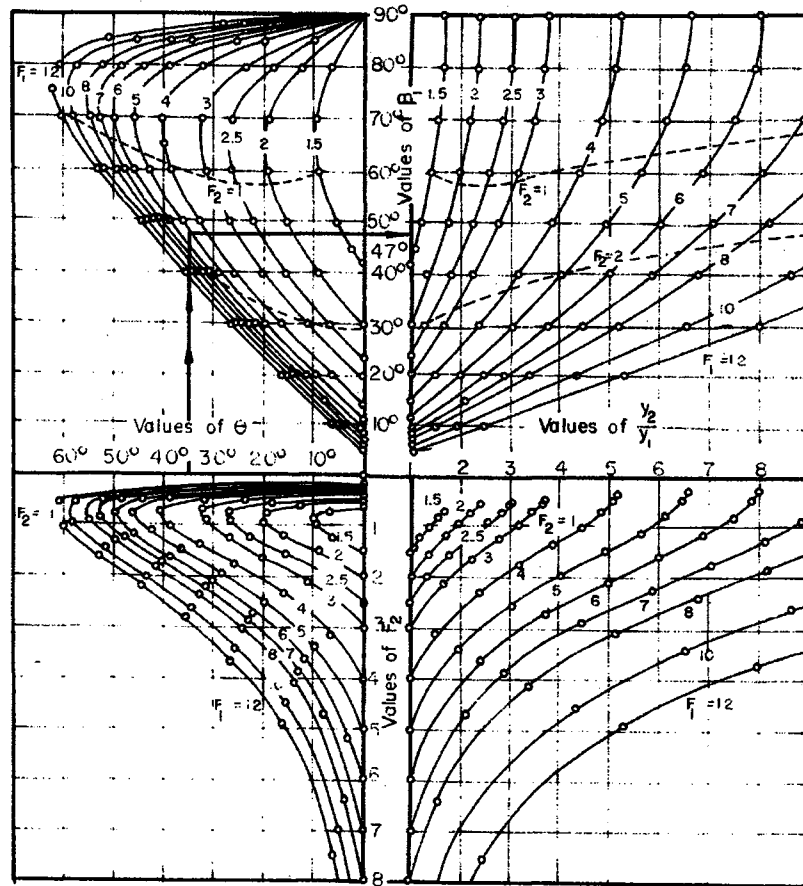
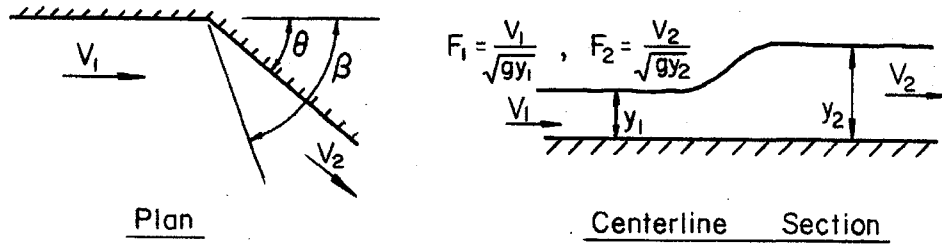
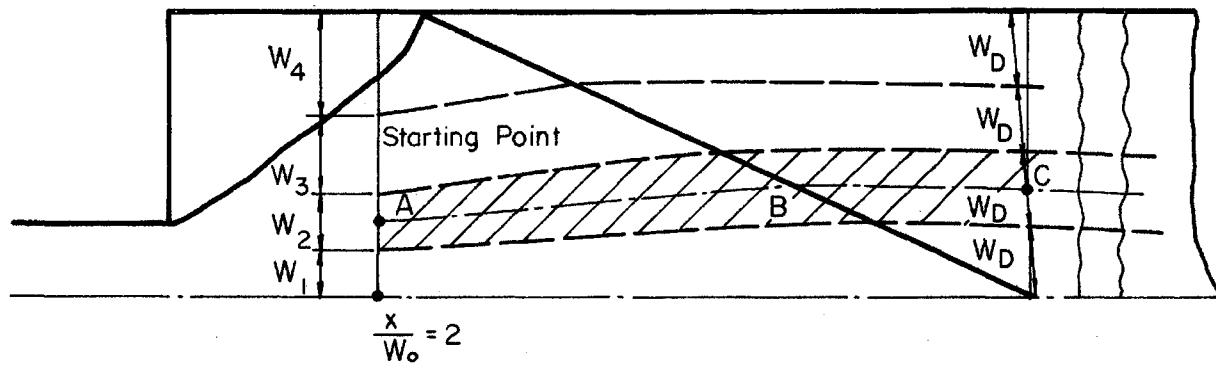
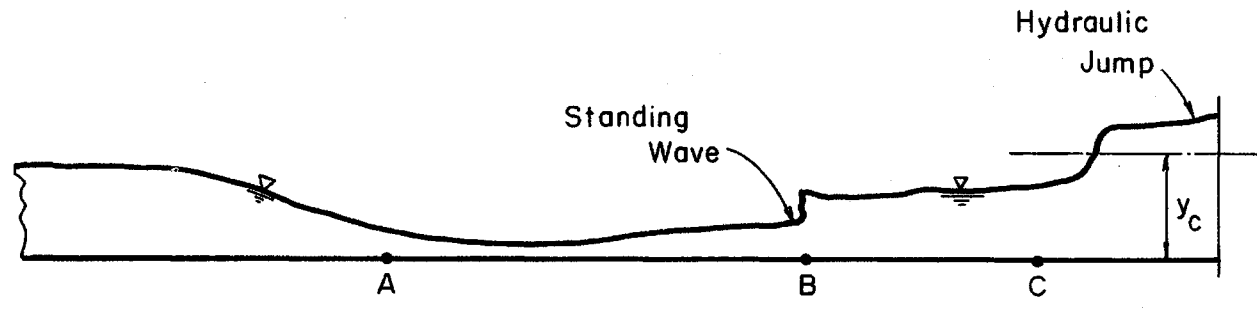


Fig. 24 General Relations Among F_1 , θ , β , y_2/y_1 and F_2 for Oblique Hydraulic Jumps (after A.T. Ippen, Reference 7)



Half Plan



Section Along Stream Tube

Fig. 25 Definition Sketch for Backwater Computations, Smooth-floor Rectangular Basin

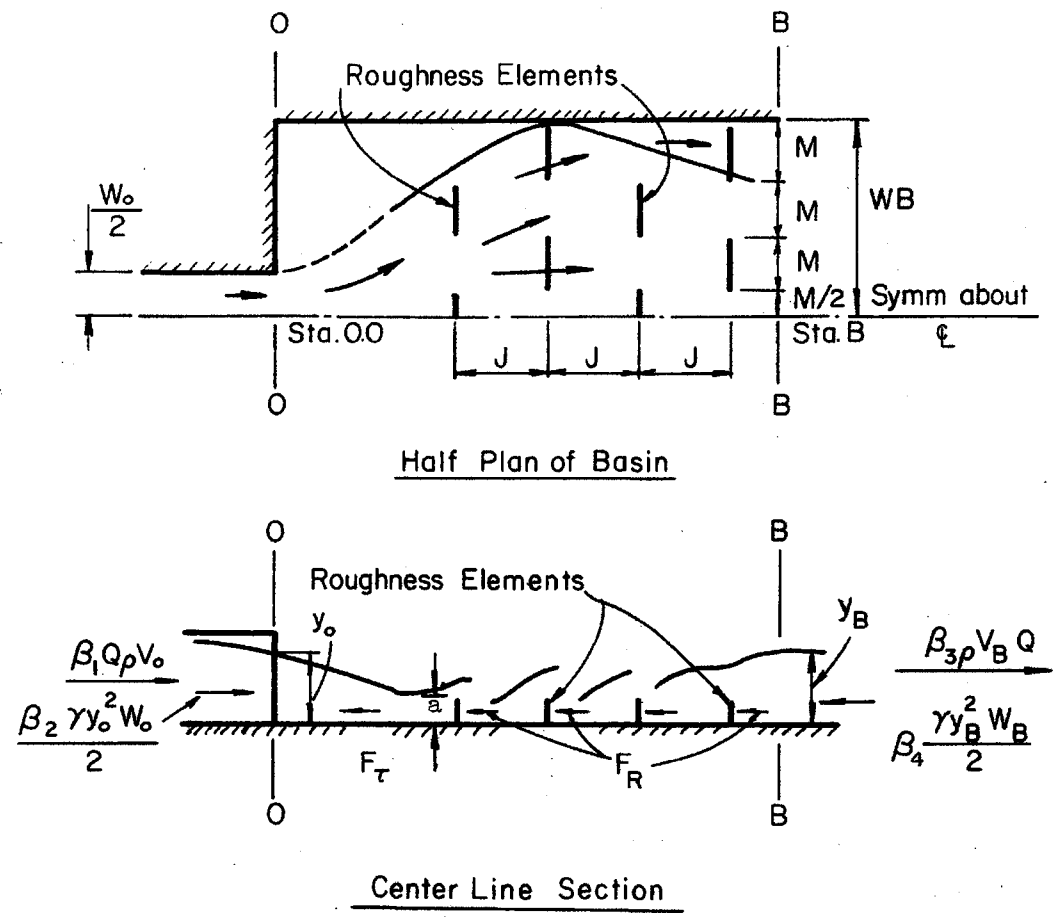


Fig. 26 Definition Sketch for a Rough-floor Basin

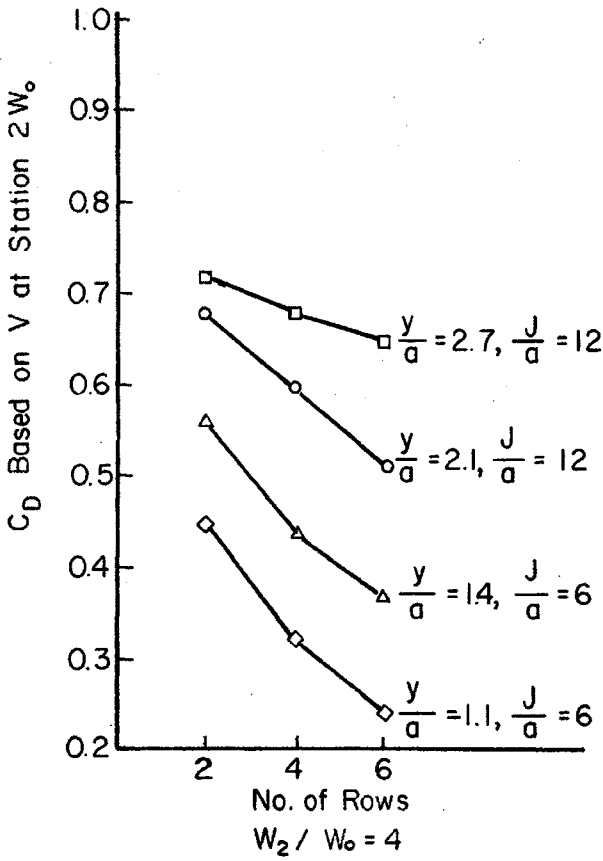
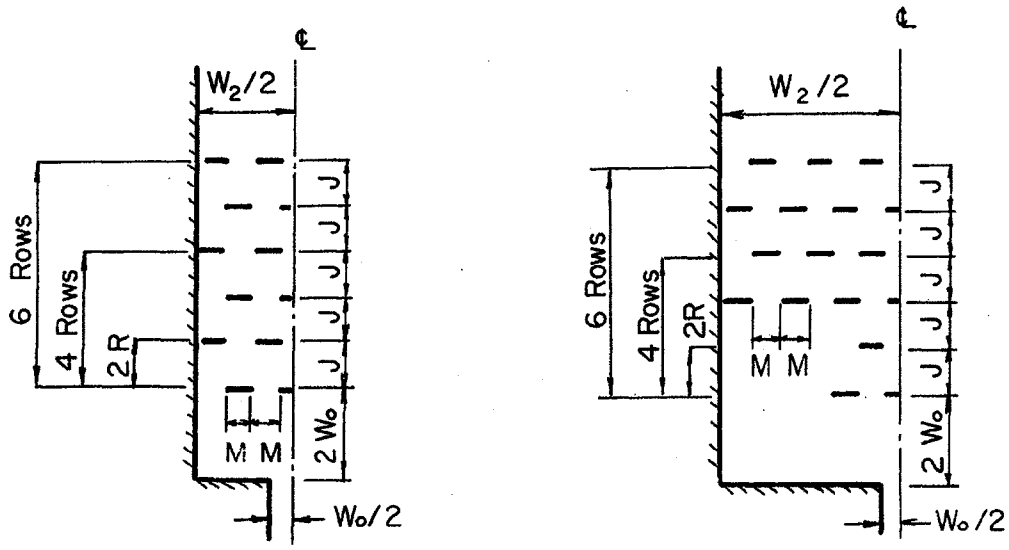


Fig. 27

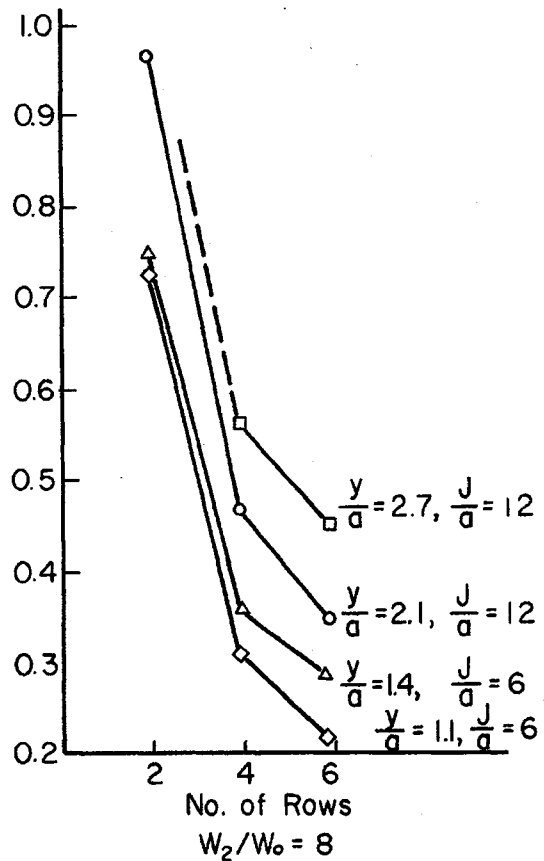


Fig. 28

Coefficients of Drag for Roughness Elements, Rectangular Approach Pipe

a = Amplitude of Roughness Element

y = Depth of Flow

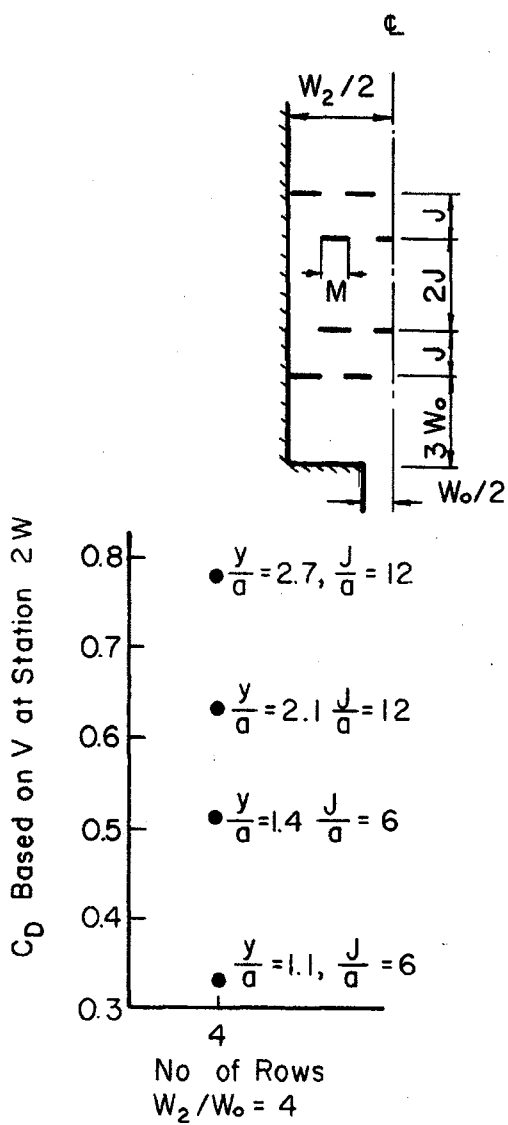


Fig. 29

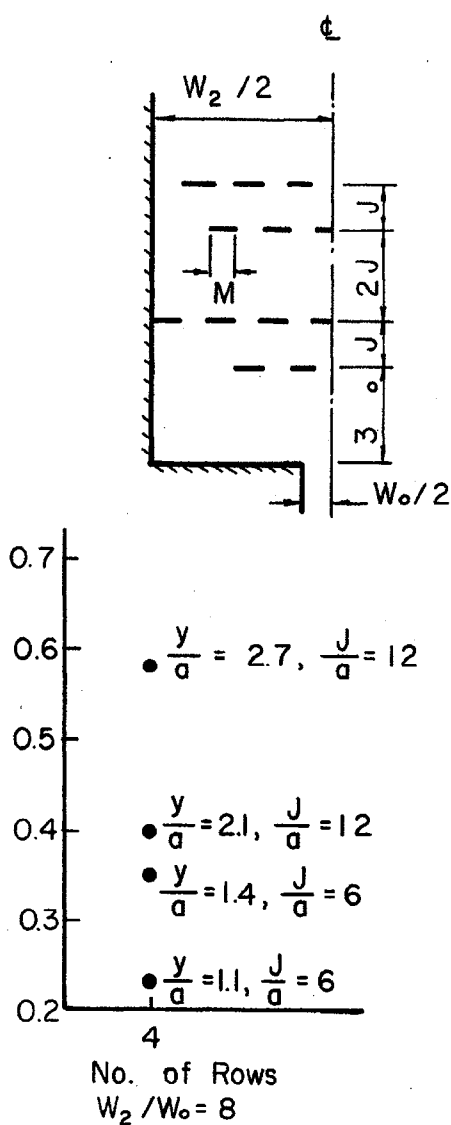


Fig. 30

Coefficients of Drag for Roughness Elements, Rectangular Approach Pipe

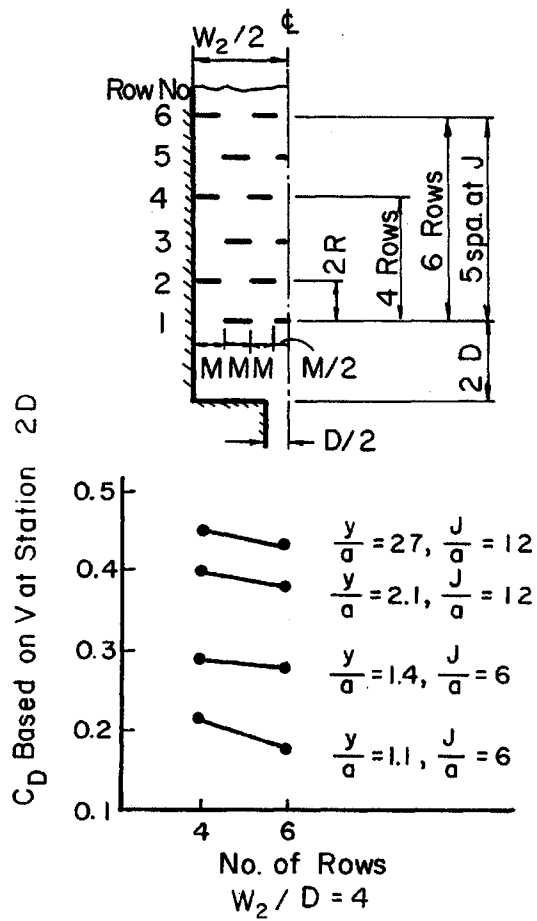


Fig. 31

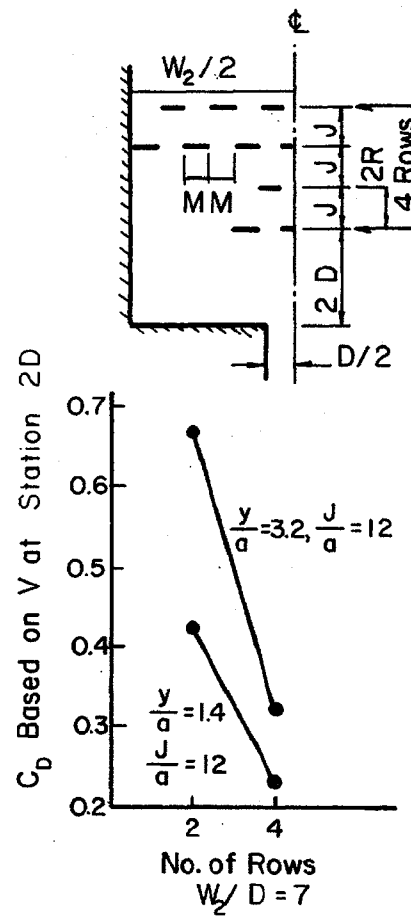


Fig. 32

Coefficient of Drag for Roughness Elements, Circular Approach Pipe

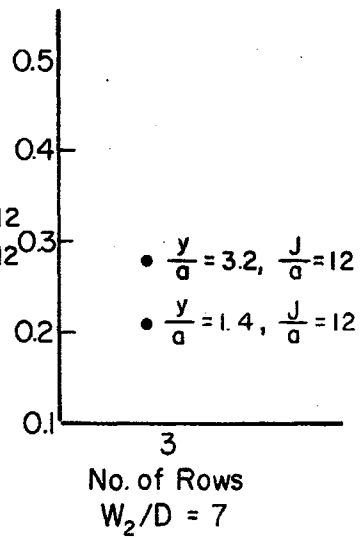
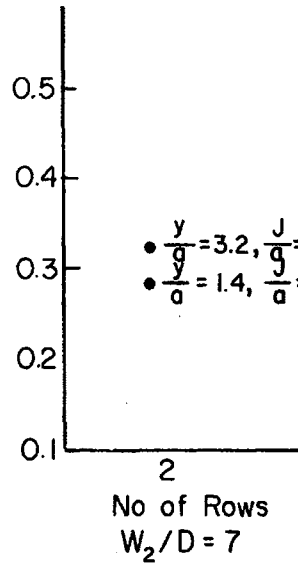
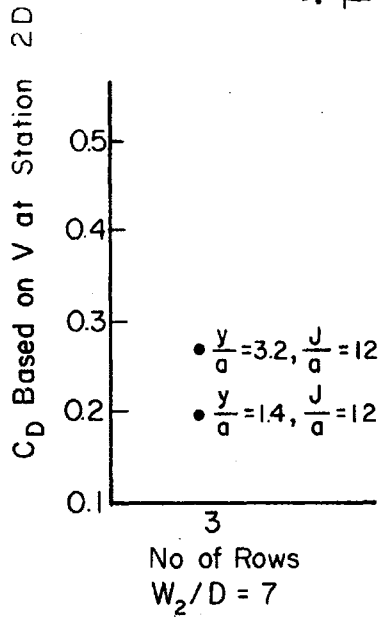
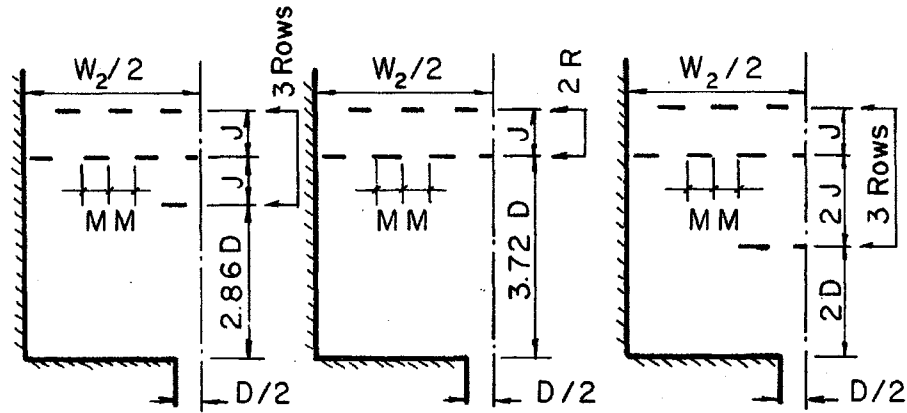


Fig. 33

Fig. 34

Fig. 35

Coefficients of Drag for Roughness Element, Circular Approach Pipe

Not Recommended

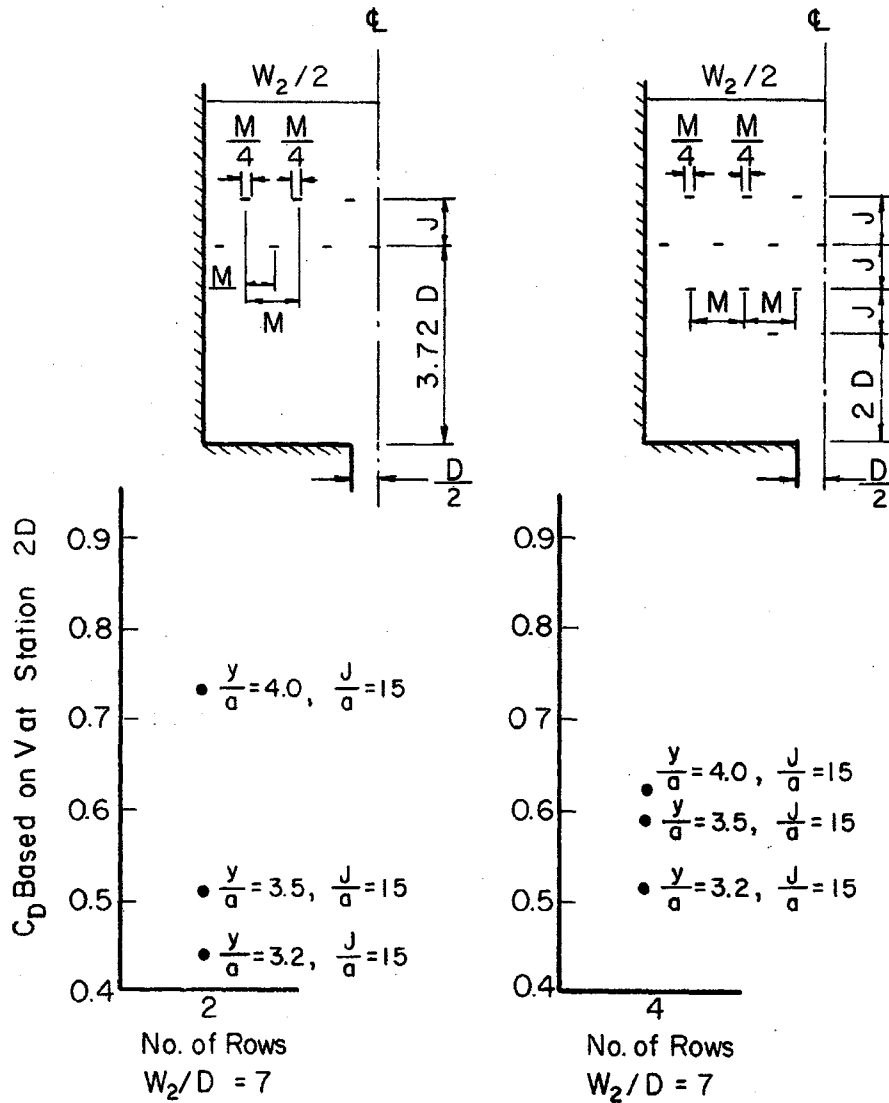


Fig. 36

Fig. 37

Coefficient of Drag for Roughness Elements,
Circular Approach Pipe

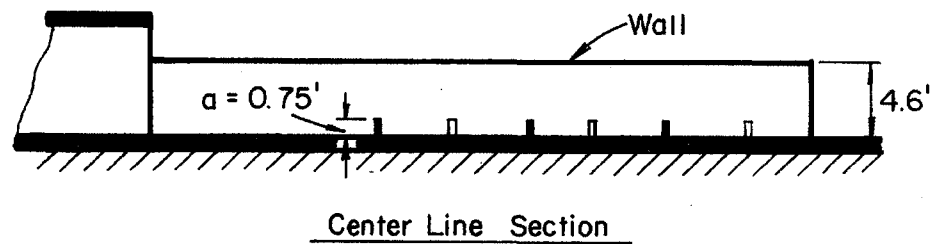
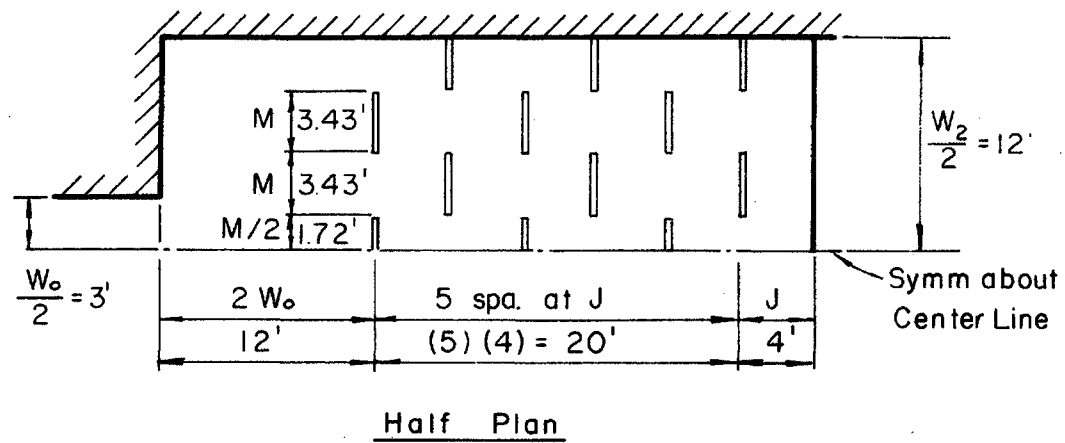
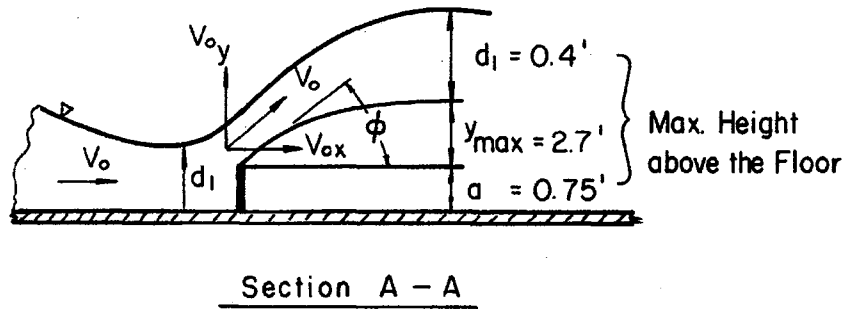
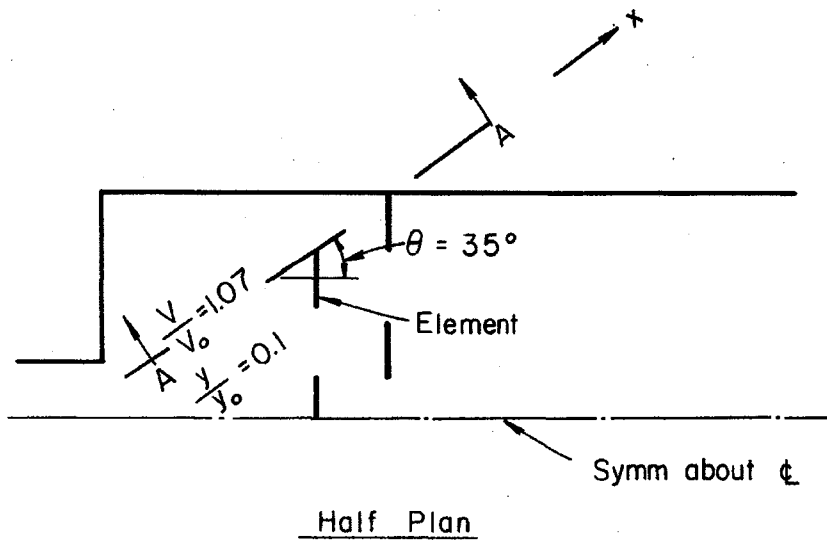


Fig. 38 Rough-floor Basin



Trajectory Equations

$$V_{ox} = V_o \cos \phi \qquad V_{oy} = V_o \sin \phi$$

$$y_{max} = V_{oy}(t) - \frac{1}{2}gt^2 \qquad x = V_{ox}(t)$$

Fig. 39 Definition Sketch, Trajectory Equation

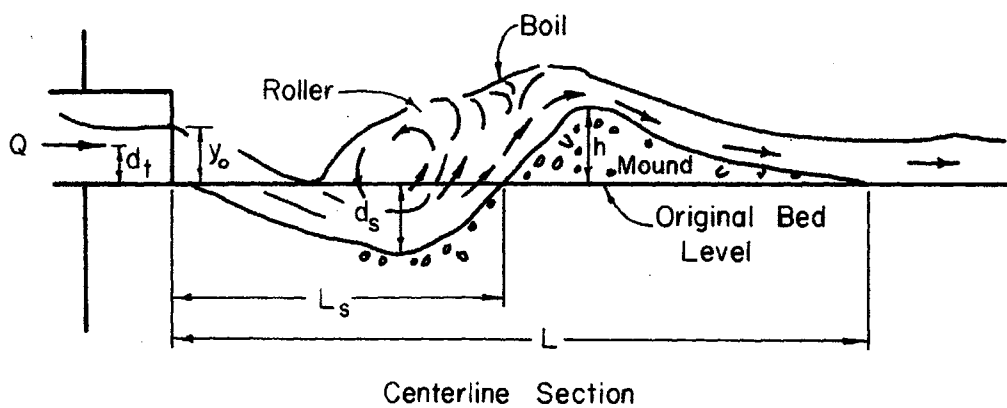
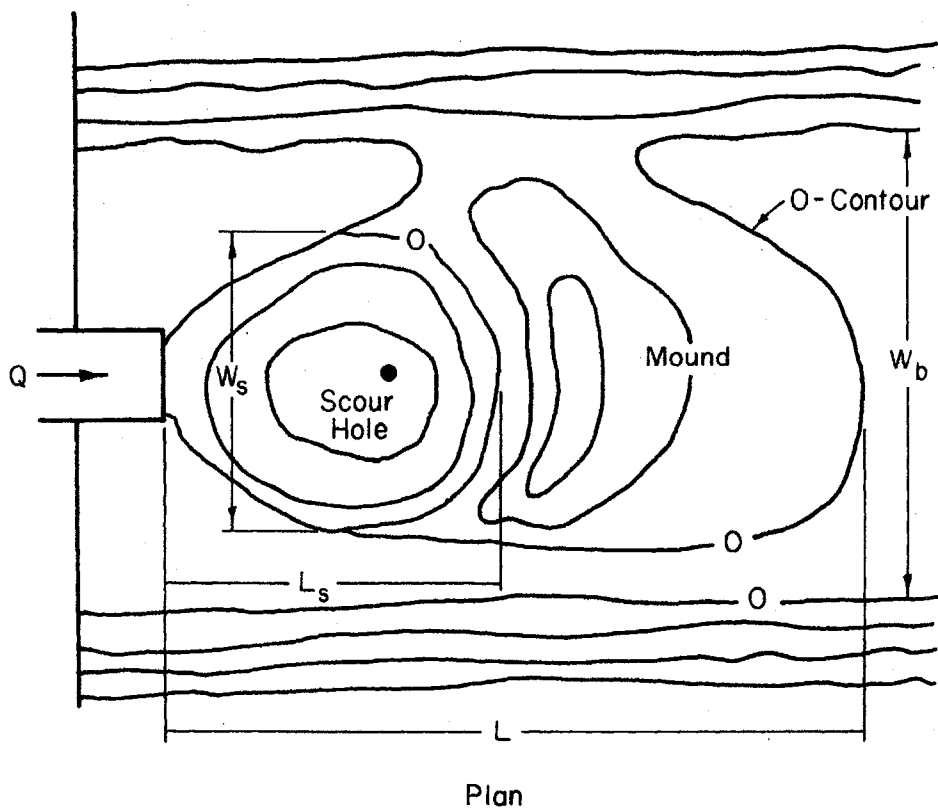


Fig. 40 Definition Sketch of Riprapped Basin

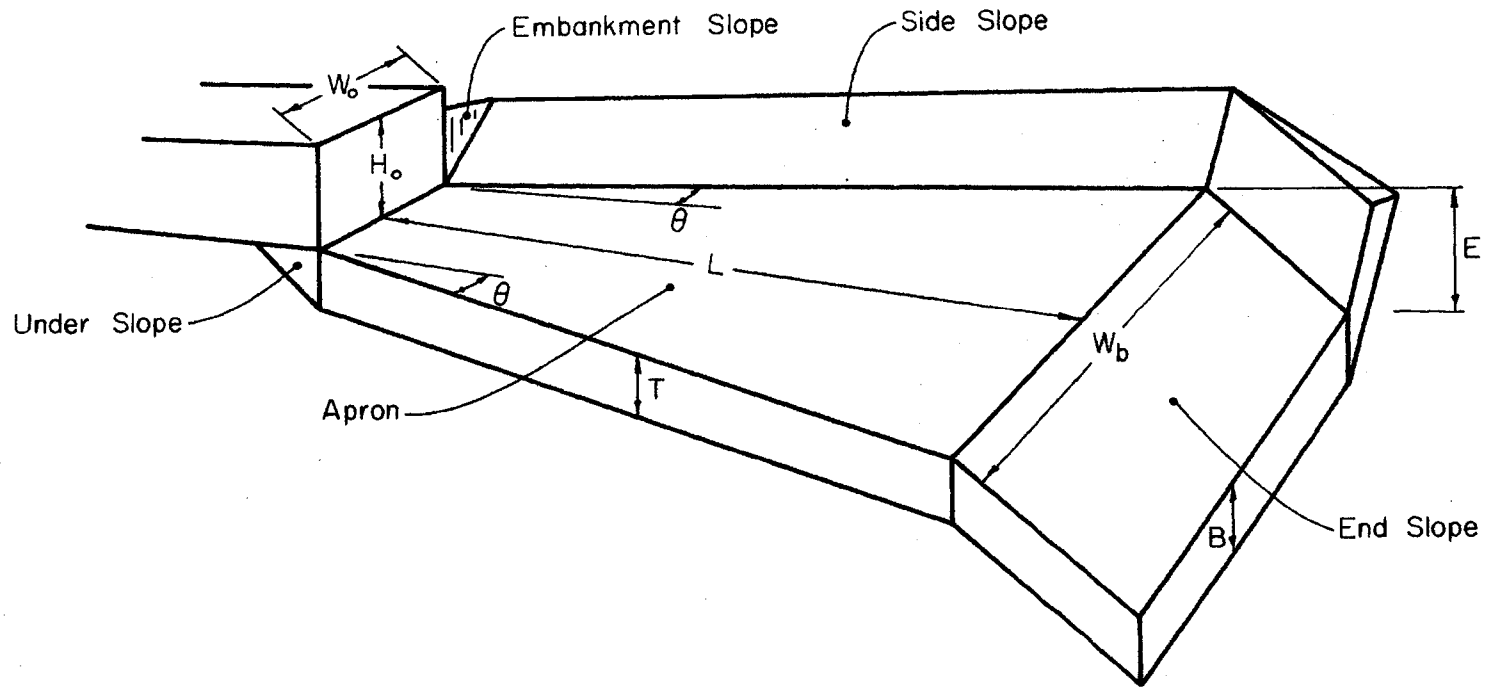


Fig. 41 Standard Non-Scouring Riprapped Basin

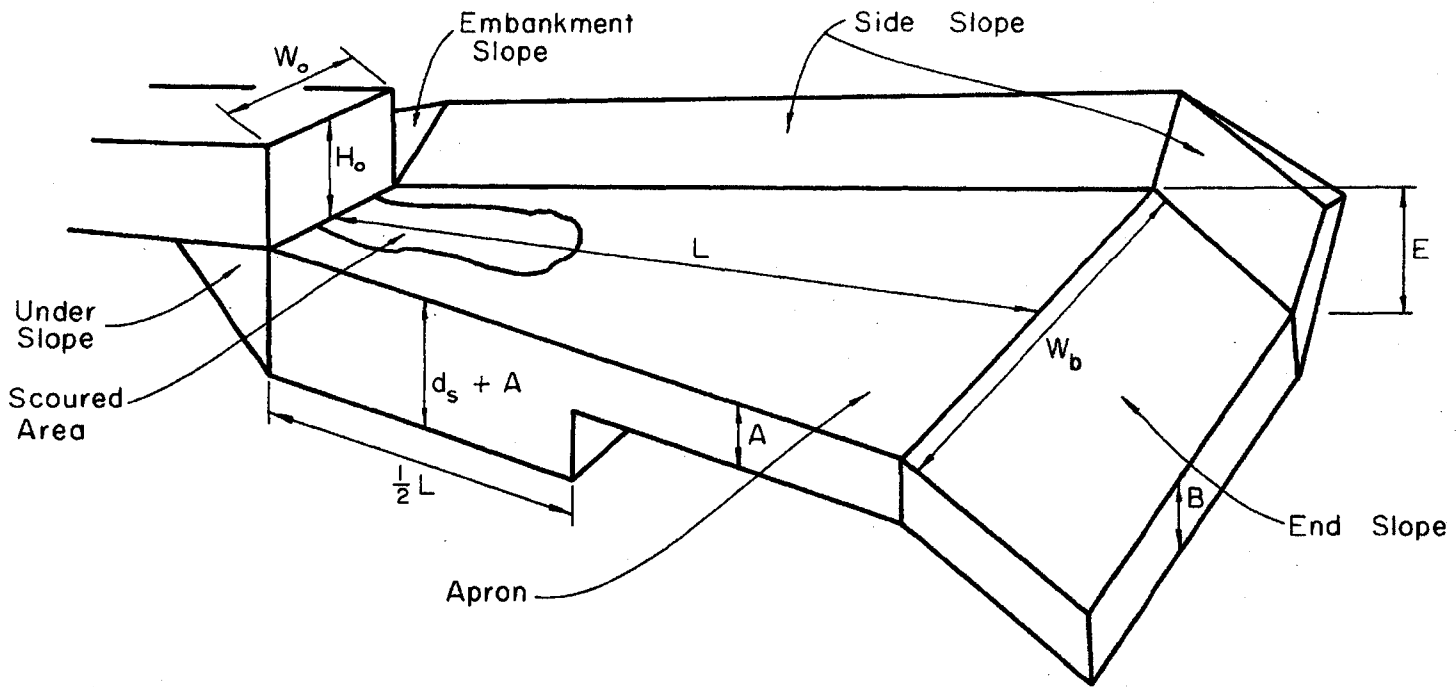


Fig. 42 Standard Hybrid Riprapped Basin

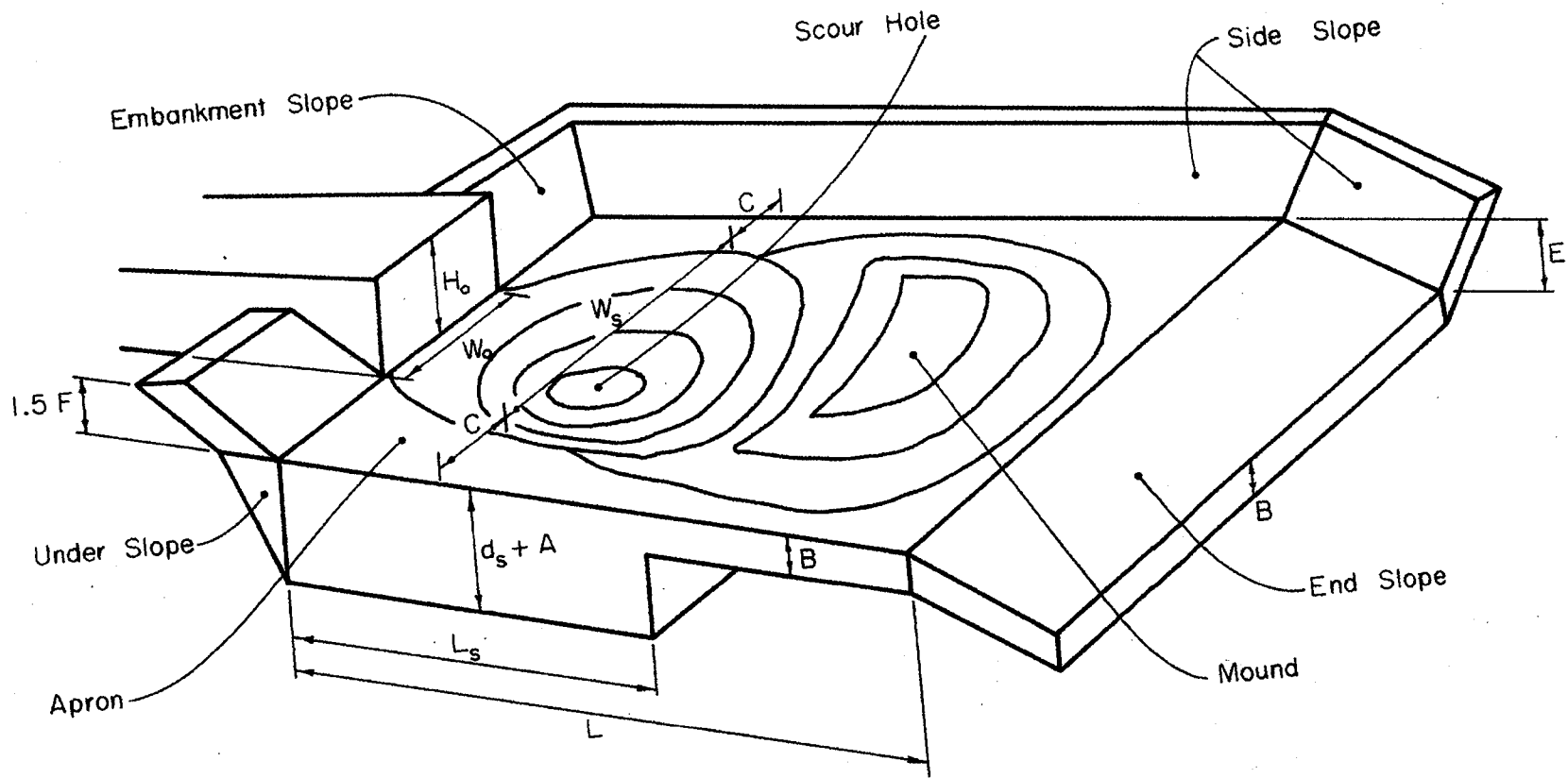


Fig. 43 Standard Scoured Basin

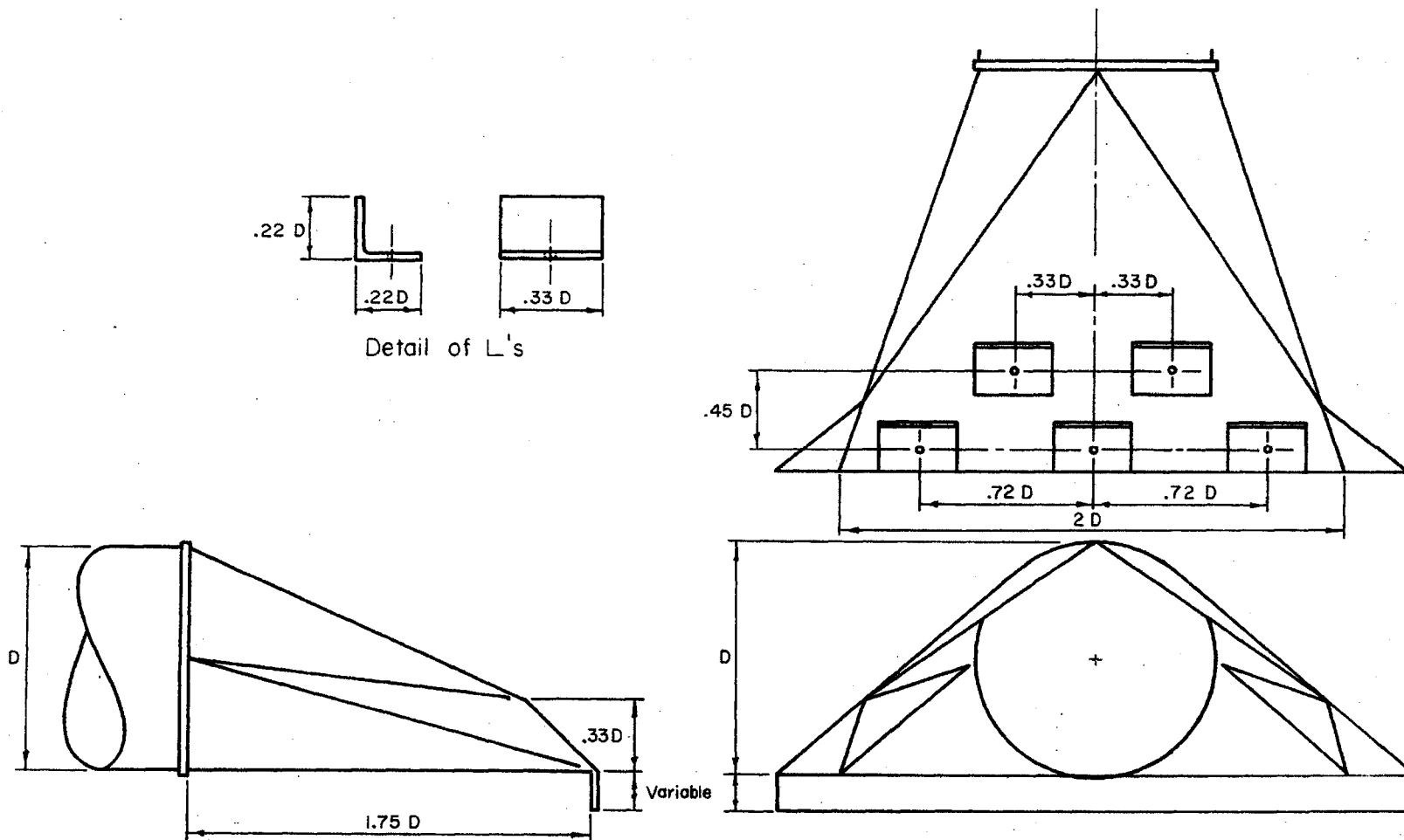


Fig. 44 Metal End Section

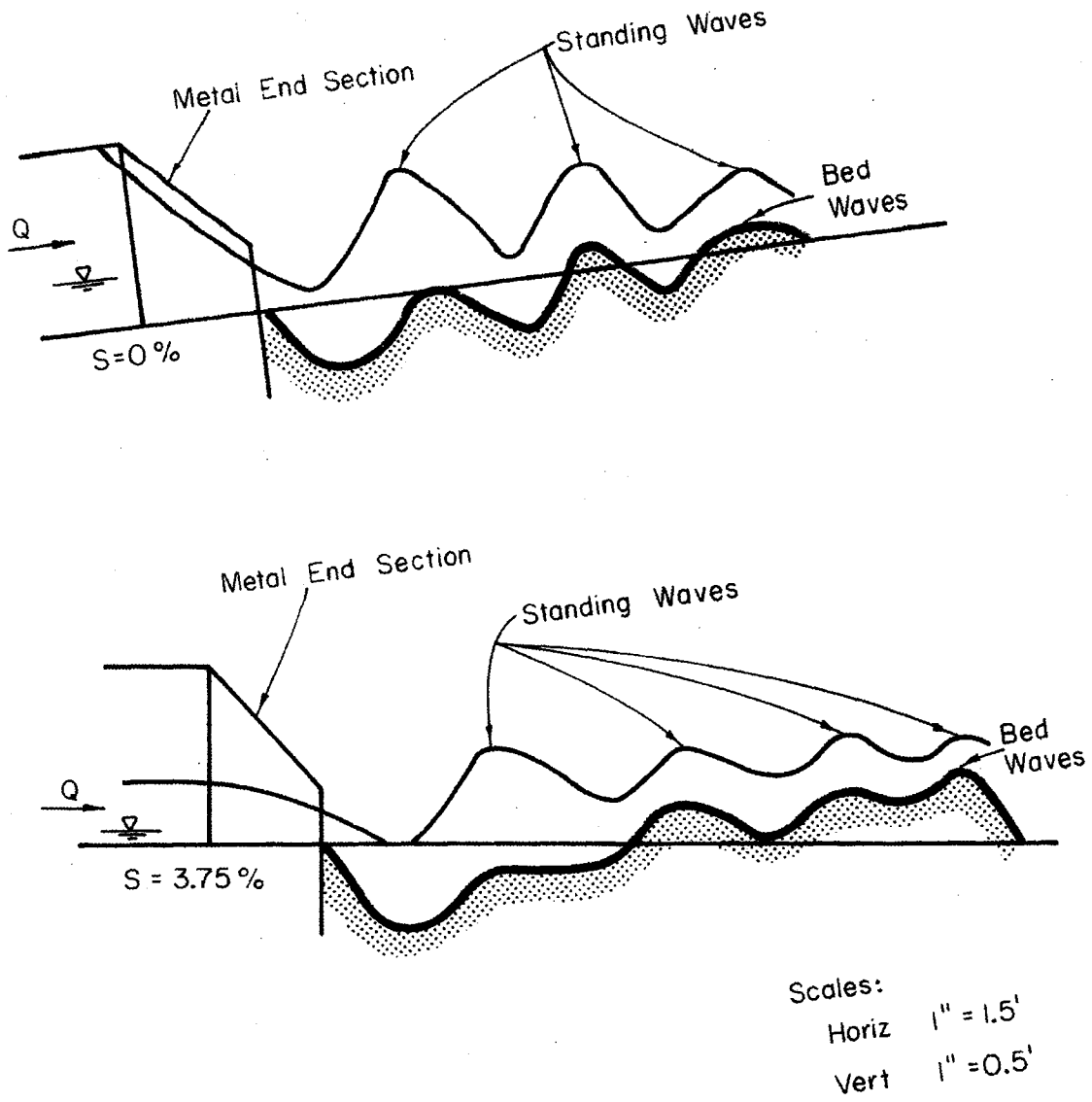


Fig. 45 Standing Waves

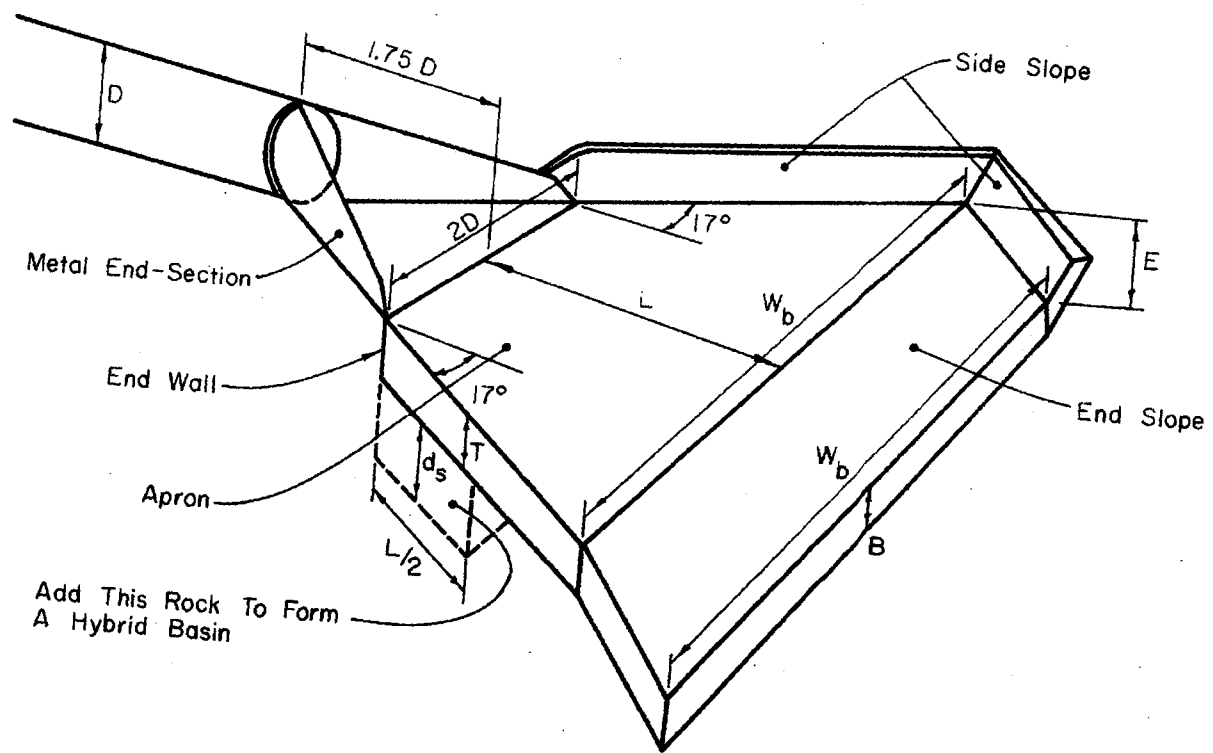


Fig. 46 Non-Scouring Basin with a Metal End Section

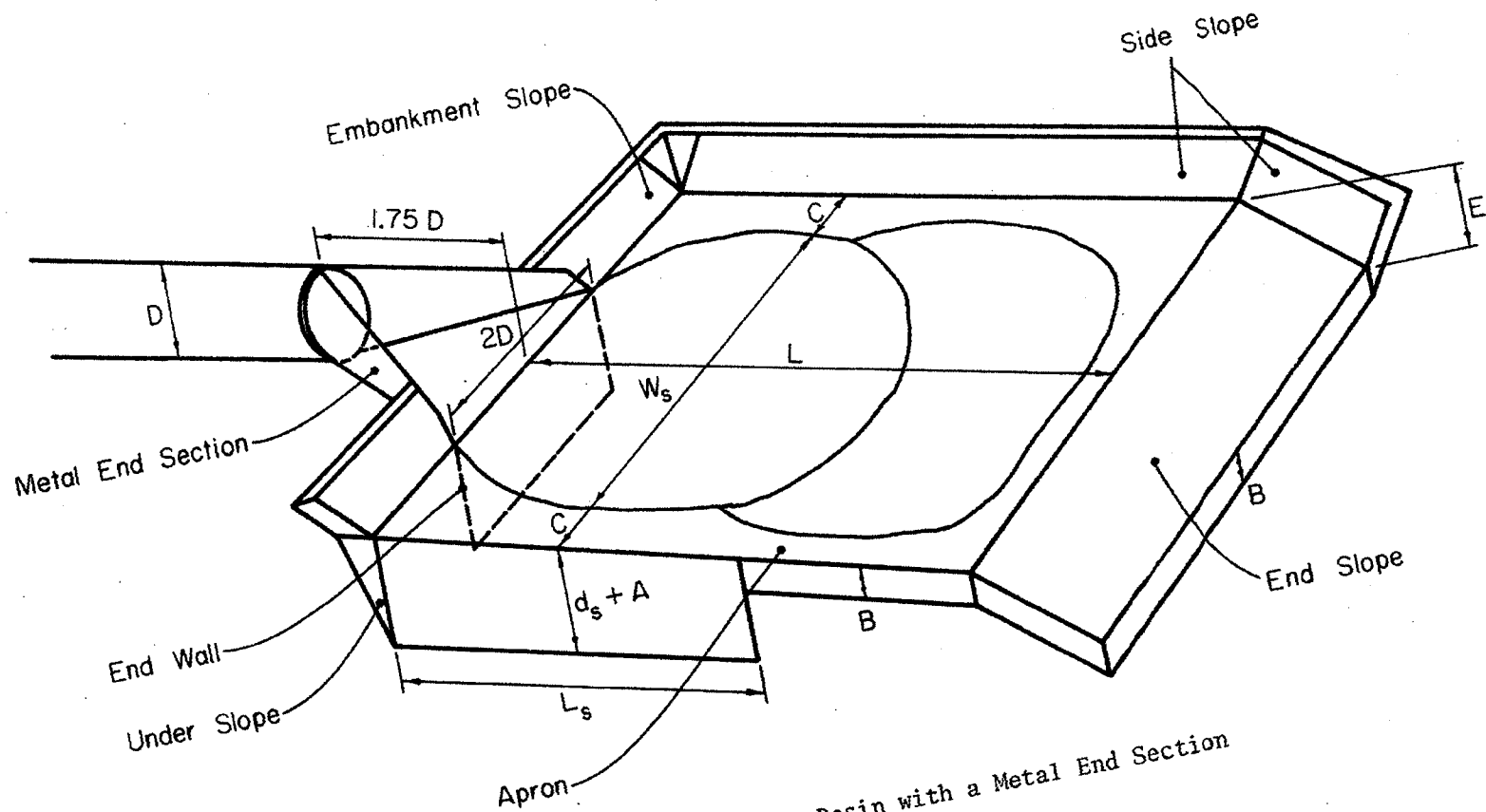


Fig. 47 Scouring Basin with a Metal End Section

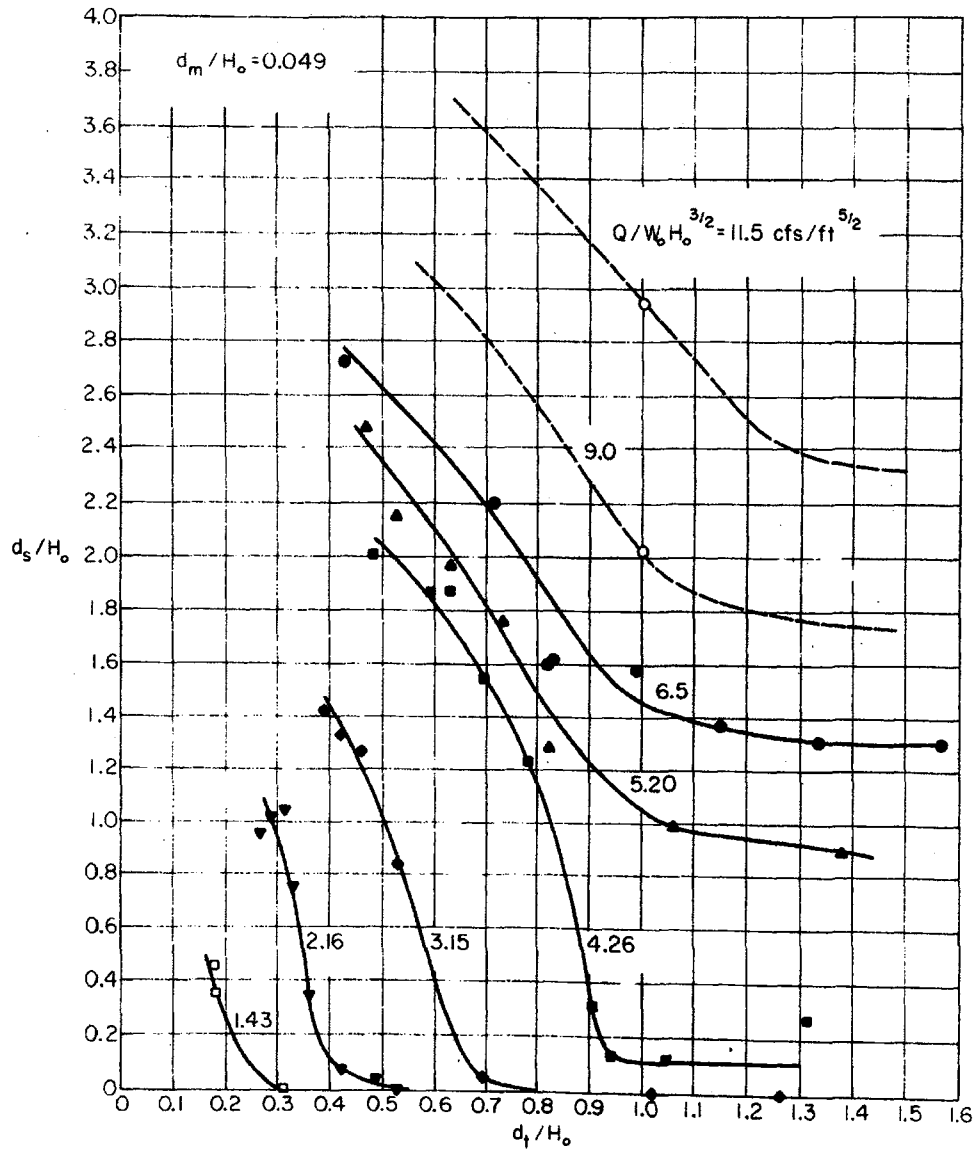


Fig. 48 Scour: Plain Rectangular Outlet

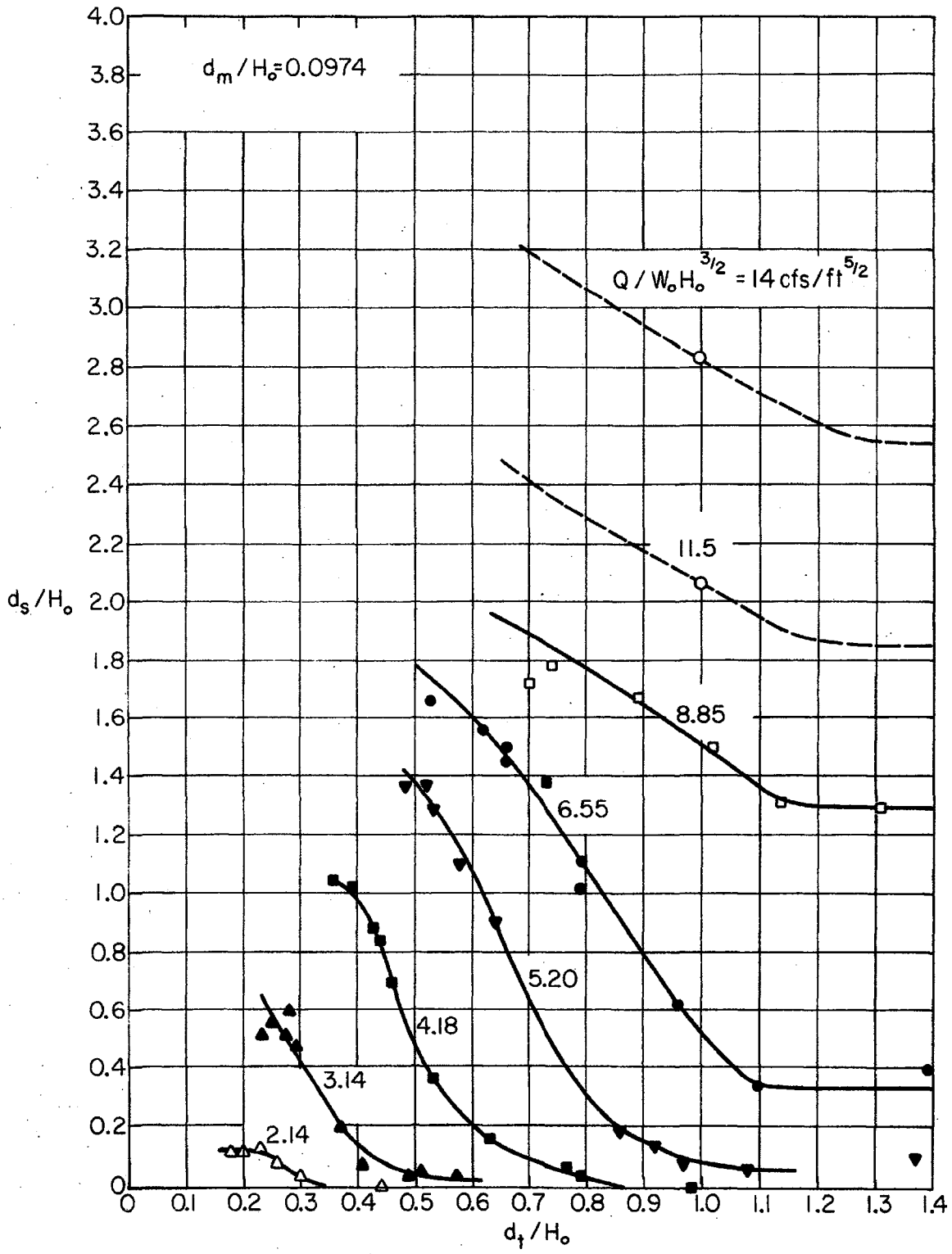


Fig. 49 Scour: Plain Rectangular Outlet

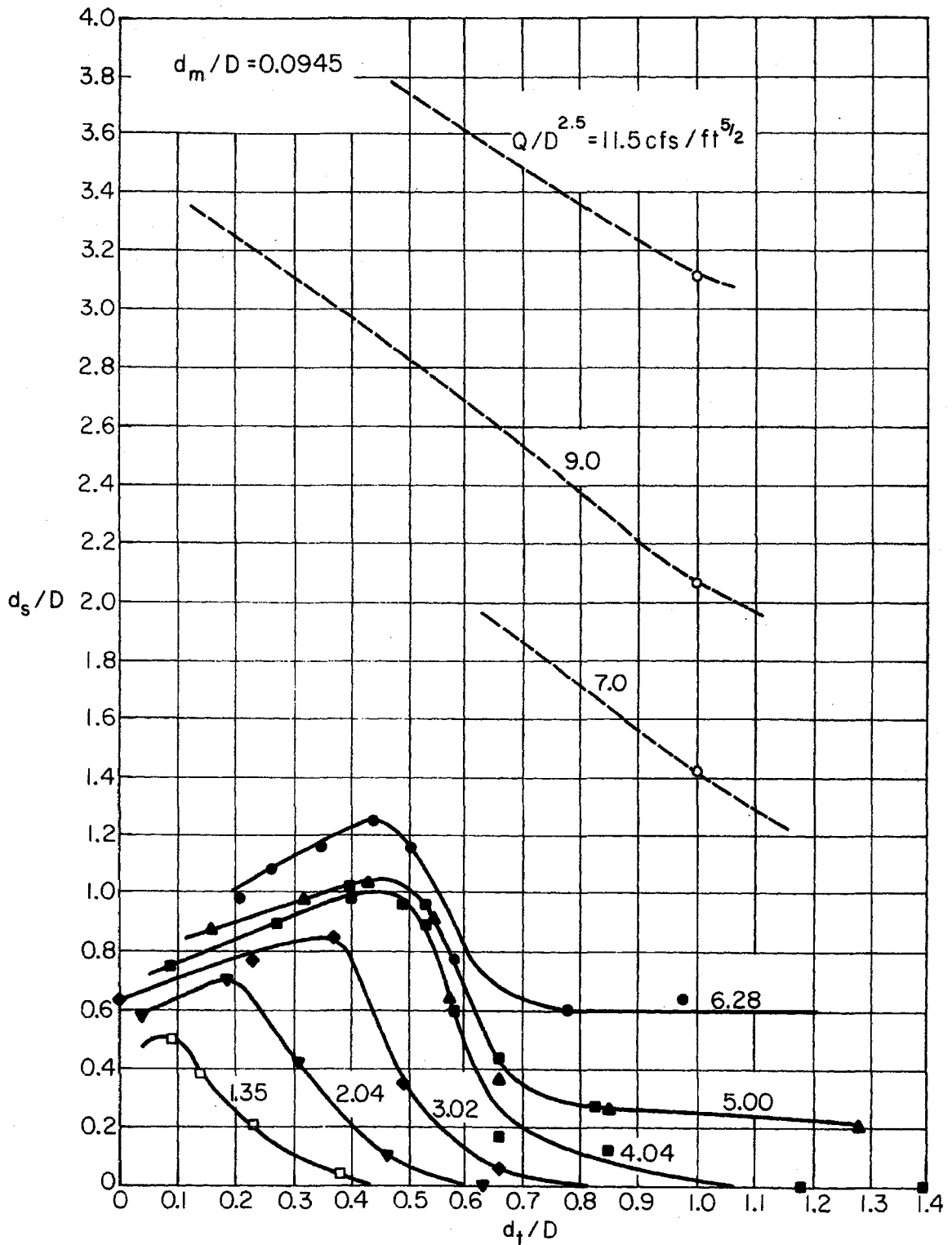


Fig. 50 Scour: Plain Circular Outlet

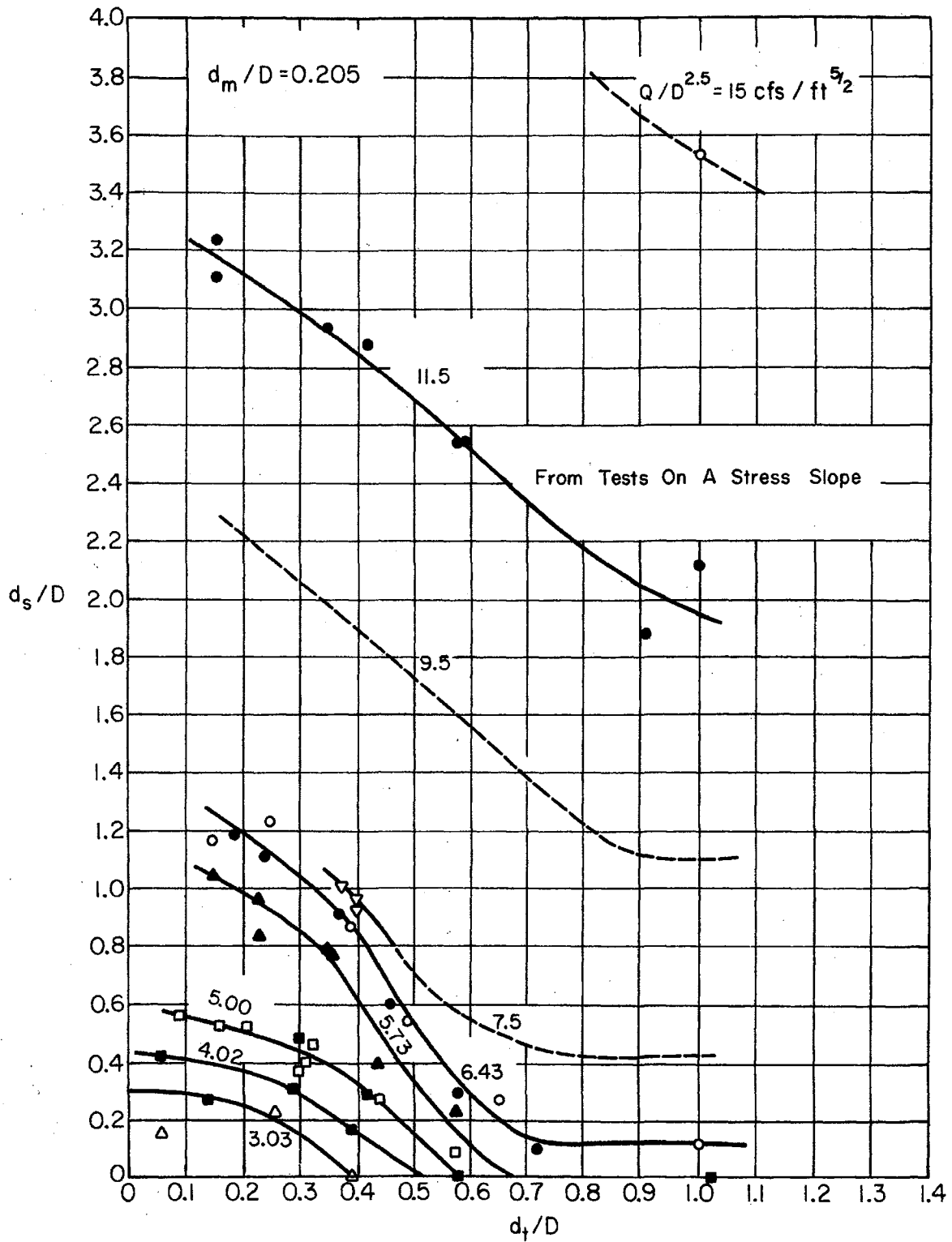


Fig. 51 Scour: Plain Circular Outlet

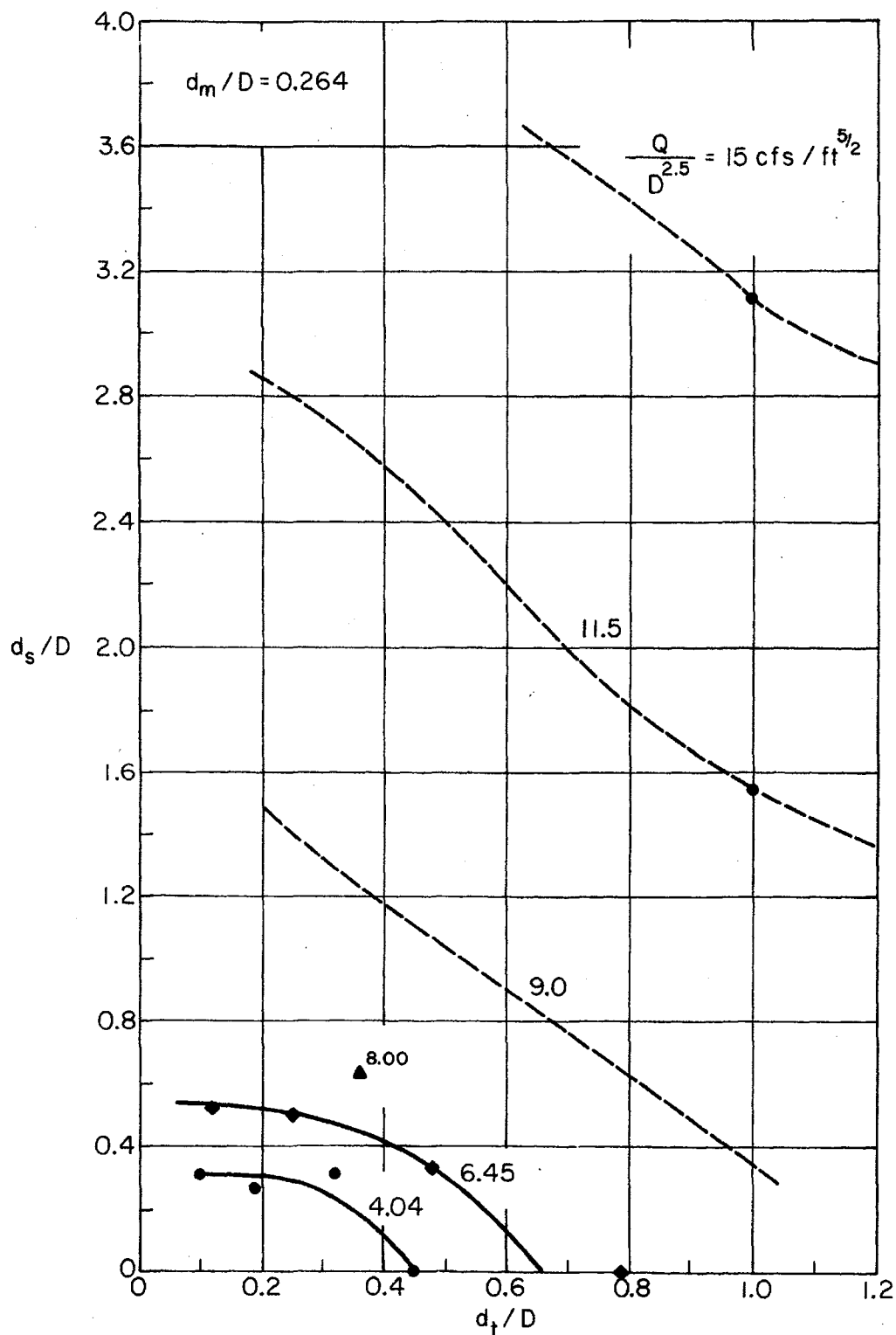


Fig. 52 Scour: Plain Circular Outlet

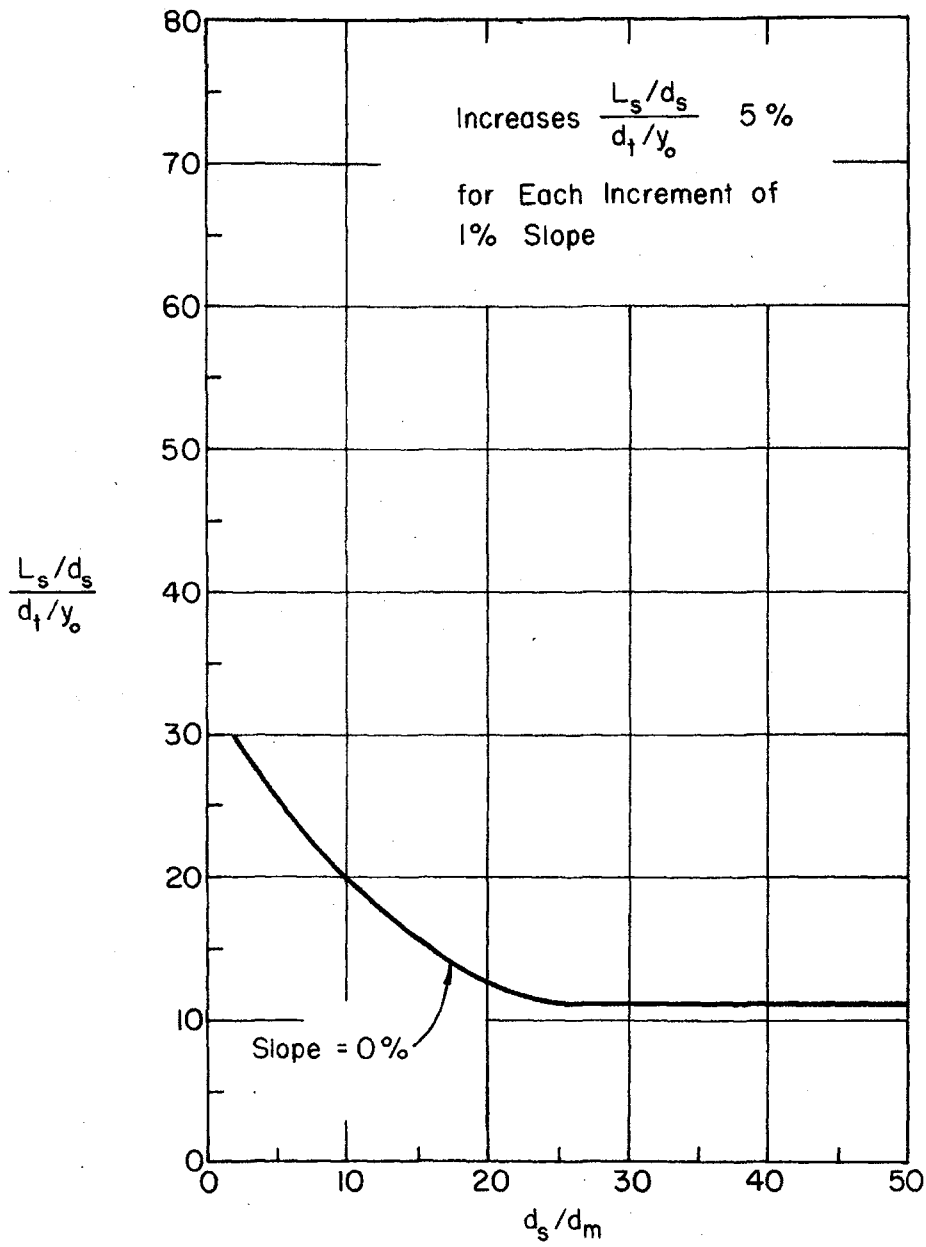


Fig. 53 Length of Scour Hole

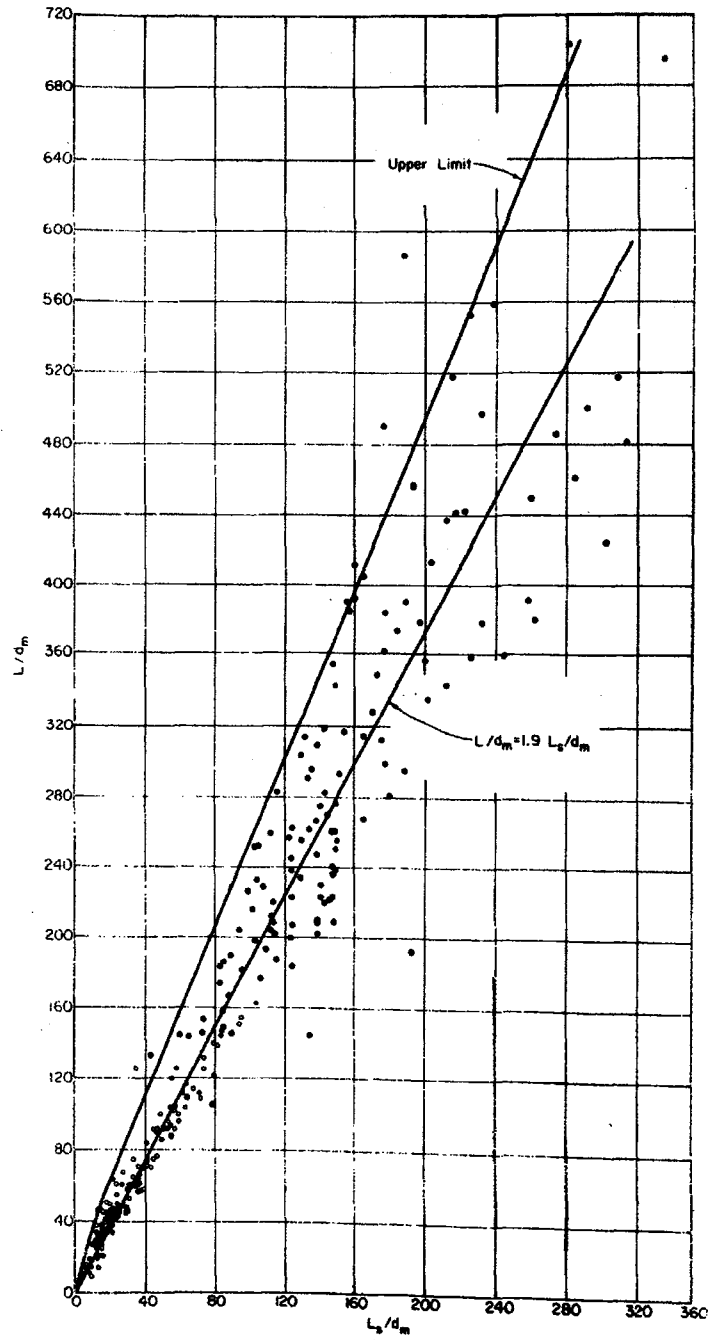


Fig. 54 Length of Basin

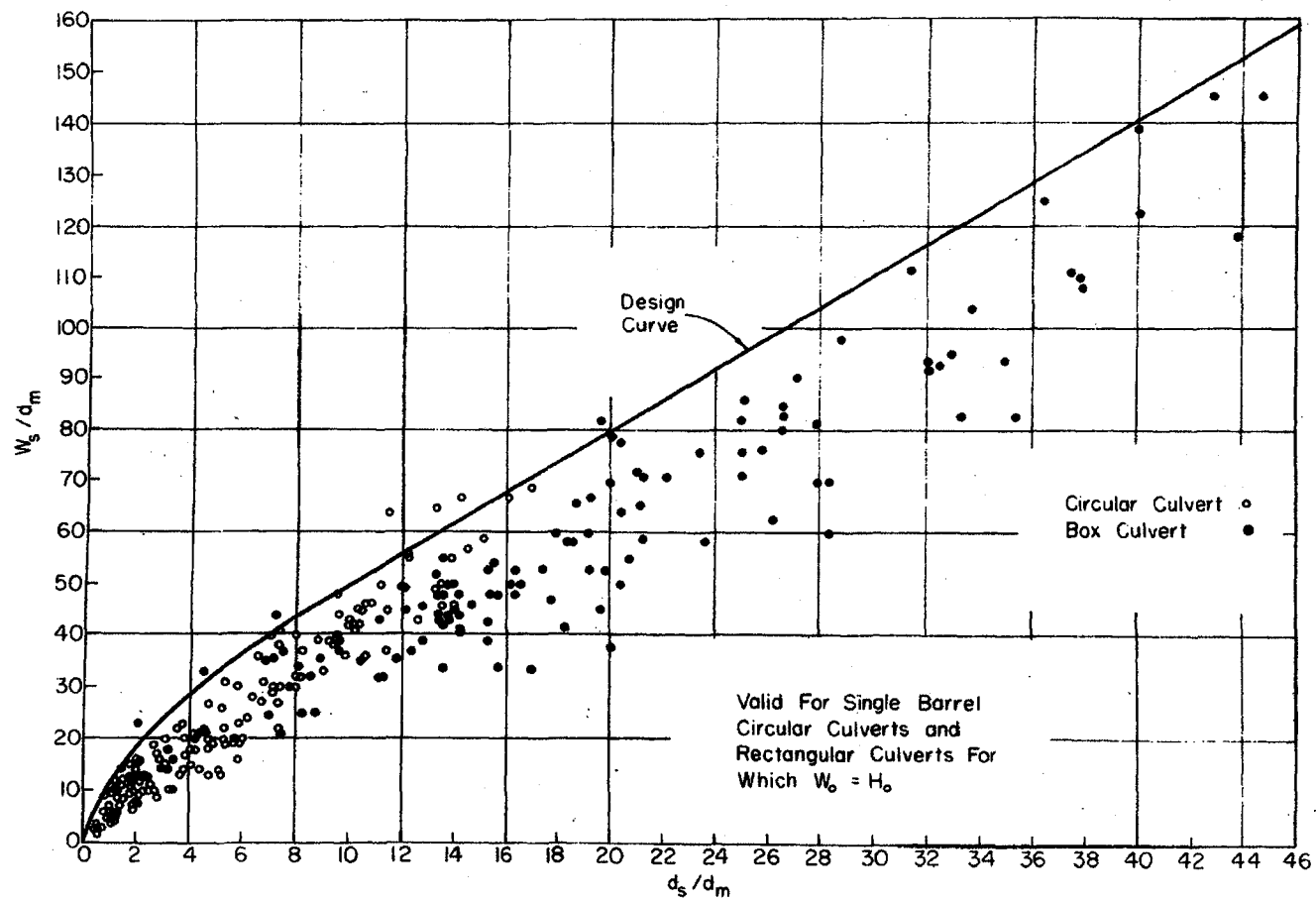


Fig. 55 Width of Scour Hole, Plain Outlets

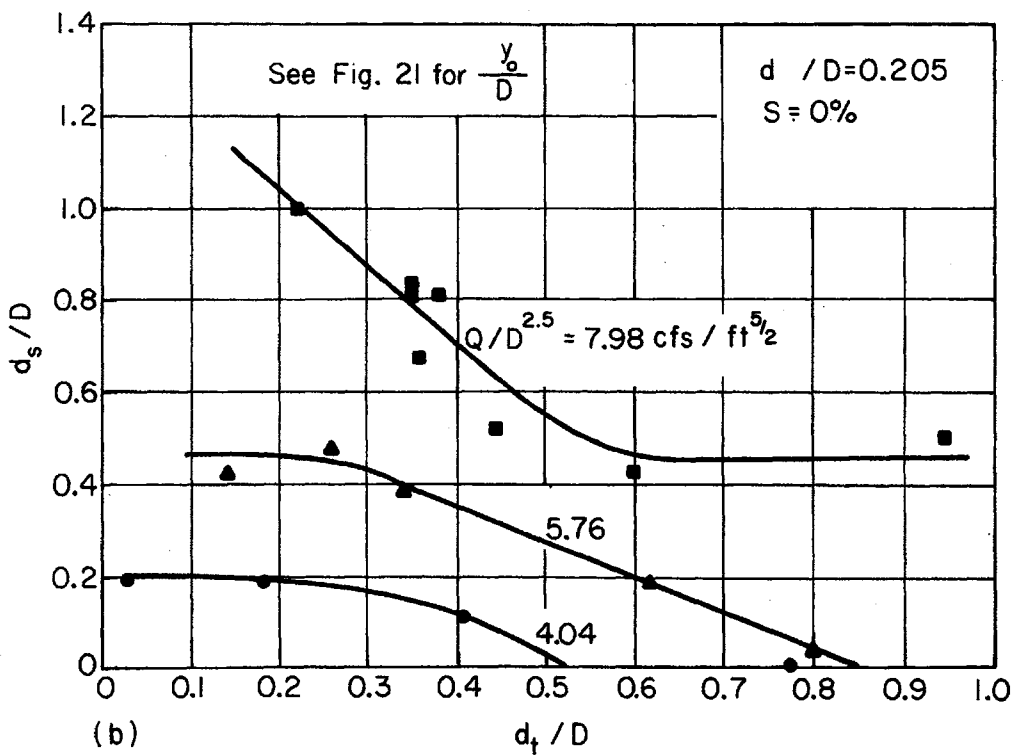
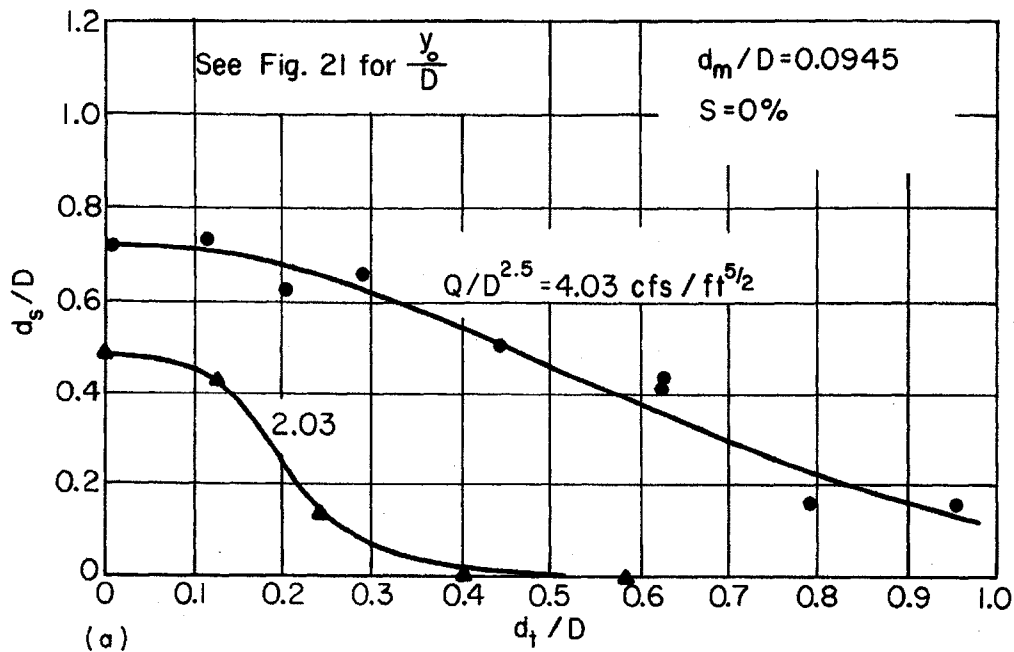


Fig. 56 Scour: Metal End Section

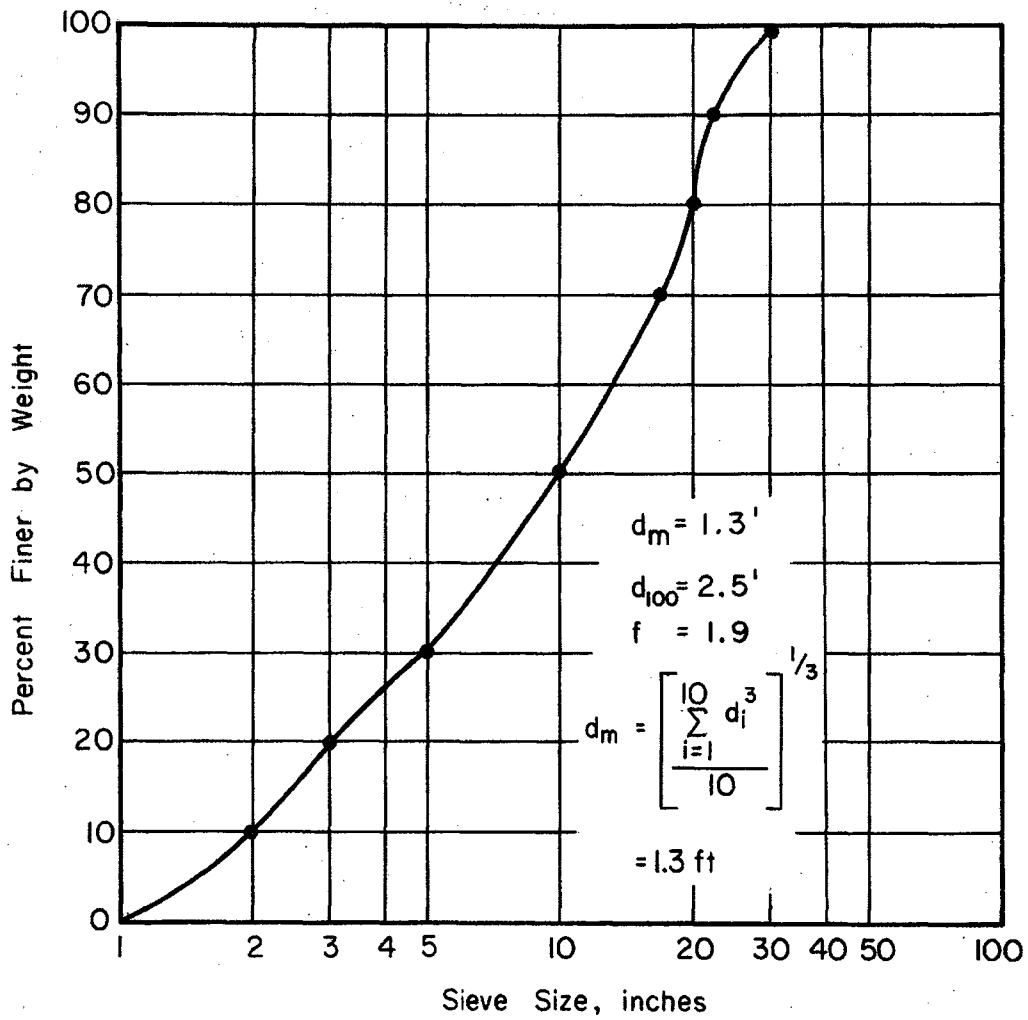


Fig. 57 Gradation Curve, Example 1

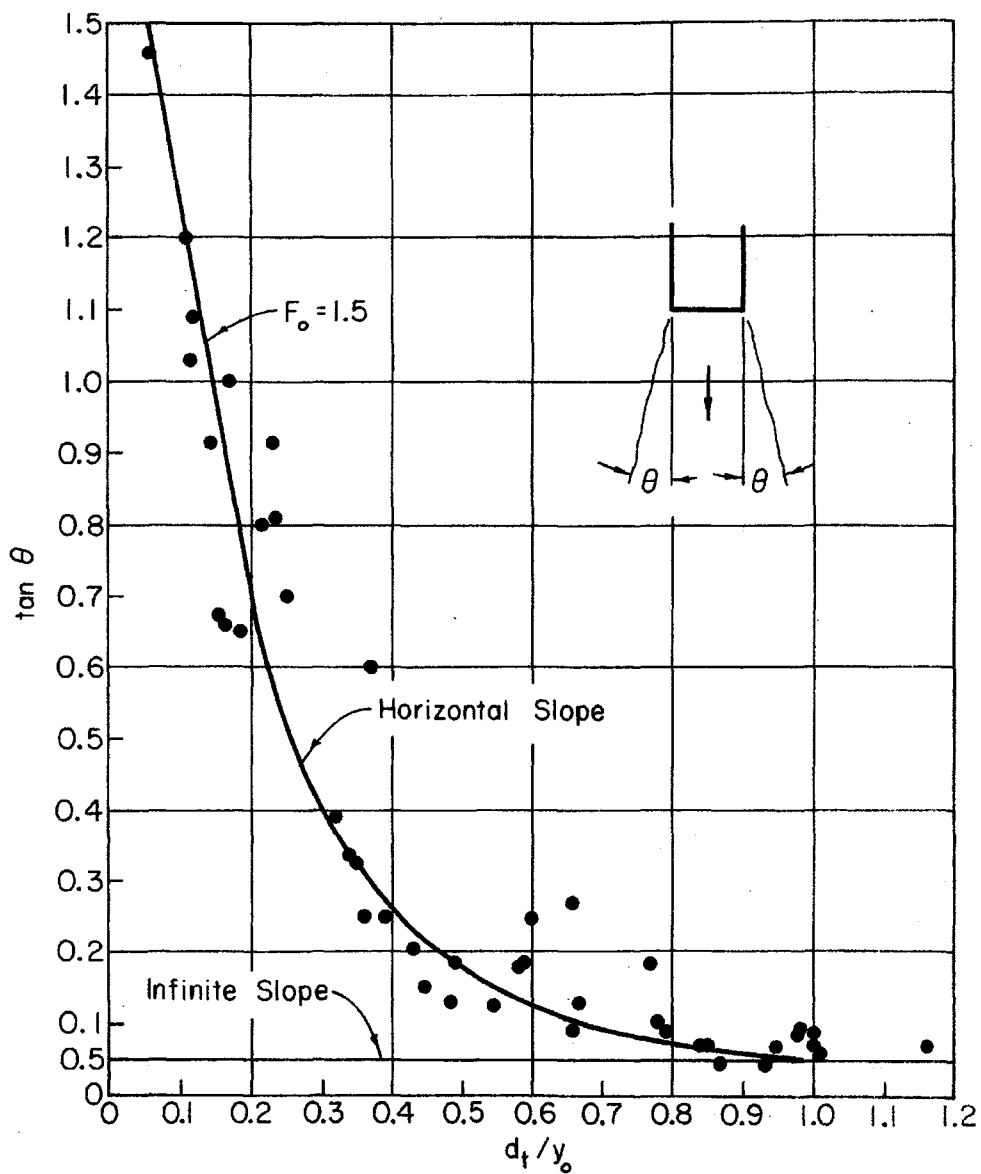


Fig. 58 An Estimate of the Angle of Lateral Expansion for Horizontal and Mild Sloping Circular Culverts

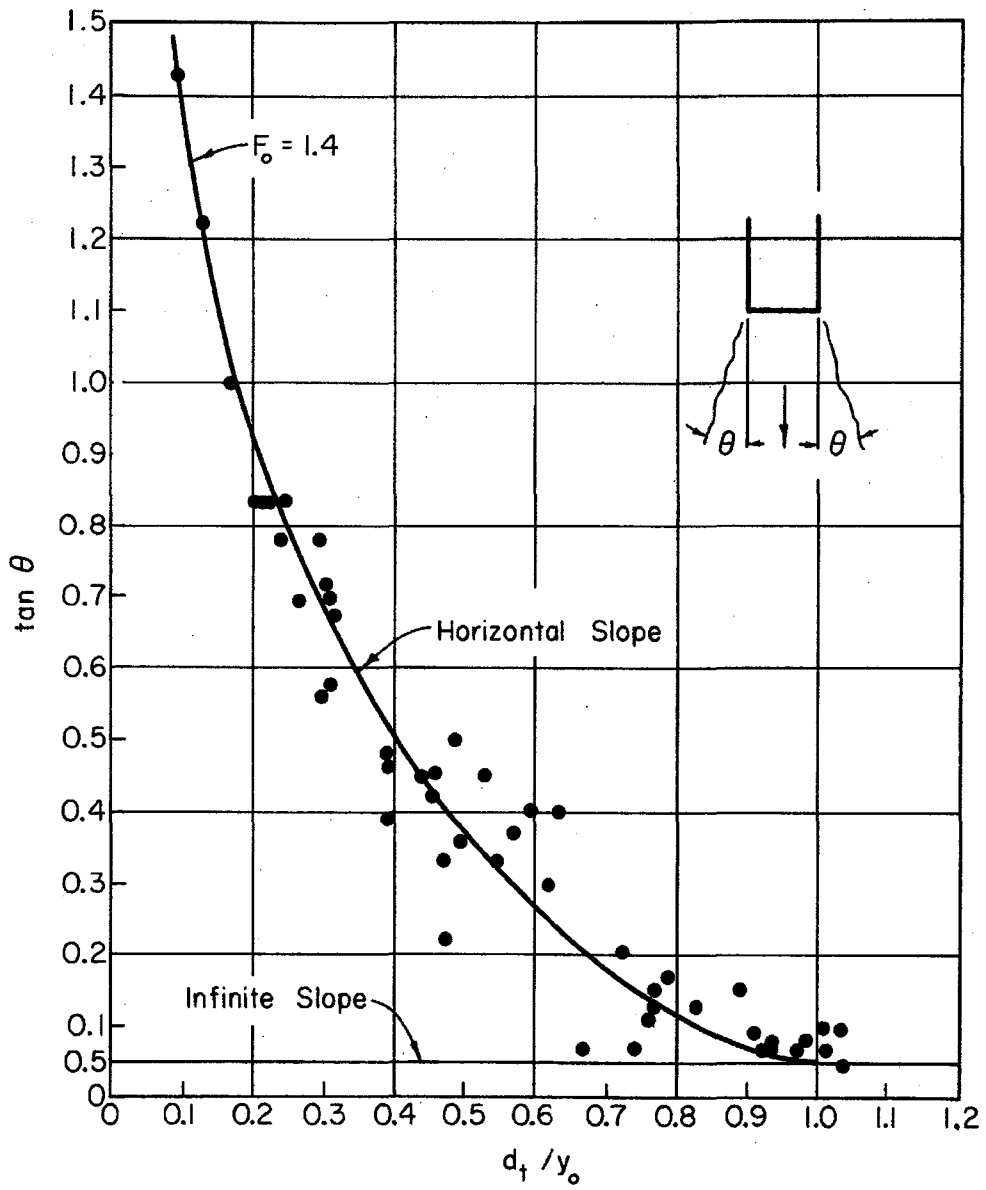


Fig. 59 An Estimate of the Angle of Lateral Expansion for Horizontal and Mild Sloping Rectangular Culverts

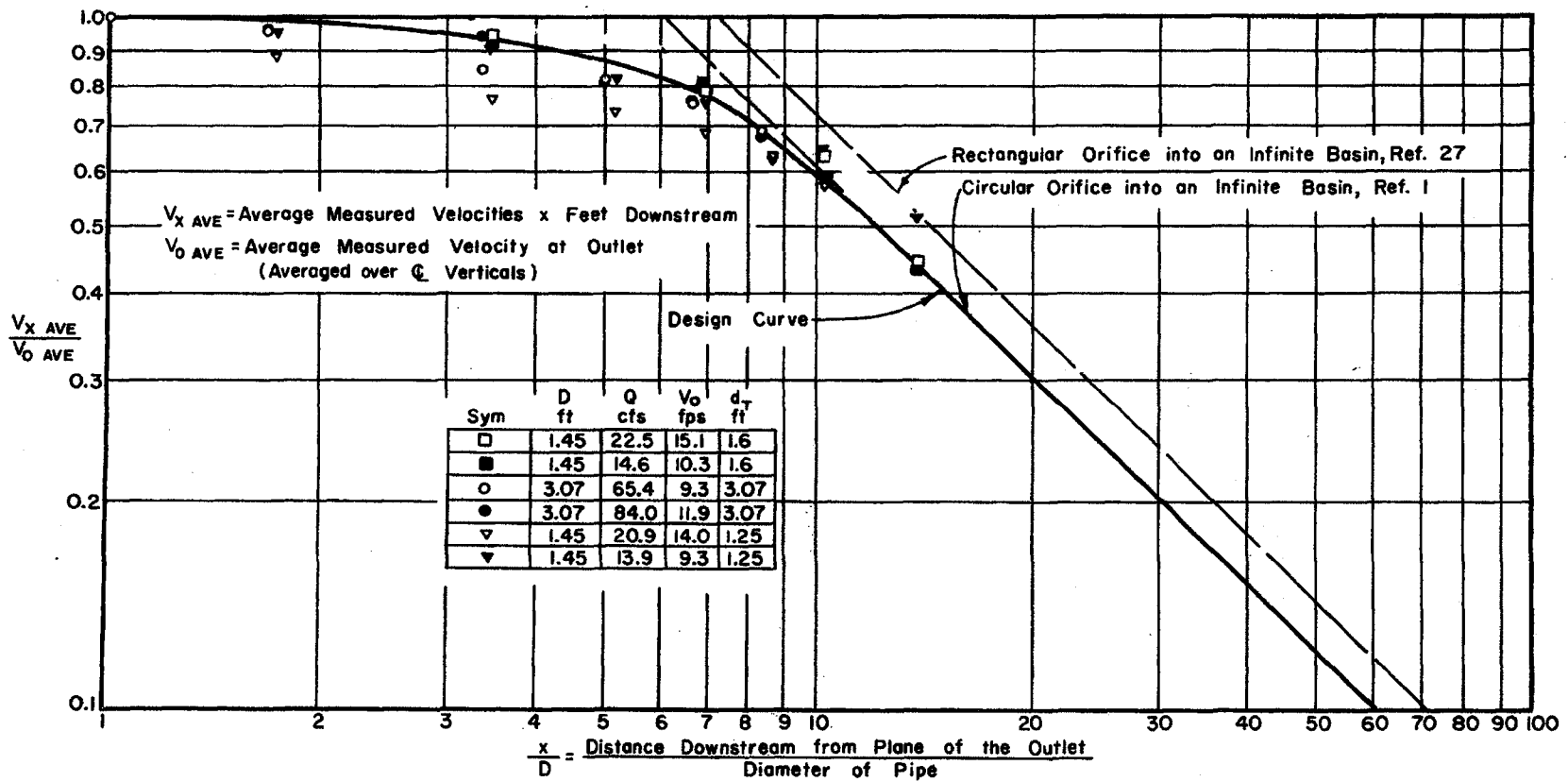


Fig. 60 Distribution of Centerline Velocity for Flow from Submerged Outlets (after Reference 1)

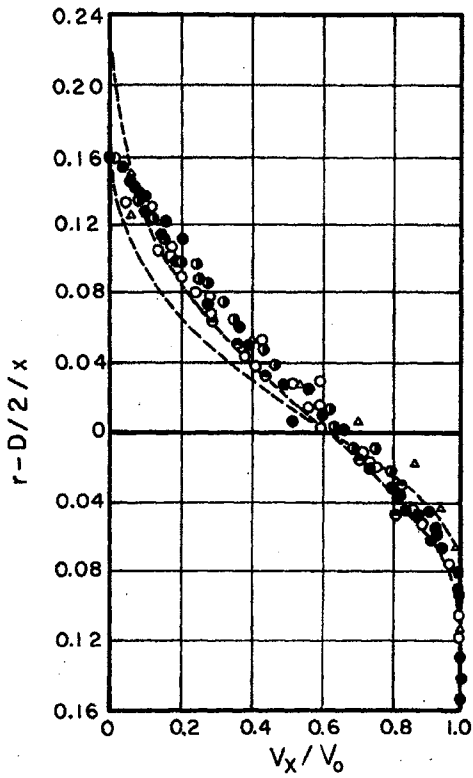
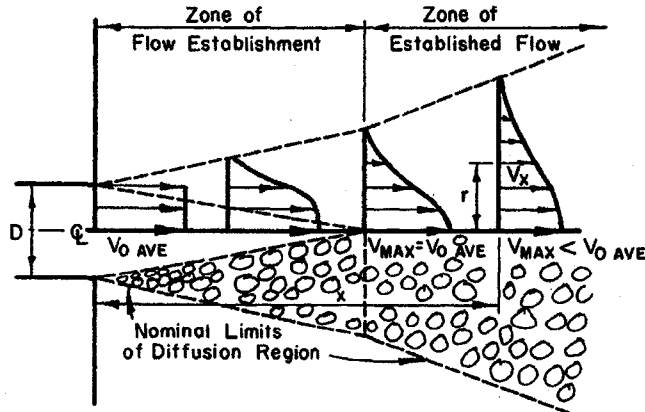


Fig. 61

Distribution of Longitudinal Velocity for $\frac{x}{D} < 6$ (after Reference 1)

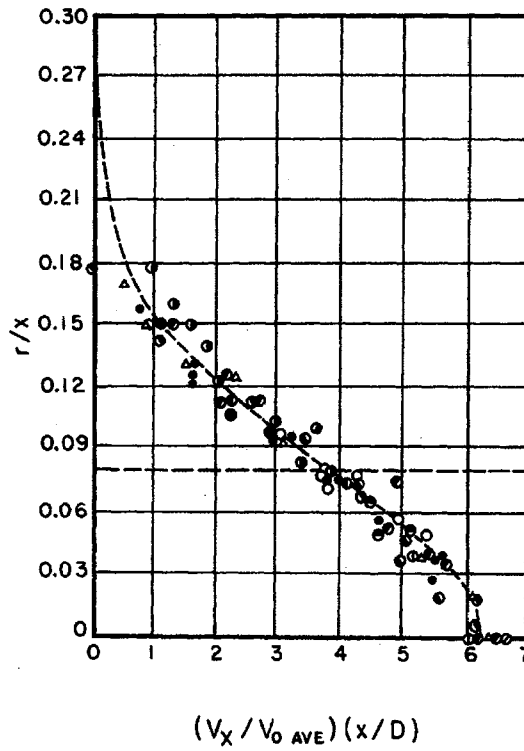


Fig. 62

Distribution of Longitudinal Velocity for $\frac{x}{D} > 6$

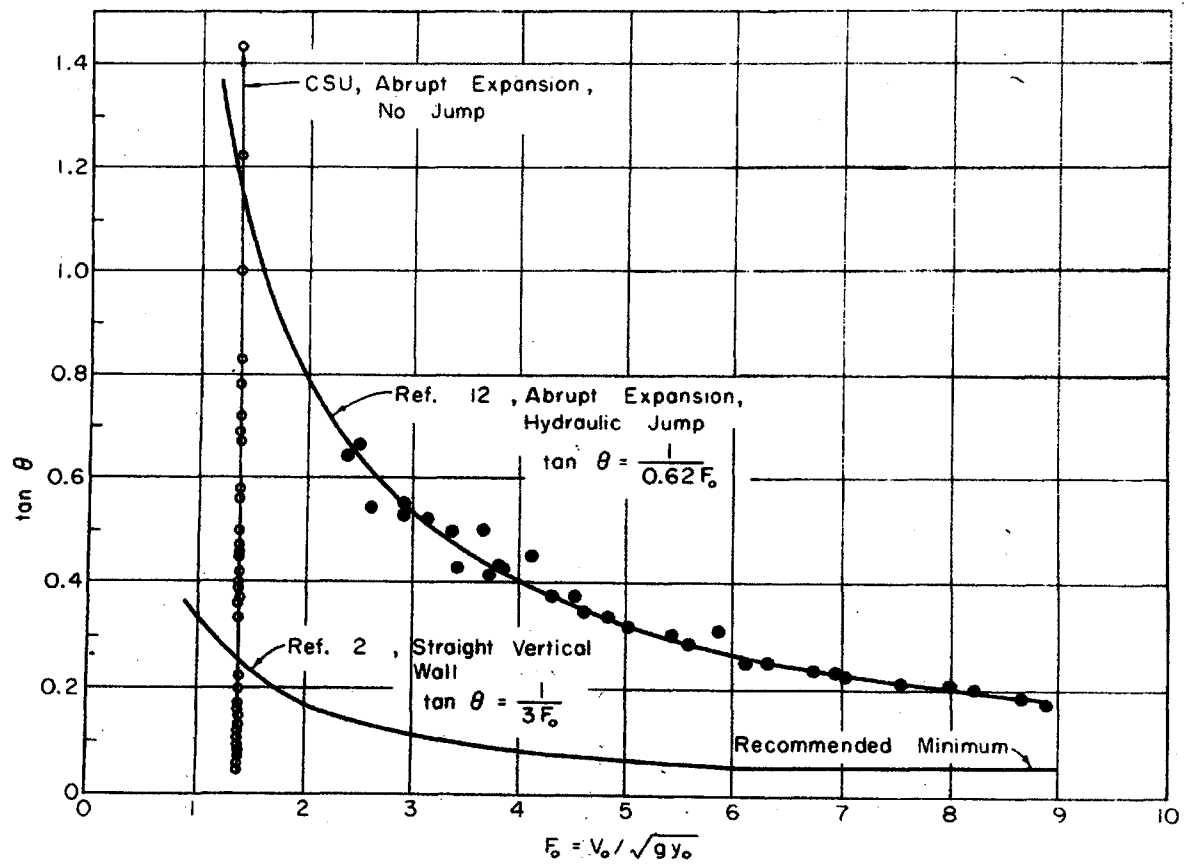


Fig. 63 Comparison of Expansion Angles for Different Basin Geometries

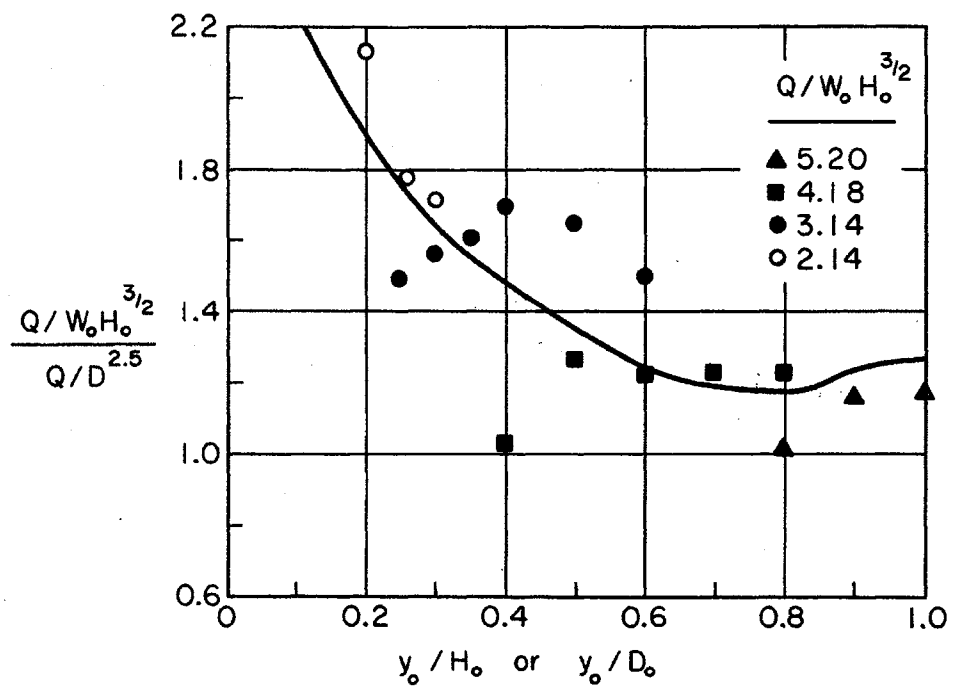


Fig. 64 Discharge Ratios for the Two-Dimensional Flow Approximation

APPENDIX C

FLARE ANGLE AT THE CULVERT OUTLET

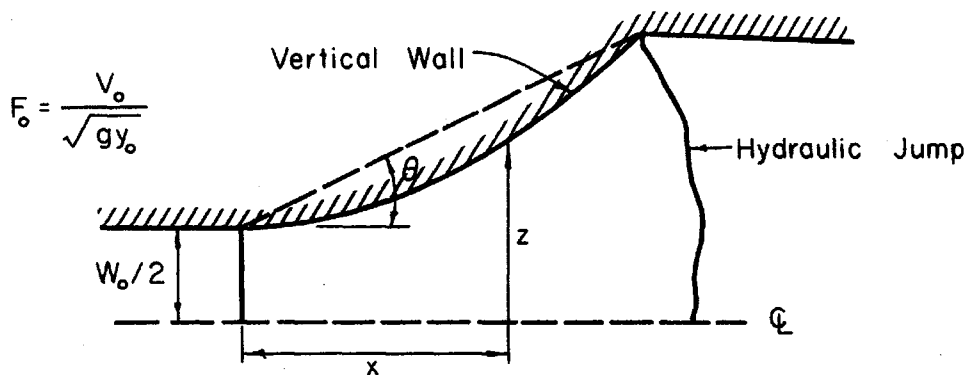
FLARE ANGLE AT THE CULVERT OUTLET

It can be reasoned that the rate of lateral expansion of the jet scouring the culvert outfall is a function of the outfall Froude number, $V_o/\sqrt{gy_o}$, the ratio of the basin width to culvert width, W_b/W_o or W_b/D (if the basin is rectangular), and the ratio of the tailwater depth at the outfall d_{to} to the brink depth y_o . If the jet expands rapidly the basin length is shorter and less material is required to construct the basin.

Rouse, Bhoota, and Hsu (14) have recommended a curved outlet with a vertical wall. The coordinates of the expanded wall are given by the equation

$$\frac{z}{W_o} = \frac{1}{2} \left(\frac{x}{W_o F_o} \right)^{3/2} + \frac{1}{2}$$

for rectangular outlets. The variables are shown in the plan view sketched below.



This geometry, tested in models with $1 \leq F_0 \leq 8$, provides a transition that prevents the formation of waves in the section, and the gradual increase in boundary angle does not cause any large changes in depth across any normal section; that is, the variation in depth from wall to wall at a normal section does not exceed 30 percent of the centerline value.

The vertical wall is matched to a rectangular basin as shown in the preceding sketch. Ideally, one would want the hydraulic jump to form at the end of the transition. Then the basin performs very well hydraulically. However there is a problem, the jump will move with changes in discharge and/or downstream tailwater depth. Rouse, Bhoota, and Hsu (14) recommended an abrupt drop in the floor of the basin at the end of the transition wall.

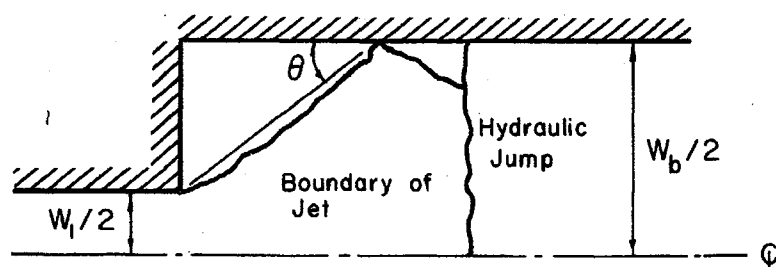
The basin with the curved wall transition is probably one of the best hydraulic designs that can be achieved. However, the curved vertical walls are costly, so efforts have been made to replace this curved wall with a straight vertical wall.

Blaisdell (2) has established criteria for the maximum permissible sidewall flare for the straight vertical walled transition. In the evaluation of his model test results ($1 \leq F_0 \leq 50$), Blaisdell considered that (1) the flare must be as extreme as possible to reduce the depth in the shortest possible distance, and (2) any disturbances created at the walls must not be objectionable from a practical point of view. His conclusion was that the maximum permissible sidewall flare is given by the equation

$$\tan\theta = \frac{1}{3F_0} .$$

The angle θ is shown in the previous sketch.

If an abrupt expansion to a rectangular basin of width W_b is used (no transition is provided), then the jet will choose a flare angle governed by the hydraulic conditions at the outlet. Rajaratnam and Subramanya (12) studied jumps occurring at sudden expansions with the geometry shown in the following sketch



The angle θ was measured in model tests in which the Froude number was varied from 2 to 9 and the expansion ratio, W_b/W_o , was varied between 1.2 and 6. It was found that

$$\tan\theta = \frac{1}{0.62 F_o}$$

when the jet is free to choose the angle of lateral expansion within the rectangular basin -- at least in the range $1.2 \leq W_b/W_o \leq 6$ and $2 \leq F_o \leq 9$.

In the CSU model studies employing a 6-in. by 12-in. rectangular culvert and a rectangular basin 6-foot wide ($W_b/W_o = 6$), an entirely different relationship was found. It is shown in Fig. 59. In this case the culvert was on a zero slope; for the discharges tested the Froude number, F_o , was essentially constant. It can be shown that for

a large portion of the data

$$F_o = \left(\frac{y_c}{y_o}\right)^{3/2} .$$

The relationship between d_t/y_o and y_c/y_o is given in Fig. 14 so F_o can be related to d_t/y_o . The relationship is tabulated below:

d_t/y_o	y_c/y_o From Fig. 14	F_o
0.0	1.31	1.50
0.1	1.30	1.483
0.2	1.29	1.465
0.3	1.28	1.448
0.4	1.27	1.431
0.5	1.265	1.423
0.6	1.26	1.415
0.7	1.25	1.398
0.8	1.23	1.264
0.9	1.22	1.348
1.0	1.00	1.00

Hence, F_o in the CSU model can be considered constant at a value of 1.4. Then, the angle of lateral expansion is a function of d_t/y_o .

It is now apparent that for abrupt expansions $\tan\theta$ is a function of F_o for high Froude numbers ($F_o > 2$), at least for $W_b/W_o < 6$, and $\tan\theta$ is a function of d_t/y_o for low Froude numbers ($F_o < 1.5$), at least for $W_b/W_o > 6$.

A study is required to establish the relationship among $\tan\theta$, F_o , W_b/W_o , d_{to}/y_o , and d_t/y_o for abrupt expansions. Here d_{to} is the tailwater depth at the plain of the culvert outfall and d_t is the tailwater depth at the end of the rectangular basin. As a starting point, application of the momentum equation to the control volume of fluid in the basin yields the expression

$$\left(\frac{d_t}{y_o}\right)^3 - \frac{d_t}{y_o} \left[W_r + \left(\frac{d_{to}}{y_o}\right)^2 (1-W_r) + 2F_o^2 W_r (1-C_s) \right] + 2F_o^2 W_r^2 = 0$$

$$(d_{to} \leq y_o)$$

in which

$$W_r = W_o/W_b,$$

and the total integrated shear force on the floor and walls is assumed to be $C_s \rho Q V_o$. The equation degenerates into the classical hydraulic jump equation

$$\frac{d_t}{y_o} = \frac{1}{2} \left[\sqrt{8F_o^2 + 1} - 1 \right]$$

if, $W_r = 1$, $d_{to} = y_o$, and $C_s = 0$.

The abrupt expansion is not an economical design because the corners of the basin at the culvert outfall serve no apparent function and yet require considerable concrete. If the corners are eliminated by a straight vertical wall flaring at an angle θ given by either $\tan\theta = 1/0.62 F_o$ for $F_o > 2$ or by Fig. 59 if $F_o \leq 1.5$, there is no certainty that the basin will perform properly. The flare angle would be much greater than that recommended by Blaisdell (2), especially at

low Froude number flows. Yet Blaisdell's criteria results in a very long basin.

One is tempted to replace the curved vertical wall recommended by Rouse, Bhoota, and Hsu with a straight vertical wall having the same terminal point. Then,

$$\tan\theta = \frac{\left(\frac{W_b}{W_o} - 1\right)^{1/3}}{2 F_o}$$

However, there is no proof that the hydraulic performance would be satisfactory in such a basin.

For culvert basin design the volume of concrete must be kept at a minimum and the length of the basin as short as possible. A large investment cannot be justified in an outlet basin structure that is utilized at its design capacity only one in 25 years. Long basins are tolerable only in limited cases because they would require the purchase of more right-of-way. This would suggest a plan of research in which one would strive to find an optimum flare angle based on certain conditions:

1. the downstream normal tailwater would be utilized to establish a hydraulic jump in the basin;
2. the flare angle would be such that the momentum on the centerline of the basin just upstream of the jump is a minimum in this sense. Any increase in flare angle would not decrease the distance from the outlet to the toe of the jump and any decrease in θ would result in the jump moving downstream.

An abrupt drop in floor level could be considered to help stabilize the jump under lower discharge and a changing tailwater condition.

At present, the only flaring straight vertical walled transition that can be recommended is that established by Blaisdell; i.e.,

$$\tan\theta = \frac{1}{3 F_o} .$$

Figure 63 has been prepared to show the variation of $\tan\theta$ with Froude number. The equation

$$\tan\theta = \frac{\left(\frac{W_b}{W_o} - 1\right)^{1/3}}{2 F_o}$$

is not shown but represents a family of curves for which

$$\tan\theta = \frac{1}{0.62 F_o}$$

and

$$\tan\theta = \frac{1}{3 F_o}$$

are two members.

An obvious conclusion is that commercial interests should consider alternate basin designs that utilize, totally or in part, manufacturable energy dissipating basin components.

APPENDIX D
R-JUMP BASIN

R-JUMP BASIN

The so-called R-jump basin reported by Rajaratnam and Subramanya (12) can be used at rectangular culvert outlets provided that

$$2.0 < F_o < 9.0, \text{ and}$$

$$1.2 \leq \frac{W_b}{W_o} \leq 6.0 ,$$

and that the designer understand the risk involved. Using R-jump basin requires that the tailwater be specified by the design charts. Any increase in tailwater above that required for the design will result in the collapse of the jump and the tailwater will spill upstream on one side of the basin. Then the jet is forced against the other wall and will leave the basin with little or no reduction in velocity. If the tailwater drops below that required for the R-jump, the jump will move downstream and possibly out of the basin. In the design, it will be necessary to establish that the design is satisfactory for all discharges up to and including the culvert design flood discharge. This type of design procedure is illustrated in a U.S. Bureau of Reclamation report (19, p. 40).

The basin geometry is shown in the sketches on the next page.

The design equations are.

$$\frac{W_o}{W_b} = \frac{\left(\frac{d_t}{Y_o}\right) - 0.75}{F_o - 0.85} - 0.30 ,$$

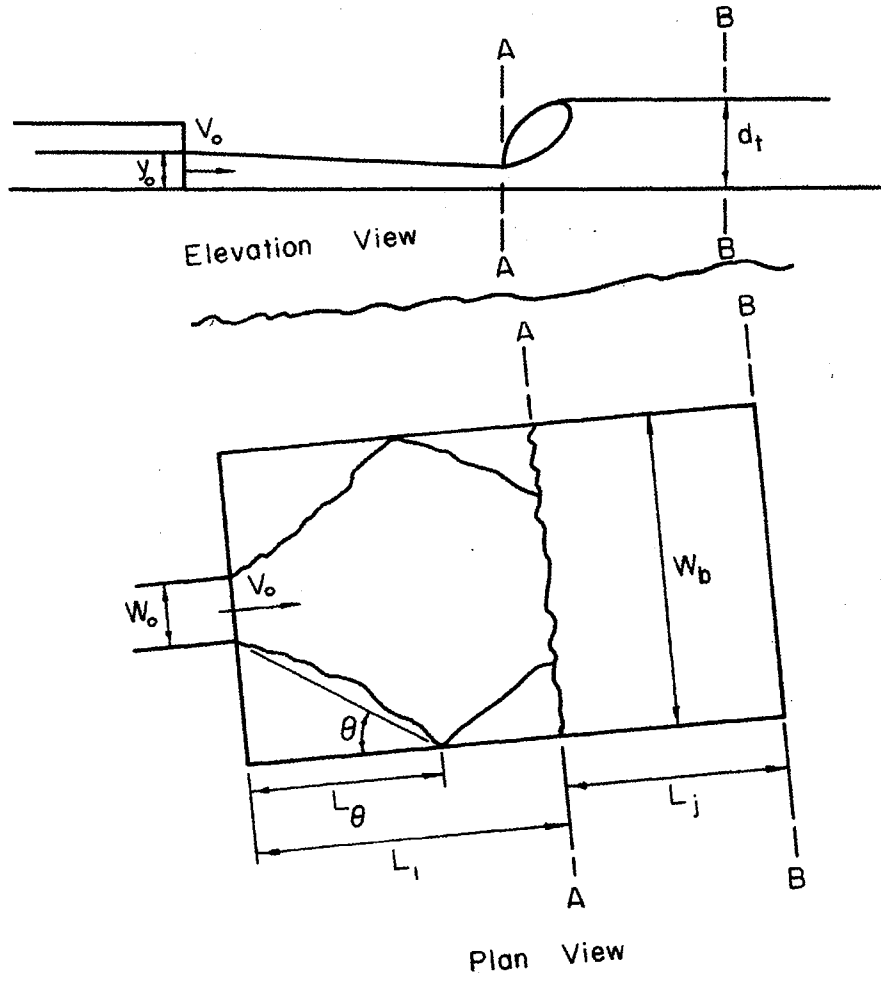
$$\frac{L_j}{d_t} = 5 ,$$

$$\frac{L_1}{W_b - W_o} = 0.62 F_o$$

$$F_o = \frac{V_o}{\sqrt{g y_o}}$$

and

$$\tan \theta = \frac{1}{0.62 F_o}$$



Example of the Design of the R-Jump Basin

Given	6 ft x 6 ft	box culvert
	Design discharge	Q = 600 cfs
	Brink depth	y _o = 2 ft
	Tailwater depth	d _t = 8 ft for 600 cfs

The solution is:

$$V_o = \frac{Q}{y_o \times W_o} = \frac{600}{2 \times 6} = 50 \text{ fps}$$

$$F_o = \frac{V_o}{\sqrt{g y_o}} = \frac{50}{\sqrt{32.2 \times 2}} = \frac{50}{8.02} = 6.25$$

$$\frac{W_o}{W_b} = \frac{(d_t/y_o) - 0.75}{F_o - 0.85} = 0.30$$

$$= \frac{4 - 0.75}{6.25 - 0.85} = 0.30$$

$$= 0.614 - 0.300$$

$$= 0.314$$

$$W_b = \frac{W_o}{0.314} = \frac{6}{0.314} = \underline{19 \text{ ft}}$$

$$L_j = 5 d_t = 5 \times 8 = \underline{40 \text{ ft}}$$

$$\frac{L_1}{W_b - W_o} = 0.62 F_o$$

$$L_1 = 0.62 \times 6.25 (19-6)$$

$$L_1 = \underline{51 \text{ ft}}$$

Hence, a rectangular basin, 19 ft by 91 ft, is required for the design discharge; the velocity leaving the basin would be 4 fps.

From the equations for flow through culverts, the discharge-brink depth relationship can be determined. Also, the discharge-stage relationship for the natural channel can be developed. With this information the 19 ft by 91 ft basin is checked for other discharges and tailwaters less than the design values.

Suppose, for example, that when $Q = 300$ cfs, $y_o = 1.25$ ft and $d_t = 6.0$ ft, then

$$V_o = \frac{300}{1.25 \times 6} = 40 \text{ fps}$$

$$F_o = \frac{40}{\sqrt{g \times 1.25}} = \frac{40}{6.34} = 6.32.$$

The required tailwater to produce a R-jump is

$$\frac{d_t}{y_o} = \left(\frac{W_o}{W_b} + 0.30 \right) (F_o - 0.85) + 0.75$$

$$\frac{d_t}{y_o} = \left(\frac{6}{19} + 0.30 \right) (6.32 - 0.85) + 0.75$$

$$= .616 \times 5.47 + 0.75$$

$$= 3.37 + 0.75 = 4.12,$$

or

$$d_t = 4.12 \times 1.25 = 5.15.$$

Since the actual tailwater depth (6.00 ft) is greater than that required for the R-jump, the high velocity jet would probably be diverted to one wall by the tailwater flooding toward the outlet and no jump

would form at $Q = 300$ cfs. Hence, an R-jump basin should not be used on this culvert.

So, in general, unless the Froude number versus the d_t/y_o curve developed from the culvert hydraulic analysis closely matches that developed from the R-jump basin hydraulic analysis at all but the lowest discharges up to the maximum, the R-jump basin cannot be used. On the other hand it provides a very satisfactory design if the basin is properly designed and utilized.

APPENDIX E
TWO-DIMENSIONAL FLOW APPROXIMATION TO PREDICT SCOUR DEPTHS
AT THE OUTFALL OF CIRCULAR AND RECTANGULAR CULVERTS

TWO-DIMENSIONAL FLOW APPROXIMATION TO PREDICT SCOUR DEPTHS
AT THE OUTFALL OF CIRCULAR AND RECTANGULAR CULVERTS

It is reasoned that if the flow velocity, V_o , tailwater depth, d_t , and the brink depth, y_o , are the same in a rectangular culvert and in a circular culvert, then the depth of scour, d_s , would be the same for a given rock size, d_m . This hypothesis is described mathematically as follows.

If

$$(V_o)_{\text{rect}} = (V_o)_{\text{cir}}$$

$$(y_o)_{\text{rect}} = (y_o)_{\text{cir}}$$

$$(d_t)_{\text{rect}} = (d_t)_{\text{cir}}$$

and

$$(d_m)_{\text{rect}} = (d_m)_{\text{cir}},$$

then

$$(d_s)_{\text{rect}} = (d_s)_{\text{cir}}.$$

In essence, this is a two-dimensional approximation for flow from culvert outlets.

The discharge ratios $\frac{Q}{W_o H_o^{3/2}} / \frac{Q}{D^{2.5}}$ from the data given in Figs. 16 and 17 have been computed for

$$\frac{y_o}{H_o} = \frac{y_o}{D}$$

and

$$\frac{d_t}{H_o} = \frac{d_t}{D}.$$

The average values of the discharge ratios have been plotted as the curve in Fig. 64. There is a slight variance between computed values (not more than 5%) about the curve because of the effect of tailwater. The curve is applicable if the water surface profile upstream of the outlet is an M2 or H2 profile.

From Figs. 49 and 50, the discharge ratio $\frac{Q}{W_o H_o^{3/2}} / \frac{Q}{D^{2.5}}$ was found for the conditions that

$$\frac{d_s}{H_o} = \frac{d_s}{D}$$

$$\frac{y_o}{H_o} = \frac{y_o}{D}$$

$$\frac{d_t}{H_o} = \frac{d_t}{D}$$

and

$$\frac{d_m}{H_o} = \frac{d_m}{D} \quad (\text{approximately}).$$

These ratios are also plotted on Fig. 64

The agreement between the scour test results and the curve is generally good. The pipe size scale effect, discussed in Chapter II, did become apparent though. For example, in Fig. 50, when

$$4.04 \leq \frac{Q}{D^{2.5}} \leq 6.28 \text{ cfs/ft}^{5/2}$$

the scour depth curves are closely bunched for tailwater depths, d_t/D , in the range between 0.4 and 0.7. This is the influence of the region of negative pressure at the crown of the pipe near the outlet. The top

surface centerline velocity vector has a pronounced downward component on small models. The effect of the downward velocity component is to cause additional scour. The same influence exists in the box culvert but to a lesser extent and at a higher discharge. Therefore, on the models, good agreement between the two-dimensional flow hypothesis and experimental scour results cannot be expected for culverts flowing nearly full unless the brink depth scale effect is eliminated.

When both the rectangular and circular model culverts flow full, the indication is that, for the same outlet velocity, brink depth, and tailwater depth, scour in the circular culvert basin is slightly less than in the box culvert basin. The difference however is only about 5 percent.

Further confirmation of the two-dimensional flow approximation is found by comparing the CSU model study results with those obtained by Valentin (21) who studied scour in sand downstream of model sluice gates. Valentin's empirical equation for scour, in terms of the variables used in this report, is

$$\left(\frac{d_s}{H_o}\right) \left(\frac{d_m}{H_o}\right)^{1/2} = e^{\frac{F_o - 2}{2.03}}$$

in which

$$F_o = V_o / \sqrt{g y_o} .$$

The equation agrees with Valentin's experimental data if a constant is added so that the scour depth will be zero when the velocity is zero; i.e.,

$$\left(\frac{d_s}{H_o}\right) \left(\frac{d_m}{H_o}\right)^{1/2} = e^{\frac{F_o - 2}{2.03} - 0.373} .$$

This latter equation should be applicable to scour below culverts if

1. the two-dimensional flow approximation is valid,
2. the pressure distribution at the outlet is hydrostatic, and
3. the ratio d_s/d_m is large.

The second qualification is met if the ratio d_t/y_o is unity.

The third qualification is necessary because the power law

$$d_s \propto \frac{1}{d_m^{1/2}}$$

is valid only if the ratio d_s/d_m is large (17). An analysis of data, independent of the CSU study, indicates that

$$\frac{d_s}{d_m} \geq 10 \text{ to } 15$$

if the scour depth is to be proportional to the inverse of the square root of the rock size.

Valentin's equation, after modification, agrees well with the CSU data for both rectangular and circular culverts provided the above qualifications are met.

It is then concluded that the two-dimensional flow approximation is sufficiently valid to predict scour depths in rock basins below culvert outlets. Valentin's equation was employed to position the dashed curves in Figs. 48 through 52.

Two examples are given below to show how the two-dimensional flow approximation is used to predict scour.

Example 1

A 6 ft box culvert ($W_o = H_o = 6$ ft) is carrying 352 cfs ($Q/W_o H_o^{3/2} = 4.0$ cfs/ft $^{5/2}$) with a depth of $y_o = 3.0$ ft on a steep slope (S2 backwater curve). The data given in Figs. 48 and 49 for $Q/W_o H_o^{3/2} = 4.0$ are for M2 and H2 water surface profiles.

However, this flow in the 6 ft box culvert is equivalent to flow in a box culvert with $W_o = H_o = y_o = 3.0$ ft (i.e., a 3 ft box culvert flowing full) with the same velocity and the same tailwater depth as for the 6 ft box. The equivalent discharge in the 3 ft box on a mild slope is

$$\begin{aligned} \frac{Q}{W_o H_o^{3/2}} &= 4.00 \times \left(\frac{6}{3}\right)^{3/2} \\ &= 11.30 \text{ cfs/ft}^{5/2} . \end{aligned}$$

In each case, the velocity at the outfall is 19.5 fps and the brink depth is 3.0 ft. If $d_t/H_o = 0.20$ for the 6 ft box culvert, then in the equivalent box culvert $d_t/H_o = 1.2/3 = 0.40$.

Now, the data in Figs. 48 and 49 can be utilized. In Fig. 48

$$\frac{d_s}{H_o} = 4.1$$

for

$$\frac{d_m}{H_o} = 0.049$$

$$\frac{Q}{W_o H_o^{3/2}} = 11.3$$

and

$$\frac{d_t}{H_o} = 0.40.$$

Then $d_s = 4.1 \times 3 = 12.3$ ft
 and $d_m = 0.049 \times 3 = .15$ ft.

Thus, the supercritical flow at a velocity of 19.5 fps would scour the 0.15 ft diameter rock to a depth of 12.3 ft.

Example 2

In Fig. 48, for the conditions that

$$\frac{Q}{W_o H_o^{3/2}} = 3.15 \text{ cfs/ft}^{5/2},$$

$$\frac{d_t}{H_o} = 0.40, \text{ and}$$

$$\frac{d_m}{H_o} = 0.049,$$

the depth of scour is

$$\frac{d_s}{H_o} = 1.45$$

provided that the flow depth at the plain of the outlet is

$$\frac{y_o}{H_o} = .55 \quad (\text{Fig. 16}),$$

i.e., it is a mild sloping culvert.

Now, the Fig. 64, for

$$\frac{y_o}{H_o} = .55$$

$$\frac{Q}{W_o H_o^{3/2}} / \frac{Q}{D^{2.5}} = 1.48.$$

Hence, if

$$\frac{Q}{D^{2.5}} = \frac{3.15}{1.48} = 2.13 \text{ cfs/ft}^{5/2}$$

$$\frac{d_t}{D} = \frac{d_t}{H_o} = 0.40$$

$$\frac{d_m}{D} = \frac{d_m}{H_o} = 0.049$$

and

$$\frac{y_o}{D} = \frac{y_o}{H_o} = .55$$

then

$$\frac{d_s}{D} = \frac{d_s}{H_o} = 1.45 .$$



Fig. 22 Smooth Floor 45° Flare, $Q = 21.6$ cfs (from Watts, Reference 22)

This page is reproduced at the back of the report by a different reproduction method to provide better detail.

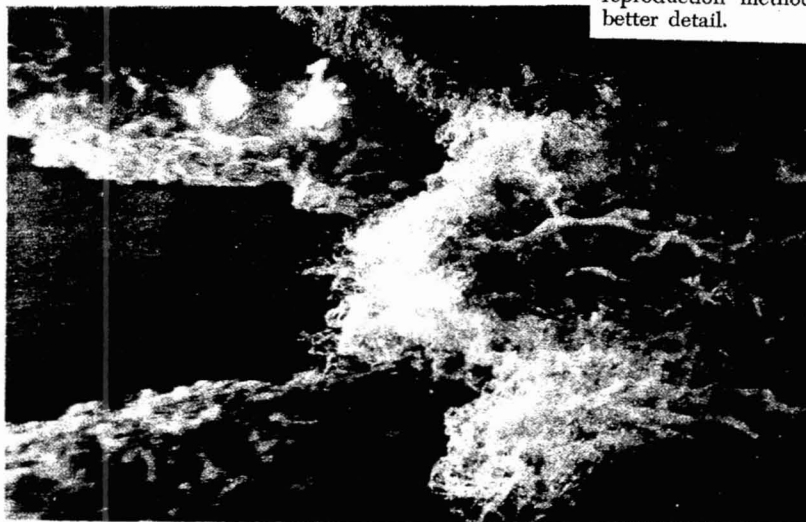


Fig. 23 Smooth Floor Plain End, $Q = 14.9$ cfs (from Watts, Reference 22)



Fig. 22 Smooth Floor 45° Flare, $Q = 21.6$ cfs (from Watts, Reference 22)

This page is reproduced at the back of the report by a different reproduction method to provide better detail.

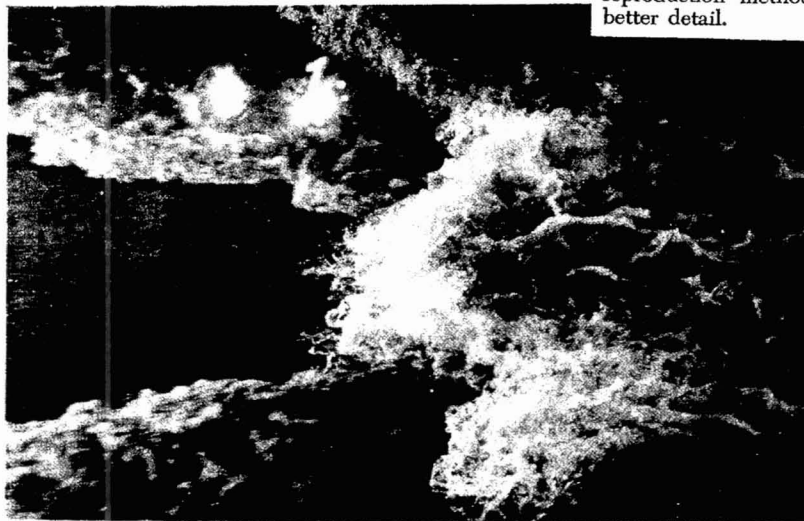


Fig. 23 Smooth Floor Plain End, $Q = 14.9$ cfs (from Watts, Reference 22)



Fig. 22 Smooth Floor 45° Flare, $Q = 21.6$ cfs (from Watts, Reference 22)

This page is reproduced at the back of the report by a different reproduction method to provide better detail.

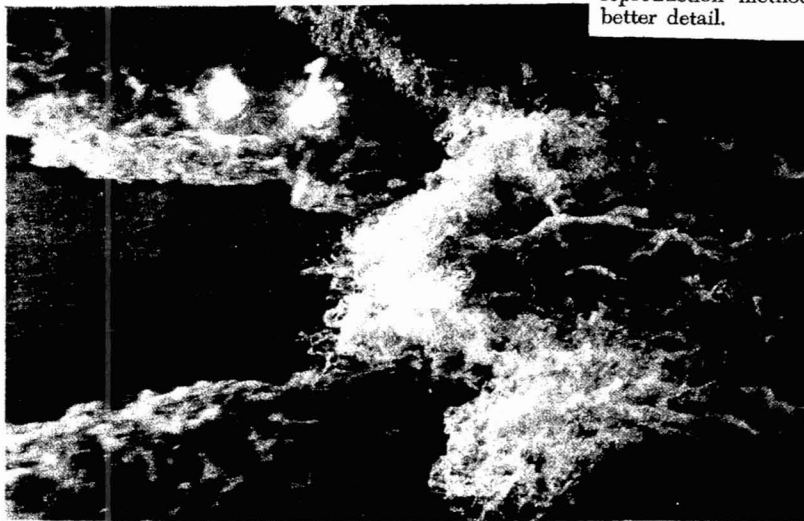


Fig. 23 Smooth Floor Plain End, $Q = 14.9$ cfs (from Watts, Reference 22)



Fig. 22 Smooth Floor 45° Flare, $Q = 21.6$ cfs (from Watts, Reference 22)

This page is reproduced at the back of the report by a different reproduction method to provide better detail.

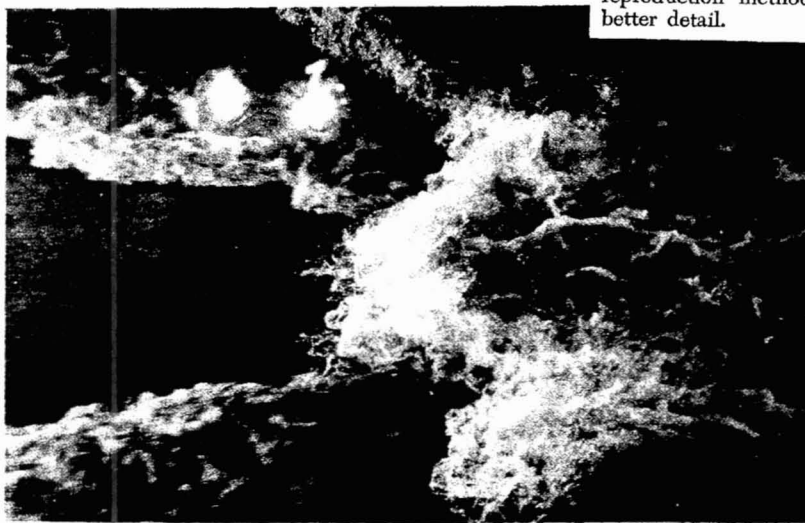


Fig. 23 Smooth Floor Plain End, $Q = 14.9$ cfs (from Watts, Reference 22)

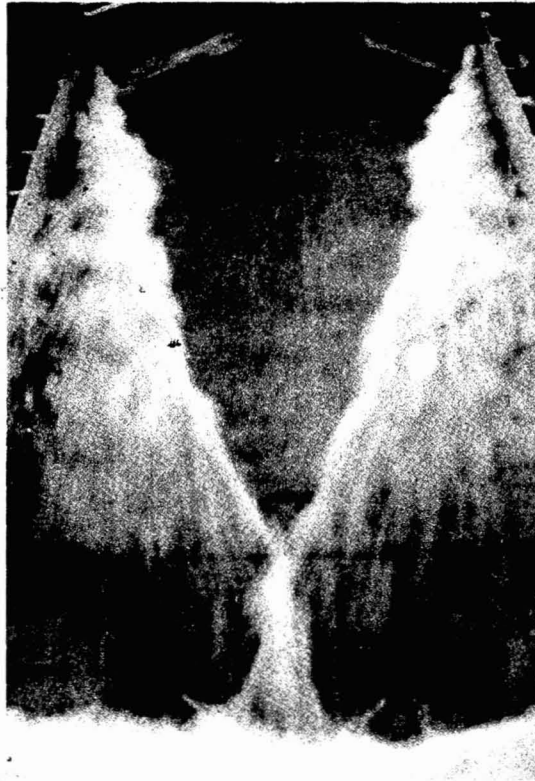


Fig. 22 Smooth Floor 45° Flare, $Q = 21.6$ cfs (from Watts, Reference 22)

This page is reproduced at the back of the report by a different reproduction method to provide better detail.

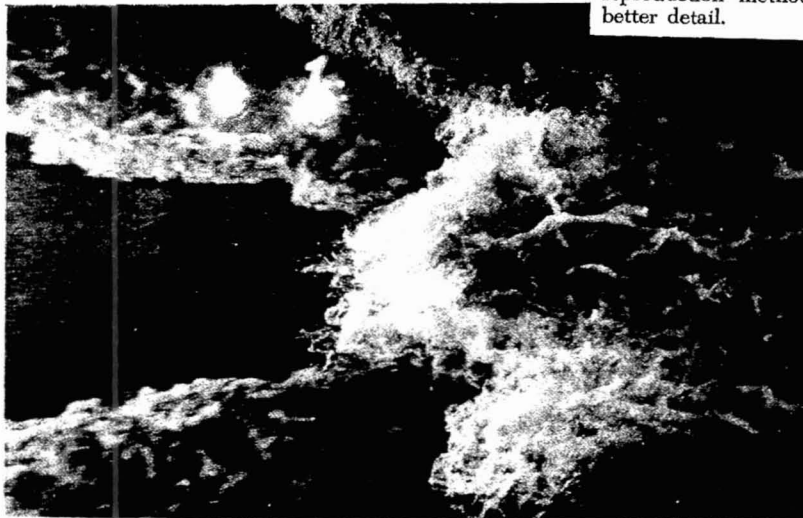


Fig. 23 Smooth Floor Plain End, $Q = 14.9$ cfs (from Watts, Reference 22)